User Facilitated Real-Time Inter-Operator Resource Sharing

vorgelegt von
Ahmet Cihat Toker, M.Sc.
aus Ankara

Von der Fakultät IV - Elektrotechnik und Informatik
der Techischen Universität Berlin
zur Erlangung der akademischen Grades:
Doktor der Ingenieurwissenschaften
Dr.-Ing.

genehmigte Dissertation

Promotionsausschuss:

Vorsitzender: Prof. Dr. Peter Pepper
Gutachter: Prof. Dr.-Ing. habil. Sahin Albayrak
Gutachter: Prof. Dr. rer. nat. habil. Dr. h. c. Alexander Schill

Tag der wissenschaftlichen Aussprache:17.3.2011

Berlin, 2011
D 83

Erklärung der Urheberschaft

Ich erkläre hiermit an Eides statt, dass ich die vorliegende Arbeit ohne Hilfe Dritter und ohne Benutzung anderer als der angegebenen Hilfsmittel angefertigt habe; die aus fremden Quellen direkt oder indirekt übernommenen Gedanken sind als solche kenntlich gemacht. Die Arbeit wurde bisher in gleicher oder ähnlicher Form in keiner anderen Prüfungsbehörde vorgelegt.

Berlin, den 18.03.2011 Ahmet Cihat Toker

Abstract

Ein Historiker der Technologie im Jahr 2100 könnte das Apple Iphone mit dem T-Model Henry Ford's vergleichen. Wie das T-Model vom letzten Jahrhundert, stellte das Iphone dem Endbenutzer, eine Vielfalt von schon existierenden Technologien in einem benutzerfreundlichen Paket zur Verfügung. Dadurch ermöglichte Apple, dass die Massen auf ihre beliebten Internet-Diensten unabhängig von ihrer Mobilität und ihrem Aufenthaltsort zugreifen könnten. Das war ein wichtiger Wendepunkt für die Telekom Operatoren, die seit Anfang der 2000er Jahren in Kommunikationinfrastruktur investierten, die solche Datendienste für ein großes Publikum anbieten sollten. Diese Investitionen wurden begleitet durch Werbekampagnen, die ein großes Versprechen verkündeten: "Always Best Connected" - immer die beste Verbindung- oder "Anytime, anywhere"- jederzeit und überall- lauteten die Devisen. Jetzt wollen die Benutzer dieses Versprechen mit den Nachbebenwellen der Iphone-Revolution, den sogenannten "Smart Phones", ausleben.

Für die Telekom Operatoren stellt diese Entwicklung sowohl Herausforderungen als auch Geschäftschancen dar. Um Kapital aus der rasch zunehmenden Datenverkehrlast schlagen zu können, müssen die Operatoren dafür sorgen, dass dieser Anstieg die Qualität der Dienste nicht stört, die die Benutzer empfinden. Ein neuer Begriff namens "Quality of Experience (QoE) " -Qualität des Diensterlebnis- bezeichnet die subjektive Beurteilung der Benutzer, wie befriedigend die Ablieferung eines Datendienstes über ein bestimmtes Operator-Netzwerk ist. Je mehr Benutzer es in einem Netzwerk gibt, desto schwieriger wird es, die Bedürfnisse der Benutzer zu erfüllen. Der Grund dafür ist die Tatsache, dass die Kapazität der verschiedenen Knoten der Operator-Netzwerke begrenzt ist. Für die Übertragung der Datendienste braucht ein Operator eine drahtlose Funkschnitstelle, verschiedene Router und Hochgeschwindigkeitsverbindungen zwischen diesen Elementen. Alle diese Komponenten haben limitierte Ressourcen. Wenn die Anzahl der Benutzer, die diese Elemente teilen, steigt, sink die Leistungsfähigkeit dieser Elementen. Dies führt dazu, dass die Benutzer schlechtere Qualittsmerkmale empfinden, sowie größere Verzögerungen oder ein Anstieg der Paketverluste. Letztendlich bedeuten diese niedrigen Performanzmerkmale auch niedrige QoE Werte für alle Benutzer.

Die Operatoren haben drei strategische Möglichkeiten, dieses Problem anzugehen. Die traditionelle Maßnahme gegen Kapazitätsengpässe ist mehr Investition in Infrastruktur. Diese Option hat zwei Hindernisse: das erste ist die Lage der Weltwirtschaft. Sie erlaubt es momentan kaum, Kapital in einer Industrie anzulegen, die vor ein paar Jahren eine große Menge von Investitionen erhielt. Zweitens wird es immer schwieriger für Operatoren, neue Grundstücke für die Basisstationen zu finden. Lokale Behörden folgen den Gesundheitsbedenken der Bevölkerung, und reduzieren den genehmigten Leistungspegel der Basisstationen und limitieren die minimale Entfernung zwischen Basisstationen.

Die zweite Option strebt an, das Radiospektrum effizienter zu nutzen. Es gibt zwei

Ansätze, um dieses Ziel zu erreichen. Der erste Ansatz bewahrt die jetzige Frequenzzuweisung unter den Operatoren, und setzt neue Methoden aus der Kommunikationstheorie um, um mehr Bits pro Spektrumeinheit tragen zu können. Die Reihenfolge von Akronymen wie 2.5G, 3G, 3.5G, LTE (Long Term Evolution) sind nicht mehr als Marketingnamen von Industriestandards, die neue Kommunikationsmethoden von zunehmenden Komplexität beinhalten. Diese Option hat den Nachteil, dass es Jahren dauert, bis die innovativen Kommunikationsmethoden standardisiert und serienmäßig implementiert werden können.

Eine andere Möglichkeit, die Benutzung des Radiospektrums zu verbessern ist eine Verfeinerung oder Erneuerung des jetzigen Frequenzzuweisungsschemas. Das aktuelle Schema kontingentiert Blöcke des Radiospektrums zu den verschiedenen Operatoren. Studien der Nutzung der unterschiedlichen Spektrumblöcken belegen, dass ein großer Teil des Spektrum nicht ausgenutzt bleibt. Ansätze wie der dynamische Spektrumzugang oder kognitives Radio lockern oder schaffen die heutige statische Frequenzzuweisung ab. Sie schlagen Methoden und Protokolle vor, mit denen ein dynamischer Zugang zur Spektrumeinheiten gewährleistet werden kann. Diese Ansätze brauchen etwas mehr Zeit als konsekutive Erweiterungen der Standards. Der Grund dafür ist, dass sowohl regulatorische als auch technologische Änderungen in Basisstationen und Kundenterminals gebraucht werden.

Die dritte und die letzte Option ist die Kombination der verschiedenen Radiozugangstechnologien. Ein sehr bekanntes Beispiel dafür ist die Integration von WirelessLAN Hotspots, die Operatoren in dicht bevölkerten Orten einsetzen, mit den gewöhnlichen Mobilfunknetzwerken. Wenn eins von dieser Netzwerke zu überlastet ist, kann ein Teil des Datenverkehrs auf das andere Netzwerk umgeleitet werden. Darüber hinaus, erhöht das Zusammenbringen von zwei heterogenen Netzwerken gleichzeitig die Kapazität und gleicht die Lastvariationen in beiden Netzwerken aus. "Common Radio Resource Management(CRRM)" -gemeinsames Management der Radioressourcen- ist das Konzept, in dem ein Operator das Verwalten heterogener Netzwerke, die dem Operator gehören, synchronisiert, um von den erwähnten Kapazitätsverbesserungen zu profitieren. Dieses Thema erregte in den letzten fünf Jahren große Aufmerksamkeit in der Forschungsgemeinde. Diese Interesse führte zu vielen wichtigen Forschungsergebnissen und ersten kommerziellen Anwendungen.

Unsere elementare Beobachtung war, dass die Einschränkung des gemeinsamen Managements der Radioressourcen auf Netzwerken, die alle zu einem einzigen Operator gehören, nicht technisch oder theoretisch ist. Die in der Literatur zu findenden Algorithmen machen es nötig, dass die zwei Netzwerke, die Ressourcen austauschen wollen, auch Operationsdaten wie die aktuelle Last oder Benutzeranzahl austauschen. Diese Anforderung stellt keine Hindernisse dar, wenn diese zwei Netzwerke einem Operator gehören. Aber ein Operator wäre, vermutlich aus kompetetiven Gründen nicht bereit, solche Daten einem anderen Operator zu übergeben. Aber, wenn es möglich wäre, diese Informationen durch einen anderen neutralen Weg indirekt zu erfahren, wäre es auch möglich, die Gewinne der CRRM zu den Szenarien zu erweitern, in denen die kooperierenden Netzwerke verschiedenen Operatoren gehören.

Diese alternative Methode, durch die ein Operator die Datenverkehrlast in einem

anderen Operator abschätzen kann, involviert das Zusammenspiel der Benutzer. Wir postulieren, dass die Benutzer bereit sind, ihre Performanzmerkmale und Subjektive QoE-Auswertungen in einer verteilten Datenbank zu speichern. Dieses Postulat setzt voraus, dass das Speichern dieser Daten anonym und sicher durchgeführt werden kann. Darüber hinaus, wir begründen später warum, dass es zugunsten von Operatoren und Benutzer ist, dass die Operatoren Zugriff auf diese Datenbank haben. Wenn diese Annahmen erfüllt sind, können zwei oder mehrere Netzwerken diese Datenbank nutzen, um abzuschätzen, wie belastet andere Netzwerke in der Gegend sind. Mit dieser Abschätzung, können sie sich entscheiden, ob es sinnvoll ist, ein Teil ihres Datenverkehr auf andere Netzwerke, die anderen Operatoren gehören, umzuleiten. Unser Vorschlag heißt "User Facilitated Real-Time Inter-Operator Resource Sharing" -Benutzer ermöglichte Echtzeit Inter-Operator Ressource Mitbenutzung. Der Ablauf von Interaktionen ist wie folgt.

Jeder Operator hat einen Software Agent, der sich im zentralen Netzwerk Operation Zentrum (NOC) befindet. Dieser NOC-Agent hat eine Dauerverbindung zu allen Radiozugansnetze (RAN) des Operators. Ein Radiozugangsnetz besteht von einem Basisstation oder einem drahtlosen Zugangspunkt und dem angeschlossenen Router, die die Benutzer über die Funkschnittstelle zu dem Operator Kernnetzwerk verbindet. Auf jeder Basisstation oder drahtlosen Zugangspunkt befinden sich weiter Software Agenten, die RAN-Agenten.

NOC-Agent ist dafür zuständig, die mittelfristige Belastung in jedem RAN zu betrachten. Mittelfristig bedeutet für unseren Vorschlag Zeitintervalle im Stundenbereich. Wenn der NOC-Agent feststellt, dass in einem RAN der Belastung so hoch wird, dass die QoE der Benutzer gefährdet sind, initiiert es ein Negotiationsverfahren mit einem anderen NOC-Agent von einem anderen Operator. Dieser Operator muss eine RAN in der Nähe des überlasteteten RANs haben, damit eine Ressourcemitbenutzung stattfinden kann. Wenn das Negotiationsverfahren erfolgreich abgelaufen ist, kalkuliert jeder NOC-Agent einen Controller-Algorithmus für seinen RAN-Agent.

Diese Algorithmen werden basierend auf der aktuellen Datenverkehrlast der beiden RANs berechnet. Die RAN-Agenten machen periodische Anfragen bei der von den Benutzern ausgefüllten Datenbank, um die kurzfristige Belastung in dem anderen RAN abzuschätzen. Da diese Abschätzung immer einen Fehleranteil hat, muss der RAN-Agent eine Entscheidung mit unvollständigen Informationen treffen. Für dieses Zweck benutzt der RAN-Agent den von NOC-Agent berechneten Algorithmus. RAN-Agent in den überlastete RAN muss entscheiden, wann das Weiterleiten vom Datenverkehr abgebrochen werden soll. Das weiterleiten muss eingestellt werden, wenn das andere RAN, das extra Datentraffic akzeptiert, auch überlastet ist. Auf der anderen Seite muss der RAN-Agent, der den datenverkehr akzeptiert, sicherstellen, dass der zuztzliche Datenverkehr nur dann angenommen wird, wenn das benachbarte RAN tatschlich überlastet ist. Das akzeptieren von zuätzlichem Datentverkehr von einem nicht überlasteten RAN wäre aus kompetitiven Gründen falsch.

In diesem Traktat wird eine vollständige Lösung für den obengenannten Ansatz präsentiert. Im Kapitel 4 entwickeln wir ein gemeinsames Leistungsmodelle für heterogenen RANs basierend auf dem "Processor Sharing"(PS) Warteschlangemodell. Wie dieses Modell be-

nutzt werden kann, um vergleichbare und kompatible Modelle für 3.5G HSDA und WirelessLAN RANs zu entwickeln, zeigen wir hier. Im Kapitel 5 benutzen wir den mathematische Formulierungsansatz "Queueing Networks" um das Austausch vom Datenverkehr zwischen RANs mathematisch zu beschreiben. Basierend auf dieser Beschreibung zeigen wir, wie optimale Parameter für das Trafficaustausch berechnet werden können. Im Kapitel 6 präsentieren wir zwei Negotiationmethoden, die von NOC-Agenten verwendet werden können, um sich auf die optimale Parameter zu einigen. Im Kapitel 7 zeigen wir wie der NOC-Agent einen annherend optimalen Algorithmus berechnen kann, und wie dieser Algorithmus von dem RAN-Agent umgesetzt werden kann. Im Kapitel 8 testen wir unseren Vorschlag unter realistischen Bedienungen.

Acknowledgements

Ars longa,
vita brevis,
occasio praeceps,
experimentum periculosum,
iudicium difficile.
Hippokrates of Kos

I would like to express my deepest thanks to my family for giving me the chance to pursue my learning endeavor to its furthest and for raising me to be the person that I am. My mother for kindling my curiosity from an early age, my father for challenging me in every aspect of life and my sister for giving me the opportunity to be a better person by trying to be a role model for her.

I wish to send my warmest feelings to Pınar, without whom the last and the most challenging two and a half years of my thesis would be impossible. Her encouragement and support have made these years enjoyable. I hope to make her thesis writing experience as comfortable as possible next year.

I wish to thank my advisor Professor Şahin Albayrak for his guidance and providing me a perfect work environment. I would like to thank my students Nadim El Sayed and Sebastian Peters and my colleague Mürsel Yildiz, who have taken an immense load from my shoulders. Without their support, I would have needed at least another year to finish my thesis.

My thanks also goes to my colleagues Dr. Fikret Sivrikaya and Dr. Ahmet Çamptepe and their advisor Prof. Dr. Bülent Yener, whose comments and ideas I have found immensely helpful.

Finally I would like to thank Bob Dylan, Gustav Mahler, Igor Stravinsky, Chan Marshall and Bruce Springsteen for providing the perfect musical accompaniment during long nights; Dostoyevsky and Kafka for providing alternative worlds to wonder into, when my world got too stressful.

Berlin, March 18, 2011

Contents

Nomenclature

ΔS Probability distribution over the elements of the set **S**

M $\Rightarrow$ M Markov Inputs Markov Outputs

3GPP 3rd Generation Partnership Project 2

AAA Authentication, Authorization, Accounting

ACK Acknowledgment

ADP Approximate Dynamic Programming

AI Artificial Intelligence

AMC Adaptive Modulation and Coding

AP Access Point

BOR Borrowing Action

Bps Bytes per second

bps bits per second

BS Base Station

CAC Call Admission Control

cCDF Complementary Cumulative Distribution Function

CDMA Code Division Multiple Access

CO-MDP Completely Observable MDP

CAB Coordinated Access Band

CQI Channel Quality Indicator

CRRM Common Radio Resource Management

CSMA-CA Carrier Sense Multiple Access with Collision Avoidance

CTMC Continuous Time Markov Chains

DARPA Defense Advanced Research Projects Agency

DCF Distributed Control Function

DCF Distributed Coordination Function

DCH Dedicated Channel

DEC-POMDP Decentralized POMDP

DITG Distributed Internet Traffic Generator

DON Donating Action

DP Dynamic Programming

DPS Differential Processor Sharing

DSL Digital Subscriber Line

DSL Dynamic Spectrum Lease

DSSS Direct Sequence Spread Spectrum

DTM Deterministic Turing Machine

DTMC Discrete Time Markov Chains

DSA Dynamic Spectrum Access

EV-DO Evolution Data Optimized

EXP Exponential Time

EXPSPACE Exponential Space

FCC Federal Communications Commission

FCFS First Come First Serve

FSC Finite State Controller

FSM Finite State Controller

GPRS General Packet Radio Subsystem

GSM Global System Mobile

HSDPA High Speed Download Packet Access

HSPA High Speed Packet Access

I-POMDP Interactive POMDP

IMBDP Improved Memory Bounded Dynamic Programming

JRRM Joint Radio Resource Management

KSBS Kalai-Smorodinsky

LAN Local Area Network

LB Local Balance Property

LCFS Last Come First Serve

LTE Long Term Evolution

MAC Medium Access Layer

MAN Metropolitan Area Network

MAP Mesh Access Point

MDP Markov Decision Process

MDP Markov Decision Process

MOS Mean Opinion Score

MOS Mean Opinion Score

MTDP Multi-agent Team Decision Problem

NEXP Non-Deterministic Exponential

NOC Network Operations Control Center

NOP Do Not Interact Action

NP Non-Deterministic Polynomial Time

NTM non-deterministic NTM

OFDM Orthogonal Frequency Domain Modulation

OFDMA Orthogonal Frequency Domain Multiple Access

P Polynomial Time Class

PF Product Form

PF Proportional Fair

POMDP Partially Observable Markov Decision Process

POSG Partially Observable Stochastic Games

PSPACE Polynomial Space

PWLC Piecewise linear and continuous

QoS Quality of Service

QoE Quality of Experience

r.v. Random Variable

RAN Radio Access Network

RAT Radio Access Technology

RF Radio Frequency

RR Round Robin

SLA Service Layer Agreement

SNMP Simple Network Management Protocol

SOD State Oriented Domains

TBS Transfer Block Size

TCP Transport Control Protocol

TDMA Time Domain Multiple Access

TFC Transport Format Combinations

TOD Task Oriented Domains

TTI Transport Time Interval

UDP User Datagram Protocol

UMTS Universal Mobile Telecommunications System

UWB Ultra-wideband Systems

VoIP Voice over IP

WLAN Wireless Local Area Network

WOD Worth Oriented Domains

1. Introduction

1.1. Challenges in the Mobile Data Networks

A 22th century historian studying the technological developments of the last centuries may compare Apple's iPhone with the T-Model of Henry Ford. Similar to T-Model of the last century, iPhone offered a single and user-friendly packet to the users, which was a combination of a variety of existing technologies. With this Apple allowed the users to access their internet services, irrespective of their locations and mobility status'. This was an important turning point for the telecom operators, who had been investing in wireless infrastructure since the beginning of 2000s, in order to bring the internet to the mobile users. These investments were accompanied by marketing campaigns with slogans like "always best connected" or "anytime anywhere". Now the users have the devices, the smartphones, to live out the promises of the operators.

This development poses at the same time opportunities and risks for the telecom operators. To benefit from the quickly expanding data traffic volume, the operators must make sure that the increase in traffic does not reduce the Quality of Service (QoS) offered to the users. QoS is expressed in concrete and objective technical parameters such as delay and loss rates. A newer concept, Quality of Experience (QoE) extends QoS with the subjective valuation of the user, how satisfying the service consumption over a certain network is.

As the number of users in a network grows, it gets harder to satisfy the requirements of the users. This is due to the fundamental fact, that the different nodes in an operator network have finite resources. A network operator brings together a wireless interface, various routers and high speed connections to offer data services to the users. Since these elements have finite resources, the increase in number of users sharing these elements mean a decrease in their performance, leading to worse QoS metrics, such as longer delays or higher packet loss rates. If severe enough, this decrease will result ultimately in a decrease in the subjective evaluation of the network, i.e. QoE.

1.2. Strategic Options

The operators have three strategic options to deal with this problem. The traditional remedy for performance bottlenecks in the telecommunications industry is to invest in infrastructure, and engineer the network for the peak demand. However, there are two drawbacks with this approach. The first is the situation in the world economy, which makes it hard to gather investment to an industry, which has already received substantial amount of funds in the last ten years. Secondly, even of the financing is

found, the operators find it increasingly hard to find new properties on which to build new base stations. The local civic and national regulation authorities are listening to the perceived health concerns of base stations among the population and reduce the power output or limit the maximum allowed density of base stations.

The second option aims to make the use of the currently allocated radio spectrum more efficient. There are two approaches for this. The first approach keeps the current frequency allocation methods, and incorporates innovative methods from the communications theory to be able to transmit more bits per unit spectrum. The series of acronyms 2.5G, 3G, 4G, LTE(Long Term Evolution) are simply given to industry standards, which employ increasingly complex and innovative modulation and communication techniques. The drawback of this approach is the fact that it takes decades from the inception of new methods, until they can be standardized and implemented serially for mass production.

Another possibility to increase the efficiency of the use of radio spectrum is to refine or the renew the way spectrum is allocated to users and operators. The current scheme gives blocks of spectrum to operators for exclusive usage.However studies of the long term usage of spectrum blocks show that large parts of the allocated spectrum remain under-utilized. Approaches like Dynamic Spectrum Access(DSA) or cognitive radio relax or abolish the current spectrum allocation scheme. They propose methods and protocols that allow a dynamic and more efficient access to spectrum. This approach will take even more time to be commercialized, compared to the consecutive extensions of standards we mentioned above, since both regulator and technological changes are required simultaneously.

The third option is to combine different radio access technologies (RAT). A well-known example is the combination of WLAN Hotspot networks deployed by the network operators with the cellular networks. When one of these networks is congested, a part of the traffic destined for this network can be transferred to the alternative network. In addition to protecting against congestion, the equalization of load between two different RATs also increases the total capacity, by making use of statistical multiplexing. Common Radio Resource Management (CRRM) denotes the concept of jointly managing two different RATs in an operator network, to benefit from the aforementioned effects. This approach has gathered much interest in the research community and resulted in important research results and the first commercial applications.

1.3. Our Approach

Our primary observation that lead to this work was that the limitation that the integrated networks should belong to the same operator is not theoretical or technical. The algorithms in the literature require exchange of operation information among the different radio access networks (RAN) that are managed jointly. These information are number of current users, or the congestion level in the network. This is possible if the RANs belong to the same operator. However two operators would be unwilling to share such information due to their competently status. And it is this situation that has lead to CRRM to be applied to RANs belonging to the same operator.

This information is needed to satisfy the fundamental requirements of the operators. A donor operator wishes to donate resources to a congested operator only. Doing otherwise would mean helping a competitor permanently. A borrower operator wishes to send its users to a under-utilized operator, in which the QoE requirements of the transferred users could be met. We propose a seamless transfer, in which the users are not aware of the transfer. So if the QoE is not met in the destination RAN, the users would still associate this with the original operator. For this reason, operators need to be able to gauge the load level in RANs owned by other operators.

If it were possible for operators to obtain this information indirectly over a neutral path, it would also be possible to extend the gains of CRRM to multi operator scenarios. We propose an alternative method, in which an operator can estimate the load in the RAN of another operator. This alternative method involves the cooperation of the end users. We postulate, that the users are willing to share their subjective evaluations of different networks they have access to in an open database. Naturally, we require that the storage and access to this database is anonymous and secure. If there is such a database, which stores how satisfied users are from a RAN for a specific service, we demonstrate why it is to the benefit of the users, that the operators also can query this database.

When the operators have access to such a database, they can also estimate the congestion status in the foreign RANs that are co-located with their own RANs. With this estimate, they can decide when it makes sense to transfer some part of their traffic to foreign RANs in times of congestion. Our proposal is called therefore "User Facilitated Real-Time Inter-Operator Resource Sharing". In the next section, we demonstrate the sample workflow of our proposal.

1.3.1. User Facilitated Inter-Operator Resource Sharing Workflow

Before we present a overview of similar proposals in the literature and give the details of our solution, it is beneficial to describe the workflow depicted in Figure 1.1. In this workflow we have three different types of software agents.For each operator there is a single NOC-Agent, which runs in the centrally located at the Network Operations Control center. The NOC-Agent has connections to the RAN-Agents running on each and every RAN belonging to the operator.

Finally, there is a SLA-Broker entity that is responsible for acting as a proxy between the NOC-Agents of different operators when needed. This broker entity is not depicted in the Figure Figure 1.1, since it is only SLA-Broker is employed for multi-class resource sharing. We assume that all of these entities are able to query the open user QoE database.

We assume, based on traffic measurements published in the open domain, that the arrival rate into an operator varies in an hourly basis. The NOC agent tracks the arrival rates and MOS levels in each of its RAN by querying the database and the RAN-Agents. If in a particular area, a RAN goes into congestion, the NOC-Agent controlling the congested RAN obtains the details from the RAN-Agent, and contacts another NOC-Agent, belonging to another operator and having an under-utilized RAN in the vicinity

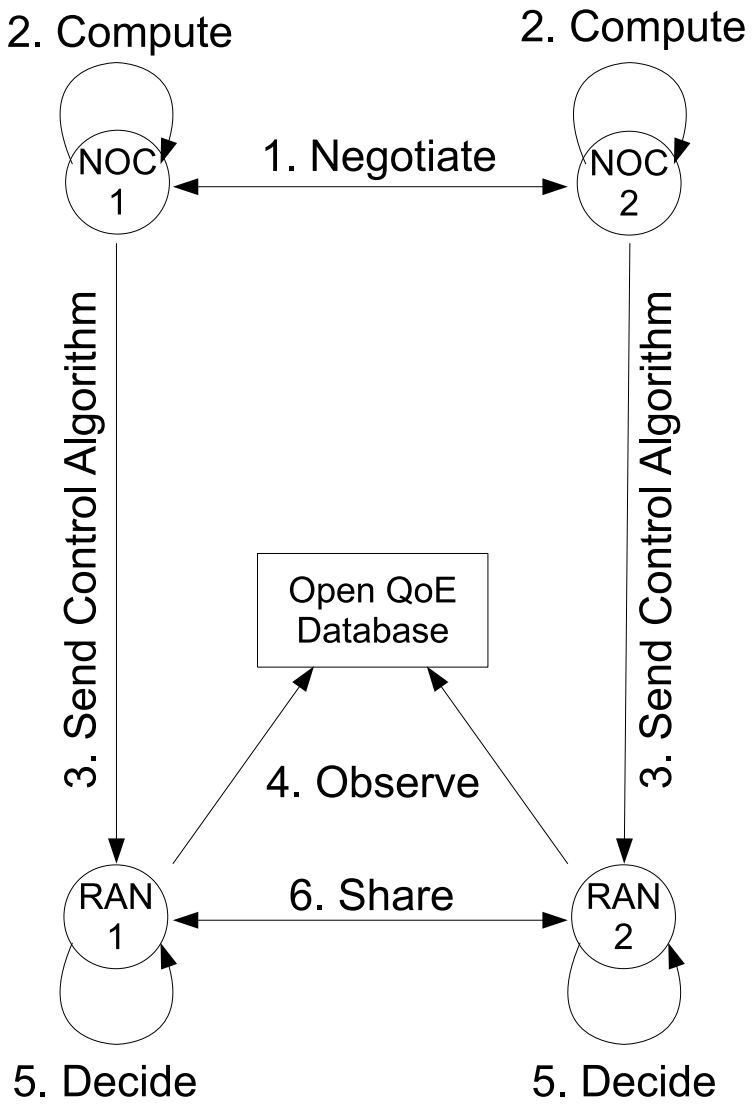

Figure 1.1.: User Facilitated Real-time Resource Sharing workflow.

of the congested RAN. In Step 1, the NOC-Agents execute a negotiation protocol to agree on a percentage of the traffic that must be transferred from the congested RAN to the normal RAN.

In Step 2, NOC-Agents compute a control policy for their RAN-Agents, using the agreed transfer probability and information that they obtain about the peer RANs from the open database. These policies, which are in the form of finite state controllers are sent along with the transfer rates to the RAN-Agents in Step 3.

With the sharing parameters available RAN-Agents, these begin querying the QoE database to track the congestion status on their peer operators in Step 4. We assume the RAN Agents will execute these observations in time scales of minutes. Using the control policies, the RAN-Agents decide on stopping or continuing the resource sharing, depending on the observations they make on the QoE Database. Resource sharing is stopped *(i)* when the overloaded operator becomes normal again, or *(ii)* the donating operator suddenly becomes overload. These are steps 5 and 6 in the workflow.

It must also be clarified what we mean by donor and borrower operator. These are in terms of radio resources. A borrower borrows additional resources, which is equivalent to transferring extra traffic to another operator. Donor operator is similarly gives unused radio resources to another operator. This is equivalent to accepting additional traffic.

1.4. Organization and Contributions

1.4.1. Organization

We organized our solution in terms of sub-problems. We first detail the discussions we introduced at the beginning of this chapter, and motivate our solution in Chapter 2. We then present a state of the art analysis, and demonstrate how our approach differs in Chapter 3. We then proceed with the individual sub-problems and their solutions.

In this work we provide algorithms for all the agents we described in 1.3.1. In order to achieve this we first present a common mathematical model based on Processor Sharing (PS) queues that can be used to abstract the queueing properties of heterogenous access networks such as WLAN and HSDPA. We term this the *Modeling Problem* , and present our results in Chapter 4.

We then formulate yet another mathematical model in Chapter5 that employs the developed queue models. This model describes the delay performance of single and multi-class resource sharing, and therefore is named the *Description Problem*.

In Chapter 6, titled the *Negotiation Problem*, we present two different negotiation mechanisms. The first method uses a peer-to-peer protocol between the NOC-Agents of individual operators, without consulting the SLA-Broker. The second model, which is developed for multi-class resource sharing relies on the existence of a trusted neutral party that is the SLA-Broker.

The workflow we described requires automated control of sharing process by exploiting the QoE database, that are computed by the NOC-Agents for the RAN-Agents. The *Control Problem* involves the development of the automated controllers and handled in

Chapter 7. We develop two such controllers, one for WLAN-WLAN sharing and one for HSDPA-WLAN.

We present finally the results of our testbed testing of the controllers in the Chapter 8.

1.4.2. Contributions

We can summarize our primary contributions as follows:

- **User Facilitated Real-Time Peer to Peer Resource Sharing Workflow:** The proposals in the literature for real-time resource sharing involve a neutral third party. We present a novel workflow summarized in Section 1.3.1 and detailed throughout this work that does not require a third party. This is made possible by using the measurements of the users. We present a complete solution for each step and component in the workflow.

- **Processor Sharing Model for HSDPA and WLAN:** Processor Sharing models have been proposed in the for both WLAN and HSDPA. We argue that these models can be used to abstract the heterogenous properties of these networks, and develop algorithms based on a common description for both technologies. We also argue that the core abstraction behind using PS models is fundamental to wireless access technologies, and therefore can be used for other future wireless air interface technologies.

- **Queueing Model for Real-time Resource Sharing:** To the best of our knowledge, there are no closed form analytical description of load balancing or resource sharing for multi-operator scenarios. The algorithms are evaluated against simulations. We present a queueing network model that use the processor sharing abstractions for heterogenous networks. We provide optimum transfer probability that minimizes delay for the single-class traffic sharing case. We also analyze and characterize multi-class sharing.

- **Incentive Compatible Negotiation Mechanism:** An incentive compatible negotiation mechanism is a mechanism in which the participants gain nothing by lying. Such mechanisms are needed for a peer to peer approach to resource sharing to be successful. We provide such a mechanism, and prove that it is incentive compatible. This mechanism can be used by two operators to agree on the optimal transfer probability derived by the queueing model.

- **Auction Mechanism for Centralized Negotiations:** For multi-class resource sharing, we were not able to provide an optimal solution for transfer probabilities. Furthermore, our proposed method requires a central entity to mediate the resource transfer. We provide an auction-base allocation mechanism to be employed by the meditating entity to allocate resources from donor operators to borrower operators.

- **User Centric Load Measure:** Calculating the real-time capacity of wireless networks is not trivial. We present a new user-centric measure of load and capacity calculated from delay values reported by the users.
- **Intelligent Controllers for Real-time Resource Sharing:** Partially Observable Markov Decision Mechanisms (POMDP) are decision making formalizations used in Artificial Intelligence (AI) domain. They are used to model decision making agents under uncertainty. We apply this formalization in conjunction with the incentive sensitive negotiation mechanism to solve the multi-agent decision problem of real-time resource sharing. We develop near-optimal heuristics for deciding when to start and when to stop real-time resource sharing.
- **Realistic Traffic Model for Heterogenous Networks:** In order to test our proposal, we need realistic models of traffic fluctuations in heterogenous networks. We present a survey of spatio-temporal traffic variations in cellular and WLAN networks. Based on this survey, we develop a traffic model that can be used to generate realistic synthetic load variations for HSDPA and WLAN.
- **Proof of Concept Implementation:** Finally, we present a proof of concept implementation of our proposal, used for automated load balancing between two WLAN networks.

1.4.3. Publications

We presented a multi-agent implementation for the policy based control of handovers between single operator heterogenous networks in [1].

We patented our proposal on how user experience reports can be used to calculate the capacity of heterogenous wireless networks in [2].

We motivated the use of decision making entities based on AI techniques on individual nodes to improve the efficiency of the networks in [3] and [4].

We participated in the EU FP7 Project, where we propose an open user experience database, and presented the approach in [5].

We first described our proposal, "User facilitated real-time resource sharing" in [6], as a concrete application of AI inspired decision makers in wireless networks.

The solution to description model, the single class queueing model, was presented in [7]. The multi-class extension and simulative evaluation was the topic of the Mr. Nadim El Sayed's Masters Thesis [8], for which the author of this dissertation served as the advisor.

We presented the auction mechanism we proposed to be used by the meditating trusted third party in [9].

We finally published our AI inspired controllers in [10].

The aforementioned publications are listed in the next section.

Bibliography

[1] C. Fan, M. Schlager, A. Udugama, V. Pangboonyanon, A. C. Toker, and G. Coskun, "Managing Heterogeneous Access Networks Coordinated policy based decision engines for mobility management," *Local Computer Networks, Annual IEEE Conference on*, vol. 0, pp. 651–660, 2007. [Online]. Available: http://dx.doi.org/http://doi.ieeecomputersociety.org/10.1109/LCN.2007.115

[2] A. C. Toker, F.-U. Andersen, and C. Fan, "Evaluation device and method for evaluating access selection in a wireless communication system," European Patent Office International Patent, WO2010057534, May 2010.

[3] S. Albayrak, M. Elkotob, and A. C. Toker, "Smart middleware for mutual service-network awareness in evolving 3GPP networks network aware applications & application aware networks," in *Communication Systems Software and Middleware and Workshops, 2008. COMSWARE 2008. 3rd International Conference on.* IEEE, 2008, pp. 44–50.

[4] S. Albayrak, K. Bur, and A. C. Toker, "Network Economy in Service-and Context-Aware Next Generation Mobile Networks," in *Personal, Indoor and Mobile Radio Communications, 2007. PIMRC 2007. IEEE 18th International Symposium on.* IEEE, 2007, pp. 1–5.

[5] A. C. Toker, F. Cleary, M. Fiedler, L. Ridel, and B. Yavuz, "PERIMETER: Privacy-Preserving Contract-less, User Centric, Seamless Roaming for Always Best Connected Future Internet," in *Proceedings of 22th World Wireless Research Forum*, 2009.

[6] S. Albayrak, F. Sivrikaya, A. C. Toker, and M. A. Khan, *User-Centric Convergence in Telecom Networks,*. Taylor & Francis, 2010.

[7] A. C. Toker, F. Sivrikaya, and S. Albayrak, "An Analytical Model for Dynamic Inter-operator Resource Sharing in 4G Networks," in *The Proceedings of the Second International Conference on Wireless & Mobile Networks*, 2010.

[8] N. E. Sayed, "A mathematical framework for the analysis and design of dynamic inter-operator resource sharing mechanisms," Master's thesis, Technische Universität Berlin, 2010.

[9] M. A. Khan, A. C. Toker, C. Troung, F. Sivrikaya, and S. Albayrak, "Cooperative game theoretic approach to integrated bandwidth sharing and allocation," in *Game*

Theory for Networks, 2009. GameNets' 09. International Conference on. IEEE, 2009, pp. 1–9.

[10] A. C. Toker, S. Albayrak, F. Sivrikaya, and B. Yener, "Inter-operator Resource Sharing Decisions Under Uncertainty," in *Proceedings of IEEE Globecom 2010.* IEEE, 2010.

2. Motivation

2.1. Challenges for Network Operators

Current business models of telecommunication operators are based on the concept of the so called *"walled garden"*: Service providers operate strictly closed infrastructures, and base their revenue-generating models on their capacity to retain current customers, acquire new ones, and effectively enact both technological and economical barriers to prevent users from being able to utilize services and resources offered by other operators. The aforementioned network management practices are strongly rooted in the monopolistic history of the telecom operator industry. The liberalization of the operators has only changed the landscape in a way that there were multiple closed operators rather than one closed operator. This trend has had related implications on the network operator and the user side.

This approach has led to the following problems:

- Lack of freedom and privacy for mobile users: users are tied by long-term contracts and are not free to move seamlessly between different operators based on their preferences when roaming. Furthermore, their privacy is compromised because excessive amount of information is exchanged between multiple administrative domains when handover is performed even though it is not required to accomplish the procedure.
- High cost of service for mobile users: while the capacity to increase operators' profits has levelled out, users can not expect significant decreases in the price of mobile network services for the foreseeable future.
- Inability of new operators to come to the market: high entrance investment costs, combined with difficulties in obtaining service level agreements (SLA) with existing operators make it next to impossible for newcomers to become actual players in this market.
- Difficulty in introducing new services over multiple administrative domains: the deployment of complex services that require interaction of the user with multiple operators becomes either impossible for technological reasons, or extremely inefficient for economical ones .
- Inefficiencies in the use of telecommunication infrastructures for socially-oriented purposes: the "walled garden" model prevents optimal re-use of the operators' under-utilized resources for non-profit or socially-oriented services, such as coverage of schools, public libraries, emergency forces, etc.

- Under-utilization of public resources and unsustainable investment models: lack of an efficient collaborative service provisioning model hinders the network and spectrum sharing efforts which aim economically and environmentally efficient networks.

The rise of Internet as the dominant driving force behind and the medium of social and economical changes in the last 10 years has put the usually centrally managed telecom operator networks which are poorly integrated with outside components, and strictly isolated from external access. On the other hand the Internet was born out of the need for integrating networks. The exposure of users to the prolific Internet services, which make extensive use of the open integration, means that similar service models will have to be provided by the next generation telecom networks. The clash between these two opposite approaches poses important challenges for network operators. This is due to the fundamental risk associated with their networks turning into mere bit-pipes. In order for future telecom networks to be economically viable, they should provide a similar user experience with Internet services, albeit in a more managed and reliable manner. Here lies the challenge of the so-called Telco 2.0 operators. The operators have to offer even more data intensive applications on their networks to make their operations profitable.

This comes in a time, when the increasing data traffic is starting to hurt user experience, and pose itself as the biggest risk facing the operators. The increase in traffic and its negative impact on user experience and thus operator revenues can be observed in the media, scientific literature and industry specialists reports. In [1], the CEO talks about the danger of a *"capacity crunch"*, and proposes the opening up of new spectrum, investment in new radio access technologies, and using existing technologies such as WLAN as possible remedies. In the technical report published by 4G Market Research and Analysis Firm Marvedis [2] designates the capacity shortfall as the primary concern of the network operators. Finally Halepovic surveys the trends in the data traffic patterns over the last 10 years in [3], and concludes that the demand for mixed data services over WLAN and 3G networks will be growing steadily as more users connect to the Internet using wireless technologies and as the current users increase the size and variety of their data consumption.

2.2. Solution Strategies

In the face of the trends and the weaknesses we described above there are three strategies that the network operators and broadband service providers can follow:

1. **Competitive:** Capacity expansion.
2. **Heterogeneous Cooperative:** Employing untapped networking resources, such as community/cooperate Wireless LAN networks.
3. **Homogeneous Cooperative:** Establishing strategic partnerships with other operators to share the existing spectrum.

Capacity expansion Strategy

Most direct method of combating missing capacity is investing directly to infrastructure. This has been the case for most of the operators who flag shipped the adoption of Apple's iPhone, such as AT&T in the United States. In a press release in March 2009 [4], the company announced that its investment for the state of Illinois alone was 3.3 billion. Industry analysts put the projected capital expenses of the company in the range of 18 billion and discern it as an industry-wide trend. Clearly, this is a brute-force solution to the problem and can only be extended to the point when the investment costs drive access prices beyond market prices. Even if one assumes that the market would adjust all prices accordingly, the emergence of "Greenfield operators" employing new technologies such as WiMAX, or a possible decrease in revenues due to the falling data traffic mean that this strategy is not sustainable.

Heterogeneous Cooperative

802.11 based WLAN are becoming ubiquitous in most urban areas, where they are mostly deployed as hot-spots on densely populated areas. Most of the network operators offer hotspot services to their data users. In the recent days the concept of traffic offloading [5] is being used to transfer data traffic that is bound to the global Internet to WLAN hot-spots operated by the wireless operators.

Operator owned WLAN hot-spots are not the only possible WLAN networks that can be used to help the operators under capacity crunch. Community networks, built from the access point of non commercial users are also possible candidates. The concept of community communication networks goes bask to the mid 90's [6]. The goal of community networks is reducing the investment costs for the most expensive part of the end-to-end path in communication networks, the access part. Main idea is to combine access points of end users into a single access network, which is then offered to other foreign users in exchange of a fee, or to new members in exchange of access point. Early incarnations of this idea used wired connections such as cable, fiber, and twisted copper networks [7]. With the ubiquity of wireless access networks, realized by the popularity of 802.11-based wireless LANs, idea has experienced a revival. Companies such as FON [8] are already offering commercial community networks, and free communities are burgeoning in European (Berlin, Rome, Athens) and US (San Francisco) cities employing the 802.11 technology. The 802.16-based solutions for lower population density rural environments are also being proposed in the literature [9], which is yet to become a reality.

The essential role of the community networks from the perspective of mobile fixed convergence is the opening up of last mile wired connectivity to the wireless domain. This new untapped wireless capacity can be used by the network operators to extend their networking resource pool. In fact, the concept of operator assisted community networks has been developed in the literature for the coexistence of community networks with wireless network operators. It has been shown[10] recently that the co-existence of a community network and a licensed operator is viable, under the condition that

community network fees are below a threshold value. Such a scenario can be seen as cooperation between the wired ISP that provides the back-haul connectivity to the wireless operator via the proxy of community network.

Homogeneous Cooperative

The final strategy that the operators can follow is to establish strategic partnerships with other operators in order to *(i)* reduce down the investment costs or *(ii)* make use of trunking gains in the case of asymmetric service demand profiles. As we will discuss in Chapter 3, such agreements between operators are already takin place. However these agreements are mostly off-line in nature and can only be reached after long legal and financial negotiations by the involved parties. Despite the difficulties associated with cooperative solutions, they represent a far more long term and sustainable solution compared to capacity extension.

2.3. User Facilitated Real-Time Inter-Operator Resource Sharing

2.3.1. Aim

We believe that the dynamic resource sharing between two licensed or virtual operators and cooperation between a licensed operator and a wireless community network are of similar nature, and provide the best solution to the operators capacity scarcity problem. We also are of the opinion that the time-scales with which the transfer of resources take place can be improved. Currently, these durations are measured in terms of days. Our aim is to enable dynamic resource exchange between heterogeneous operators within the timescales of hours or minutes. We will demonstrate that according to the latest measurements and traffic models developed for wireless networks, there are cooperation opportunities to be exploited within these time scales.

2.3.2. User-Centricity and User-Facilitated Resource Sharing

An important obstacle before executing dynamic resource sharing in sub-daily timescales is the way the ownership of digital identities of individual users are handled in the current environment. Current practices tie the users to a single operator even though the number of players in the market has long been growing. The users tend to manually combine their subscriptions to multiple operators in order to take simultaneous advantage of their different offers that are suited for a variety of services. *User-centric networking* is a new approach to the relation to the ownership of identity in next generation networking. In its most generic sense, the user-centric view in telecommunications considers that the users are free from subscription to any one network operator and are the real owners of their identities. This allows them to dynamically choose the most suitable transport infrastructure from the available network providers for their terminal and application requirements.

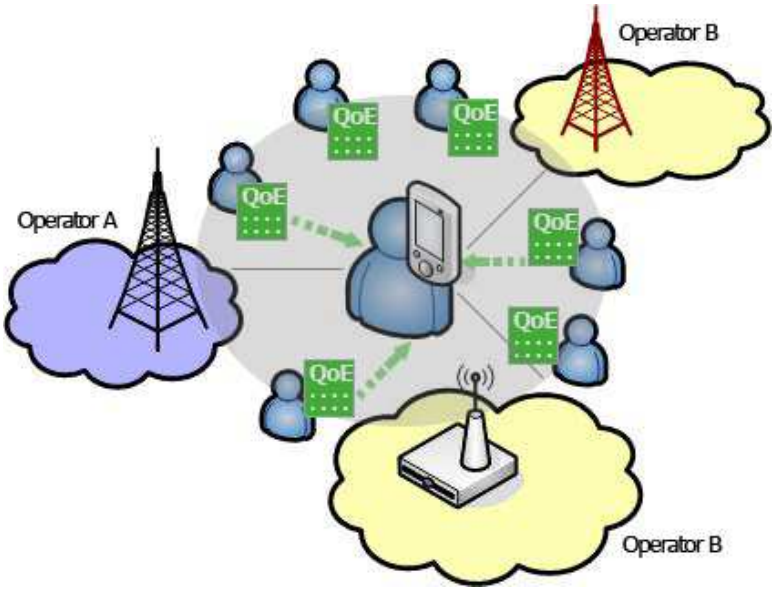

Figure 2.1.: User centric approach in Perimeter project.

The PERIMETER project [11], funded by the European Union under the Framework Program 7 (FP7), has been investigating such user-centric networking paradigm for future telecommunication networks. The key innovation in PERIMETER project is the introduction of a distributed database implemented on user terminals, which stores the *Quality of Experience* (QoE) reports associated with a certain network generated by the users as depicted in 2.1. These reports capture the objective QoS measurements, as well as subjective grading of the suitability of a given application to a specific RAN. The subjective scores that the users enter are called the Mean Opinion Score (MOS). The users utilize the reports of current and past users of networks to decide which network to choose. It is also possible for the network operators to host support nodes that store the user reports. In exchange for hosting this service, they would be able to track the subjective user performance metrics in their own networks as well as in the networks which are co-located. Even if the contract-less dynamic access part of the user-centric paradigm were not to be implemented, an open QoE database is still beneficial both to the operators and users, and therefore can be realized on its own.

Another critical aspect of sub-daily dynamic inter-operator sharing is what we call the *information asymmetry*. In the well researched intra-operator resource sharing problem the internal congestion states of different Radio Access Networks (RAN) are available to the controller, since both RANs belong to the same operator. In the case of inter-operator sharing this is not the case, since competing operators would not be willing to share mission-critical operation data with each other. In user-facilitated Inter-operator Dynamic Resource Sharing, the user QoE database helps the operators to make indirect observations about the congestion state of the peer operators. With these observations they can take cooperation decisions. Furthermore, the fact that each operator knows

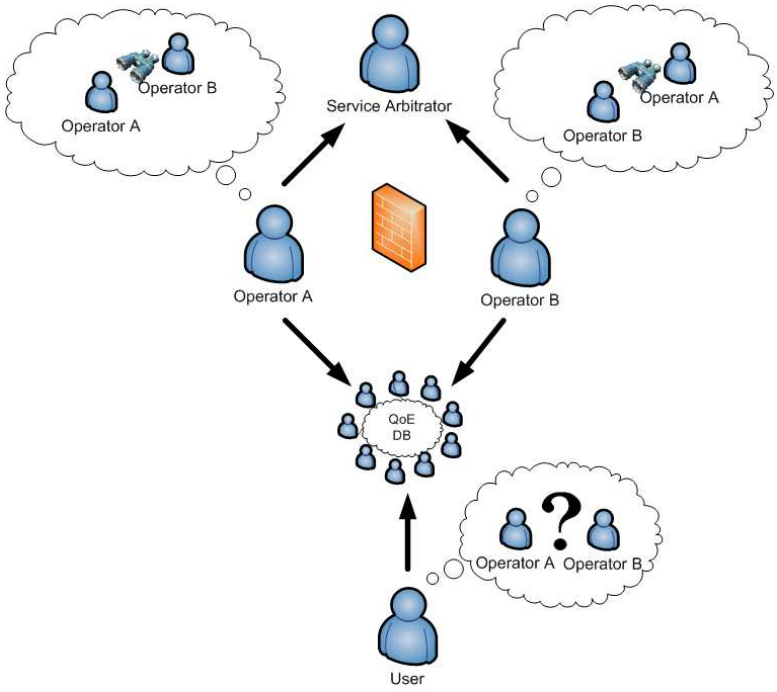

Figure 2.2.: Information Asymmetry solved by the user QoE database.

that its congestion state is indirectly available to the peer operator makes it possible for us to design efficient interactions between peer operators, in which lying about the operator internal conditions are are futile. This is depicted in 2.2.

2.4. How Realistic is a Cooperative Solution?

Our proposal requires cooperative behavior from the operators. In this section we discuss under which conditions this might be possible.

Cooperation among the end users and network side elements enable a more efficient utilization of the wireless spectrum, compared to a competitive use of the spectrum. This simple fact has not translated into reality, even in the wake of a long history of academic and industry research projects, and various commercialization attempts. Ad hoc networking has been an active research field for at least 30 years, yet to produce a civilian product that is profitable. Cognitive radios and software defined radios are all providing and demonstrating through proof-of-concept projects and implementations promising results that validate the fundamental fact about cooperation. Yet they are finding it hard to make their impact on the business front. These facts make asking the following question legitimate: "Does the success factor behind cooperative methods in 4G networks lay beyond the technical considerations?"

Dohler et. al., who are associated with France Telecom, investigate the answers in [12]. Before postulating success factors, they discern common reasons of failure that

are associated with past proposals for cooperative communications. First aspect they recognize, which does lay outside the technical realm indeed, is the short-term horizons of human decision processes. Specifically, successful cooperation necessitates the acceptance of short term losses, as condition for long term benefits. The authors propose that the instinct-driven minds of humans are not apt to make such a sacrifice. Thus their claim is that a cooperative scheme that depends *a priori* on human decisions for cooperation is doomed to fail. The second reason of failure is socio-technical in nature. The authors postulate that the number of design degrees of freedom associated with the cooperative communications proposals have made their commercialization impossible. The reasoning is that cooperative systems require the system designers to come to a consensus on the terms of cooperation beforehand. The larger the number of technical parameters, the harder for the designers to achieve an agreement. Finally, the authors note technical ground for the apparent commercial failure of cooperative systems. Successful commercial communication networks build on the premise that end-users are willing to make contracts with operators, in exchange for a reliable connection. The cooperative proposals in the literature did not lend themselves to such business model, and hence could not build a healthy ecosystem of companies needed for the success of a communication technology.

Based on these observations the authors propose the following success criteria for cooperative communication systems.

1. Cooperation decisions should be taken by decision engines with long term decision horizons.

2. The benefits of cooperation should be explicit and trackable.

3. There has to be a clear answer to the *Cui bono?* question, that is for whom the benefits are, should be demonstrated clearly.

4. Cooperation should provide reliable communication means.

5. Design degrees of freedom of the system should be kept at a minimum.

Let us analyze our proposal from these success criteria. The cooperation decisions are to be taken by the NOC-Agents, which base their decisions on long term average average rates. In an actual implementation the amount of traffic exchanged can be tracked explicitly. Furthermore, by analyzing the QoE database, the user performance can be tracked. This means the benefits such as higher revenue and increased user satisfaction are explicitly trackable. In our proposal, cooperation makes the communication more reliable, in the sense that service degradations due to congestions are less frequent. As we describe in Chapter 5, there is a single dynamic parameter that the cooperating parties must agree upon, namely the transfer probability.

It is worth discussing the *Cui bono?* question in a little more detail. The benefit of the operator who is donating resources is obvious. In the short term, it is able to increase its revenues by opening some of its under-utilized infrastructure. The benefits of the borrowing operator on the other side are long term. It sacrifices some or all of

the revenue from the transferred sessions, for the sake of increasing the QoE of the users already associated with the operator. This is compensated in the long term, since a sustained lower QoE levels leads to users leaving or not choosing the operator in the future. This is termed churning in the literature. Avoiding churning in the highly saturated telecommunications market of today is an important financial benefit.

It is tempting for an under-utilized operator to reject helping a congested operator, with the hope that the churning users of the under-utilized operator would choose the under-utilized operator in the future. This would be the case if the operators would stay under-utilized and congested for long periods of time. However this is rarely the case, and a under-utilized operator will become congested in the future. Similarly, a congested operator could become under-utilized in the future. The load fluctuations are due to random user population variations in the short term and service penetration variations in the long term, both of which the operators cannot influence directly. It is highly probable, that the cooperation agreements between operators would be based on this fact, and be reciprocal. That means, an operator would be willing to accept additional traffic from another operator, with the condition that the other operator would be willing to do the same in the future if the conditions require this. From this perspective, going into such a cooperation agreement, and loosing some short term revenue can be seen as an insurance that protects from future congestions.

Dohler's analysis is slightly more technical, compared to the analysis of Giupponi et. al. [13] which includes micro-economical components. Giupponi proposes a meta-operator, similar to the SLA-Broker we introduce in Chapter 6, that allows real-time resource sharing among operators. Operators which need additional resources apply to the meta-operator for additional resources. The meta-operator than chooses another network with extra capacity. The authors propose a neural network controller to be employed by the meta-operator, with a reinforcement learning mechanism to set the prices for unit bandwidth transferred among operators. They investigate the benefits of real-time resource sharing as a function of relative market shares and infrastructure investments of two operators. Even though the control mechanism is different from our proposal, the financial analysis is still relevant.

In the first scenario, when both operators have the same market shares and infrastructure deployment, real-time resource sharing increases operator revenues by 34% and the number of total users served by 36%. In this scenario the roles of the operators change from time to time, i.e. an operator has both donor an operator roles.

In the second scenario authors examine the effects of uneven market penetration. When Operator 1 controls two thirds of the market, this translates to 85% of traffic transfers taking place from Operator 1 to Operator 2. This means that the short term financial benefits are inclined towards the operator with the less market penetration. Operator 1's benefits are long term, in terms of reduced churn rate, i.e. keeping customers. In [14] authors quantify the churn rate as a function of market share and cooperation options. For the market share of 66.6 %, cooperation reduces user churn rate from 0.99 to 0.0001. Therefore even an operator with a larger market share would be willing to go in a cooperation agreement.

In the final scenario the authors concentrate on the effects of asymmetrical infrastruc-

ture deployments. In a region where Operator 1 has invested more in infrastructure, under high load conditions most of the traffic transfer occurs from Operator 2 to Operator 1. The cooperation agreement increases the revenue of the Operator 1, which allows the costs of infrastructure to be covered. To sum up, Giupponi et. al. show that it is beneficial for operators to go into cooperative agreements irrespective of the market and infrastructure shares.

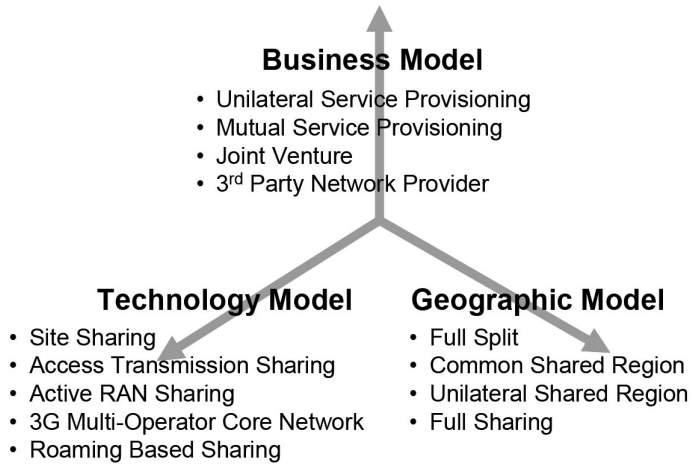

Figure 3.1.: The Infrastructure sharing dimensions and variants.

3. State of the Art

In this Chapter we present the proposals and trends in the industry and the scientific literature that are similar to our proposal. At the end of the Chapter, we compare our proposals with those we cover in the Chapter.

3.1. Infrastructure Sharing

Infrastructure sharing is a fairly new industry trend in cellular networks, in which operators share varying portions of the access networks to leverage the initial investment and reduce the operation costs of the most expensive part of their networks. Depending on the level of network sharing, the resources shared between operators may involve radio spectrum, back-haul links, and even some network layer links.

The portion of the network shared between the operators is not the only distinguishing property of Infrastructure Sharing. Frisanco provides a three dimensional categorization of Infrastructure sharing in [15], which we reproduce in Figure 3.1.

According to this view the dimensions are the technical dimension, which is related to the proportion of the 3G network that is shared. Second dimension is the business model, which defines the legal and financial roles of the the sharing operators. Final dimension is the geographic dimension, which defines in which parts of the operators networks the sharing will be effective.

On the physical dimension, one can discern a fundamental trade-off. The higher in the UMTS hierarchy the sharing goes, the higher are the savings in the investment and operation costs. But this comes at the prize of losing autonomous control over a larger part of the network for the operators. At the bottom of this hierarchy is the *passive sharing*, in which the operators have no protocol interfaces. In this scenario base station sites, or the links connecting the base stations to the base station controllers are shared. *Active sharing* means on the other hand, that the operators share the software protocol interfaces to individual nodes. Active sharing generally involves the sharing of the complete RAN. The RAN can be partitioned into logically between operators, in which the end users see a single base station ID, or physically in which the users see the base station IDs of both operators.

On the business model dimension the operators can decide to form a joint venture, let a third party handle the operations or to make separate offers to the users. Which one of these options can be chosen depends also on the technical and geographic dimension.

The fact that infrastructure is gaining popularity among operators show that there is the possibility that operators are willing to go into resource sharing contracts with other operators. In contrast to our proposal, the sharing of resources, is at least for the moment, is static.

3.2. Common Radio Resource Management (CRRM)

We discussed earlier that the operators have already deployed WLAN based hotspots. Common Radio Resource Management is the concept that such multiple radio access technologies can be combined in an operator network to diversify the service offer, as well as for making use of trunking gains. In [16] Tolli quantifies the benefits of CRRM. Fruskär provided the derivation of optimal allocation mix, which is the ratio of traffic allocated to different RANs, as a function of the service mix, which is the ratio of arrival rates of different service class sessions in [17]. The main result from this analysis is the following. According to the slopes of the joint capacity regions, each service has a particular RAT, for which it is optimal. For example data calls are served better by WLAN networks, where as voice calls are better served by UMTS. The optimum allocation strategy is to fill the WLAN with data sessions, and the UMTS with voice calls as long as the capacity of those RANs are not exceeded. Only after the capacity is exceeded should the voice calls be allocated to WLAN, or data calls to the WLAN RANs. In [18] Perez-Romero provides architectural models with which CRRM can be executed. And in [19] he shows how CRRM can be used to alleviate the effects of congestion.

3.3. Spectrum Sharing

In 2002 FCC, the regulator in USA, published the results of a large-scale spectrum occupancy survey. This was a seminal document, since it showed the variability of the occupancy of allocated spectrum varied between 15% and 85% both spatially and temporally. This was clearly seen as a shortcoming of the current spectrum allocation

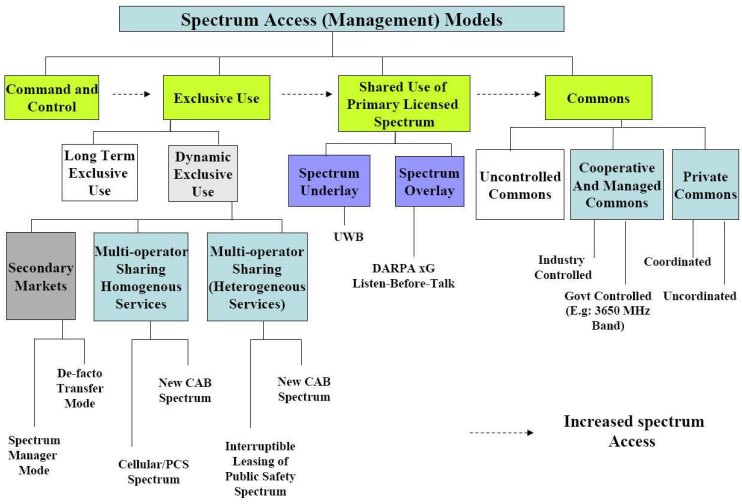

Figure 3.2.: An overview of DSA proposals from [20].

policies. The traditional method of spectrum allocation is to allocate a band to a certain technology, operator, and usage purpose. It is a natural result of this static allocation strategy, that the occupancy varied this much. Two main of complementary research directions were formed as an answer to this problem:

- Dynamic Spectrum Access (DSA)
- Cognitive and Reconfigurable Radio

3.3.1. Dynamic Spectrum Access

The aim of DSA is to replace the current static spectrum allocation regime with a more dynamic one. There number of DSA proposals in the literature is very large. Buddhikot proposes a detailed hierarchy in [20] in order to put these proposals in perspective. The hierarchy is depicted in Figure 3.2.

The current spectrum access model falls under he category of long term exclusive use, in which the owners of spectrum licenses have a long time and mostly non-transferable right to transmit in the corresponding spectrum. Buddikhot explains the current secondary market rules in USA, which allows the exchange of data transmission rights for a given spectrum rights between operators. Even the fastest mechanisms require a 15 day processing delay. The licences can be transferred for short periods of time in the range of days.These are called the non real-time secondary markets.

The author proposes two methods how real-time secondary markets can be implemented. In the first version, the operators exchange frequency carriers as an answer to load fluctuations for shorter amounts of time such as 15 minutes. Buddikhot rejects the applicability of this scenario in high density areas, and argues that this scenario is more relevant for rural areas. We will show that this is not the case in Section 8.3.3.

The author advocates an alternative approach, in which a dedicated frequency band called Coordinated Access Band (CAB) is allocated only for such dynamic short term allocation to operators which need them in the case of congestion. He proposes a trusted Spectrum Broker to allocate the radio carriers to operators according to their bandwidth requirements.

The next category in DSA hierarchy is the shared use of primary licensed spectrum. The idea is to let users of a secondary RAT to use the spectrum that is already allocated to a primary user. This can take place in two variants. In the spectrum underlay, the secondary system operates below the noise/interference threshold of the primary system, so that the secondary system appears as noise or negligible interference to the primary users. Ultra-wideband Systems (UWB) are examples of such an approach. The approach is related to configurable radios and cognitive radios we will discuss next.

3.3.2. Cognitive and Software-defined Radio

The approach in spectrum overlay is to let the the secondary users find spectrum holes in frequency and in time and transmit opportunistically. This approach requires cognitive approaches to find the spectrum holes, and transmit opportunistically during these holes. Since the spectrum holes appear on different frequencies and require different power levels, reconfigurable radios are needed. Software-defined radio is the approach, in which the radio transmission properties of the user and base station network interfaces can be controlled algorithmically. Akyildiz provides an excellent survey of the cognitive radio challenges and research results in [21].

The commons model covers coordinated and uncoordinated access to a shared spectrum, without any exclusive spectrum allocation. In fact, WLANs which operate at the licence-free ISM band is an example of such a commons model.

3.4. Proposals for Real-time Spectrum Sharing

In the literature, there are similar proposals to our solution.

Salami et. al. make a very similar proposal for dynamic spectrum sharing in the UMTS bands. They make the assumption that the operators are involved in an active sharing agreement, and thus share the same RNC and base stations. A central entity is responsible for tracking the spectrum utilization of two operator simultaneously. In [22] they let the RNC be controlled by this central entity to dynamically change the channel and code assignments between the operators according to the different load levels. In [23] they make a more similar proposal to our approach. Instead of adjusting the channel codes according to the network load, they let the RNC issue "re-connect" messages to the end users, to transfer traffic between operators.

In [24] the authors propose the technique of Dynamic Spectrum Lease (DSL). In DSL the owner of the primary spectrum, i.e. the access point, actively tries to lease some part of the spectrum to secondary users, when the traffic is low. The authors formulate the problem as a power control game. This approach takes the cooperation to a lower layer compared to our proposal.

Finally Guipponi et. al. propose an inter-operator Joint Radio Resource Management (JRRM) mechanism in [13]. In this proposal the operators forward the user requests that they cannot answer to a meta-operator. This meta operator is responsible for finding a suitable operator as well as the bit rate for these requests. It is able to calculate these values, since the operator internal JRRM entities constantly update the meta-operator JRRM about the spare capacity in their RANs. The architecture resembles our SLA-Broker based multi-class negotiation mechanism we present in Chapter 6. Instead of using auctions to calculate these values, the authors use fuzzy logic. Another important similarity to our approach is the processor sharing abstraction the authors employ for WLAN RANs in their systems.

3.5. Comparison with State of the Art

Lets compare our proposal with the approaches we presented above.

When seen from the DSA hierarchy perspective given by Buddhikot [20], our proposal is an example of DSA, within the Dynamic Exclusive Use category. It is a real-time secondary market, which is implemented in the already existing cellular and WLAN bands. Unlike the example given by the authors, our proposal does not involve actual exchange of radio carriers, but exchange of user sessions between operators. This means our approach does not require any changes to the base station hardware or controller software.

From the perspective of the infrastructure sharing, our approach can be categorized as a roaming based infrastructure sharing. The geographic scope of infrastructure sharing is limited to the congested area. During the resource sharing period, all the nodes in the donor operator is shared. To the best of our knowledge, there is no current implementation or proposal to use real-time roaming to overcome congestion.

Our proposal can be seen as an extension of the CRRM approach to include foreign operators. The framework architecture presented by Perez Romero shows the practical applicability of our solution, since the same architecture used for CRRM can be used for User-Facilitated Dynamic Inter-Operator Resource sharing by considering RANs from foreign operators as possible traffic diversion destinations.

Finally, real-time spectrum sharing proposals we discussed in Section 3.4 share the common characteristic of relying on a trusted third party to meditate and control resource sharing. Our primary improvement on the state of the art is the possibility share resources directly between operators, without the third party. We believe it is an important improvement, since trust establishment between two operators is simpler than building from meta operator from scratch.

4. Modeling Problem

In the *Modeling Problem* we are interested in developing comparable and compatible performance models for heterogenous radio access technologies such as HSDPA and WLAN.

4.1. Introduction

Processor Sharing (PS) is a queueing service discipline first analyzed by Kleinrock in [25] in 1967. It is an idealized version of the Round Robin (RR) service discipline, in which the service quanta that each job in the queue receives is infinitesimal. In the limit the server operates in a manner that each job receives a service rate equivalent to the overall server capacity divided by the number of jobs in the queue.

We will use PS abstraction in order to abstract the performance of heterogeneous radio access networks. In this Chapter we present a summary of the results in the literature that have used PS abstraction for WLAN and 3GPP RANs. The intuition that the wireless access network can be modeled as a service station that simultaneously serve the active users can be traced back to the work of Telatar [26]. Furthermore, it has been shown that the Weighted Fair Queueing service discipline, used widely in radio network base stations, approximates processor sharing when the packet size is small compared to the session size [27].

Another important feature of PS, which has lead us to consider it as an abstraction model is the fact that combination of PS queueing stations have a separable joint probability distribution thanks to the BCMP theorem [28]. We will investigate this in Chapter 5.

In this Chapter we first provide a mathematical background on PS in Section 4.2. In Section 4.3, we first present an overview of the 802.11 MAC and then argue that WLAN MAC can be modeled with a PS queue, especially for TCP traffic. In Section 4.4, the issue of how 3GPP family of RATs handle different service classes is discussed. We make a summary of the of the HSDPA technology, which is an example of evolution of traditional UMTS based 3G networks that focuses on bursty traffic. We finally argue that the data transmission performance of HSDPA can be modeled via a PS model similar to the WLANs. We conclude therefore that the PS abstraction can be used as an umbrella model for interacting heterogeneous RANs.

4.2. Mathematical Background

4.2.1. Time Shared Systems

Time shared systems were the pioneering paradigm that heralded the arrival of the current Internet and World Wide Web. They were conceptualized after the Second World War, as a means of making the few high computation powered computers in the United States accessible to the researchers across the country. The computers would be shared between users over different time blocks. Round Robin (RR) discipline was the first candidate for regulating the access to the computers.

In the RR service discipline the customer at the head of the queue receives Q seconds of service on the server, then is returned to the tail of the queue. In the next service interval, the new head of the queue customer also gets Q seconds of service and send to the back of the queue after finishing its service quantum Q.. The process repeats. Thus the customer would cycle the queue n times when his service demand equals nQ.

While investigating the delay characteristics of the RR disciplines used for time shared systems, Kleinrock introduced PS is the limiting service discipline of RR, when one lets $Q \to 0$. Practically, this happens when the size of the service quantum Q is infinitesimal compared to the job sizes. Ideally, in this discipline each customer receives C/k service rate when there are k users using the server of capacity C. From this perspective, the PS is the ideal time shared discipline, treating the users fairly.

4.2.2. Derivation of PS Results

Let us assume that the job size in a RR queue is distributed geometrically with a parameter σ. Geometric distribution is chosen, since it is the only memoryless discrete distribution. Let s_n donate the probability that the request size is of size n service quanta:

$$s_n = (1 - \sigma)\sigma_n^{n-1} \tag{4.1}$$

One has to be careful in taking the limit. Simply letting $Q \to 0$ would mean the service time of a request nQ would also go to zero. Instead, one keeps the average service time constant as the limit is taken. If the average size of the request is $1/\mu$ operations or resources, and the server capacity is C operations or resources per second, the average service time is given by $1/(\mu \cdot C)$. From the RR discipline average service time is given by $E[s_n] \cdot Q$. Since s_n is Geometric r.v. , $E[s_n] = 1/(1 - \sigma)$. Equating both of the expressions for average service time we get 4.2:

$$\frac{1}{\mu C} = \frac{Q}{1 - \sigma} \tag{4.2}$$

$$\sigma = 1 - Q\mu C \tag{4.3}$$

So taking the limit $Q \to 0$ by keeping the average service time same necessitates $\sigma \to 1$. It is well known for the limit $\sigma \to 1$ the geometric r.v. s_n converges to a exponential r.v.

with parameter μ. Under this conditions the PS server reduces to a M/M/1 server with load dependent service rate, in whihc *(i)* jobs arrive according to a Poisson process, *(ii)* jobs have an exponential size distribution, *(iii)* jobs see a service rate of C/n when there are n other non-completed jobs.

Kleinrock formulated the expected sojourn time in a PS queue conditioned on the job size x in [25], by letting $Q \to 0$ and $\sigma \to 1$ in the formulations for RR queue. $T(x)$, which describes the average time spent in the system of a customer requiring x operations, is given by (4.4):

$$T(x) = \frac{x/C}{1-\rho} \tag{4.4}$$

The importance of this result is two-folds. First of all, the sojourn or the total time a x-sized job has to wait is linear with x. This means shorter jobs are not lengthened by longer jobs, which makes the PS discipline fair in a narrow meaning of the word. Secondly, it was later shown that Equation (4.4) is valid for arbitrary job size distributions, as long as $\rho = \lambda E[S]$, where $E[S]$ is the first moment of the size distribution S. This is the celebrated insensitivity result of PS, the conditional sojourn time is only linked to the mean service size, not on its distribution.

The fact that there are abrupt changes in the service rates with the arrival and departure of jobs makes the analysis of the number of the jobs in the system slightly more complicated. The number of jobs in a system depends on the remaining service times of all the jobs in the system at the time of the arrival of a new job. It was not until 1979, that it was shown by Kitayev in [29] that the number of jobs in a M/M/1 PS queue has the same distribution as a M/M/1 FCFS queue. The actual distribution, rather than the mean as given in Equation (4.4), of the sojourn time was first given by Coffman in [30]. Ott extended this result, and gave the distribution of sojourn time conditioned on the number of jobs upon the arrival of a new job for an arbitrary job distribution size in [31]. The queueing properties of PS abstraction and the application of it to real world problems is an active research field. An excellent survey on this topic is given by Yaskhov in [32].

4.3. Wireless Local Area Networks

4.3.1. Overview of 802.11 MAC

Wireless Local Area Networks (WLAN), based on the IEEE 802.11 family of standards, have been experiencing rapid growth since the introduction of the standards. The standards have paved the way to a sustainable technological ecosystem, in which standard conforming equipment are able to function together, and bring the forces of the economies of scale in action. Through these forces the 802.11 based user and network equipment are available to the general public for affordable prices. It may be argued that the success of the 802.11 standard is a result of its simplicity, especially as seen from the network side. It adopts the standard 802 logical layer protocol, and a best effort multiple access (MAC) layer based on the well-known carrier sense multiple (CSMA) access with col-

	Transmission	Operating Frequency	Physical Layer Rate
802.11a	OFDM	5 GHz	54 Mbps
802.11b	DSSS	2.4 GHz	11 Mbps
802.11g	OFDM	2.4 GHz	54 Mbps

Table 4.1.: Normal form representation of the first level game.

lision avoidance (CA) , while providing optimized physical layer techniques which are completely transparent to the network and user side. However, the very fact that the legacy 802.11, i.e. 802.11a, b and g, support a best effort MAC which led to its success is also its main weakness. The lack of QoS support in the forms of service differentiation or resource reservation prohibits the usage of WLAN's for real-time and mission critical applications, and necessitates changes or variations to the original standards and investment on devices that support the improved standards. However there is a economical incentive for the network operators to undertake such investments, as QoS support in WLANs allows segmenting market and allowing charging premium to real-time or mission critical applications.

With legacy 802.11 we mean the family of standards 802.11a, 802.11b, 802.11g which share identical MAC properties but differ in the physical layer. The different properties of legacy WLAN standards are summarized in Table 4.1.

The mobile stations running 802.11 protocols can support two types of basic service sets (BSS), the infrastructure and independent BSSs. In independent BSS, also known as the ad-hoc mode, two or more 802.11 supporting mobile stations communicate with each other directly. In infrastructure the mobile stations communicate with an access point (AP), which then is connected to an infrastructure network. Furthermore more then one AP can be connected to offer what is referred as extended BSS. Our survey will concentrate on the infrastructure BSS.

There are two MAC protocols defined in legacy 802.11, the distributed coordination function (DCF) and point coordination function (PCF). We will summarize these in detail, as they are the fundamental mechanisms on which the extensions built up upon. We summarize the important parameters used in 802.11 MAC before going in to detail.

DCF Interframe Space (DIFS) Duration that the medium should be free in DCF before a MAC entity can start a random back-off.

Short Interframe Space (SIFS) Duration that the medium should be free before RTS, CTS, Data, and ACK packets can be sent.

PCF Interframe Space (PIFS) Duration that the medium should be free in PCF before a MAC entity can start a random back-off.

Contention Period Period defined in PCF during which mobile stations contend for channel access.

Target Beacon Transmit Time Planned absolute time in terms of slots when the AP transmits a new beacon.

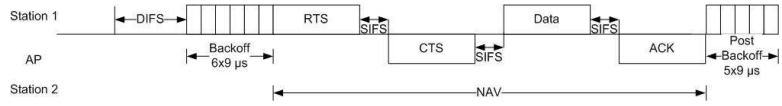

Figure 4.1.: 802.11 DCF timing.

Network Allocation Vector Time when a station cannot transmit when RTS/CTS is used.

Distributed Coordination Function

The basic 802.11 MAC protocol DCF is a CSMA/CA type of MAC scheme. The stations are able to determine if the medium is free or not. After listening the medium for a predetermined period of time (DIFS) and assuring it is free, each station initiates what is called a random backoff procedure, which is choosing a random integer between 0 and contention window (CW). The station can only start transmitting if the channel remains idle for another CW times slot time, which is 9 microseconds in 802.11a and changes from standard to standard. In the case when the channel is occupied by another mobile station or the AP during the backoff period the backoff timer is saved. When the mobile station starts the next backoff procedure, instead of generating a new random integer, it uses this saved value.

The transmission of data can optionally be protected from the interference of exposed or hidden nodes by using request to send (RTS) and clear to send (CTS) messages. The sending station or AP transmits RTS indicating its wish to send data, to which the receiving station replies with a CTS. Both of these messages contain information on how long the data and corresponding acknowledgement frames will occupy the channel. The stations in the range of the communicating parties set their network allocation timers, according to the information contained in RTS/CTS frames, and retain from sending any data or control frame during the specified time. The data can then be sent either in fragmented form, or in complete form which are acknowledged by the receiving station. After each successful data frame transmission the value is set to a global parameter CWmin, which is broadcasted by the AP, and after each failure the value of CW is doubled, up to a system-wide limit CWmax. RTS, CTS, data and acknowledgement frames are separated by a SIFS, which is shorter than DIFS, which keeps other stations from transmitting. Finally after the data transmission is completed, another backoff procedure is initiated which is named the post-backoff. Post-backoff assures there is at least one backoff procedure between transmissions. The procedure is demonstrated in Figure 4.1.

The only parameter which would allow differentiation of channel allocation probabilities in legacy 802.11 DCF is CWmin, the smaller its value, the more possible it is for a mobile station to get the channel access, as on the average it would have to wait (CWmin x Slot Time)/2 seconds to access the channel. In DCF all the mobile stations use the same value of CWminand therefore cannot be separately treated. This is the main reason why there is no QoS support in terms of service differentiation inlegacy

WLAN MAC protocol. Furthermore due to the probabilistic nature of the MAC protocol, and there is no control on how long a mobile station can occupy -there is only a maximum limit- guarantees cannot be given on QoS defining parameters such as jitter and delay for real-time applications.

Point Coordination Function

Point coordination function (PCF) attempts to introduce prioritization to 802.11 MAC. This is achieved by introducing a central component that coordinates the medium access known as the point coordinator (PC), which usually is the AP. The resilience of DCF is traded of for a central architecture, with a single point of failure, for the sake of providing prioritized access.

In PCF, PC is responsible for transmitting beacon frames in regular intervals, in which synchronization and other protocol specific information are carried. One such information is TBTT, which is the time when the next beacon is scheduled. Note that this is the target time, and the fact that it cannot be met under certain circumstances is the main shortcoming of PCF, as we will see shortly. Each beacon starts a period of two alternating MAC regimes, the contention period (CP) and the contention free period (CFP). In CP, normal DCF is employed. The PC must schedule at least one CP. In CFP, whose duration is set by the PC, the PC polls the individual stations. Data is piggybacked to polling request and response frames. CFP ends with a special CF-End Frame.

The main problem with PCF is tied to the fact that PCF has no control over the amount of time the mobile stations can occupy the medium. This means that the last polled station may occupy the channel beyond the previously scheduled TBTT, which would mean that the next CFP is spoiled. Therefore it is not possible to give guarantees on delay or bandwidth with PCF. Furthermore, it is highly unlikely that PCF can operate without degrading the performance of mobile stations employing DCF only. Lastly, PCF is suboptimal in terms of bandwidth utilization as the stations which possess data to send must wait to be polled, during when stations without data might be being polled. Due to this inadequacies PCF has not gained popularity in the research community, which has gone in the direction of extending DCF with service differentiation, and admission control and bandwidth reservation via Layer 3 protocols such as DiffServ[33] and IntServ[34]. An alternative approach has been providing a service differentiation in the MAC layer which we discuss in the next section.

802.11e

The aforementioned weaknesses in 802.11 MAC lead to the standard makers to concentrate their efforts on modifying the 802.11 MAC, without fundamental changes to the standard itself, which resulted in the 802.11e amendment.

The main improvements to the legacy MAC of the 802.11 MAC can be summarized as:

- The introduction of transmission opportunity (TXOP), which sets an upper bound to the duration which a mobile station can occupy the medium.
- The stations are not allowed to start transmission if their TXOP runs beyond the next TBTT, these two properties make it possible to give time based guarantees.
- The mobile stations in range can exchange data among each other, after executing direct link protocol. This may be seen as an hybrid mode between infrastructure and independent BSS's.

802.11e defines the hybrid control function (HCF), which is a mixture of PCF and DCF. Just like in the PCF a superframe between beacon frames is divided into a contention based channel access period and, contention free, controlled channel access periods. Enhanced distributed channel access (EDCA) is an extension of DCF and is used only during the contention based channel access. During both the controlled channel access and contention based channel access period the HCF controlled channel access (HCCA) can be employed. 802.11 also introduces the concept of a QOS supporting BSS (QBSS) which is composed of a hybrid coordinator (HC), which is usually the AP, and mobile stations running an implementation of 802.11e standard.

In the core of EDCA lies the introduction of 4 access categories (AC), namely voice, video, best effort and background. Each of these AC's is represented by 4 backoff entities running on the same mobile station which contend with each other for a TXOP. These backoff entities run a similar backoff algorithm as defined in the legacy 802.11, with the only difference being the ability of HC to adjust certain parameters of the backoff algorithm that the backoff entities of individual ACs are running. These parameters are:

- Arbitration interframe space (AIFS): This replaces DCF defined in legacy 802.11. Smaller the value of AIFS, the higher the possibility of an individual AC gaining a TXOP.
- CWmin, CWmax: By lowering the contention window maximum and minimum sizes one can increase the probability of a certain backoff entity obtaining a channel access. However this increases the possibility of frame errors, as collisions become more often occurring.
- TXOPlimit: By changing the maximum duration a AC can hold the medium, one can adjust the amount of capacity allocated to that AC.

It is worth mentioning that each back-off entity of a certain AC on every mobile station of a QBSS has the exact same backoff algorithm parameters above. Also within an mobile station if a collision occurs between different backoff entities of different AC's the access is priotorized according to the priority of voice, video, best effort and background. During contention based channel access the backoff entities access the channel according to EDCA.

HCCA allows the HC having the highest priority, when it comes to accessing the shared medium. This is achieved by setting PCF, which is the amount of time the HC

should observe the channel to be free, before it can transmit, to be smaller than AIFS. With this condition it can obtain a TXOP to itself anytime it needs, both in contention based channel access period, and controlled channel access period. It can use this TXOP to deliver downlink data to a certain mobile station, or to directly poll a mobile station.

In contention based period the TXOP obtained by the HC can be delayed by max-ACTXOPlimit at most. By contending for a TXOP maxACTXOPlimit earlier then required, HC can poll and therefore give time guarantees to certain flows even in the contention based period. In contolled channel access period, the backoff entities only transmit as answer to polling HC, and there fore HC is in complete control over the time aspects of channel accesses of different mobile stations.

As described above EDCA and HCCA combine the best aspects of PCF and DCF, and allows service differentiation and time guarantees while not degrading the performance of contention based channel access. However there are two main shortcomings of 802.11e as described in [35]. First of all service differentiation does not scale well, and perform badly under high network load. Secondly when two or QBSS working on the same frequency channel interfere with each other, the performance degrades substantially. However 802.11e has been commercially more successful than the previous PCF attempt. Currently 802.11e compliant hardware is being sold under the WiFi-Multimedia label given by the WiFi consortium industry alliance.

We conclude that 802.11 family of protocols lack a strict QoS capability. The best approach to guaranteeing users quality is to keep the utilization of the access point low. This can be done with pricing, Call Admission Control or load balancing.

4.3.2. Theoretical Analysis of 802.11 MAC

One of the pioneering works of the the formal theoretical analysis of 802.11 MAC layer performance is due to Bianchi [36]. This influential work was simplified and generalized by Kumar et. al. in [37].

This strand of analysis aims at finding the aggregated throughput of the 802.11 MAC layer when there are n nodes using the layer. There can be data flow between any two nodes in the system, thus the analysis is valid for both ad-hoc and infrastructure modes. They make the *saturation assumption*, which means that the nodes always have a packet to transmit when they get the chance to transmit. In a real life scenario the throughput obtained with this assumption sets an upper bound to the traffic arrivals at each node. If the traffic arrivals are less than the saturation throughput, the node queues remain stable.

The analysis depends on the key observation that for the throughput performance analysis, the modeling of the back-off process is sufficient. It is enough to compare the event flows in the cases of a successful attempt and a collision given in Table 4.2.

What can be observed from the the events is the following. MAC protocol swing between a deterministic and stochastic part. The time intervals in which transmissions occur and the time intervals after collisions when no transmission occurs are deterministic. The time between attempts, which can be successful or result in a collision, is the stochastic component. This component is completely described by the evolution of the

Success	**Collision**
A single node's back-off timer timeouts	More than one nodes' back-off timers timeout
Transmitter Send a RTS	Wait for an amount of time equal to RTS transmission
Non-transmitting nodes freeze back-off timers	All nodes freeze back-off timers
Recipient Sends CTS	All nodes wait for a fixed amount of time
Data Transmission	All nodes resume their timers
ACK Transmission	-
Transmitting node restarts back-off timer, the others resume their timers	-

Table 4.2.: Flow of MAC events.

back-off process in the individual nodes. Since the back-off counters are frozen during the deterministic periods, it is sufficient to study the aggregated back-off process.

The value of the back-off counter is dependent on the number of retransmissions already suffered due to the exponential back-off employed in the MAC protocol. Therefore the back-off process is not inherently Markovian. Bianchi introduces the *decoupling approximation* that transforms the process into a Markovian process, for which he develops a DTMC. The decoupling approximation is defined as [36]:

> [**Decoupling approximation**] is the assumption of constant and independent collision probability of a packet transmitted by each station regardless of the number of retransmissions already suffered.

The approximation results are more accurate when the contention window size is large. The approximation has been shown to be accurate with the help of simulations. With the further is assumption that the nodes have the same back-off parameters, the nodes time out the back-off timers with the same rate, and thus attempt to access the channel with an equal probability. This rate is termed the attempt rate β, and is the key parameter in this strand of analytical performance evaluation.

The attempt probability is not equal to the probability of successfully accessing the channel. This is because multiple nodes try to access the channel independently with the rate β and experience collisions as a result. The collision probability γ is thus a function of the attempt probability β. On the other hand, the attempt rate is also a function of the collision probability, since the nodes make more attempts to transmit a packet when there are more collisions. Fixed point analysis uses this exact dual relation between the two rates to calculate the β and γ. Specifically, attempt rate is a β is a function of collision probability γ, i.e. $\beta = G(\gamma)$. Similarly the collision probability is dependent on

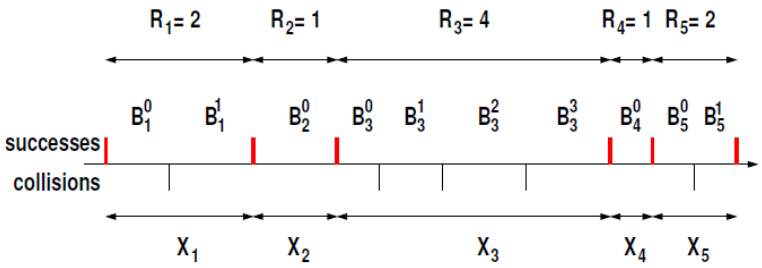

Figure 4.2.: Back-off process from [37].

the rate which the nodes are attempting to transmit, i.e. $\gamma = \Gamma(\beta)$. Composing these two relations gives $\beta = G(\Gamma(\beta))$, which is a fixed point equation. By the well know Brouwer's fixed point theorem, the equation always have a solution. Using the attempt rate one can calculate the aggregate throughput.

Whereas Bianchi solves a two dimensional DTMC modeling the back-off process and uses the state probabilities, Kumar use the reward-renewal theorem [38] to calculate the throughput without solving the DTMC in [37]. They work with the stochastic back-off process is depicted in Figure 4.2 .X_k is the total back-off time for k-th packet, and the R_k is the number of attempts required for the same packet. B_k^j is the length of j-th attempt, and is characterized by the parameters in the 802.21 standard. Attempt rate can be calculated by treating X_k as a renewal process, and R_k as the associated reward process, $\beta = E[R]/E[X]$. Both the expected length of back-offs, $E[X]$, and the expected number of attempts $E[R]$ are polynomials in γ and allows us to calculate $G(\gamma)$:

$$\beta = G(\gamma) = \frac{P(\gamma)}{Q(\gamma)} \tag{4.5}$$

Similarly the collision probability is equivalent to the probability that at least one of $(n-1)$ stations attempt a transmission. With the help of the decoupling assumption, the aggregated attempt process is Bernoulli with parameter γ. With this information one can calculate γ as one minus the probability that $(n-1)$ nodes do not transmit simultaneously:

$$\gamma = \Gamma(\beta) = 1 - (1-\beta) \tag{4.6}$$

Solving (4.5) and (4.6) together numerically, one can obtain β and γ values. This is depicted graphically in Figure 4.3. The intersection of $\Gamma(G(\gamma))$ functions plotted for increasing number of nodes with the line γ gives the collision rate achieved. One can observe that collision rate increases with the number of nodes.

Once the attempt rate is calculated, the calculation of overall throughput is simpler. The analysis relies on the fact that all the nodes have the same probability of winning the allocation race, since they run the back-off process with the same parameters. To calculate the system throughput, the same renewal process used to calculate attempt and collision rates is expanded with the deterministic time intervals spent after collisions

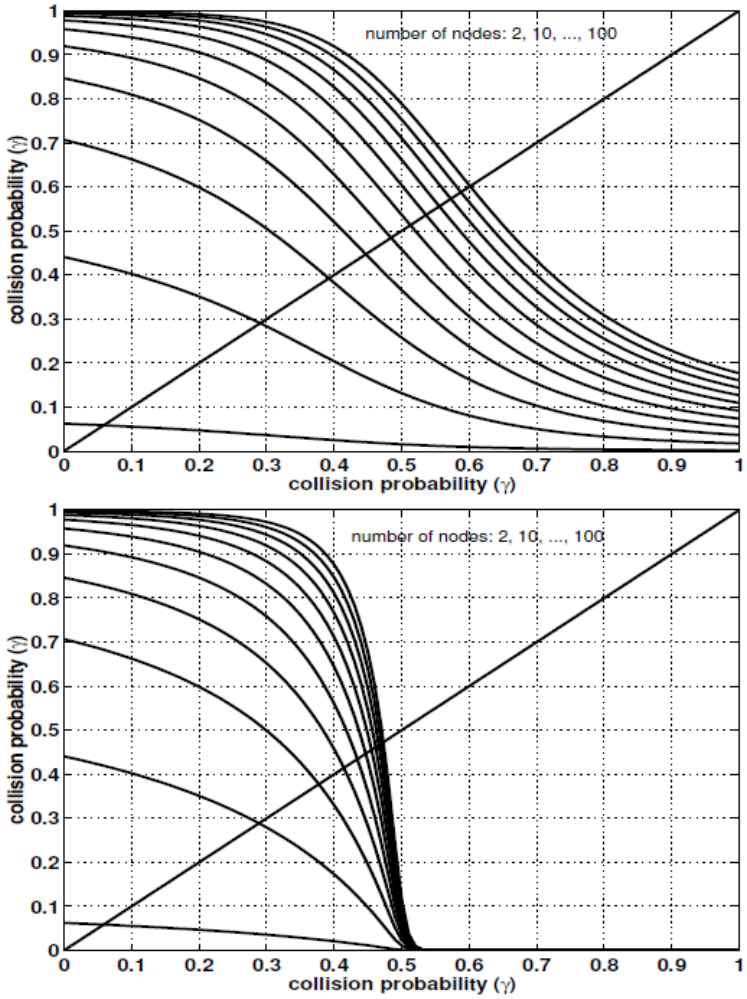

Figure 4.3.: Collision probabilities from [37].

and transmissions. These deterministic time intervals happen with probabilities that are functions of the attempt and collision rates. The reward is taken as the number of bits that are transmitted during a renewal interval, and is a function of the average packet size. Average aggregated throughput is again calculated using the renewal-reward theorem, which is plotted against increasing number of users and compared to simulations in Figure 4.4. It is important to note that the analysis is valid for UDP-like open loop data exchanges. When the stations use the same back-off parameters, the total system throughput is shared equally between the stations.

4.3.3. PS Models for WLAN

Both Kumar and Bianchi's analysis are for situations in which the number of active sessions are fixed. Making use of the results of these important papers authors have

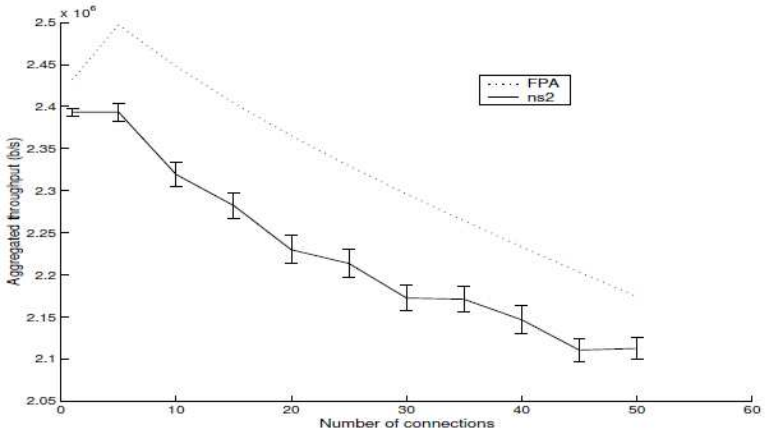

Figure 4.4.: Aggregated throughput from [37].

extended the analysis of 802.11 DCF to account for non-saturation situations, varying number of active stations and TCP type of traffic. We shortly review the important results.

Miorandi et. al. consider asymmetric HTTP traffic over an infrastructure 802.11 network in [39]. They are interested in the interaction between the 802.11 MAC and the TCP congestion control mechanism. The authors begin their analysis with a single persistent TCP session. They calculate the collision probability with a fixed point analysis similar to Kumar's. This probability is used to calculate the average time spent in back-off and collisions by this single session when it has back-logged packets. The packet size divided by the total average time between two successive packet transmissions give the average TCP throughput. In order to extend their analysis to n concurrent persistent TCP sessions the authors make the assumption that the probability that an user station has a backlogged packets to send is equal to the same probability for AP, which is 0.5. This assumption is validated by comparing the analytical results to simulations. With this assumption the authors calculate the probability distribution of number of end user stations which have backlogged packets to send. This probability distribution is finally used to calculate the expected aggregate throughput, which is a function of the number of backlogged stations and the packet lengths.

The average aggregated TCP throughput is given in Figure 4.5. It is worth noting that the aggregated throughput stays the within a narrow band around 2.4 Mbps . This aggregate bandwidth is shared equally among the individual TCP connections if same advertised TCP window size is used among all the connections in addition to the same back-off parameters. The authors use this property to derive a queueing model for the TCP traffic over 802.11 based WLANs. Specifically, they propose a processor sharing model with state dependent service rates. When there are k connections in the system, each connection is served with the rate $\mu_k = \frac{C(k)}{k}$ where the state dependent capacity $C(k)$ is simply the aggregated TCP throughput given in Figure 4.5. Notice that if one takes the average value of aggregated throughput to be constant over k this model

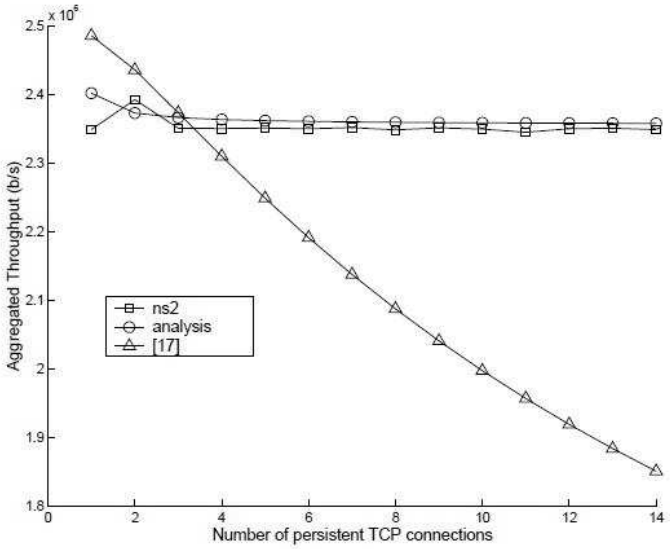

Figure 4.5.: Aggregated TCP throughput vs. number of stations from [39].

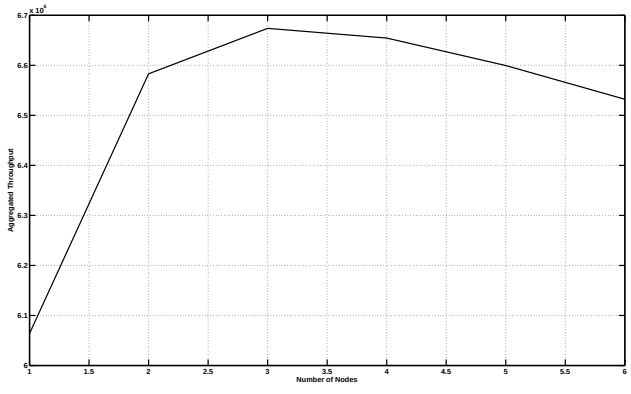

Figure 4.6.: Average Delay versus number of nodes for state independent and dependent capacity models.

reduces to a traditional processor sharing queue.

Litjens was among the first researchers to take processor sharing modeling that Miorandi demonstrated for TCP traffic to shorter timescales. In other words, he demonstrated that a state dependent capacity processor sharing models can be applied in MAC layer packet timescales. He uses the aggregated MAC layer throughput as a function of active stations calculated via Bianchi's fixed point analysis as the state dependent capacity in his thesis [40].

Medepalli et. al. expand Bianchi's fixed point analysis to include non-saturated nodes in [41]. Their analysis includes the average idle time that a non-saturated node spends

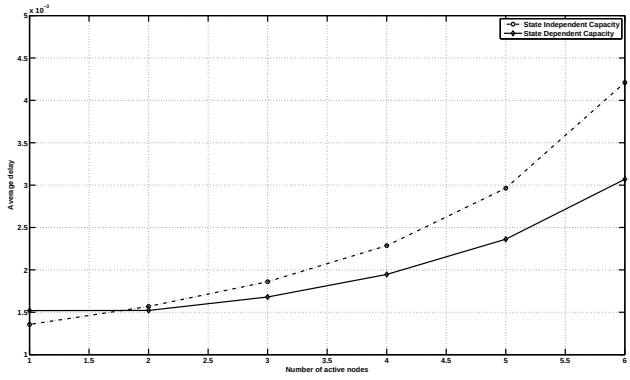

Figure 4.7.: Average Delay versus number of nodes for state independent and dependent capacity models.

when it doesn't have a packets to send to the average regeneration time in the reward-renewal analysis used to calculate the attempt rate β. This idle time is function of two parameters. First is the the probability that a node has a packet send and it is equal to $\rho_s = \lambda/\mu_s$. In this expression λ represents the rate with which the packets are generated and $1/\mu_s$ is the average service time of the 802.11 MAC. This ratio is equivalent to the time in which a central server of average service rate μ_s is busy with a single node. This service rate itself is a function of the collision rate γ. The second variable is the average delay a packet experiences, D_T, which is again a function of the average service rate, which is a function of the collision rate. Authors propose calculating this delay by using a state dependent processor sharing model with average rate μ_s similar to Litjens. By using the closed form expressions for the delay one is able to calculate attempt rate as a function of the collision rate $\alpha = \Gamma(\gamma)$. Similar to Kumar, they use the relation between the attempt rate and collision rate, i.e. $\gamma = 1-(1-\alpha)^{(N-1)}$, to solve for γ and α via fixed point analysis. The result of the analysis gives the aggregated throughput, again shared equally among the nodes, depicted in Figure 4.6 . What we observe is that the overall throughput increases slightly with the increasing number of users, only to stabilize at the saturation value of 6.5 Mbps. The average delay values for increasing number of users are plotted for two different processor sharing models in Figure 4.7. In one model we used state dependent capacities calculated with the fixed point analysis, and in the other one we use a fixes capacity equal to the saturation value. The approximate fixed capacity model estimates the delay only slightly lower than the state dependent model for the initial two values. For the rest the approximate delay values are more conservative than the state dependent capacity model. This is due to the interesting phenomenon of overlapping back-off processes across the nodes as the number of nodes increase. This results on the performance being slightly better than a traditional processor sharing, in which the degradation in service rate is strictly monotonic.

Another important research direction was opened by Bruno et. al. in [42]. In this work the authors investigate the situation when N 802.11 stations are connected to

a AP and are making bulk TCP downloads similar to Miorandi. Since 802.11 DCF doesn't distinguish between the AP and the stations, it is assumed that most of the data packets are queued in the AP, while the stations always have a single ACK to send. The authors use an alternative iterative approach to solve for system and node throughput with a modified back-off mechanism called *p-persistent back-off*. In this alternative MAC mechanism the back-off interval length is sampled from a geometric distribution of parameter p. Kuriakose et. al. extended the same model to work with standard DCF in [43] by making use of the attempt rates obtained via Bianchi's fixed point analysis. Their results are also identical to Miorandi's, that is the system throughput stays almost the same as the number of active stations increase and that this system throughput is shared equally among the active stations.

Finally, Ferragut and Paganini extended the processor sharing approach to analytical modeling of TCP over 802.11 DCF to the case when there are stations with different data transfer rates in [44]. The 802.11 standard allows increasing data rates to be applied with decreasing distance between nodes. Their analysis is split into two, in which they investigate downlink and uplink traffic separately. This separation is not to be understood from a physical perspective, since the 802.11 MAC layer does not distinguish between packets from AP to the stations, i.e. the downlink packets, and the packets from the stations to the AP, i.e. the uplink packets. Rather, the authors name the scenario discussed by Miorandi and Bruno, where the majority of packets are from the AP to the stations as the downlink scenario.

For the downlink scenario they derive the aggregated throughput assuming that the collisions are negligible. In such an environment the delay a packet experiences is only due to the AP choosing a random interval between zero and minimum collision window size for back-off for each packet. The authors derive connection level rates for each physical rate possible in 802.11 standard (there are seven of them ranging from 54 Mbps to 6 Mbps). They also show that the connection level throughput achieved by each node is equivalent to a Differential Processor Sharing queue (DPS) . Specifically, if the nodes whose physical rate is R_j achieve a connection level rate of C_j, where $j = 1, 2, ...7$ and there are n_j nodes in each physical rate class the rate achieved by all of the individual nodes is given by:

$$r(n_1, ...n_7) = \frac{1}{\sum_{j=1}^{7} \frac{n_j}{C_j}} \tag{4.7}$$

Equation (4.7) reduces to a traditional processor sharing queue when there is a single rate in the system. An important result of this analysis is the fact that the rate achieved by the nodes is independent of their physical rates. The rate is determined by the slowest node in the system. This means increasing the transmission rate above the slowest rate in the system does not bring any performance improvements. This counter-intuitive result can be explained easily by remembering that all the faster nodes should wait for the slower node's transmission to finish. This property makes application of multiple rates within an infrastructure WLAN served by a single AP problematic, since increasing

the rate does not bring any throughput benefits. It is much more sensible to employ a single rate, in which the analysis of Ferragut and Paganini is equivalent to a traditional processor sharing queue as noted earlier.

We can conclude that a load dependent capacity PS model is appropriate describing the TCP performance over 802.11 MAC. However, the load dependency is not very drastic. A constant capacity PS model will only result in a model that is more conservative delay estimate, which is not necessarily a drawback.

4.4. 3Gpp Family

4.4.1. QoS Support in UMTS

It is the key goal of 2.5G and 3G systems to increase the data throughput capabilities for both the individual user and the network. In 2.5G such as Universal Mobile Telecommunications System (UMTS), which incorporates wideband CDMA for the radio interface and GSM/GPRS for the network architecture, the goal of the increased capacity is to efficiently provide wireless Internet services. In order to maintain an acceptable user experience without sacrificing network capacity, wireless network designers and operators must incorporate the means to manage quality of service (QoS).

QoS provisioning in UMTS is achieved through the concept of *bearers*. A bearer is a service providing a particular QoS level between two defined points invoking appropriate schemes for either the creation of QoS guaranteed circuits or enforcement of special QoS treatments for specific packets between two nodes on the end to end path. The radio bearer is between the user equipment and the base station. The so called *IuB* bearer is between the base station and the RNC controller in running on the backbone. Each UMTS bearer is characterized by a number of quality and performance factors. One of the most important factors is, bearer's traffic class. Following four different classes have been proposed in the scope of UMTS framework:

- Conversational (e.g. voice, video conferencing): Delay is much less than 1 second
- Interactive (e.g. web browsing, gaming): Delay can be around 1 second
- Streaming (e.g. video streaming): Delay is less than 10 seconds
- Background (e.g. background email download): Delay can be greater than 10 seconds.

In UMTS, in order to provide end to end QoS to the users, the network elements on the path should set up the required bearers, providing the required QoS parameters on the respective bearers. This means a connection establishment phase before the actual communication is required. This connection setup involves the exchange of so called UMTS attributes for individual calls. UMTS attributes serve to map the end-to-end QoS requirements to appropriate requirements for each bearer service used by a connection. The QoS parameters are transported from the terminal to the UMTS

network in various *PDP context messages*. If the requested QoS by the user terminal match the users subscription profiles, the nodes on the path are instructed to set up the bearers with QoS properties matching the user request. At the wired part of the UMTS network, QoS max be provisioned by overprovisioning, DiffServ, IntServ, or setting up MPLS tunnels for the calls. On the radio access part, the base station controller sets up an individual radio access bearer for the terminal, which is equivalent to allocating the user a WCDMA code. After the code is established, the user has an end to end channel that provides the required QoS for the duration of the session. configure the radio access bearer. If the QoS is granted, the radio bearer is set up. If for some reason the radio bearer cannot be set up due to the resource restriction in the cell, the user is notified that the request is not granted. The user may then initiate a new session set up with new QoS requirements.

There are two main shortcomings of the described approach. First of all, even thought suited for a voice like services that demand a constant bit rate, the reservation scheme is not efficient for bursty traffic that dominates the next generation applications. Secondly, the service differentiation or prioritization applied do not consider fairness between different service classes. There is always the possibility of lower priority classes starving out of bandwidth in case of congestion. These concerns have led the 3GPP to consider a new MAC approach at least at the radio bearer, which has led to the development of a new access technology called High Speed Packet Access (HSPA) which we summarize in the next section.

4.4.2. QoS Support in HSDPA/HSPA

High Speed Packet Access can be considered as a 3.5G technology. Even though it makes radical changes in the physical layer and the MAC layer, the changes do not go as far as changing the multi access type, say for example like the change from TDMA to CDMA in going from GSM to CDMA. The multiple access scheme is still CDMA. There is an ongoing standardization effort for the next generation standards, which will replace CDMA with OFDMA under the name Long Term Evolution (LTE). For technical and financial reasons it is deployed in two steps. First the techniques we will summarize below are employed on the downlink only, when HSPA is called High Speed Download Packet Access (HSDPA).

The primary change in the physical layer is the adoption of *Adaptive Modulation and Coding* (AMC). A cornerstone of W-CDMA based UMTS is the dynamic power adaptation loop used to keep the received power levels from different users same at the base station. In order to achieve this, a closed loop power control is implemented between the user terminals and the base station to adjust the transmission power with respect to the physical distance between the base station and the terminal. Radio Frequency hardware that is able to adjust the power level dynamically are more expensive and have a shorter lifetime compared to hardware optimized for a constant power level transmission. Instead of increasing the power level for terminals which are either away from or which are experiencing multi-path fading, the base station automatically adapts the modulation type and coding strength to match the quality offered by the radio

channel. To facilitate this, users send a quantized version of the signal ti interference and noise ratio to the base station as Channel Quality Indicator (CQI) messages. The base station chooses from a set of standard Transport Format Combinations (TFC) , which is a combination of modulation type, number of W-CDMA codes and the Coding Rate. For the next transmission between base station and the user terminal the matching Transfer Block Size (TBS) , which is the number of information bits corresponding to a certain TFC, is used.

The most important conceptual change from the dedicated channels used for each session in UMTS to HSDPA is the introduction of the HS-DSCH (High Speed Downlink Shared Channel) to the base station. The operators are free to reserve some of their allocated frequency to be used as a shared channel that the users and base station access jointly. This also means that the the number of HS-DSCH is deployed along legacy Dedicated Channels (DCH) used to transmit voice and other applications that require dedicated channels. The number of channels and the power budget allocated to HS-DSCH is a function of the capacity allocated to the legacy DCH channels. This allocations can be static, or can vary according to the current voice traffic in the cell.

The notion of a shared channel is reminiscent of the 802.11. Instead of the distributed CSMA-CA protocol that regulates the access to the shared medium in 802.11, the base station is responsible for scheduling the transmission from and to each active user terminal. In fact this can be seen as conceptually equivalent to the PCF described in 4.3.1. Unlike PCF, in which there are both contention free and contention periods, in HSDPA there are no contention periods. Base station scheduler is responsible for selecting the user terminal that will have access to the shared channel in the next Transport Time Interval (TTI) , according to the scheduling algorithm it implements. During the TTI, the scheduled user sole access to the shared channel.

Similar to the 802.11 standard, 3GPP standards do not enforce a particular scheduling algorithm to foster innovation. As a result, the choice of the scheduling algorithm has important results on the system and user level performance. There are many scheduling algorithms proposed in the literature. Scheduling algorithms can be channel blind, meaning that they do not use the CQI reports from the users to make the decisions. A very basic RR is an example of such an algorithm. The channel aware algorithms make use of the channel quality reports to take decisions. The MaxTBS, which is also known as the Greedy Algorithm, chooses the user with the best transmission quality. The greedy algorithm brings with it the danger of users, which are close to the base station and having a better channel quality draining all the resources of the base station. The Proportional Fair Scheduler (PF) is a remedy for this problem. The algorithm keeps a track of the average throughput achieved by the users within a certain time window. It then chooses the user with the lowest average throughput to access the channel. This increases the average throughput of that particular user until the next TTI decision, which avoids this particular user draining the resources. As the name suggests, the PF scheduler is more fair compared to RR and MaxTBS regimes. A more detailed analysis of the HSDPA architecture is given by Mäder in [45], along with a comparasion of the performances of different scheduling regimes in [46].

4.4.3. PS Models for 3Gpp Family

Cite Litjens was the first author to apply processor sharing abstraction to 3GPP family of radio access technologies [40]. He was concerned with the throughput characteristics of data traffic running on GPRS networks.

In [47] Pederson et. al. obtained simulative results on the network layer average cell throughput in a cell that simultaneously serves dedicated channels and HSDPA channels. When five codes and a constant power level (7W) are allocated to the HSDPA channels, the total throughput of the cell is 1320 KbpsKilobits per second, 900 Kbps of which is transmitted over HSDPA channels. The authors use a web-browsing type of TCP traffic model on the HSDPA channels with Poisson arrivals and lognormal request sizes. They also report that a increase in the average number of users by a factor of three decreases the per user throughput by a factor smaller than three. This is due to the multiuser detection gains made possible by the HSDPA protocols.

Processor sharing abstraction was used for 3G family of wireless access technologies by Borst in [48] for modeling the user level delay and system throughput in CDMA 1xEV-DO system. CDMA 1xEV-DO is the set of standards developed by the North American focused 3GPP2 consortium that is comparable to the HSDPA standards. Borst deals with a set of users, whose data rates vary according to stationary and ergodic stochastic processes $\{R_1(t), ..., R_M(t)\}$. This is a salient feature of all the evolutionary extensions of 3GPP and 3GPP2 family of standards, which employ adaptive modulation and coding to modify the data rate to match the channel conditions. It is assumed that all of the rates vary around their long term averages $C_i = E[R_i(t)]$ according to identical distributions. Borst examines the time average rate seen by users of a base station that employs a weight based scheduling under identical distributions. In the weight based scheduling scheme, at a given time slot t, the channel is assigned to the user with the maximum $\alpha_i \cdot R_i(t)$ value, where α_i is the weight of the user i. It is shown, if the weights of the users are chosen to be the inverse of their average rates, i.e. $\alpha_i = \frac{1}{C_i}$, the scheduler behaves as a processor sharing system, in that the M users experience the time average rate of $\frac{G(M)}{M}$. Furthermore, it is argued that the Proportional Fair(PF) Scheduling implemented in CDMA 1xEV-DO roughly behaves like a weighted scheduler. Under Poisson arrivals of file transfer requests, the system behaves like a processor sharing queue. If the variance of rates around their means are nor statistically identical, a discriminatory processor sharing abstraction can be applied. However, this version of PS abstraction is yet mostly intractable, and a detailed model is not possible. Wu presents a similar analysis in [49].

Another important and related result on the PS models for data networks is given again by Borst in [50]. This paper is concerned with the sojourn time distributions of two classes of data traffic running over a network that can be abstracted by a processor sharing model. The important result is a variant of *reduced load equivalence* established for other queueing systems in the literature. Assuming two classes have a normalized average rate of ψ_1 and ψ_2, the sojourn time distribution of class 1 is equivalent to a constant rate processor sharing queue with a capacity $1 - \psi_2$. The sojourn time distribution of class 2 is similarly equivalent to a system with the capacity $1 - \psi_1$. This result is very important, since the performance of a certain class is affected only via

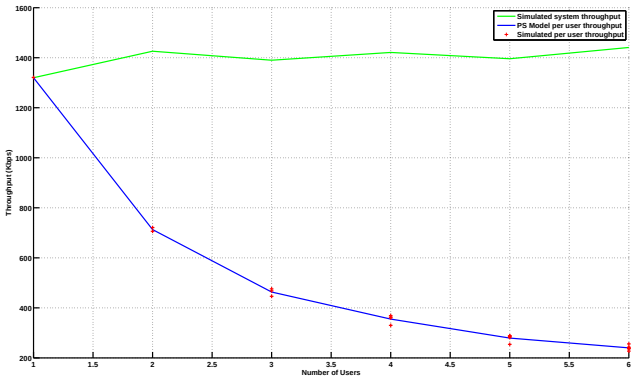

Figure 4.8.: System and per users throughput in a HSDPA cell.

the average rate of the other class, but not with the actual distribution or the higher moments. This relation can be used to model HSDPA with a processor sharing model, even when the HS-DSCH is implemented along with DCH, and the capacity of the HS-DSCH is adjusted dynamically according to the DCH load. Without the need to of the actual distribution of the voice traffic, an equivalent HSDPA capacity can be calculated by subtracting the average DCH load.

Fitzpatrick and Ivanovich apply this approach to a generalized beyond 3G network, which includes LTE and WiMAX standards in [51].

The Engineering Services Group of Qualcomm presents the results of a simulative analysis of HSDPA cell in [52]. The results of simulative per user and system throughput is depicted in Figure 4.8. It can be seen in the Figure, that the simulative per user results are very close to what a processor sharing model, such as the one proposed by Borst in [48]. Furthermore, it can be observed that the average system throughput varies slightly around 1.4 Mbps .

Van den Berg, Litjens and Laverman extend the processor sharing abstraction to SNR-Based scheduling. In this scheme a greedy approach is applied, and at every transmission interval, the channel is allocated to the user with the best channel condition, as it is inferred from the CQI reported from the user devices. It is shown that PF and SNR-based scheduling outperforms Round Robin (RR) in terms of delay and throughput metrics. SNR-based performs slightly better than PF, with the disadvantage of being not fair to users far away from the base station. Finally, Kouvastos has modeled the performance analysis of hypothetical 4G base stations accommodating different services [53] and [54] with the help of PS abstraction. A hypothetical 4G cell is modeled as a combination of three service centers. Voice calls are handled by a classical Erlang loss system, the data calls are handled by a PS (Processor Sharing) system and finally streaming calls are handled by a FCFS (First Come First Serve) system. It must be noted that since the proposed LTE standard employs a similar scheduler based shared channel for data calls, a processor sharing model can be used to model it.

4.5. Conclusion

We have demonstrated that the data traffic performance of both 802.11 based WLANs and HSDPA based 3.5G cellular based networks can be modeled by a PS queue. We will use this modeling approach in Chapter 5 to develop a BCMP queueing network describing load exchange between heterogenous RANs belonging to different operators. In Chapter 7 we use this description to develop automated software agents controlling the resource exchange dynamically.

5. Description Problem

In *Description Problem*, we present a separable analytical model that can be used to analyze resource sharing between two different operators. The description framework we lay is used in order to develop negotiation mechanisms in Chapter 6 as well as automated control mechanisms for resource sharing in Chapter 7. We start the chapter by introducing the requirements and motivations of the analytical model. We formulate the problem formally in Section 5.2 and compare it to the state of the art in Section 5.4. We propose the single class analytical model in Section 5.5 and apply it to a single class resource sharing scenario in Section 5.5.3.We extend our single class model to handle multiple service classes in Section 5.6. We finally verify the results of this chapter via OPNET simulation we summarize in Appendix B.

5.1. Motivation and Requirements

The problem we are addressing is the minimization or avoidance of possible degradation in user perceived quality of experience in an access network as the number of users increases in an open user-centric network environment. The delay a session request experiences is a common performance measure that can be used to handle a variety of service types. Therefore, we choose the delay as the performance metric of dynamic resource sharing mechanisms.

The method with which the avoidance or minimization is achieved is by borrowing network layer resources from an access network that belong to another operator (community, virtual or real operator). In a user-centric environment, the operators have to find additional resources, not to degrade the QoE, otherwise the users will be moving away to alternative operators. What would be the incentives for the donor operator to lend some of its resources to the borrower? A quick answer would be that if the donor operator is under-utilized at that particular point of time, then it could increase its utilization to a point where it still can serve its current users, thereby increasing its revenues. However, the challenge of user centricity comes from the fact that users can instantaneously decide on the operators they choose. The donor operator may choose to ignore the borrowing operator, in an attempt to drive the QoE in the borrowing network down, and gain more users. Therefore the dynamics of the resource sharing between two operators become strategy dependent, and not trivial.

The aforementioned problem is not specific to the dynamic resource sharing in user-centric networking. As Dohler discusses in [12], the problem is not only technological, but also strategic. We adhere to Dohler's approach, in which he proposes that the success of any cooperative solution to any communications problem is more possible if the cooperation decisions are taken by software agents, and the benefits of these decisions

i	operator index, $i \epsilon A, B$.
P_i	Probability that users prefer Operator i.
$P_{R,i}$	Blocking probability in Operator i.
$P_{T,i}$	Transfer probability in Operator i.
$D_{\max,i}$	Maximum allowed average delay in Operator i.
$1/\lambda$	External average inter-arrival time ($secs$).
$1/\mu$	Average request size($bits$).

Table 5.1.: Model variables.

are clear to the owners of these agents. Therefore we derive a simple and intuitive formula for the relation between the average delay and cooperation parameters.

Another important requirement to the model is the separability. Under separability we mean the following. Generally, the state space describing two independent systems interacting with each other is two dimensional. The solution of the probability distribution of such a distribution requires the knowledge of the states of the independent systems. This is not possible for two cooperating operators, since the operators will be reluctant to share their operation information with each other. If the performance metrics can be calculated by openly available information, without requiring the knowledge about the operative status of the other operators we call such a model separable.

Final requirement on the modeling approach is the capability to efficiently model heterogenous wireless networks. It is foreseen that the 4G networks will be composed of heterogenous wireless access technologies. Therefore the model should be able to accommodate a variety of them.

5.2. Problem Formulation

In this section we define formally the abstraction level we employ in modeling the problem of dynamic resource sharing in user-centric networking. We consider a location where the users have two wireless operators to choose from, operator A and operator B. The users generate requests with exponential inter arrival times of mean $1/\lambda$, which have sizes that are also exponentially distributed with mean $1/\mu$. Since these users are not in contractual agreements with the operators, they can choose either one of the operators with probabilities P_A and P_B. The operators utilize a call admission control (CAC) mechanism that block incoming requests with probability P_R, or transfer to the other operator with a probability P_T. The operators employ these techniques in order to provide a maximum delay guarantee to the users given by $D_{\max}$. The variables of the model are summarized in Table 5.1.

5.3. Mathematical Background

Considering the requirements we listed in Section 5.1, we have decided to use Queueing Networks [55] as the modeling framework. Queueing networks are a generalization of

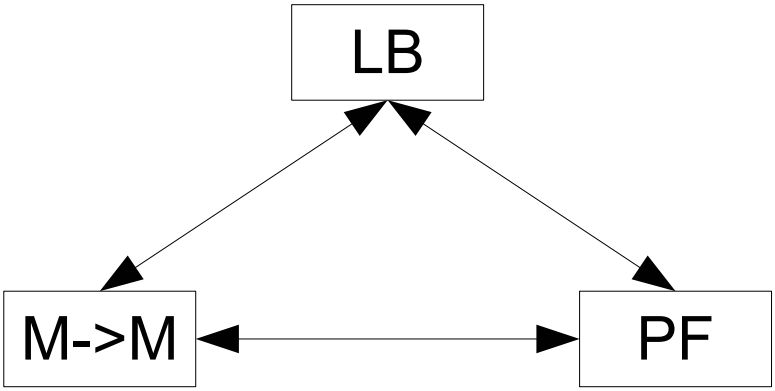

Figure 5.1.: Relationship between $M \rightarrow M$, LB and PF properties.

the classical queueing systems. They are concerned with the performance modeling of systems that are composed of interconnected queueing stations. The main goal of the queueing networks is the derivation of the joint probability distribution of the number of jobs in each service station. One of the most important results of Queueing Networks is the Baskett, Chandy, Muntz and Palacios (BCMP) theorem, named after the researchers who jointly developed the theorem in [28]. The theorem states that the joint probability distribution of a queueing network can be written as the product of marginal probability distributions of the individual service stations. Furthermore, each service stations behaves like a traditional M/M/1 queue, with a modified input traffic rate, reflecting the network topology. This formulation satisfies the separability and simplicity requirements.

The Continuous Time Markov Chain (CTMC) describing the BCMP type of networks have the *local balance property*, which allows efficient solutions of the probabilities.The global balance equations of the CTMC can be written as:

$$\pi_i \sum_{j \epsilon S} q_{ij} = \sum_{j \epsilon S} \pi_j q_{ji} \tag{5.1}$$

These equations can be interpreted as the balancing of probability flows out of and into each state in the CTMC description. Simultaneous numerical solution of these global equations can be prohibitive, when the size of the state space grows. Furthermore, analytical solutions are unattainable in most cases. The global balance equations can be separated into sum of smaller *local balance equations*. Local balance equations equate the probability flows going into and out from a state that are due to transitions associated with an individual node in the queueing network. When added up, they result in the original global balance equations.

For certain node types, these local balance equations have solutions, in which case the node is said to have *local balance property* . If all the network nodes do have the local balance property, than the whole network has a product form solution (PF) , in terms of the product of the solutions to the individual local balance equations. A necessary

and sufficient condition for a node to be locally balanced is for that node to posses the *Markov inputs, Markov outputs* ($M \rightarrow M$) property. As the name suggests nodes with this property have Markovian outputs when the inputs are Markovian. Figure 5.1 depicts the relation between $M \rightarrow M$, LB and PF properties.

BCMP Theorem for Single Class Networks

BCMP theorem is applicable to any Queueing Network that is composed of processing centers that are of the following four types:

1. *Type 1*: ·/M/m - FCFS .
2. *Type 2*: ·/G/1 - PS .
3. *Type 3*: ·/G/1 - IS .
4. *Type 1*: ·/G/1 - LCFS .

The BCMP theorem states that given a Queueing Network, composed of N processing centers, the steady state probabilities of the joint state vector $\mathbf{S}$ has a product form. S is a vector of N dimensions, $S = (k_1, k_2, ..., k_N)$, where k_i denotes the number of jobs in processing center i. The form is given by:

$$\pi(\mathbf{S}) = \frac{1}{G(\mathbf{K})} d(\mathbf{S}) \prod_{i=1}^{N} f_i(k_i). \tag{5.2}$$

The first term $\frac{1}{G(\mathbf{K})}$ is a normalization constant which is a function of the population vector $\mathbf{K} = (k_1, k_2, ..k_N)$. It is obtained from the total probability condition (5.3), which says that the probability of all the states should sum up to unity:

$$\sum_{\forall S \epsilon \mathbf{S}} \pi\{S\} = 1. \tag{5.3}$$

The second term $d(\mathbf{S})$ is able to accommodate state-dependent arrival rates. It is given by $d(\mathbf{S}) = \prod_{i=0}^{K(\mathbf{S})-1} \lambda(i)$, where $K(\mathbf{S}) = \sum_{i=1}^{N} k_i$ represents the total number of jobs in the system.

The final term takes different forms according to the type of the service center under consideration. Specifically:

$$\begin{aligned} f_i(k_i) &= \left(\frac{e_i}{\mu_i}\right)^{k_i} \qquad \textit{Type 2}. \\ f_i(k_i) &= \frac{1}{k_i!} \cdot \left(\frac{e_i}{\mu_i}\right)^{k_i} \qquad \textit{Type 3}. \end{aligned} \tag{5.4}$$

The term e_i is an important parameter of queueing networks. They represent the *visit ratio* or the *relative arrival rate* of jobs at node i. They are defined as the ratio of arrival rate at node i to the external arrival rate, i.e. $e_i = \frac{\lambda_i}{\lambda}$. The arrival rates λ_i can be found by solving the traffic equations. For open networks they can be expressed as:

$$\lambda_i = \lambda \cdot p_{0,i} + \sum_{j=1}^{N} \lambda_j \cdot p_{j,i}, \quad i = 1, ..., N. \tag{5.5}$$

where λ is the external arrival rate, and $p_{i,j}$ represent the routing probability between service stations i and j where the subscript 0 denotes the external environment.

5.4. State of The Art

Historically, queueing networks have provided very attractive models for a wide variety of communication networks and applications running on these networks. Early applications include [56] Conway's queueing model for the performance evaluation of Signalling System 7 (SS7).

One of the most active application of queueing networks to the 4G networking has been the work of Kouvastos et al. Kouvastos first employed a queueing network model to analyze the performance of ATM Asynchronous Transfer Mode switches developed for the ISDN Integrated Services Digital Networkss [57]. The challenge he addressed was the development of an analytical performance model for the switches that can be used during the design and development phase. The model regarded the switching matrix at the core of the switch as a medium that had to be shared among flows of different service types.

The author applied the same queueing model first to performance analysis of GSM/GPRS base stations [58], and subsequently to the performance analysis of hypothetical 4G base stations accommodating different services [53] and [54]. A hypothetical 4G cell is modeled as a combination of three service centers. Voice calls are handled by a classical Erlang loss system, the data calls are handled by a PS (Processor Sharing) system and finally streaming calls are handled by a FCFS (First Come First Serve) system. These service centers exchange resources among themselves according to the state of the cell, which consists of $\mathbf{n} = (n_1, n_2, n_3)$ where n_1, n_2, n_3 are the number of calls in the respective service centers. The state space is three dimensional and therefore not analytically tractable. The authors make use of the maximum entropy principle to find a product form approximation that yields a closed form solution. Maximum entropy principle was introduced by Jaynes in 1960s [59], and can be seen as an equivalence principle between statistical and information theoretical entropy definitions. It states that given a constraint on the mean values of a family of probability distributions that may describe a physical process, the distribution that maximizes the entropy is the least biased estimate of the probability distribution. The constraints on the mean values under investigation are:

$$\lambda_i(1-p_i) = \mu_i U_i, \quad i = 1,2,3 \tag{5.6}$$

where λ_i is the overall flow into a server center, p_i is the blocking probability, μ_i is the service rate and U_i is the utilization of the service center associated with the service types described before. This equality is a reformulation of global balance conditions, equating the flows into and out of a state. The goal is to find the probability distribution of $\mathbf{n}$. Maximum entropy method involves solving the maximization problem with the method of Lagrange multipliers. These Lagrange multipliers are then used to formulate equivalent flows into the individual service centers, which can then be analyzed independently. Similar to this work, we use PS service stations to model heterogeneous access networks. Our model not only takes into account multiple access networks, but also different operators. Furthermore, we use the BCMP method to provide exact solution to the queueing model. Our solution is also computationally more efficient than this, as it does not include any recursive solutions.

Fukushima et al. present an innovative application of queueing networks to the wireless communications domain in [60]. Specifically, they employ queueing networks to model the interplay between user mobility and bursty nature of packet traffic in wireless systems. The mobility of the users between cells and their service requests evolve with different timescales. The authors utilize queueing networks to model these two aspects jointly. In their formulation each cell has two service centers. The first service center, which is an infinite server (IS) center, models user mobility, where users move from one infinite server to the other based on routing probabilities obtained from an external mobility model. The second server is a PS center, which models the sharing of base station transmission capacity among the service requests of users in the cell. The service demand at the second service station is a function of the state of the first service station. It can be said that the authors use a queueing network with state-dependent routing. The state dependency expresses itself as non-linear traffic equations, which can be solved using fixed point iterative methods. The authors use this model to analyze a hierarchical WLAN-cellular integration, with static *"WLAN first"*policy, similar to [61].

In [61]the authors provide an analysis of a hierarchically integrated WLAN and cellular network by employing queueing networks. In a hierarchical integration architecture [62], the WLAN cells are used as high-speed hot spots, and are carefully positioned as an overlay on the cellular infrastructure. The natural question that arises in such an architecture is when the overlay will be used. Assuming that the network operator has the final say on this decision, the authors employ the *"WLAN first"* resource allocation policy. In this policy the calls are admitted to the WLAN cell as long as the capacity is not reached. The calls are then admitted to the underlay cellular cell, once the capacity is reached. The authors assume that the data calls can be modeled by discrete bandwidth units they fill in different subsystems. With this assumption, they are able to model the individual overlay and underlay cells as classical Erlang loss-systems. The availability of a static allocation policy, the interaction between different cells are modeled by static and additive traffic flows. The authors mention that the overall system is represented by a multi-dimensional Markov chain, but do not propose a solution for the global equations.

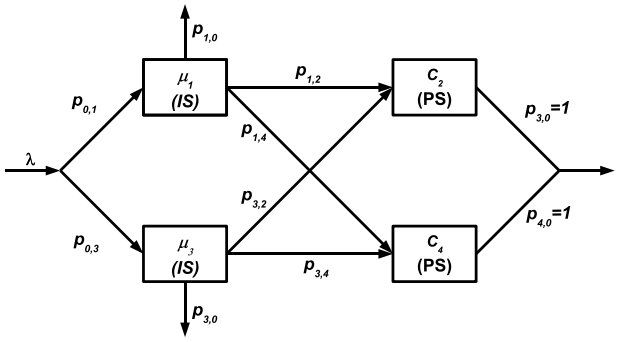

Figure 5.2.: The single class queueing network model.

Subsequently, no relation between the marginal probabilities and the global probabilities are presented. Based on the marginal probabilities, the authors are able to derive closed-form blocking probabilities. Both of these works consider a single operator owning the heterogeneous access networks.

Early applications of BCMP theorem to data communication networks include the analysis of general sliding window type flow control, such as the one used in TCP by Reiser [63]. Recent application fields include the modeling of multi-tier Internet applications and the operational optimization of data centers hosting these services. A typical Internet application is provisioned by a multi-tier arrangement of servers. In the front end is the load balancer that routes the application requests to replicated first tier web servers. The first tier web servers route the session requests to the second tier application servers that host the applications are replicated. Finally, the application servers use the third tier data base servers to compose the applications. In [64] Urgaonkar models this architecture via a single class closed BCMP network and present analytic solutions for the average delay. Data centers that host these applications on identical server clusters can also be modeled as closed BCMP networks. In this case the server clusters become the service centers, and the different applications represent the different applications. The authors use such an analytical model to optimize the energy use and scaling of data servers in [65]. To the best of our knowledge BCMP networks have not been applied in modeling 4G networks.

5.5. Single Class Resource Sharing

5.5.1. Single Service Class Queueing Network Model

In order to develop a tractable, closed form, and separable solution for the delay performance metric we use the BCMP theorem on the queueing network depicted in Figure 5.2. Each wireless operator is modeled by a tandem of queues. The first stage IS queue, represents the CAC decision making. The traffic exiting the first stage queue enters the PS queue which jointly models the shared air interface and access router that connects the base station to the backbone.

5.5.2. Closed Form Solution of BCMP Equations for Our Model

By making the relevant substitutions in (5.5) we obtain the expressions for the input rates of the different service stations as:

$$\begin{aligned} \lambda_1 &= \lambda \cdot p_{0,1}. \\ \lambda_2 &= \lambda \cdot p_{0,1} \cdot p_{1,2} + \lambda \cdot p_{0,3} \cdot p_{3,2}. \\ \lambda_3 &= \lambda \cdot p_{0,3}. \\ \lambda_4 &= \lambda \cdot p_{0,3} \cdot p_{3,4} + \lambda \cdot p_{0,1} \cdot p_{1,4}. \end{aligned} \tag{5.7}$$

The main challenge involved in finding the solution of the steady-state probabilities is the computation of the normalization constant $G(\mathbf{K})$. For single class open networks a closed form solution is possible as we demonstrate below. We first apply the total probability condition to our network:

$$\sum_{i=1}^{4} \sum_{k_i=0}^{\infty} \pi(k_1, k_2, k_3, k_4) = 1. \tag{5.8}$$

If one replaces e_i with $\frac{\lambda_i}{\lambda}$ in (5.4), one gets the term $\frac{\lambda_i}{\mu_i}/\lambda$. This correspond to the utilizations of individual servers, ρ_i, divided by the external arrival rate, λ, and we get the following expressions f_i:

$$\begin{aligned} f_i(k_i) &= \rho_i^{k_i} \lambda^{-k_i} \qquad i = 2, 4. \\ f_i(k_i) &= \frac{1}{k_i!} \rho_i^{k_i} \lambda^{-k_i} \qquad i = 1, 3. \end{aligned} \tag{5.9}$$

Since our model does not involve state-dependent arrival rates, hence $d(\mathbf{S})$ simplifies to:

$$d(\mathbf{S}) = \lambda^{(k_1+k_2+k_3+k_4)}. \tag{5.10}$$

The $\lambda_i^{k_i}$ terms in $d(\mathbf{S})$ and in $f_i(k_i)$ cancel out each other. We obtain the following form of (5.8):

$$\frac{1}{G(\mathbf{K})} \cdot \sum_{k_1=0}^{\infty} \frac{1}{k_1!}\rho_1^{k_1} \sum_{k_2=0}^{\infty} \rho_2^{k_2} \sum_{k_3=0}^{\infty} \frac{1}{k_3!}\rho_3^{k_3} \sum_{k_4=0}^{\infty} \rho_4^{k_4} = 1. \tag{5.11}$$

The summations involving factorials are the Maclaurin expansion of the exponential function. Other terms can be simplified using the well known formula for the computation of geometric series [66]:

$$\begin{aligned} \sum_{i=0}^{\infty} \frac{\rho_i^{k_i}}{k_i!} &= e^{-\rho_i}. \\ \sum_{i=0}^{\infty} \rho_i^{k_i} &= \frac{1}{1-\rho_i}. \end{aligned} \tag{5.12}$$

Replacing these values in (5.11) we obtain the value of $\frac{1}{G(\mathbf{K})}$

$$\frac{1}{G(\mathbf{K})} = (1-\rho_1) \cdot e^{-\rho_2} \cdot (1-\rho_3) \cdot e^{-\rho_4}. \tag{5.13}$$

One can use the traffic equations (5.7) and the service rates of the individual server stations to calculate the individual utilizations. Once these modified utilizations are computed, the joint probability distribution can be written as:

$$\pi(k_1, k_2, k_3, k_4) = \prod_{i=1,3} e^{-\rho_i} \frac{\rho_i^{k_i}}{k_i!} \cdot \prod_{i=2,4} (1-\rho_i)\rho_i^{k_i}. \tag{5.14}$$

Let us substitute the routing probabilities of the BCMP model with the system parameters we defined in Section 5.2. The indices $i = 1, 2$ describe the operator A and $i = 3, 4$ the operator B. $p_{0,1}$ and $p_{0,3}$ correspond to the users operator preferences, P_A and P_B respectively. $p_{3,2}$ and $p_{1,4}$ are the transfer ratios of the operators, $P_{T,A}$ and $P_{T,B}$. The CAC mechanisms reject calls with probabilities $P_{R,A}$ and $P_{R,B}$, hence we have $P_{1,0} = P_{R,A}$ and $P_{3,0} = P_{R,B}$. By using total probability principle we obtain $P_{1,2} = 1 - P_{T,A} - P_{R,A}$ and $P_{3,4} = 1 - P_{T,B} - P_{R,B}$. Let us analyze the utilization of the PS part of the individual operators. Given that the users generate requests whose sizes are distributed according to an exponential distribution of average μ bits and the operators access networks have a capacity of C_A and C_B bits per second, we have $\mu_1 = \mu \cdot C_A$ and $\mu_2 = \mu \cdot C_B$. Thus we have:

$$\begin{aligned}\rho_{PS,A} &= (P_A \cdot (1 - P_{T,A} - P_{R,A}) + P_B \cdot P_{T,B}) \cdot \tfrac{\lambda}{\mu C_A}. \\ \rho_{PS,B} &= (P_B \cdot (1 - P_{T,B} - P_{R,B}) + P_A \cdot P_{T,A}) \cdot \tfrac{\lambda}{\mu C_B}.\end{aligned} \tag{5.15}$$

These equations show an intuitive and linear relationship between operator utilizations and transfer and blocking probabilities. Specifically, an operator may increase its utilization by accepting additional traffic from the other operator, or may decrease its utilization by transferring traffic to the other operator or by increasing the CAC level. When increasing the utilization, the condition $\rho_{PS,A}, \rho_{PS,B} < 1$ should be considered to guarantee stability. These utilizations can be used to find the expected delay conditioned on the request size x given in bits at the PS side of the operators. These are given by:

$$\begin{aligned}D_{PS,A}(x) &= \frac{x/C_A}{1 - \rho_{PS,A}}. \\ D_{PS,B}(x) &= \frac{x/C_B}{1 - \rho_{PS,B}}.\end{aligned} \tag{5.16}$$

5.5.3. Application of the Model to Single Class Resource Sharing

a In a single service class scenario, the sharing of resources to avoid overload situations becomes mutually exclusive with the under-utilization situations. This means that the borrowing operator will not donate resources, and the donor operator will not borrow resources from each other. Let us arbitrarily assign operator A to be the donor operator, and operator B to be the borrowing operator. The borrower operator A borrows resources and sends a given portion of traffic to the donor operator B, which accepts additional traffic. Furthermore, let us assume the average service demand x is fixed.

In this case the delays become a function of the transfer probability P_T and the operator preferences of the users P_A, P_B. This means that the exchange of resources is one way, i.e. $P_{T,A} = 0$. We can simply use the transfer probability P_T in the place of $P_{T,B}$. The problem of finding an optimal P_T is then characterized the relative operator preferences of the users P_A, P_B; the delay thresholds $D_{\max,A}, D_{\max,B}$; and the CAC probabilities $P_{R,A}$ and $P_{R,B}$.

In a resource sharing scenario, the donor operator has to find the amount of traffic it can accept, equivalently the amount of resources it can donate, without increasing the expected delay of the already accepted users above a threshold $D_{\max,A}$, described by (5.17). The donor operator finds the maximum P_T value that satisfies this condition described by which we term P_T:

$$D_A(P_T) = D_{PS_A}(P_T) = D_{\max,A} \tag{5.17}$$

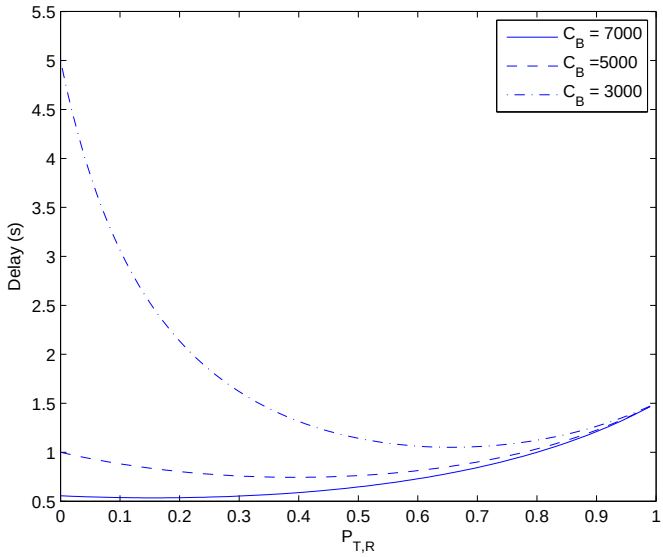

Figure 5.3.: The variation of average delay versus transfer probability for $C_A = 5000bps, D_{A,init} = 0.6$.

On the other side the borrowing operator has to calculate how much traffic it should transfer, or equivalently how much resources it should borrow, in order to reduce the expected delay in its access network to a threshold. However, it also has to consider the increase in delay it induces on the donor operators. We are considering a *seamless* scenario, in which the transferred users are not aware of the fact that their session request is served by an alternative operator. The borrowing operator should not load the donor operator excessively, since this excessive loading would increase the delays experienced by the transferred users, who would associate this with the borrowing operator.

There are two approaches for considering this aspect. One can consider the maximum of the delays in the two networks as in (5.18).

$$\max\{D_{PS_A}(P_T), D_{PS_B}(P_T)\} \leq D_{\max,B}(x) \tag{5.18}$$

An alternative is to consider the average delay as experienced by the users of the borrowing operator, as in (5.19).

$$E\{D_B(P_T)\} = (1 - P_T) \cdot D_{PS_B}(P_T) + P_T \cdot D_{PS_A}(P_{T,R}) \leq D_{\max,B}(x) \tag{5.19}$$

In both cases, the borrowing operator chooses the transfer probability value P_T that minimizes the delay. We choose the second option, as it is more fair to the users of the borrowing operator. In order to calculate $E\{D_B(P_T)\}$ operator B has to be able to calculate the utilization of operator A, which requires the knowledge of $P_{R,A}$. This is an private information that is not available to operator B. However this can be solved

by utilizing the open user experience database, proposed by PERIMETER. We assume operator B is able to gather the initial average delay in operator A, $D_{A,init}$, by exploiting the database. From this value it can calculate initial value of the utilization via (5.16). Employing (5.15) allows us to formulate the utilization of operator A after resource sharing, by consulting only to the publicly available average delay. Using this value one is able to write down the expression for $E\{D_B(P_T)\}$:

$$E\{D_B(P_T)\} = \frac{\frac{x}{C_A} \cdot P_T}{\frac{x}{C_A D_{A,init}} - \frac{P_B \lambda}{\mu C_A} \cdot P_T} + \frac{\frac{x}{C_B} \cdot (1 - P_T)}{1 - P_B(1 - P_{R,B} - P_T)\frac{\lambda}{\mu C_B}} \tag{5.20}$$

Equation 5.20 is plotted for varying borrowing operator capacities in Figure 5.3. It can be observed that the amount of reduction in the average delay is directly proportional with the capacity of the donor operator. For all cases the delay is a rational function of transfer probability with global minimum. Of course a compromise should be found, if the P_T value that the donor can support does not match the optimum P_T value that minimizes borrower delay. The negotiation mechanisms for establishing jointly a agreed P_T are developed in Chapter 6. For the rest of this chapter we assume both donor and borrower have agreed upon the optimal P_T value.

In order to find the optimal P_T we apply the standard calculus techniques. We consider the expected delay for the users of operator B $E\{D_B(P_T)\}$, as a function of P_T as in Equation (5.20). For this function, we calculate the first derivative and set it to zero. The solutions are the candidates for the minima. Afterwards, we calculate the second derivative, and search for the negative second derivatives corresponding to the of the minimum. In this way we define a closed form solution for the optimal sharing parameter $P_{T,B,opt}$.

In Appendix A, we show that the Equation 5.20 can be reshaped in Equation 5.21:

$$D_B(P_{T,B}) = \frac{P_{T,B}}{m - k \cdot P_{T,B}} + \frac{1 - P_{T,B}}{n + k \cdot P_{T,B}} \tag{5.21}$$

where $m = \frac{1}{D_{A,init}}$, $n = \frac{1}{D_{B,init}}$, and $k = \frac{C_B}{x(1-P_{R,B})} \cdot \rho_{B,init}$. Furthermore we prove that we have a minimum and we give a closed form solution for $P_{T,B,opt}$ as:

$$P_{T,B,opt} = \frac{m}{k} \cdot \frac{\sqrt{\frac{n+k}{m}} - \frac{n}{m}}{\sqrt{\frac{n+k}{m}} + 1} \tag{5.22}$$

This is valid under the assumption that:

$$\frac{D_{A,init}}{D_{B,init}} \leq \frac{n}{n+k} \tag{5.23}$$

This condition can be interpreted as follows. An optimal sharing parameter exists, in case the donor operator is advertising a lower initial delay then the borrower operator's initial delay. This condition is satisfied when an overloaded operator is borrowing resources from a normal operator.

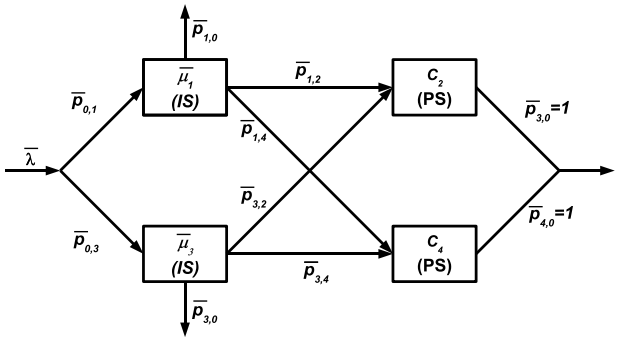

Figure 5.4.: The multi class queueing network model.

5.6. Multi-Class Resource Sharing

In this section we try to extend the description framework to the scenarios in which multiple classes of services are running on the interacting operators.

5.6.1. Multi Service Class Queueing Network Model

We extend the single class model we developed in 5.5.1 to include multiple service classes that represent either different service types such as video, audio, background or to represent different user classes such as premium and standard.

Different user classes arise out of service differentiation efforts of the operators. In order to differentiate users who are willing to pay more for better quality of experience from

5.6.2. BCMP Solution for Multi Class Networks

The BCMP theorem can be extended to multiple service classes. Given that there are R different service classes, the traffic equation for the arrival of service class r jobs in node i is given by:

$$\lambda_{ir} = \lambda \cdot p_{0,ir} + \sum_{j=1}^{N} \sum_{s=1}^{R} \lambda_{js} \cdot p_{js,ir}. \tag{5.24}$$

where the term $p_{js,ir}$ represent the probability of a class s finishing processing at service station j and joining service station i as a class r job. In this case the state of the service station i is given by the vector $\mathbf{S_i} = (k_{i1}, ..., k_{iR})$, where k_{ir} is the number of class r users in service center i. The overall state of the network is given by the vector

of vectors $\mathbf{S} = (\mathbf{S_1}, ..., \mathbf{S_N})$. The product form which the state probabilities obey is then given by:

$$\pi(\mathbf{S_1}, ..., \mathbf{S_N}) = \frac{1}{G(\mathbf{K})} d(\mathbf{S}) \prod_{i=1}^{N} f_i(\mathbf{S_i}). \tag{5.25}$$

The forms of the constituent parts are given by the following formulas.

$$d(\mathbf{S}) = \prod_{i=0}^{K(\mathbf{S})-1} \lambda i \quad \text{where} \quad K(\mathbf{S}) = \sum_{i=1}^{N} \sum_{r=1}^{R} k_{ir}. \tag{5.26}$$

$$\begin{aligned} f_i(\mathbf{S_i}) &= k_i! \prod_{r=1}^{R} \frac{1}{k_{ir}!} \left(\frac{e_{ir}}{\mu_{ir}} \right)^{k_{ir}} \qquad \textit{Type 2}. \\ f_i(\mathbf{S_i}) &= \prod_{r=1}^{R} \frac{1}{k_{ir}!} \left(\frac{e_{ir}}{\mu_{ir}} \right)^{k_{ir}} \qquad \textit{Type 3}. \end{aligned} \tag{5.27}$$

e_{ir} is the *relative visit ratio* of class r jobs to node i and it is given by the expression $\frac{\lambda_{ir}}{\lambda_r}$. λ_r is the external input rate of class r jobs. It can be calculated by the expression $\lambda_r = \sum_{i=1} N\lambda \cdot p_{0,ir}$. k_i term represent the total number of jobs in node i, i.e.$k_i = \sum_{r=1}^{R} k_{ir}$

5.6.3. Application of BCMP Solution Our Multi Class Model

Our model does not involve class switching. This means that once a job enters the system as a service class r, it will never change its service class until it leaves the system. This means that the only transition probabilities that are allowed to have non-zero values are of the form $p_{ir,jr}$. As a result the traffic equations for our system have the following form:

$$\lambda_{ir} = \lambda \cdot p_{0,ir} + \sum_{j=1}^{4} \lambda_j \cdot p_{jr,ir}. \tag{5.28}$$

Introducing the different transition probabilities, we obtain the following traffic equations:

$$
\begin{aligned}
\lambda_{11} &= \lambda \cdot p_{0,11}. \\
\lambda_{12} &= \lambda \cdot p_{0,12}. \\
\lambda_{21} &= \lambda \cdot p_{0,11} \cdot p_{11,21} + \lambda \cdot p_{0,31} \cdot p_{31,21}. \\
\lambda_{22} &= \lambda \cdot p_{0,12} \cdot p_{12,22} + \lambda \cdot p_{0,32} \cdot p_{32,22}. \\
\lambda_{31} &= \lambda \cdot p_{0,31}. \\
\lambda_{32} &= \lambda \cdot p_{0,32}. \\
\lambda_{41} &= \lambda \cdot p_{0,31} \cdot p_{31,41} + \lambda \cdot p_{0,11} \cdot p_{11,41}. \\
\lambda_{42} &= \lambda \cdot p_{0,32} \cdot p_{32,42} + \lambda \cdot p_{0,12} \cdot p_{12,42}.
\end{aligned}
\tag{5.29}
$$

Similar to the single class solution, we proceed by formulating the total probability condition:

$$
\sum_{i=1}^{4} \sum_{r=1}^{2} \sum_{k_{ir}=0}^{\infty} \pi((k_{11}, k_{12}), ..., (k_{41}, k_{42})) = 1. \tag{5.30}
$$

Similar to the single class case, the form of $d(\mathbf{S})$ simplifies, since the arrival rate is state independent. In the multi-class case $d(\mathbf{S})$ is given by:

$$
d(\mathbf{S}) = \lambda^{\{\sum_{i=1}^{4} \sum_{r=1}^{2} k_{ir}\}} \tag{5.31}
$$

Let us expand the expression for e_i to simplify the form of $f_i(\mathbf{S_i})$. In order to do this, we have to calculate λ_r:

$$
\begin{aligned}
\lambda_r &= \sum_{i=1}^{4} \lambda_{0,ir}. \\
\lambda_r &= \sum_{i=1}^{4} \lambda \cdot p_{0,ir}. \\
\lambda_r &= \lambda \sum_{i=1}^{4} p_{0,ir}. \\
\lambda_r &= \lambda.
\end{aligned}
\tag{5.32}
$$

where we used in the last step the fact that the incoming traffic in any given traffic class is distributed to one of the operators with probability one, i.e. $\sum_{i=1} 4p_{0,ir} = 1$. This leads the simplification of $\frac{e_i r}{\mu_i r}$ to $\rho_{ir} \cdot \lambda^{-1}$. We have therefore the following form of $f_i(\mathbf{S_i})$:

$$f_i(\mathbf{S_i}) = k_i! \prod_{r=1}^{2} \frac{1}{k_{ir}!} \rho_{ir}^{k_{ir}} \lambda^{-k_{ir}} \qquad \textit{Type 2}.$$
$$f_i(\mathbf{S_i}) = \prod_{r=1}^{2} \frac{1}{k_{ir}!} \rho_{ir}^{k_{ir}} \lambda^{-k_{ir}} \qquad \textit{Type 3}.$$

(5.33)

Similar to the single class case, the four individual terms $\prod_{r=1}^{2} \lambda^{-k_i r}$ multiplied with each other equate to $\lambda^{\left\{-\sum_{i=1}^{4}\sum_{r=1}^{2} k_{ir}\right\}}$ and cancel out the $d(\mathbf{S})$ term (5.31). Finally, after substituting k_i with $k_{i1} + k_{i2}$ We end up with the following simplification of the total probability condition, which will be used to calculate the value of the normalization constant:

$$\begin{aligned} 1 \;=\; & \frac{1}{G(\mathbf{K})} \\ & \times \sum_{k_{21}=0}^{\infty} \sum_{k_{22}=0}^{\infty} (k_{21}+k_{22})! \frac{\rho_{21}^{k_{11}}}{k_{21}!} \frac{\rho_{22}^{k_{22}}}{k_{22}!} \\ & \times \sum_{k_{41}=0}^{\infty} \sum_{k_{42}=0}^{\infty} (k_{41}+k_{42})! \frac{\rho_{41}^{k_{41}}}{k_{41}!} \frac{\rho_{42}^{k_{42}}}{k_{42}!} \\ & \times \sum_{k_{11}=0}^{\infty} \frac{\rho_{11}^{k_{11}}}{k_{11}!} \sum_{k_{12}=0}^{\infty} \frac{\rho_{12}^{k_{12}}}{k_{12}!} \\ & \times \sum_{k_{31}=0}^{\infty} \frac{\rho_{31}^{k_{31}}}{k_{31}!} \sum_{k_{32}=0}^{\infty} \frac{\rho_{32}^{k_{32}}}{k_{32}!}. \end{aligned}$$

(5.34)

The first two double sums in (5.34) correspond to the PS service nodes, whereas the last two correspond to the IS nodes. The IS node summations are Mclaurin expansions of the natural exponential function and converge for all the values of ρ_{ir}. However the summations related to PS nodes do not lend themselves for closed form solution, since the factorials terms $(k_{i1} + k_{i2})!$ $\frac{1}{k_{i1}!k_{i2}!}$and do not cancel out each other. If they were to cancel out, it would mean that the different traffic classes in a single PS node were independent random variables. This is physically not possible, since different service classes physically share the same server.

The authors approach this problem by aggregating the service classes in a node [28]. This means the aggregate state is given by $\mathbf{S} = (k_1, \ldots, k_4)$. This has the consequence that the utilizations are also combined, i.e. $\rho_i = \rho_{i1} + \rho_{i2}$. With this aggregation, a closed form solution for the state probabilities are possible:

$$\pi(k_1, k_2, k_3, k_4) = \prod_{i=2,4} (1-\rho_i)\rho_i^{k_i} \prod_{i=1,3} e^{-\rho_i} \frac{\rho_i}{k_i!} \tag{5.35}$$

One question that remains open is how to account for the distribution of individual service classes. It is theoretically possible, but computationally not feasible to compute the distributions of individual service classes as we illustrate next.

The theoretic analysis uses the basic relation of conditional probability:

$$\pi(k_{11}, k_{12}, \ldots, k_{41}, k_{4,2}) = \sum_{\mathbf{K=0}}^{\infty} \pi(k_{11}, k_{12}, \ldots, k_{41}, k_{4,2})|\mathbf{K}) \cdot \pi(\mathbf{K}) \tag{5.36}$$

where $\mathbf{K}$ represents the aggregated state, whose distribution can be calculated by using (5.35). Then for all the possible combinations of K, one can hold k_i values constant, and solve the system as a closed queueing network, which would give the $\pi(k_{11}, k_{12}, \ldots, k_{41}, k_{4,2})|\mathbf{K})$ terms. There are efficient iterative algorithms based on convolution for calculating the normalization constants and the state probabilities such as one given in [67]. Even when one limits the number of possible states in $\mathbf{K}$, to include only those states for which there is a significant probability of occurrence, the solutions will not be closed form and not be in accordance with our motivations.

Even though the marginal distributions are not explicitly obtainable, one can use the concept of utilization in a Multi-class Processor Sharing (MCPS) Queue is defined by Kleinrock in [25] . This type of queue is also used as the multi-class extension of BCMP networks in [55]. In a MCPS queue, the total utilization is defined as the sum over all the per class utilizations. For the sake of simplicity we assume we have two service classes. In this case we have

$$\rho = \rho_1 + \rho_2 \tag{5.37}$$

with and ρ_i is given by:

$$\rho_i = \frac{\lambda_i}{\mu_i C} \tag{5.38}$$

where λ_i represents the arrival rate of class-i requests, and $\frac{1}{\mu_i} = x_i$ is the average request length of class-i requests. C represents the total capacity of the queues. It must be noted that no service differentiation is applied in this model. The extensions of PS queue that allow service differentiation such as Kleinrock's original Priority Processor Sharing , Discriminatory Processor Sharing [68] or Generalized Processor Sharing [69] have yet to be incorporated to the queueing network framework and therefore not applicable to our approach. We can reformulate the equation (5.37) as:

$$\rho = \frac{\lambda_1 x_1}{C} + \frac{\lambda_2 x_2}{C} \tag{5.39}$$

This shows that, given a certain overall utilization ρ the relationship between the arrival rate of the two classes is linear, i.e. in order to keep the utilization same, one

must counter the increasing arrival rate of users of one type by decreasing the arrival rate of the other type. We assume that there is a ρ_max that is required to be met, in order to meet the performance metrics of both of the service classes. In this case we have:

$$\begin{aligned} \rho_1 + \rho_2 &\leq \rho_{\max} \\ \frac{\lambda_1 x_1}{C} + \frac{\lambda_2 x_2}{C} &\leq \rho_{\max} \end{aligned} \tag{5.40}$$

In Section 7.4.3 we describe how one can obtain $\rho_{\max,i}$ values for individual service classes $i = 1, 2$ given their statistics, maximum delay values and the grade of service values.

Sharing Options

Once the x_1 and x_2 values are set, say to the average request sizes of the individual classes, the inequality (5.40) can be represented as a triangular region on the $\{\lambda_1, \lambda_2\}$ axes, as shown in the Figure 5.5. The points on the figure are given by: $P_1 = \frac{\rho_{\max} C}{x_1}$, $P_2 = \frac{\rho_{\max} C}{x_2}$. Note that the slope is independent of the server capacity C and is given by $\alpha = -\frac{x_2}{x_1}$. Naturally, the server can serve more traffic coming from the service class with a smaller average size.

We define the state of an operator i by the arrival rate in different service classes: $S_i = (\lambda_{i1}, \lambda_{i2})$. With this definition the linear boundary in Figure 5.5 defines a region in the state space, in which the delay guarantees can be met. For states outside to the right and above the boundary, these delay guarantees cannot be met. For states inside to the lower and left side of the boundary the guarantees are met. A congested operator has a state outside the boundary, and tries to come closer to the boundary by borrowing resources from a normal operator which lies inside the boundary. An example is depicted in Figure 5.6, in which the states of the operators are depicted by dots. Operator 1 tries to move closer to the boundary in order to meet the delay guarantees. Operator 2 tries to move towards its boundary in order to increase its utilization and revenues.

Table 5.2 shows all possible cases of sharing between two operators. We can see that cases 1, 2, and 3 are analog to the cases 8, 7, and 6. In these cases we have one donor operator and one borrower operator. In cases 4 and 5, different classes of shared traffic, go in different directions. Thus each operator plays a dual role: donor respective to class-i traffic and borrower for class-j traffic, where $i \neq j$ and $i, j \in \{1, 2\}$.

The symmetry in the sharing cases, reduces our discussion to two scenarios:

1. **Single-role scenario:** where we have one pure donor operator and another pure borrower operator irrespective of the traffic's class.

2. **Dual-role scenario:** where each operator, who is involved in resource sharing plays different roles (donor and borrower) in different traffic classes.

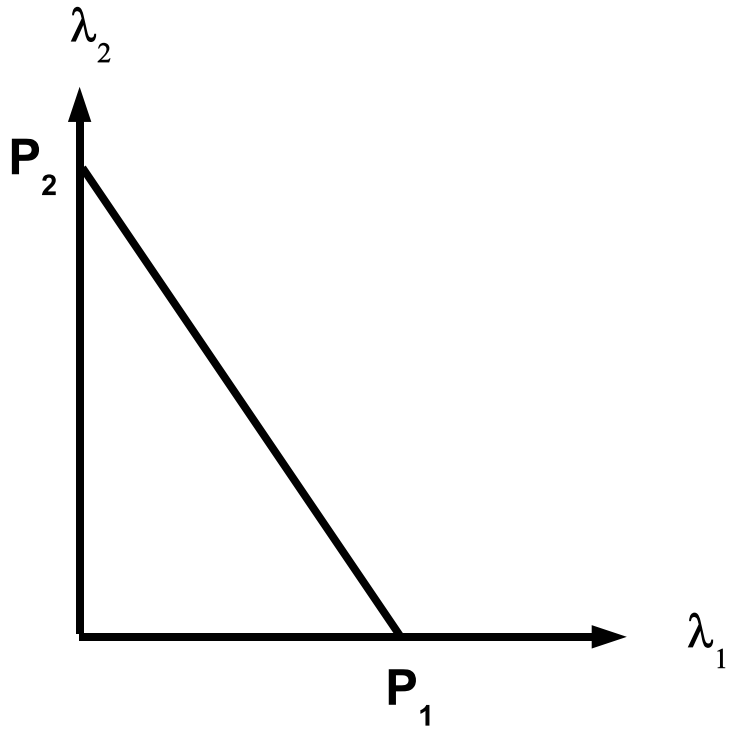

Figure 5.5.: Arrival rate regions.

In the following sections, we will discuss those scenarios, and provide some equations, that can be used for calculating each operator's sharing needs and potentials (donate or borrow) on one side, and facilitate the decision making (to share or not to share) of each single operator on the other side.

An important aspect of resource sharing, is the information available at each operator. Each operator knows its own capacity, and the type of traffic its is serving, thus it is able to calculate his own boundary line. The operator cannot have the same information about the peer operator due to the information asymmetry we discussed earlier. Similar to the single class case we assume that the software agents controlling the sharing use the user experience database.

Multi-Class BCMP Model

Considering a location, where users have two co-located wireless operators to choose from: operator A (Op-A) and operator B (Op-B). Users of different types (or classes) have a Poisson arrivals, with class respective arrival rates λ_1 and λ_2. The users of each class can decide to choose Op-A with the probabilities $P_{A,1}$ and $P_{A,2}$, or Op-B with the probabilities $P_{B,1}$ and $P_{B,2}$. Of course this products $\lambda_1 P_{A,1}$ and $\lambda_2 P_{A,2}$ yield the actual arrivals at Op-A. Thus the following derivations are also suited for the traditional

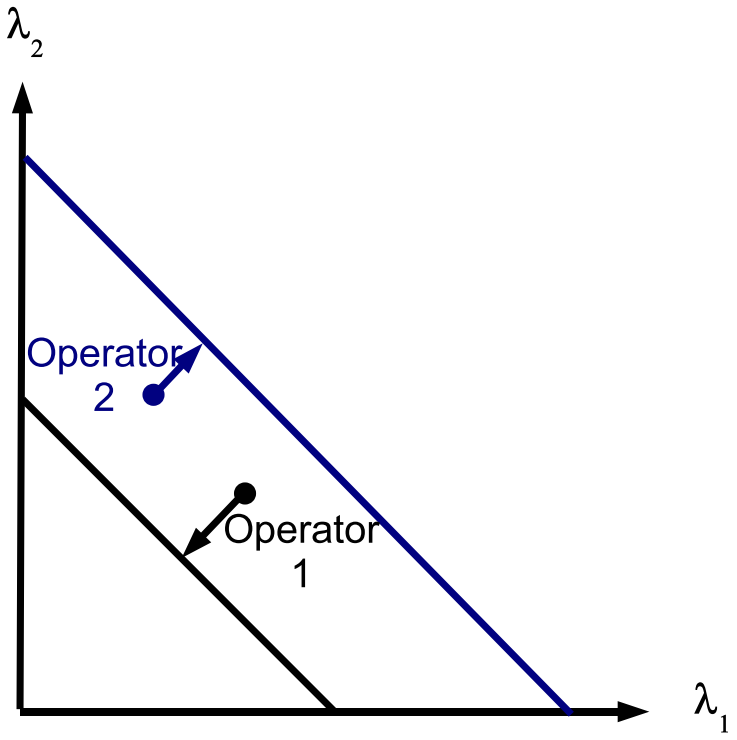

Figure 5.6.: Multi class resource sharing.

operation of wireless networks where user identities are owned by (and tied to) their respective operator. The sizes of the requests have a general distribution with a mean of $\frac{1}{\mu_1} = x_1$ and $\frac{1}{\mu_2} = x_2$ for the classes 1 and 2 respectively. The Grade of Service g, guaranties that no more then g % of the class respective requests excesses the maximum acceptable response times $D_{max,1}$ and $D_{max,2}$.

Using a call admission control (CAC) mechanism the operators can choose to block a certain request with the probabilities $P_{R,A,1}$, $P_{R,A,2}$, $P_{R,B,1}$, $P_{R,B,2}$, or to transfer the request to another operator with the probabilities $P_{T,A,1}$, $P_{T,A,2}$, $P_{T,B,1}$, $P_{T,B,2}$. As discussed before when two operators Op-A and Op-B are involved in some resource sharing, there will be only one direction for the traffic respective to its class. In this case if $P_{T,A,1} \neq 0$, thus we automatically have $P_{T,B,1} = 0$, and so on. The wireless operators,simultaneously serving many users are modeled as a multi class processor sharing queue. Furthermore, different technologies implemented by the different operators, yield different capacities C_A and C_B for the correspondent operator's PS Queue. The CAC is modeled by an IS server, similar to single class model. The BCMP network is depicted in Figure 5.4.

Sharing possibilities			
Operator	case	Class-1 traffic direction Class-2 traffic direction	Operator
Op-B	case-1	$\rightarrow$.	Op-A
	case-2	. $\rightarrow$	
	case-3	$\rightarrow$ $\rightarrow$	
	case-4	$\rightarrow$ $\leftarrow$	
	case-5	$\leftarrow$ $\rightarrow$	
	case-6	$\leftarrow$ $\leftarrow$	
	case-7	. $\leftarrow$	
	case-8	. $\leftarrow$	

Table 5.2.: Sharing Possibilities

Parameter	Description
g	Grade of service
i	Operator index $i \in \{A, B\}$
r	Class index $r \in \{1, 2\}$
λ_r	overall arrival rate of Class-r users
$\frac{1}{\mu_r} = x_r$	average demand size of Class-r requests
$P_{i,r}$	probability that a Class-r user chooses Op-i
$P_{R,i,r}$	probability that Op-i blocks a Class-r request
$P_{T,i,r}$	probability that Op-i transfers a Class-r request
$D_{max,r}$	maximum acceptable response time for Class-r requests
C_i	Capacity of Op-i

Table 5.3.: System's parameters

5.6.4. Multi-Class Load Balancing Variants

Using the traffic equations 5.29, we can write down the individual utilizations as:

$$\rho_{A,1} = \frac{\lambda_1}{\mu_1 C_A} \cdot \Big(P_{A,1}(1 - P_{B,A,1} - P_{T,A,1}) + P_{B,1} P_{T,B,1} \Big)$$
$$\rho_{A,2} = \frac{\lambda_2}{\mu_2 C_A} \cdot \Big(P_{A,2}(1 - P_{B,A,2} - P_{T,A,2}) + P_{B,2} P_{T,B,2} \Big)$$
$$\rho_{B,1} = \frac{\lambda_1}{\mu_1 C_B} \cdot \Big(P_{B,1}(1 - P_{B,B,1} - P_{T,B,1}) + P_{A,1} P_{T,A,1} \Big)$$
$$\rho_{B,2} = \frac{\lambda_2}{\mu_2 C_B} \cdot \Big(P_{B,2}(1 - P_{B,B,2} - P_{T,B,2}) + P_{A,2} P_{T,A,2} \Big) \tag{5.41}$$

These equations form the base of our derivations for the load balancing between the operators. We are interested in defining the suitable transfer probabilities $P_{T,A,1}$, $P_{T,A,2}$, $P_{T,B,1}$ and $P_{T,B,2}$. Let us assume for the sake of illustration that the blocking rate is zero on both of the operators. In this case the utilizations after resource transfer can be reformulated in terms of the initial utilizations as:

$$\rho_{init,A,1} = \frac{\lambda_1}{\mu_1 C_A} P_{A,1}$$
$$\rho_{init,A,2} = \frac{\lambda_2}{\mu_2 C_A} P_{A,2}$$
$$\rho_{init,B,1} = \frac{\lambda_1}{\mu_1 C_B} P_{B,1}$$
$$\rho_{init,B,2} = \frac{\lambda_2}{\mu_2 C_B} P_{B,2} \tag{5.42}$$

$$\rho_{A,1} = \rho_{init,A,1}(1 - P_{T,A,1}) + \frac{C_B}{C_A} \rho_{init,B,1} P_{T,B,1}$$
$$\rho_{A,2} = \rho_{init,A,2}(1 - P_{T,A,2}) + \frac{C_B}{C_A} \rho_{init,B,2} P_{T,B,2}$$
$$\rho_{B,1} = \rho_{init,B,1}(1 - P_{T,B,1}) + \frac{C_A}{C_B} \rho_{init,A,1} P_{T,A,1}$$
$$\rho_{B,2} = \rho_{init,B,2}(1 - P_{T,B,2}) + \frac{C_A}{C_B} \rho_{init,A,2} P_{T,A,2} \tag{5.43}$$

Let us further define the concept of surplus and debt of the donor and borrower operator respectively. Surplus is a measure of resources that donor can donate, and debt is a measure of the needed resources by the borrower.

- **Surplus Op-A:** $\alpha_A = \rho_{A,max} - \rho_{init,A}$
- **Debt Op-A:**$\alpha_B = \rho_{init,B} - \rho_{B,max}$

Letting Op-B be the congested, thus the borrowing operator, and Op-A the normal

and thus the donor operator. We have the following relations:

$$\begin{aligned} \rho_{init,B,1} + \rho_{init,B,2} = \rho_{init,B} \geq \rho_{B,max} \\ \rho_{init,A,1} + \rho_{init,A,2} = \rho_{init,A} \leq \rho_{A,max} \end{aligned} \tag{5.44}$$

After the resource exchange the utilization of Op-A will increase by the amount $\Delta\rho_A = \rho_A - \rho_{init,A}$. Similarly the utilization of Op-B will decrease by the amount $\Delta\rho_B = \rho_{init,B} - \rho_B$. The increase in the utilization should not exceed the surplus of the donor, and the decrease in the borrower utilization should be more than the debt of the borrower. These conditions can be summarized as:

$$\begin{aligned} \Delta\rho_A \leq \alpha_A \\ \Delta\rho_B \geq \alpha_B \end{aligned} \tag{5.45}$$

Observing the equation (5.43), the operators need to have access to ρ_{init} values across all the networks and service classes in order to built a model of the state space positions of each other. By consulting to the delay values of the QoE database, the operators are able to find out these values. However, in order to check the conditions given by inequalities (5.45) they need to be able to guess the maximum utilizations that peer operators are aiming for. Only this way they would be able to calculate each others debt and surplus. However, it is not realistic, that operators would be exchanging such a detailed internal operating parameter. This is why we believe that a peer to peer negotiation mechanism we foresee for single class sharing is not suitable for the multi-class sharing. Instead of this, we postulate the existence of a neutral third party, which we term the SLA broker, that handles the setting of P_T value. It would have access to the debt an surplus of both of the operators. We present the design of such an entity in Section 6.2.

As discussed previously, within a service class the resources will be transferred only in one direction. This leads to the eight different combinations summarized in Table 5.2. Due to the symmetry, we will investigate the Cases 1 through 4.

Single Role

Case 1: In this case class-1 traffic goes from Op-B to Op-A. Thus we have $P_{T,A,1} = P_{T,A,2} = P_{T,B,2} = 0$, and only $P_{T,B,1} \neq 0$. The equation 5.41 yields:

$$\begin{aligned} \rho_{A,1} &= \rho_{init,A,1} + \frac{C_B}{C_A}\rho_{init,B,1}P_{T,B,1} \\ \rho_{A,2} &= \rho_{init,A,2} \\ \rho_{B,1} &= \rho_{init,B,1}(1 - P_{T,B,1}) \\ \rho_{B,2} &= \rho_{init,B,2} \end{aligned} \tag{5.46}$$

Using the definition of $\Delta\rho_A$, $\Delta\rho_B$ and 5.45 we obtain:

$$\begin{aligned}\Delta\rho_B &= \rho_{init,B,1}P_{T,B,1} \geq \alpha_B \\ \Delta\rho_A &= \frac{C_B}{C_A}\rho_{init,B,1}P_{T,B,1} \leq \alpha_A\end{aligned} \tag{5.47}$$

Sharing is only possible if $P_{T,B,1,max}$ as dictated by donor is greater than or equal to the minimum $P_{T,B,1,min}$ needed by the borrower. These values can be calculated with the Equation (5.49). Expanding the values, one obtains the condition for a successful transfer as $\alpha_A C_A \geq \alpha_B C_B$.

$$P_{T,B,1,min} = \frac{\alpha_B}{\rho_{init,B,1}} \tag{5.48}$$

$$P_{T,B,1,max} = \frac{\alpha_A \cdot C_A}{C_B \cdot \rho_{init,B,1}} \tag{5.49}$$

Case 2: is the same as Case 1 except for the shard traffic class.

Case 3: is a generalization of the previous two cases. In this case, the equation 5.41 yields:

$$\begin{aligned}\rho_{A,1} &= \rho_{init,A,1} + \frac{C_B}{C_A}\rho_{init,B,1}P_{T,B,1} \\ \rho_{A,2} &= \rho_{init,A,2} + \frac{C_B}{C_A}\rho_{init,B,2}P_{T,B,2} \\ \rho_{B,1} &= \rho_{init,B,1}(1 - P_{T,B,1}) \\ \rho_{B,2} &= \rho_{init,B,2}(1 - P_{T,B,2})\end{aligned} \tag{5.50}$$

Using the definition of $\Delta\rho_A$, $\Delta\rho_B$ and 5.45 we get:

$$\begin{aligned}\Delta\rho_B &= \rho_{init,B,1}P_{T,B,1} + \rho_{init,B,2}P_{T,B,2} \geq \alpha_B \\ \Delta\rho_A &= \rho_{init,B,1}P_{T,B,1} + \rho_{init,B,2}P_{T,B,2} \leq \frac{C_A}{C_B}\alpha_A\end{aligned} \tag{5.51}$$

We reshape these inequalities according to $P_{T,B,2}$ and we get two inequalities in the $\{P_{T,B,1}, P_{T,B,2}\}$Plane as follows:

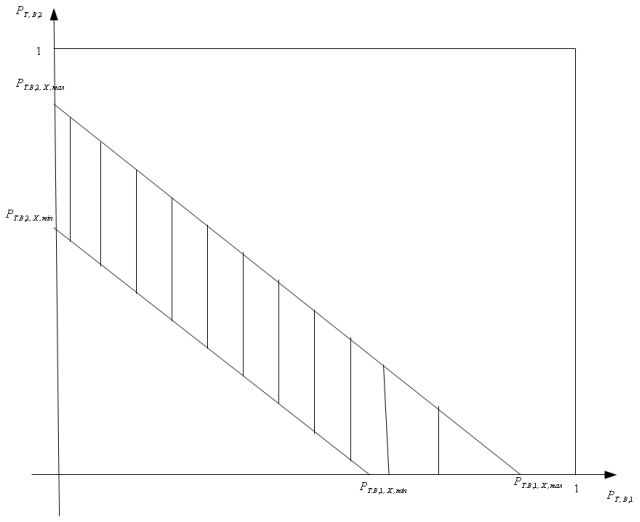

Figure 5.7.: Case 3: Intersection region of sharing.

$$P_{T,B,2} \geq -\frac{\rho_{init,B,1}}{\rho_{init,B,2}} \cdot P_{T,B,1} + \frac{\alpha_B}{\rho_{init,B,2}}$$
$$P_{T,B,2} \leq -\frac{\rho_{init,B,1}}{\rho_{init,B,2}} \cdot P_{T,B,1} + \frac{\alpha_A C_A}{C_B \rho_{init,B,2}} \tag{5.52}$$

As we can see, each one of these inequations defines a region in the $\{P_{T,B,1}, P_{T,B,2}\}$ plane. Each one of these regions is bounded by a line. The two lines have the same slope. The intersection of those regions would be a region of acceptable $(P_{T,B,1}, P_{T,B,2})$-pairs. This relationship is depicted in Figure 5.7. This shows that intersection (therefore sharing) is possible if $C_A \alpha_A \geq C_B \alpha_B$.

Dual Role

In this scenario each traffic class is transferred in another direction. Initially, we will assume that that Op-A is in a normal congestion state whereas Op-B is overloaded, thus we can say that Op-A has a surplus and Op-B is in debt. We will handle the the case when both of the operators are overloaded at the end of this section.

Single Overloaded Operator In Case 4, Class-1 traffic is transferred form Op-B to Op-A, and Class-2 traffic is transferred from Op-A to Op-B. This means we have $P_{T,B,2} = P_{T,A,1} = 0$. Thus the equations 5.41 yield:

$$\begin{aligned}
\rho_{A,1} &= \rho_{init,A,1} + \frac{C_B}{C_A}\rho_{init,B,1}P_{T,B,1} \\
\rho_{A,2} &= \rho_{init,A,2}(1 - P_{T,A,2}) \\
\rho_{B,1} &= \rho_{init,B,1}(1 - P_{T,B,1}) \\
\rho_{B,2} &= \rho_{init,B,2} + \frac{C_A}{C_B}\rho_{init,A,2}P_{T,A,2}
\end{aligned} \tag{5.53}$$

Using the definition of $\Delta\rho_A$, $\Delta\rho_B$ and 5.45 we get:

$$\begin{aligned}
\Delta\rho_B &= \rho_{init,B,1}P_{T,B,1} - \frac{C_A}{C_B}\rho_{init,A,2}P_{T,A,2} \geq \alpha_B \\
\Delta\rho_A &= \frac{C_B}{C_A}\rho_{init,B,1}P_{T,B,1} - \rho_{init,A,2}P_{T,A,2} \leq \alpha_A
\end{aligned} \tag{5.54}$$

We reshape the inequalities again to obtain a description in the $\{P_{T,A,2}, P_{T,B,1}\}$ plane:

$$\begin{aligned}
P_{T,B,1} &\geq \frac{C_A\rho_{init,A,2}}{C_B\rho_{init,B,1}}P_{T,A,2} + \frac{\alpha_B}{\rho_{init,B,1}} \\
P_{T,B,1} &\leq \frac{C_A\rho_{init,A,2}}{C_B\rho_{init,B,1}}P_{T,A,2} + \frac{\alpha_A C_A}{C_B\rho_{init,B,1}}
\end{aligned} \tag{5.55}$$

The inequalities in 5.55 define two regions in the $\{P_{T,A,2}, P_{T,B,1}\}$ plane. Each one of them is bounded with a line having the same slope $\frac{C_A\rho_{init,A,2}}{C_B\rho_{init,B,1}}$. Sharing is possible when the two regions overlap. This is the case when the condition $\alpha_A C_A \geq \alpha_B C_B$ is satisfied. These relations are depicted in Figure 5.8.

Two Overloaded operators In case Op-A is overloaded α_A, which represented his surplus will become negative. The Figure 5.9 shows the impact of having tow overloaded operators.

The two regions won't have any intersection except for the case that $\alpha_A = \alpha_B = 0$. This is the case that both operators are on their boundary lines.

In conclusion sharing is possible only when we have spare resources, that is when some operator is underloaded. Moreover, sharing between an overloaded Op-B and an underloaded Op-A is possible when the following condition holds

$$\boxed{\alpha_A C_A \geq \alpha_B C_B}$$

This condition was concluded for each one of the sharing cases, and is pretty intuitive: sharing is possible when spare resources are larger then the resources, that the overload needs.

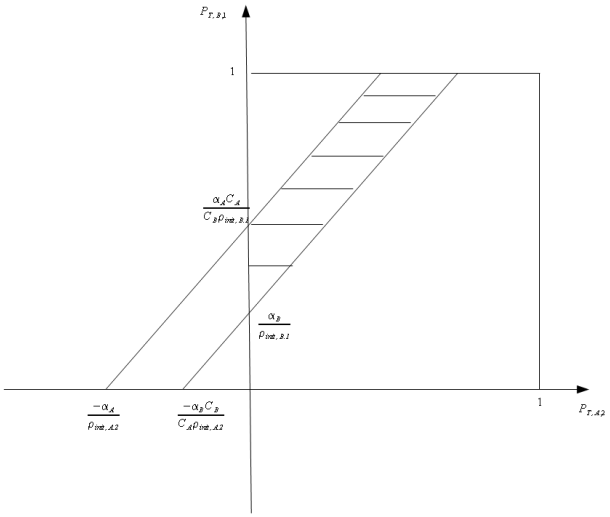

(a) Case 4: Dual Role sharing region

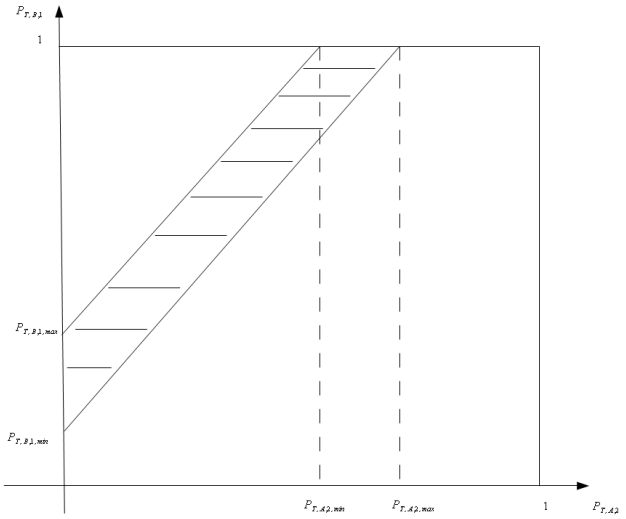

(b) Possible values for sharing

Figure 5.8.: Case 4: The intersection region.

5.6.5. Optimal Transfer Probabilities

In the single role sharing depicted in Figure 5.7, operators have a whole region of acceptable P_T values. This section discusses the impact of costs of sharing on the choice of the sharing parameter.

We Assume that each operator offers a Flat-Rate for the users. Thus there will be no

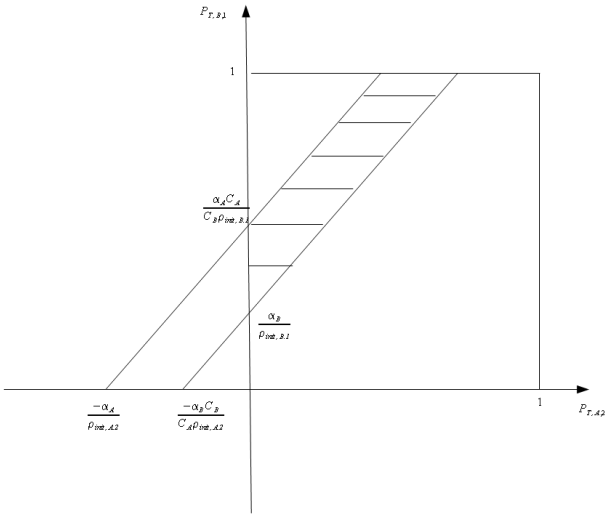

(a) Op-A normal.

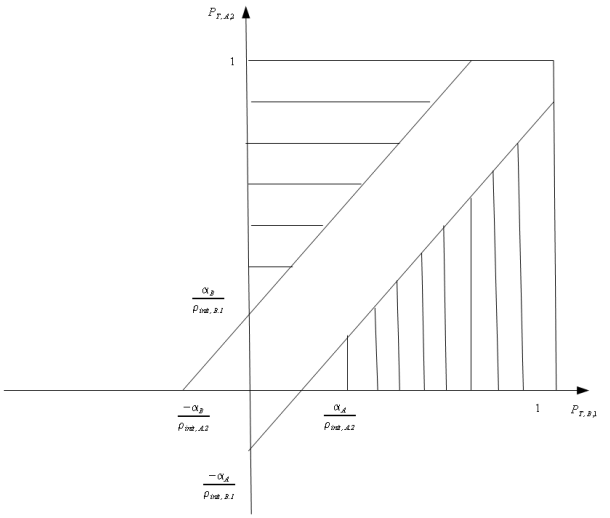

(b) Op-A congested.

Figure 5.9.: Impact of overload Op-A

difference in the utility in case users who choose him, produce Class-1 or Class-2 traffic. On the other hand transferring different traffic types could be associated with different costs. In total the overloaded operator (Op-B) wishes to minimizes the costs arising from sharing.

From the region depicted in the Figure 5.7, it would intuitively want to go to the

lower line, since more transfer will be automatically associated with higher costs. The equation of this line is given by Equation (5.56). The goal is to find which point on this line is associated with the lowest costs.

$$\rho_{init,B,1} P_{T,B,1} + \rho_{init,B,2} P_{T,B,2} = \alpha_B \tag{5.56}$$

The transfer of a class-1 and class-2 session, will be associated with costs of c_1 and c_2 respectively. Thus the total cost Op-B by transferring a mix of sessions from service class 1 and 2 is given by:

$$K = n_1 \cdot c_1 + n_2 \cdot c_2 \tag{5.57}$$

where n_1 and n_2 are the class respective numbers of transferred sessions. These can be calculated over a specific sharing duration D by:

$$\begin{aligned} n_1 &= D \cdot P_{T,B,1} \cdot \lambda_{init,B,1} = D \cdot \frac{P_{T,B,1} \cdot \rho_{init,B,1} \cdot C_B}{x_1} \\ n_2 &= D \cdot P_{T,B,2} \cdot \lambda_{init,B,2} = D \cdot \frac{P_{T,B,2} \cdot \rho_{init,B,2} \cdot C_B}{x_2} \end{aligned} \tag{5.58}$$

Using equation 5.58 in equation 5.57 yields:

$$f(P_{T,B,1}, P_{T,B,2} = \frac{K)}{D \cdot C_B} = \frac{c_1}{x_1} \cdot P_{T,B,1} \cdot \rho_{init,B,1} + \frac{c_2}{x_2} \cdot P_{T,B,2} \cdot \rho_{init,B,2} \tag{5.59}$$

which represents a function of $(P_{T,B,1}, P_{T,B,2})$ we want to minimize under the constraint in Equation 5.56.

Now we plug equation 5.56 in 5.59 and obtain:

$$f(P_{T,B,1}) = \frac{c_2 \cdot \alpha_B}{x_2} + P_{T,B,1} \cdot \rho_{init,B,1} \cdot \left(\frac{c_1}{x_1} - \frac{c_2}{x_2} \right) \tag{5.60}$$

The minimum of this function depends on the relationship of $\frac{c_1}{x_1}$ and $\frac{c_2}{x_2}$. If the two fractions are equal, thus we would have a constant cost for sharing. In this case it does not matter which point, on the line defined in equation 5.56 we choose.

In case the of $\frac{c_1}{x_1} \leq \frac{c_2}{x_2}$ the minimum of equation 5.60 will be at:

$$\begin{aligned} P_{T,B,1} &= \frac{\alpha_B}{\rho_{init,B,1}} \\ P_{T,B,2} &= 0 \end{aligned} \tag{5.61}$$

In the last case, the term $\frac{c_1}{x_1} \geq \frac{c_2}{x_2}$, the minimum of equation 5.60 will be at:

$$P_{T,B,1} = 0$$
$$P_{T,B,2} = \frac{\alpha_B}{\rho_{init,B,2}} \tag{5.62}$$

Thus we conclude that under the mentioned cost assumptions, it it not optimal to transfer mixed traffic.

5.7. Conclusion

In this Chapter we presented a mathematical description for single and multi-class resource sharing between two operators. For the single-class case, we were able to present a closed form expression for the delay variation as a function of transfer probability. We also provide the derivation of optimal transfer probability. For multi-class sharing, we established the conditions for resource sharing and characterized different sharing options. We will use this model for the rest of the work as the fundamental mathematical description. In Chapter 6, we will demonstrate how transfer probabilities can be negotiated between operators, by using the models developed in this Chapter.

6. Negotiation Problem

Negotiation Problem is concerned with the following question: "How can two or more operators agree on a transfer probability?"

In this Chapter we present two different solutions to the negotiation problem. The borrowing and donating operators have to agree on the amount of traffic to be exchanged between them, which is the negotiation problem. We first present in Section 6.1 a bilateral negotiation mechanism, which is able to come up with the optimal transfer probability that corresponds to the minimal borrower delay with out any central entity. For this purpose we employ the principles of *Mechanism Design* . The bilateral mechanism is developed for the single class scenario. Multi-class scenario cannot be solved using the same techniques. For the solution of the multi-class negotiation problem, we use auction mechanisms involving a central and trusted third party, that acts as a mediator for resource sharing among two or more operators. We present these results in Section 6.2.

6.1. An Incentive Compatible Negotiation Mechanism for Single Class Resource Sharing

6.1.1. A Primer on Negotiation Mechanisms

Our primary reference for negotiation mechanism design in is Zlotkin and Rosenschein's book [70]. The authors focus on automated systems that are involved in resource allocation related tasks, where it may to the designers interest if the automated systems coordinate to share resources. In other cases automated systems are obliged to cooperate in order to function properly, since their actions may be interfering with each other. So there are decisions that are to be taken in accordance with other machines. The aim is to enable development of protocols that allow flexible and constructive agreements between machines, that represent the interest of their designers, that reach compromises if it is for the benefit to the designer.

The focus of the book is distributed systems, consisting of components that are designed by self-interested designers, with disparate interests. The approach can be seen as the application of Game Theory to the area of multi-agent systems. The Game Theory is the mathematics of encounters of decision making entities, and is perhaps more suitable to machine to machine encounters then the human encounters, for which it was originally developed for. The multi-agent systems is on the other hand is a branch of artificial intelligence, where the agents are:

- designed by self interested designers,

- not benevolent to other agents by default,
- and the utility is defined at the agent level, not at the system level.

The authors approach can be summarized as applying the mathematical tools of game theory in the engineering problem of designing multi agent systems. This effort can be seen from a social engineering for a machine society perspective. This social engineering is composed of designing of punitive mechanisms, incentive mechanisms and protocols. The goal of these mechanisms and the protocol is to make it beneficiary for the self interested designer of the agent to design his agent in a way that is parallel to the desired system behavior. A protocol, from the perspective of negotiation mechanism design, denotes the public rules to which agents should comply with, when they are interacting with other agents. Related with each protocol is a strategy, which is the way an agent behaves in an interaction, given the protocol.

Domains

Negotiation is the act of multiple agent searching for an agreement. The search process involves a combination of exchange of information between agents, the relaxing of initial agent goals, lies or threats. Negotiation processes are associated with *domains*. These domains are:

- *Task Oriented Domains (TOD)*
- *State Oriented Domains (SOD)*
- *Worth Oriented Domains (WOD)*

Tasks are indivisible jobs that have to be executed by the agents. The TOD's are characterized by the agent activity is limited to a set of tasks that has to be completed.There are no interference between the agents. All the agents have the necessary capabilities and resources to complete the tasks. Cooperative opportunities arise from the fact that a redistribution of tasks among the agents may lead to a more efficient solution. For this reason TOD's are inherently cooperative.

In the SOD's the agents are interested to change the state of the world that the agents reside. This facts complicates the analysis and design, compare to the TOD's. The main difference between SOD and TOD is that the elementary actions that one of the agents execute may bring the environment to a state that is closer or further to the goal of the other agent. Thus both have positive or negative interactions are possible between agent actions. Therefore the SOD's are not intrinsically cooperative. More than this, there is also the possibility of goal conflicts, when there exists no environment state that satisfies the goals of the involved agents.

WOD's are generalizations of SDO's. In WDO's each state is associated with a worth measure by each of the agents. The SOD's than, can be seen as a subset of WOD, where the worth function is binary one, i.e. a state is either desirable on not-desirable. Such an extensions of the worth function allows more interesting cooperation opportunities

between the agents, that may involve the relaxing of the worths that the agents associate to different states.

Properties of Negotiation Mechanisms

There may be more than one suitable negotiation mechanism that is suitable for a given domain. To be able to compare these mechanisms there have to be certain attributes of the mechanisms that must be compared. These attributes include:

- **Efficiency:** The agreements reached after the negotiation should not waste any agent resources. The efficiency can be seen from Pareto terms, or global terms.
- **Stability:** No agent should have an incentive to deviate from the agreed upon strategies. Related with this property is the concept of self perpetuating behavior. If in an open system it is to the benefit of the each agent to behave according to the agreed upon rules, the social behavior will be stable even in the case of members leaving or joining the society.
- **Simplicity:** The amount of resources devoted to the negotiation mechanism should be smaller than the gain achieved by the negotiation.
- **Distribution:** Central decision makers should be avoided.
- **Symmetry:** The negotiation mechanism should not be biased against or for any of the involved agents.

Assumptions

The authors make certain important assumptions in the book, which we list here.

- Agents will always try to maximize their expected utilities. This means they will take risks if the outcome will bring a higher utility.
- The negotiations are isolated. Agents behavior in a certain negotiation does not affect his behavior in his later negotiations.
- The agents can compare their utilities with each other, through common utility units.
- The agents are symmetric, that is they all have the same capabilities.
- If an agent makes a commitment it is binding. This is possible if the commitments are followable through public behavior.
- There is no way of transferring utility between agent through the use of a currency. That is, an agent cannot convince another agent to give up his expected utility maximizer property by giving him the currency.

Deception-Free Protocols

There is a distinction between *public* and *private* behavior of the agent is necessary. The adherence to the protocol is the public behavior, and the strategy used is the private behavior associated with an agent. As the protocol and the offers are public, it will be relatively easy to track the public behavior of the agents. This cannot be said for the private decision making of the agents, as it is practically impossible to track the strategy of the agents, even if their strategies are made public in terms of software. Thus it cannot be taken for granted that the agents will be following a strategy that is agreed upon. It is therefore desired that the strategies are self-enforced. Negotiation mechanism in which certain strategies are enforced are called *incentive compatible* mechanisms.

Encounter Types

The aim of the negotiation mechanisms is to come up with a joint plan that will bring the world to a state that will be a member of both agents goals. There are four possibilities in SOD, depending on the goals of the different agents.

1. There exists no world state that satisfies the agent goals.
2. There exists a world state that satisfies the agent goals.
3. There exists a world state that satisfies the agent goals, but it is not *reachable* with primitive agent operations.
4. There exists a world state that satisfies the agent goals, and is reachable though primitive operations, but it is too expensive, so the agents choose not to proceed.

There are different types of non-cooperative encounters, which are summarized in Figure 6.1 in which the Euclidian distance represents the cost of a plan. In 6.1a by choosing a state in the intersection of the goal sets, they can beat any other one agent plan in their goal sets. In 6.1b the agents have to do additional work by agreeing on a state in the intersection, however the increase in the costs are symmetric. Note that these increased costs should not exceed the worth of the individual agents. 6.1c is different from the previous case, the agent with the horizontal goal set benefits from the joint plan, whereas the one with the vertical set has to compromise. Finally 6.1d represents the conflict situation.

6.1.2. A Mechanism Design for Bilateral Resource Negotiations

Our aim is to design an *efficient*, *incentive compatible*, *decentralized* negotiation mechanism based on the QN description of the interaction between two operators developed in Chapter 5. The interaction can be modeled as a SOD, in which the states of the world are the congestion statuses of the individual operators. Each operator wants to avoid congestion.

We provide a hierarchical solution to the mechanism design problem. In the first part of the interaction, the players declare their congestion states. We formulate this

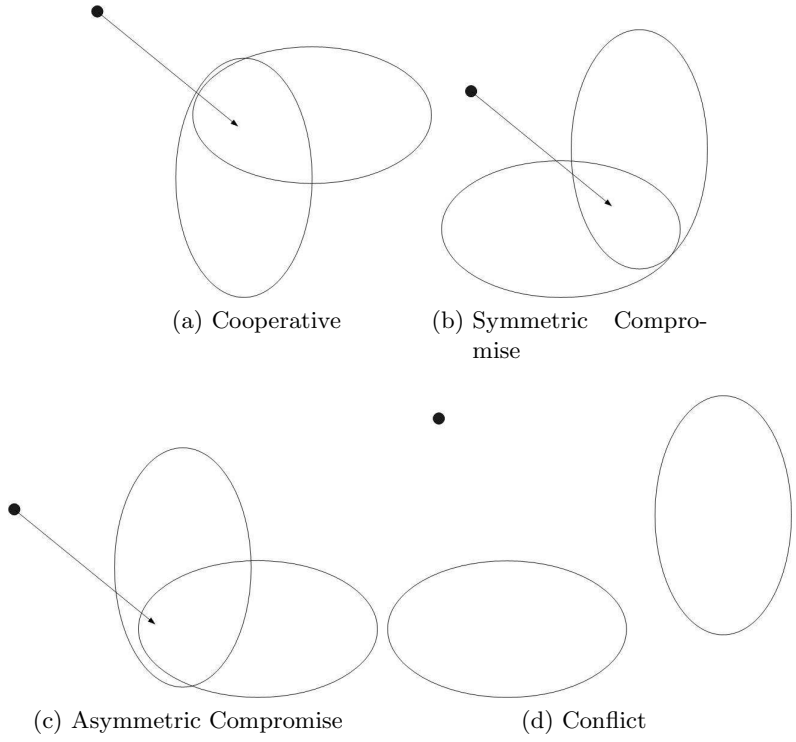

(a) Cooperative (b) Symmetric Compromise

(c) Asymmetric Compromise (d) Conflict

Figure 6.1.: Different encounter types taken from [70]

interaction in the presence of a user-generated QoE database as the First Level Game. By providing the solution to this game, we show that it is futile to lie about the congestion state. Once the congestion states are known to both operators, each operator knows its role as a borrower or a donor.The second part of the interaction involves making an offer and a counter offer on the acceptable and desired transfer probabilities. We solve the second level game, to show that the mechanism we propose is incentive compatible, and it is futile to lie about the transfer probability offer and the counter offer.

First Level Game

The first level game is defined by the *n-tuple* :

$$< N, A, \Theta, u(\cdot) > \tag{6.1}$$

There are $N = 2$ players, labeled with $i \in \{1, 2\}$. Each player can choose between two actions, constituting the action space $A = \{\text{tell truth, lie}\}$. Each player's type θ_i can be one of the two members of the type space $\Theta = \{\text{normal, congested}\}$. Furthermore each player has a belief about the type of the other player, given by $b_i(\theta_{-i})$. This belief is updated by making observations on the data available in the QoE database, which we will discuss shortly.

At the beginning of the interaction, the players declare their types, these *declared types* are denoted by θ_i^d Both players use the results of their observations in order to decide on a *assumed type* of the peer player, denoted by θ_i^a. Each player compares the assumed type about the peer player with the type that the peer player declares. If the assumed type does not match the declared type, the second game is not played. Thus the second game is played, and the interaction is continued only if the declared type and the assumed type matches for both players. Since overall payoff depends on the second game, we define the following unitary utilization function for the first game:

$$u(\theta_i, \theta_{-i}) = \begin{cases} 1 & \text{if } \theta_{-i}^d = \theta_i^a \\ 0 & \text{otherwise.} \end{cases} \tag{6.2}$$

We now elaborate how the user QoE database is exploited by the players to build assumed types of their peers. The database is filled by the users, and contain subjective MOS values which summarize users satisfaction with a certain application running on a certain RAN. It also contains objective QoS values such as end to end delay, jitter and average bandwidth. The operators are able to query these records according to the RANs that the reports are describing. Each player queries the reports originating from the other player. The results of the query constitutes an observation O, such as: *"the probability that delay is larger than 1 seconds is 0.001"* or *"95% percent of the users report a MOS value of 3"*. We assume that the players can calculate to *a priori* distributions of the observations, i.e. $P(O|\theta_{-i} = \text{normal})$, $P(O|\theta_{-i} = \text{congested})$. The players also can estimate $P(\theta_{-i} = \text{congested})$ $P(\theta_{-i} = \text{normal})$ by observing the delay values of the peer player for a long period of time. The calculation of these probabilities depend on the actual observation, the congestion condition, and the distribution of network loads, and outside the scope of this section. We give a concrete example in Chapter 8. With the observation O available to the player, it evaluates the Bayesian *a posteriori* probabilities:

$$P(\theta_{-i} = \text{congested}|O) = \frac{P(O|\theta_{-i} = \text{normal}) \cdot P(\theta_{-i} = \text{normal})}{P(O)} \tag{6.3}$$

$$P(\theta_{-i} = \text{normal}|O) = \frac{P(O|\theta_{-i} = \text{congested}) \cdot P(\theta_{-i} = \text{congested})}{P(O)} \tag{6.4}$$

The assumed type is set to the type that maximizes the a posteriori probability, since this is the best estimate given the evidence. This means comparing Equations (6.4) and (6.4) :

$$\theta_i^a = \underset{\theta \in \Theta}{\text{argmax}}\, P(\theta_{-i} = \theta|O) \tag{6.5}$$

With the definition of the assumed type and the utilization function, we are ready to present the first level game in its normal form in and its solution in Table 6.1. The solution of this game is for both operators to tell the truth about their types. This is

	TRUE $\theta_1^d = \theta_1$	**LIE** $\theta_1^d = \overline{\theta}_1$
TRUE $\theta_2^d = \theta_2$	(1,1)	$\leftarrow$ (0,1)
LIE $\theta_2^d = \overline{\theta}_2$	$\uparrow$ (1,0)	$\leftarrow$(0,0)

Table 6.1.: Normal form representation of the first level game.

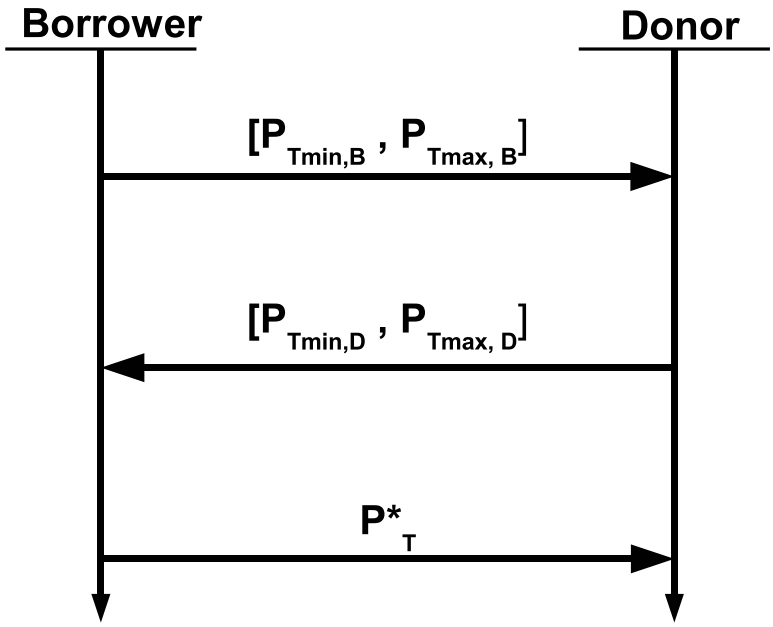

Figure 6.2.: Negotiation Mechanism

made possible by the availability of the QoE database, which allows players to detect the lies. After the declaring their true congestion types, the operators go ahead with the second game, which involves an agreement on the P_T value.

Second Level Game

We have shown through the first game, that it is rational for both operators to declare their true types. After type declaration the congested operator is designated as the borrower, and the normal operator is designated as the donor. The sequence of interaction after this point is given in Figure 6.2. The borrower first sends a message containing the minimum and maximum P_T values that it needs, which constitute the feasibility $S_B = [P_{T_{\min},B}, P_{T_{\max},B}]$. The donor operator replies with its own feasibility set $S_D = [P_{T_{\min},D}, P_{T_{\max},D}]$. Obviously, the solution should lie in the intersection of the two feasibility sets, i.e. $P_T^* \in S_B \bigcap S_D$.

The type of the intersection set is a function of the relative traffic levels of the operators. We discern three different encounter types.

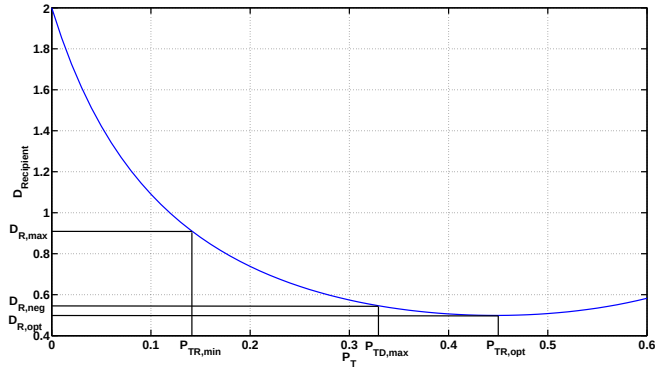

(a) Recipient delay.

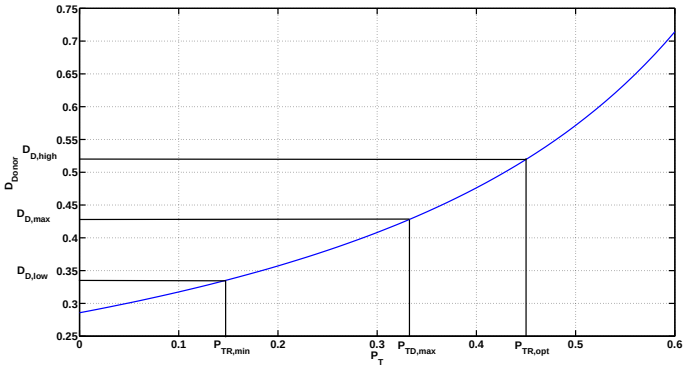

(b) Donor delay.

Figure 6.3.: Case 1.

Encounter Type 1 In the first type of the encounter depicted in Figure 6.3, the intersection set is given by $[P_{TR,\min}, P_{TD,\max}]$. The set is limited on the right with the maximum P_T that can be supported by the donor operator and the minimum P_T that is required by the borrower operator. The intersection does not include optimum minimum delay, thus is not feasible in this encounter.

Encounter Type 2 In the next type of encounter depicted in the Figure 6.4, the donor can tolerate delay larger than the optimal borrower delay value. The intersection set is given by $[P_{TR,\min}, P_{TR,\max}]$. Since the joint feasibility set is bounded to the right by the P_T corresponding to optimal minimum delay, the optimum borrower delay is feasible.

Encounter Type 3 In the final encounter type, depicted in Figure 6.5, the feasibility set is empty. The borrower operator should increase its blocking probability, and re-initiate the negotiation. The amount with which blocking probability that should be increased is given by $P_{TR,\min} - P_{TD,max}$.

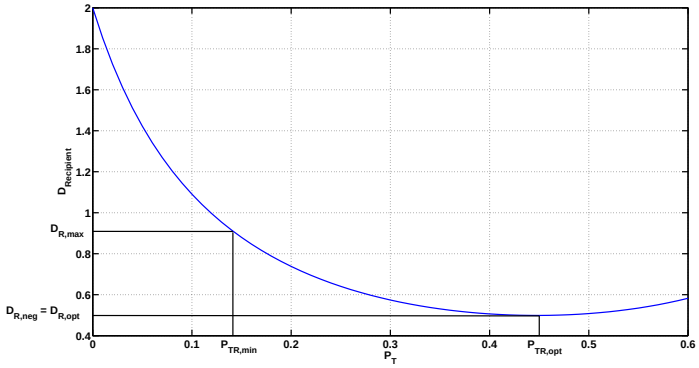

(a) Recipient delay.

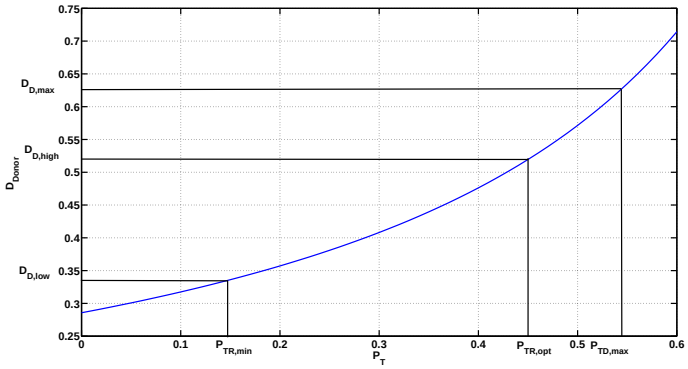

(b) Donor delay.

Figure 6.4.: Case 2.

The Mechanism A mechanism M is defined by the outcome it assigns to the actions of the donor and the borrower, denoted by σ_d and σ_b. In our case the output of the mechanism is a p_T^* value that has to be agreed upon:

$$P_T^* = M\left(\sigma_i, \sigma_j*\right) \tag{6.6}$$

The actions of the operators are the values they assign to the maximum and minimum P_T values in their offers. Our aim is to design the mechanism, or the rule that chooses the agreed P_T^* value out of the joint feasibility set, in a manner that the operators are obliged report the correct P_T values in their offers.

The design of the mechanism is dependent on the utility functions of the individual operators. Let us investigate costs an benefits of the individual operators in order to define the utilities. The borrower gains from sacrificing some of its traffic, by offering its customers a better QoE. On the other side, this involves a financial compensation that constitute the cost of borrowing. In order to formulate an utility function for

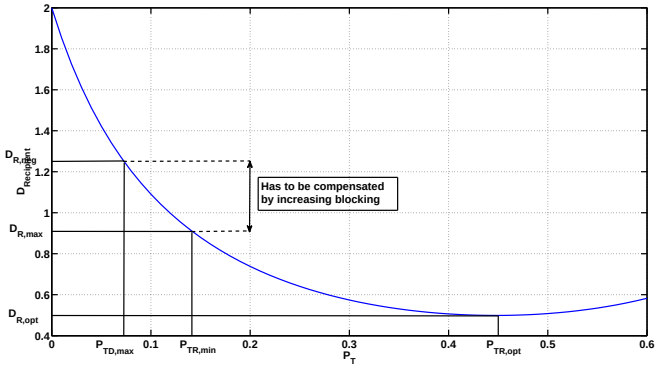

(a) Recipient delay.

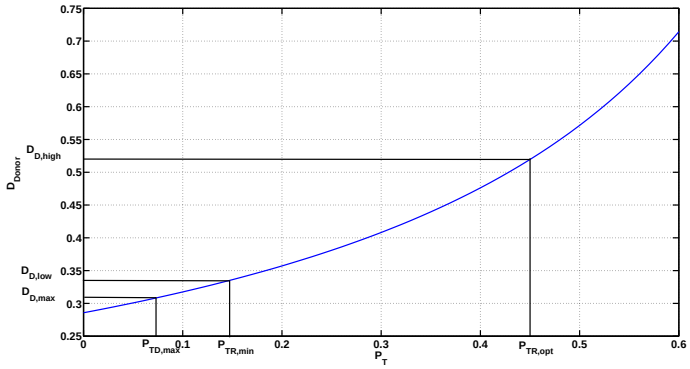

(b) Donor delay.

Figure 6.5.: Case 3.

the borrower, one must account for the financial benefit of the decrease in delay and subsequent increase in user QoE. In [71] Lin et. al. present a relation between the blocking probability and the churn rate, i.r. the rate with which users break their contracts. This relation is given in Equation (6.7).

$$C(P_b) = \frac{1}{1 + e^{\chi(\beta - P_b)}} \tag{6.7}$$

The authors choose blocking parameter as their QoE parameter in this relation. The delay guarantees we employed in Chapter 7 can also be used in the place of the blocking probabilities. This would mean that a higher probability with which the delay guarantees are not met, i.e. a higher P_b in Equation (6.7), the higher the churn rate will be. The relation is exponential. A higher churn rate means a loss of revenue for the congested operator. Offering a lower delay, and increasing the QoE is beneficial, by reducing the churn rate, and avoiding loss of revenue due to churning. We do not have access to

actual internal figures of the operators, but judging by the importance of keeping churn rates low by the operators, we make the following assumption: The long term financial benefits of offering a better QoE by offering a lower delay is comparably larger than the instantaneous cost of transferring traffic to another operator, and sharing a part of the revenue with the resource donating operator.

At the first glance, the donor operator might look like to be working without any costs. As long as the P_T does not exceed a critical value above which delay bound cannot be made, an increasing P_T means increasing financial benefit. However, one has to take into account the opportunity cost associated of not accepting any traffic from the other operators under any other circumstance. Due to the dynamic nature of the user demand, operators will be in position to be donor and borrower on different time instants. Lets assume there are two operators A and B. The operator A might refuse to be the donor when Operator is in a borrower position, with the hope that the users of operator B will churn to operator A as a result of low QoE during the congestion period. However this decision would mean that the operator A will not be able to find a donor, when congestion strikes it, since Operator B would be unwilling to help operator A. This would mean Operator A would have to suffer a lower QoE during congestion periods, leading to an increased churn rate and lost revenue according to Equation (6.7). In the competitive market of the network operators, keeping users is more important than gaining new users. This is the reason why we assume that the instantaneous benefit of being a donor is comparably larger than the long term opportunity costs.

Under these conditions, we can define the utility function as an increasing function of P_T for both operators. This means both the donor an borrower operators are satisfied more with a larger P_T within their prospective feasibility regions. For the donor, the form of the function is linear since more accepted additional traffic means more revenue. For the sake of simplicity, we also choose a linear function for the borrower. Thus the utility function of the operators is given by (6.8), where α is a positive constant:

$$u(P_T) = \alpha P_T + \beta \tag{6.8}$$

We are now in a position to define the mechanism. Given that the operators report their respective feasbility sets S_d and S_b, our mechanism chooses the P_T^* as the right bound of the joint feasibility set:

$$M\left(S_d, S_b\right) = \max P_T \in S_d \bigcap S_b \tag{6.9}$$

With the utility function defined in Equation (6.8), we claim that this mechanism is strategy proof:

Lemma 6.1.1 *Given the outcome of the first game, the mechanism forces a unique solution. For any other sets T_b and T_d we have: $u(T_b, T_d) < u(S_b, S_d) \forall T_b \neq S_b$ and $T_d \neq S_d$*

The donor has a single value to report. The lower boundary of the donor feasibility set is always zero, since the donor can work without any transfer. We claim that the

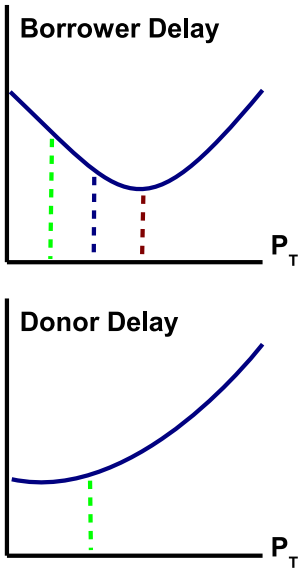

Figure 6.6.: A futile lie.

right boundary of the offer is $P_T(D_{\max,D})$, where it represents the P_T value corresponds to the maximum donor delay value $D_{\max,D}$. Any P_T value larger than $P_T(D_{\max,D})$ is outside of the feasible set, since delay is above $D_{\max,D}$. Any P_T value smaller than P_T reduces the utility of the donor according to Equation (6.8). Therefore the strategy to make the offer$[0, P_T(D_{\max,D})]$ is dominant for the donor.

For the borrower, there are two non-zero values to report. For the right boundary, it is always beneficial to report the $P_{TR,opt}$. Any P_T above this value is outside the feasible region, since the same delay is achievable by a P_T to the left of the $P_{TR,opt}$, which is inside the feasibility set. Reporting any value smaller than $P_{TR,opt}$ results in a smaller utility according to Equation (6.8). So it is rational to use $P_{TR,opt}$ as the right boundary of the offer.

The left boundary to be used in the offer is a little bit more complicated. Due to the increasing utility with increasing P_T, the borrower may be tempted to report a value larger than $P_T(D_{\max,B})$, the delay corresponding the delay bound it offers on its network. This logic would result in the borrower making the offer $[P_{TR,opt}P_{TR,opt}]$, due to the monotonic increasing utility. However, this strategy would risk an empty joint feasibility set as in Encounter Type 3 described in Section 6.1.2, which results in zero utility. This is depicted in Figure 6.6. If the borrower lies and makes the offer $[P_{TR,opt}P_{TR,opt}]$ depicted in red, the joint feasibility set is empty. If it makes the offer $[P_T(D_{\max,B})P_{TR,opt}]$, depicted in green, the joint set is bounded by the right by the maximum delay that the donor can offer. Since the borrower is the first one that makes the offer, and therefore does not have the access to $P_T(D_{\max,D})$, this is not a risk worth taking. Therefore it is rational for borrower to make the offer $[P_T(D_{\max,B})P_{TR,opt}]$. This proves our lemma.

To summarize, the mechanism we propose in Equation (6.9), for the interaction depicted in Figure 6.2, forces the borrower to make the offer $[P_T(D_{\max,B})P_{TR,opt}]$ and the donor to make the counter offer $[0P_T(D_{\max,D})]$. When the intersection of these sets are non empty, the mechanism chooses the utility maximizing right boundary of the intersection set. It is not beneficial for any operator to deviate from the rules of the encounter, and thus the mechanism is strategy proof. Combined with the first step game, the interaction provides a simple and trustable interaction mechanism between two operators which are willing to share resources in times of congestion.

6.2. Centralized Solution for Multi-class Resource Sharing

6.2.1. Introduction

As we discussed in Section 5.6, the multi-class resource sharing requires a neutral third party that both operators trust. The QoE database is not strong enough to overcome the information asymmetry problem for multiple service classes. In this chapter we present an integrated solution that involves a neutral third party we call the SLA broker. With this entity, multiple operators who are in a resource sharing agreement are able to exchange resources among each other to overcome congestion situations involving multiple classes of service.We formulate the interaction in terms of two games, the intra-operator and the inter-operator games. In the former, the RANs belonging to an operator play a bargaining game to share the bandwidth of an incoming service request. If an operator needs extra bandwidth to support the service request, it does so by playing the second game with other operators, who share the bandwidth offered to the service request.

6.2.2. State of the Art

As in many areas of the networking field, application of game theory concepts to CRRM problem has been considered using both cooperative ([72, 73]) and non-cooperative / competitive ([74, 75, 76]) game models to obtain efficient resource allocation schemes. Badia et al. provided a comparison between non-cooperative and cooperative models in resource allocation and demonstrated that collaborative strategies are able to improve the overall system performance [77]. A *bankruptcy game* is used in [72] to model the problem, but within a limiting scenario regarding the composition of available access technologies. All these studies that apply game theory to CRRM are confined to a single network operator scenario. Our approach differs from these work from the perspective that the resource sharing takes place across operator boundaries.

6.2.3. Model and Assumptions

We consider a coverage region R covered by various *radio access networks* (RAN) owned by different operators. The region R is divided into coverage areas a. An area is defined to be the geographical region which is covered by element(s) from the set of RANs.

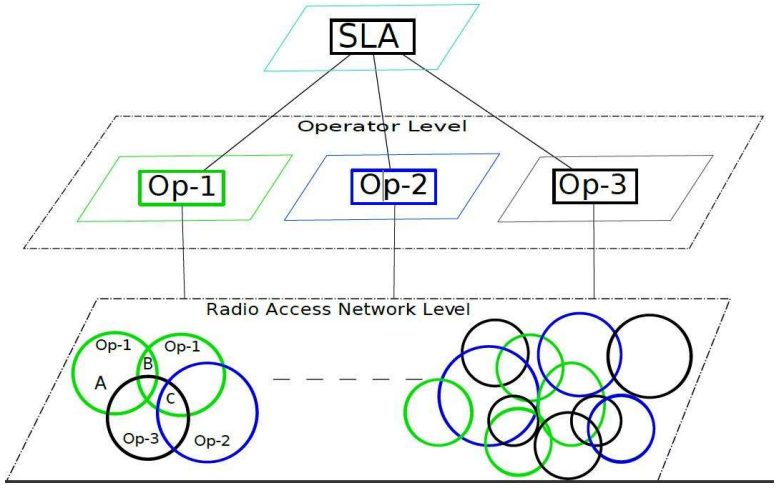

Figure 6.7.: Different coverage cases in a multi-operator multi-technology scenario

An area may be covered by a single RAN, by multiple RANs belonging to a single operator, or by multiple RANs belonging to multiple operators. We assume there are n different *radio access technologies* (RAT) which are combined into RANs by the network operators, and m different operators. This topology is depicted in Figure 6.7

A consequence of this hierarchy is the different definition of load and congestion for the RAN and area that is covered by different RANs:

1. RAN congestion: A RAN is said to be in *RAN congestion region* if its available bandwidth falls below some pre-defined threshold value.

2. Aggregated Congestion: An operator network is said to be in the *aggregated congestion region* in an area a if the aggregated available bandwidth of the RANs belonging to the operator in this area falls below some threshold value.

We assume that users have contractual agreements with a *home operator* and generate application requests of different QoS classes. We further assume that applications are divisible meaning thereby that an application can run on multiple interfaces of different characteristics simultaneously. Upon initial access selection, which is not a part of this work, a user connects to the home network using some RAN belonging to its home operator first, and generates bandwidth requests for applications of different service classes. The home operator first allocates this bandwidth request to different *home* RANs in the area. We assume there is a functional CRRM entity that coordinates RANs of an operator in the area. If the operator is experiencing aggregated congestion in the area where the user is located, it will not allocate the bandwidth right away, but will request additional bandwidth from *foreign operators* which have RANs in the area, and are willing to share bandwidth. We assume that operators are in contractual agreements with each other to share resources, in terms of *service level agreements* (SLA). The interaction between operators is monitored by a *SLA broker*, which is an independent

neutral entity. After the interaction, the requested bandwidth is distributed among those operators who are willing to share bandwidth and their RANs are present in the area. Each operator treats its share of the bandwidth as a new bandwidth request.

The first step in which the requested bandwidth is shared between the RANs of the same operator is called the *intra-operator resource allocation*, and the second allocation step is called the *inter-operator resource distribution*. In this paper we extend our previous work [78], in which we formulate the intra-operator step as an bankruptcy problem and find the estate allocation to creditors using *Kalai-Smorodinsky* bargaining solution . Application of bargaining solution to bankruptcy problem is natural in that bankruptcy problems create the situation of conflict over distribution of estate and to resolve the conflict the creditors (players) negotiate to get to the point of agreement. Such negotiations are best framed using bargaining solutions. In this paper we also formulate the inter-operator game on the same lines and find the suitable utility distribution rule using KSBS. KSBS suits our problem formulation because of its *individual monotonicity axiom*, which is further detailed in the later sections.

In Chapter 5, and especially in Section 5.6, the debt and surplus of the operators were given in unit-less differences in utilization. However in our description in this Section we are interested in bit rates. These two values are interchangeable via the capacity of the individual RANs. A $\Delta\rho$ increase or decrease in a RAN with a capacity of C Kbps is equivalent to a traffic exchange of $C \cdot \Delta\rho$. We continue the discussion with this exchange factor in mind.

6.2.4. Game Theory Background

Let us start by reviewing several basic definitions and concepts related to the bankruptcy problem and bargaining solution of cooperative games.

Bankruptcy Problem

Bankruptcy is a distribution problem, which involves the allocation of a given amount of good among a group of agents, when this amount is insufficient to satisfy the demands of all agents. The available quantity of the good to be divided is usually called estate and the agents are called creditors. The question is: *How to distribute estate amongst creditors?* A number of distribution rules have been proposed to deal with such problems. The solution to a bankruptcy problem can be interpreted as the application of an allocation rule that gives sensible distribution of estates as a function of agents' claims. Formally bankruptcy is the pair (E, C), where E represents the estate to be distributed among a set C of the claims of n creditors, such that

$$C = (c_1, \ldots, c_n) \geq 0 \quad \text{and} \quad 0 \leq E \leq \sum_{i=1}^{n} c_i. \tag{6.10}$$

An allocation x_i of the estate among creditors should satisfy

$$\sum_{i=1}^{n} x_i = E \text{ given that } 0 \leq x_i \leq c_i. \tag{6.11}$$

In our case creditors correspond to the access networks belonging to a single or multiple cooperating operators and estate correspond to the required bandwidth by applications.

Bargaining Solutions of Cooperative Games

Bargaining [79, 80] refers to the negotiation process (which is modeled using game theory tools) to resolve the conflict that occurs when there are more than one course of actions for all the players in a situation, where players involved in the games may try to resolve the conflict by committing themselves voluntarily to a course of action that is beneficial to all of them. Application of bargaining solution to bankruptcy problem is natural in that bankruptcy problems create the situation of conflict over distribution of estate and to resolve the conflict the creditors (players) negotiate to get to the point of agreement. Such negotiations are best framed using bargaining solutions.

Kalai-Smorodinsky Bargaining Solution

Given a pair (S, d) that defines the general bargaining problem, with S denoting the set of feasible utilities and $d \in S$ representing the disagreement point, the unique Kalai-Smorodinsky bargaining solution $X^* = F(S, d)$ fulfills the following axioms:

1. Individual Rationality: $X_i \geq d_i$ for all i
2. Feasibility: $X^* \in S$
3. Pareto Optimality: X^* should be Pareto optimal. A solution is Pareto optimal if it is not possible to find another solution that leads to a strictly superior advantage for all players simultaneously [81].
4. Translation Invariance: $\forall(S, d), \forall h \in \mathbb{R}^n : F(S + h, d + h) = F(S, d) + h$
5. Individual Monotonicity: Consider two bargaining problems (S^1, d) and (S^2, d) such that $S^1 \subset S^2$, and the range of attainable utility by any player j is same in both (S^1, d) and (S^2, d). Then individual monotonicity implies that utility of player $i \neq j$ is higher in (S^2, d). In other words, an expansion of the bargaining set in a direction favorable to player i always benefits i.

KSBS suits our problem formulation because of its *individual monotonicity axiom.*This can be illustrated in the Figure 6.8, which is plotted for two players. Keeping utility of one player fixed and increasing the utility of second player results in two feasibility sets S^1 and S^2 such that $S^1 \subset S^2$. In this case player 1 will attain the same utility in both sets however player-2 will attain more utility in set S^2 than in set S^1, therefore as a consequence of individual monotonicity axiom $KSBS$ will always allocate more utility to player 2.

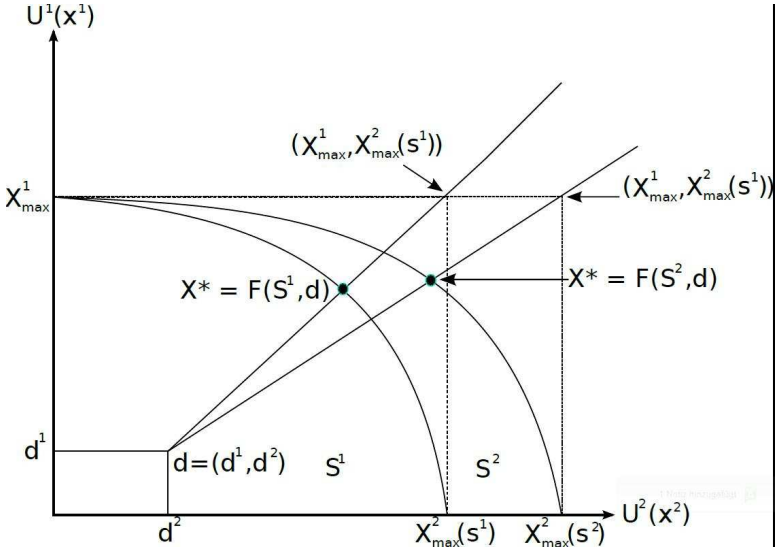

Figure 6.8.: Illustration of axiom of individual monotonicity

6.2.5. Cooperative Game Theoretic Resource Allocation

We use cooperative games to formulate the resource allocation management problem in multi-operator heterogeneous wireless networks at two levels. At the intra-operator level operator's RANs in an area bargain over the requests coming from users that belong to the operator. Executing intra-operator at this stage among the network technologies belonging to an operator over any divisible bandwidth request enable the operator to make optimal utilization of its bandwidth resource. The superiority of our intra-operator game in the context of bandwidth utilization is witnessed in our previous contribution [78]. The request is *allocated* to different RANs, and the utility function of different RANs is set to be the amount of allocated bandwidth above a certain disagreement point.

If a bandwidth request cannot be fulfilled by the RANs of a home operator, the inter-operator game is played. The inter-operator resource *distribution* problem is formulated such that each operator present in a coverage area bargain over the excess bandwidth requests. The utility function is defined similar to the intra-operator case.

There are different sequences of these games being played according to the area in which a particular user is located. Different sequences are elaborated in Fig. 6.7.

1. Area A: User is in his home network, and there is a single RAN. No games played.

2. Area B: User is in his home network, and there are multiple RANs belonging to the home RAN. Intra-operator game is played only.

3. Area C: User is in his home network, and there are multiple RANs belonging to multiple operators are available. Intra-operator game is played in the home network, followed by the inter-operator game if necessary. Intra-operator game is

played once more in home and foreign networks with the new requests that result after the distribution by the inter-operator game.

We model the allocation and distribution problems as bankruptcy problems and obtain the utility distribution rules. These rules dictate the allocation of requested bandwidth to RANs and the distribution of excess bandwidth to operators. We employ well known game theoretic approach of *bargaining* and a well-known bargaining solution KSBS to come up with the allocation and distribution rules. The distribution rule is enforced by the SLA-broker, whereas the allocation rule is enforced by the CRRM manager. We also present algorithms that calculate the offers that the players in different games make, given the distribution rules. The choice of *KSBS* in our resource allocation and distribution problem formulation is dictated by its *individual monotonicity* axiom. As this enables any access network technology (in intra-operator game) or operator (in inter-operator game) to attain more portion of requested bandwidth by increasing their *offered bandwidth*. Hence providing operators with more control over utility maximization for specific technologies.

Bargaining problem at the Intra-Operator Level

Let $r_o^a(q)$ be the requested bandwidth of service class q in area a coming from the users belonging to operator o where $o \epsilon O = \{1, ..., m\}$. Since the applications are partitionable and application requests can be allocated to different available network technologies within coverage area simulteneously, therefore playing intra-operator game the operator fairly allocates the application requests among their available network technologies. Furthermore, the operator o may have to serve bandwidth requests from other operator(s) in that area, which are in their aggregated congestion regions. These requests are denoted by $r_{\tilde{O}}^a(q)$, where $\tilde{O}$ represents the set of operators in their aggregated congestion region. In such a case inter-operator game is played first, which results in distribution of different portions of excess bandwidth requests to cooperating operators, this game is then followed by intra-operator game among RANs of operators over the portion of requested bandwidth won by operator in inter-operator game. Together these requests form the vector $Q_o^a(q) = (r_o^a(q), r_{\tilde{O}}^a(q))$, which represents the requests from a particular service class q belonging to home and foreign operators respectively that will be allocated to different RANs belonging to the home operator in this area. The RANs of that operator in the area a are members of the set $W_o^a = \{1, ..., n\}$.

$Q_o^a(q)$ is analogous to the estate of the bankruptcy game. The creditors of the game in turn correspond to the members of W_o^a. Each RAN $w \epsilon W_o^a$ makes a bandwidth offer $b_{o,w}^a$, which form the vector $B_o^a(q)$. Given $Q_o^a(q)$ and $B_o^a(q)$ the bargaining game comes up with allocation $x_{o,w}^a(q)$ of requested bandwidth to each RAN of the operator o, which must be the member of the compact and convex intra-operator feasibility set as defined below:

$$S(Q_o^a(q), B_o^a(q)) = \{x_{o,w}^a(q) : x_{o,w}^a(q) \in \mathbb{R}_+^n, \sum_{i \epsilon W_o^a} x_{o,i}^a \leq \sum_{i \epsilon W_o^a} b_{o,i}^a(q), \sum_{i \epsilon W_o^a} x_{o,i}^a(q) \leq r_o^a(q) + (r_{\tilde{O}}^a(q))\}$$

The set S above represents all possible allocation of bandwidths to the requests at intra-operator level over which RANs bargain. The first condition is natural, as bandwidths are positive quantities. The last two conditions dictate that the total allocation cannot exceed the total offered bandwidth or the total requested bandwidth. Furthermore in order for this problem to be formulated as an bankruptcy problem, the following condition should be satisfied:

$$r_o^a(q) + r_{\tilde{O}}^a(q) \leq \sum_{i \epsilon W_o^a} b_{o,i}^a(q) \leq \sum_{i \epsilon W_o^a} C_{o,i}^a \tag{6.12}$$

in which $C_{o,w}^a$ represents the total capacity of RAN w. The total requested bandwidth should be smaller then the total offered bandwidth, which should in turn be smaller than the total capacity of the operator o in the area.

Furthermore we define $d = (d_1, \ldots, d_n) \in \mathbb{R}^n$ as the given disagreement point. Setting the value of d in our bargaining problem associated with bankruptcy problem $(S(Q_o^a(q), B_o^a(q)), d)$ influences cooperation among the RANs. Since any of the RANs can always guarantee its disagreement utility by refusing to negotiate, the disagreement point defines the lower bound of the solution. The existence of a disagreement point is natural, since it endows one with a reference point from where utility comparison can be made. The problem with disagreement point is that there is no universally accepted criterion to select it[82]. However in the case of the intra-operator game, since the RANs belong to a single operator, all the available network technologies in the coverage area should participate in a game. Therefore, we keep the disagreement point as zero which means that all network technologies will have utility equal to zero if they do not collaborate.

With these definitions, we are able to formulate the corresponding 0-associated bargaining problem is $S(Q_o^a(q), B_o^a(q), 0)$. The recommendations made by *KSBS*, when applied to 0-associated bargaining problems, coincides with the proportional allocation rule[83]. Therefore, the total requested bandwidth will be distributed proportionally by the CRRM entity amongst the RANs based on their offered bandwidths according to the allocation rule:

$$x_{o,w}^a = \frac{b_{o,w}^a}{\sum\limits_{i \epsilon W} b_{o,i}^a} \left(r_o^a(q) + r_{\tilde{O}}^a(q) \right) \tag{6.13}$$

We illustrate this for two networks scenario in the Figure 6.9, where payoffs of RAN-1

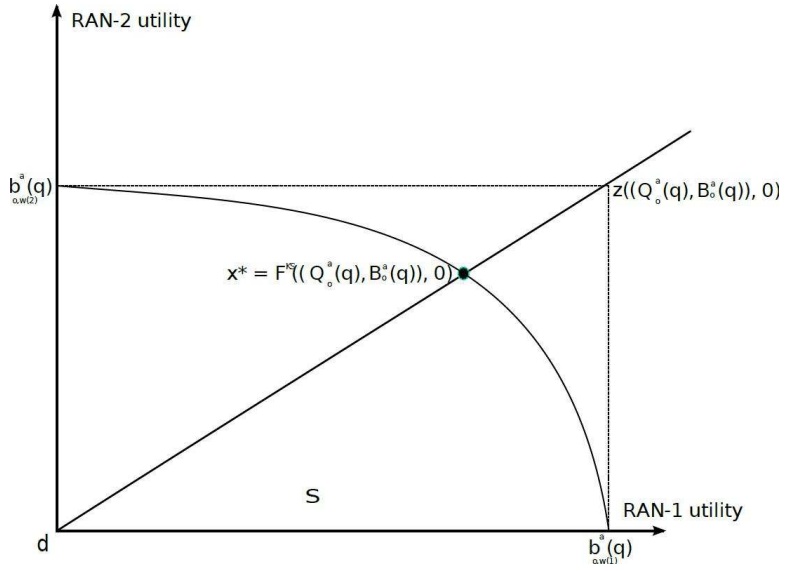

Figure 6.9.: KSBS solution in a 2 Network Scenario.

and RAN-2 are plotted along $x - axis$ and $y - axis$ respectively. Set S represent the feasibility set bounded by offered bandwidths of both the RANs along $x - axis$ and $y - axis$. As utility of RANs is function of allocated requested bandwidth to them, therefore in an attempt to increase utility network technology may increase the feasible set in its direction by increasing its offered bandwidth. Since we are plotting it for intra-operator scenario, therefore $d = 0$. Let the KSBS solution here be represented by X^*. Ideally, the allocated bandwidth by both networks should be equal to their corresponding offered bandwidth, which is depicted by the ideal point $z(Q_o^a(q), B_o^a(q), 0)$. But the ideal point lies outside the feasible set. Hence the efficient point i.e. X^* on the line joining ideal point with disagreement point represents the KSBS bargaining solution.

Bargaining problem at the Inter-Operator Level

Let us formulate the inter-operator game on the same lines as before. Let $\bar{r}_o^a(q)$ represents the excess bandwidth request for a service class q that an operator o cannot answer, and would like to offer in the inter-operator game to other operators, and the vector $\bar{Q}^a(q)$ represents all these requests from different operators in the region who are in aggregated congested regions.The operators play the game by making a bandwidth offer b_o^a, which can be grouped into the vector $B_o^a(q)$. The bargaining comes up with allocation of requested bandwidth to different operators, x_o^a, which should be a member of the compact and convex feasibility set:

$$S(\bar{Q}^a(q), B_o^a(q)) = \left\{ x_o^a : x_o^a \leq b_o^a, \sum_{i \epsilon O} x_i^a \leq \sum_{i \epsilon O} \bar{Q}^a(q) \right\} \tag{6.14}$$

Let C_o represents the aggregated capacity of operator o, that is calculated from the

capacities of the RANs belonging to operator o in that area. Similarly the condition for the bankruptcy formulation is:

$$\sum_{i \epsilon O} \bar{r}_i^a(q) \leq \sum_{i \epsilon O} b_i^a \leq \sum_{i \epsilon O} C_i \tag{6.15}$$

Contrary to the intra-operator game the disagreement point $D(q) = (d_1(q), \ldots, d_n(q)) \in \mathbb{R}^n$ is calculated from the bandwidth requests and offers of the operators. To depict the realistic scenario we select the disagreement point as characteristic function in our bankruptcy problem at inter-operator level. The characteristic function of a bargaining problem is defined as the amount of utility conceded to a player by all other players. What this implies is that an operator will cooperate with other foreign operators if and only if the operator receives at least the amount of bandwidth not covered by the offers of the other operators. That is, for an operator i and foreign operators $\forall j \neq i$ the disagreement bandwidth is given by:

$$d_i(q) = max\{0; \sum_{k \in O} \bar{r}_k^a(q) - \sum_{i \neq j} b_j^a(q)\} \tag{6.16}$$

Let the solution obtained by applying KSBS to our inter-operator bargaining problem be denoted by be denoted by $X^a = (x_1^a, ..., x_m^a)$. Then

$$X^a = F^{KS}(S(\bar{Q}^a(q), B^a(q)), D(q)) \tag{6.17}$$

The bargaining problem above is D associated bargaining problem in this case. Thus recommendations made by *KSBS*, when applied to D associated bargaining problem coincides by adjusted proportional distribution rule [83]. In other words:

$$x_o^a = d_o(q) + \frac{(b_o^a(q) - d_o(q))}{\sum\limits_{i \in O} (b_i^a(q) - d_i(q))} \cdot (\sum_{i \in O} \bar{r}_i^a(q) - \sum_{i \in O} d_i(q)) \tag{6.18}$$

This distribution rule is applied by the SLA broker.

Bandwidth Offer Algorithm at Intra-Operator Level

Here we present an algorithm for the individual RAN's given the proportional allocation rule. For each RAN, $\bar{b}_{o,w}^a(q)$ is the pre-defined bandwidth offer associated with service class q, which is defined by the operators. If the current used bandwidth $l_{o,w}^a$ is larger than the *RAN capacity threshold*, described as a percent of the total capacity $C_{o,w}^a$ in a RAN, then the pre-defined bandwidth is scaled with the *load factor* $\psi_{o,w}^a = e^{\frac{-l_{o,w}^a}{C_{o,w}^a}}$, in order to find the bandwidth offer for that RAN.

As a result of this scaling, some of the RANs belonging to the same operator offer less bandwidth compared to the pre-defined values. Since they belong to the same operator, this represents a lower utilization of the operator resources. To overcome this problem, we allow the RANs that are not in the RAN congestion to share the aggregated

difference between the pre-defined and actual offered bandwidths of the congested RANs proportionally to their own pre-defined bandwidths. In other words, let $\bar{W}_o^a \subset W_o^a$ be the set of congested RANs, then the algorithm for calculating the bandwidth offer $b_{o,w}^a$ is given by:

$$b_{o,w}^a = \begin{cases} \bar{b}_{o,i}^a(q) \cdot \psi_{o,i}^a & \text{if } i \in \bar{W}_o^a \\ \bar{b}_{o,i}^a(q) + \tilde{b}_{o,i}^a(q) & \text{if } i \in W_o^a - \bar{W}_o^a \end{cases} \tag{6.19}$$

where $\tilde{b}_{w,o}^a(q)$ stands for the proportional additional bandwidth that the uncongested RANs include in their offers, which is calculated by:

$$\tilde{b}_{o,w}^a(q) = \frac{\bar{b}_{o,w}^a(q)}{\sum\limits_{i \in W_o^a - \bar{W}_o^a} \bar{b}_{o,i}^a(q)} \cdot \sum_{i \in \bar{W}_o^a} \bar{b}_{o,i}^a(q)(1 - \psi_{o,i}^a) \tag{6.20}$$

Note that this algorithm requires exchange of information between individual RANs, which may be implemented by direct connection of RANs, through a central CRRM or a distributed CRRM as described in [76]. Since the RANs belong to the same operator, this is a valid assumption.

Bandwidth offer Algorithm at the Inter-Operator Level

The algorithm for the operators turns out to be relatively simpler than the RANs, given the most actual bandwidth offers that the RANs made for a specified service class contain a considerable amount of information about the status of the operator network in an area. Specifically, the operator sums the most up-to-date bandwidth offers from the RANs in the area for the service class. Then this aggregated offer is scaled with the motivation factor of the operator $0 \leq \mu_o \leq 1$. By setting this factor, the operator is able to adjust the cooperative nature of its strategy. There is an incentive for cooperative behavior, as operators can allocate unused bandwidth to increase revenue and utilization. Thus:

$$b_o^a(q) = \mu_o \cdot \sum_{i \in W_o^a} b_{o,i}^a(q) \tag{6.21}$$

6.2.6. Results and Analysis

In order to observe solely the effects of an allocation scheme in a given scenario, we have developed our own Java-based discrete event simulator, which generates user defined network operators, access technologies, and coverage areas with user defined RANs belonging to different operators. We investigate the performance of our approach in randomly generated coverage areas for multi-operator heterogeneous wireless networks. A snapshot of the user interface for our simulator is shown in Fig. 6.10.

To investigate the gain of cooperative operators in terms of bandwidth utilization, we select a coverage area within randomly generated scenario, which is covered by different RANs of three different operators as follows:

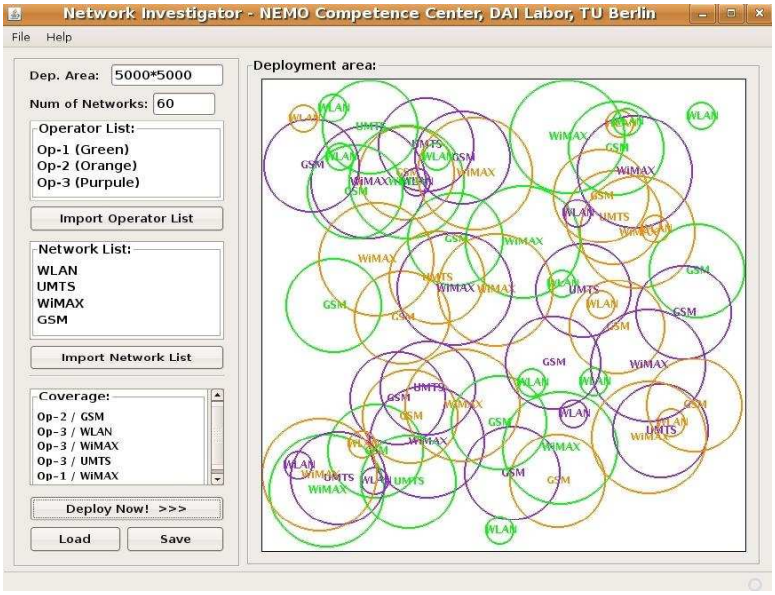

Figure 6.10.: The user interface for our discrete event simulator.

- Operator-1:WiMAX
- Operator-2: WiMAX, GSM
- Operator-3: WiMAX, WLAN, UMTS

We observe the gain of operator-2 for different levels of cooperation (for different values of motivation factor in our approach) and write it as *home operator* hereafter. The bandwidth requests of different quality classes are generated by users belonging to home operator using Poisson process with the mean 20. Simulation run is kept as 30 events, where events effectively present time instance for arrival of bandwidth requests. Simulation run for 30 events is justified here because of greater poisson process mean value. We consider three different cases here, i) When home and foreign operators are fully motivated to cooperate ($\mu = 1$ for all operators). We name this case as *fully cooperative* ii) When home operator and one foreign operator(Operator-1 in this case) are motivated to cooperate only, we name this case *selective cooperative* and iii) When no operators cooperate ($\mu = 0$), this case is called *non-cooperative case*. Results for *Fully cooperative* case can be seen in Fig. 6.11a, where the home operator offers bandwidth to its users' requests until it gets into congestion, as can be seen at event-4 and onwards the excess load is shared by foreign operators. In this case no call drops are observed. In *Selective cooperative case* 6.11b although home operator gets into congestion very soon, but no call drops are observed unless cooperating foreing operator(operator-1 in this case) is congested from event 13 and onwards. Foreign operator-3 in this case is not motivated to bargain over the excess bandwidth requests by home operator. Coming to *Non-cooperative case* 6.11c, where greater call drop is observed since no foreign operator

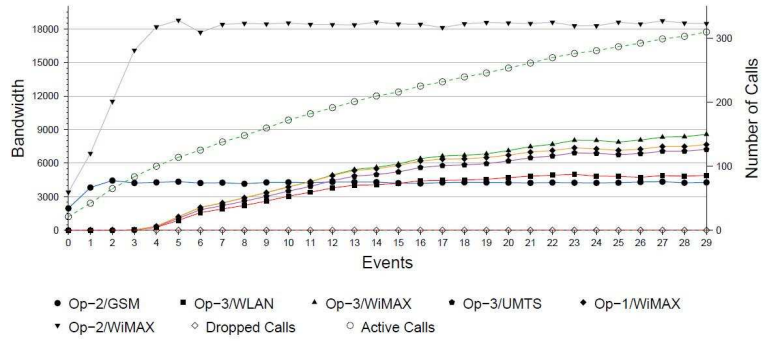

(a) Fully Co-operative

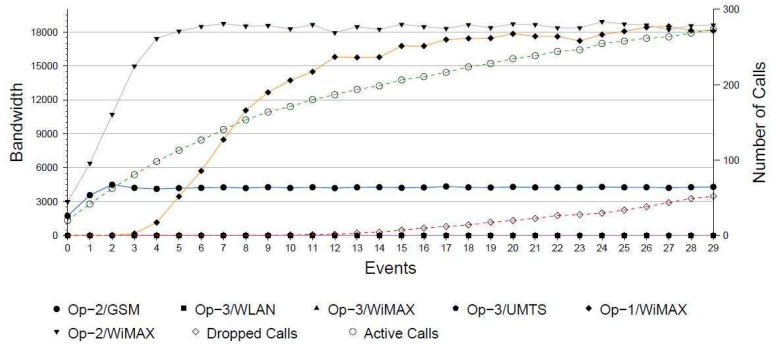

(b) Selective Co-operative (OP-1 cooperates with OP-2)

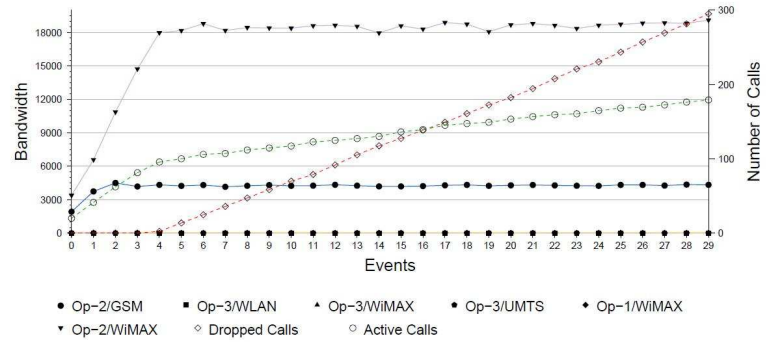

(c) Non-Cooperative

Figure 6.11.: Network Technologies Bandwidth Utilization

take part in the inter-operator bargaining. These results motivate operators to cooperate to achieve the objective function of satisfied and increased user pool cost effectively. Setting the value of motivation factor a foreign operator can make good use of his resources and increase revenue.

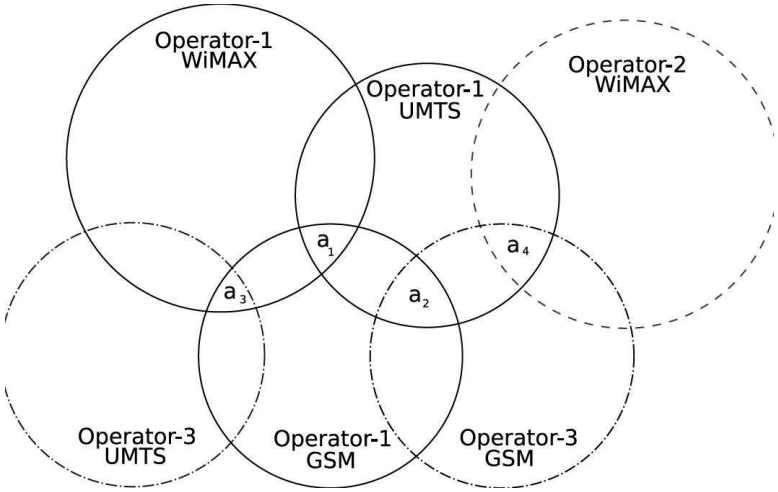

Figure 6.12.: Simulation Scenario for comparison

Table 6.2.: Predefined offer bandwidth

QoS Class	GSM	WiMAX	UMTS
Voice	500	240	400
Data	900	1000	800
Video	500	1600	500

6.2.7. Comparison with other approaches

To assess the performance of our proposed approach compared to other approaches, we implement service-based and capacity-based allocation schemes as described in the Introduction section. We consider the simulation scenario given in Fig. 6.12, where simulations are run on area granularity $(a_1, \ldots, a_4)$ with service requests arriving for different types of applications.

The arrival of requests is modeled by a Poisson process, and the service class is chosen randomly among voice, data, and video uniformly. The sizes of the requests are assumed to be static, and are 60 kbps, 150 kbps, and 500 kbps for voice, data, and video respectively. After the allocation and distribution algorithms, the allocated bandwidths are subtracted from the bandwidth pools of the RANs, assuming the users have an infinite channel holding time. This allows us to simulate the overload conditions in the areas, which results in inter and intra-operator games being played. We simulate a random topology with GSM, UMTS, and WiMAX. A GSM RAN has a capacity of 4500 kbps, UMTS 12000 kbps, and WiMAX 20000 kbps. The RAN overload thresholds are set to 10% for UMTS, GSM, and 3% for WiMAX. The operators share the same predefined offered bandwidth values in kbps, which are given in Table 6.2.

We then compute the call blocking probability in all areas a_1, a_2, a_3, and a_4 as a function of the simulation steps. We also plot the number of accepted requests as

a function of traffic intensity in calls per minute, assuming a simulation time of 100 minutes. The results for these regions are given in Fig. 6.13 and 6.14. In area a_1, a single operator has RANs of all the possible RATs. In area a_2 operator-1 has UMTS and GSM, and the operator-3 has only GSM. In area a_3 operator-1 has deployed WiMAX and GSM, and operator-3 UMTS and in area a_4 operator-1 has UMTS, operator-2 has WiMAX and operator-3 has GSM.

These results are compared with the results obtained by the capacity-based and service-based approaches discussed earlier. In the capacity based approach the players report their available bandwidths to the SLA broker and the CRRM. The service request is then allocated to the RAN or the operator with the largest amount of free bandwidth. In the service-based approach, service classes are associated with certain RANs, and are allocated to other RANs only if the associated RANs are overloaded. In this scheme voice is allocated to GSM, then to UMTS, and finally to WiMAX. Data is associated to UMTS, and allocated to WiMAX in overload. For video the sequence is UMTS and then WiMAX. In this scheme the intra-operator game is played by individual RANs submitting the type of traffic they can support to the CRRM. CRRM chooses the RANs that are willing to support the service class of the request, and divide the requested bandwidth equally among these RANs. The inter-operator game follows the same lines by operators submitting the traffic class they wish to support to the SLA broker.

Our approach outperforms both the service-based and capacity-based solutions in all coverage areas. In the area a_1, where only the intra-operator game is played, we can support 12% more calls, with the same call blocking probability as the service-based approach. In area a_2, where the operator-3 only has GSM, we allow operator-3 to make use of operator-1's UMTS and GSM, and are able to support 44% more calls, while reducing the call blocking probability from 45% to 36% . Note that this higher rate of call drop rate is due to the fact that operators have most GSM RANs, which has limited support for video or data requests. In the area a_3, where there is plenty of bandwidth to be shared in the inter operator game we outperform the service-based approach by 28% and the capacity-based by 11%. We almost halve the call drop probability compared to capacity- based scheme in the area. In area a_4 a somewhat similar behavior to the area a_1 is observed in terms of bandwidth utilization however we improve 50% in terms of call blocking probability. It is also important to note that compared within each other the capacity-based solution is able to support more calls, but has an inferior call blocking rate.

In the light of the results, we can draw the conclusion that our solution outperforms both of the compared approaches, and its virtue becomes more spoken when there is abundant bandwidth to be shared for better utilization as in area a_3, or when there is a asymmetry between the capacities of operators as in the case of area a_2.

6.3. Conclusion

In this Chapter we provided two negotiation mechanisms to be used by NOC agents to decide on the transfer probabilities. For multiple-class sharing we propose an auction based central solution that relies on a trusted third party. For single class we propose a peer to peer negotiation mechanism, which can be used without the trusted third party. We show by using the descriptive queueing model we developed in Chapter 5, that deviating from the conditions of the mechanism is not rational for RAN agents. This is important for our development of the decision making algorithm in Chapter 7. If there is no utility to be gained by lying, there is no utility in designing agent control algorithms that take into account the possibility of the other agent lying. This allows us to develop simpler agents.

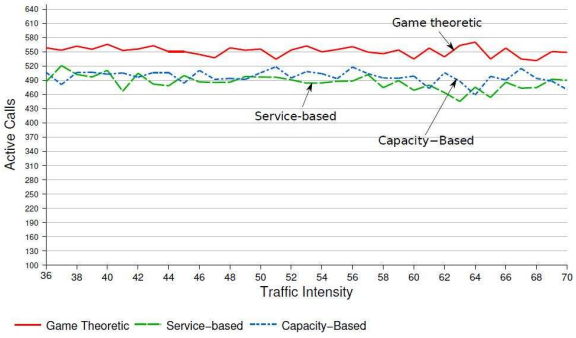

(a) Area a_1

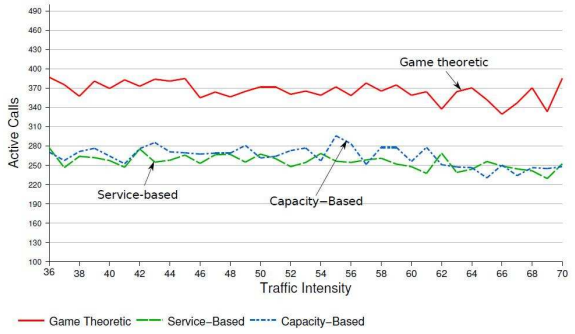

(b) Area a_2

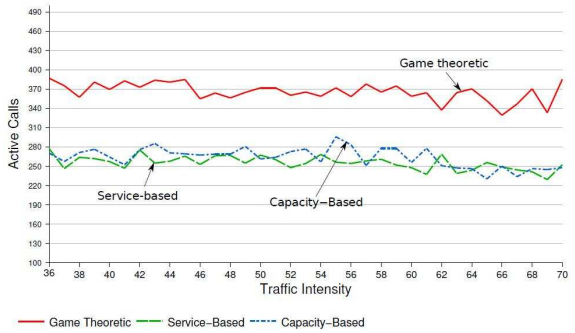

(c) Area a_3

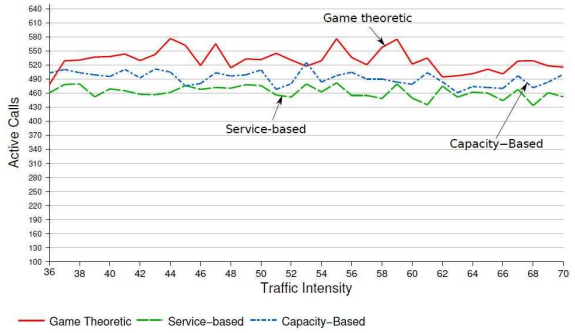

(d) Area a_4

Figure 6.13.: Number of Active Calls vs. Traffic Intensity in calls per min.

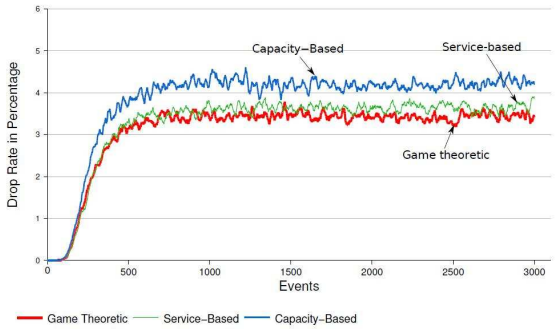

(a) Area a_1

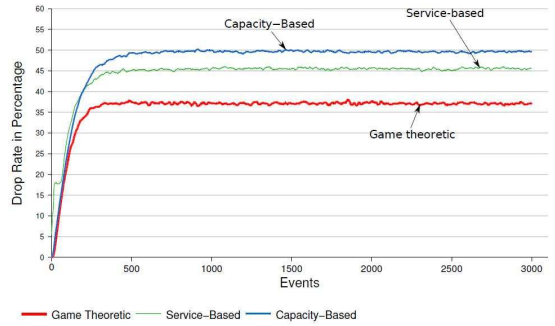

(b) Area a_2

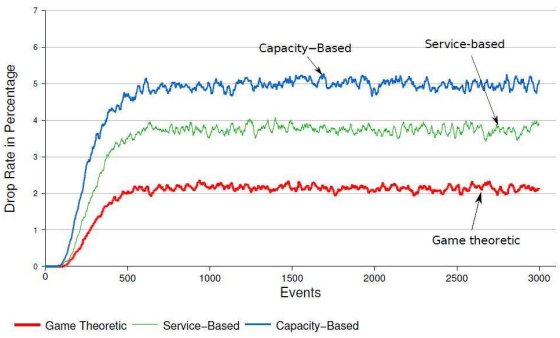

(c) Area a_3

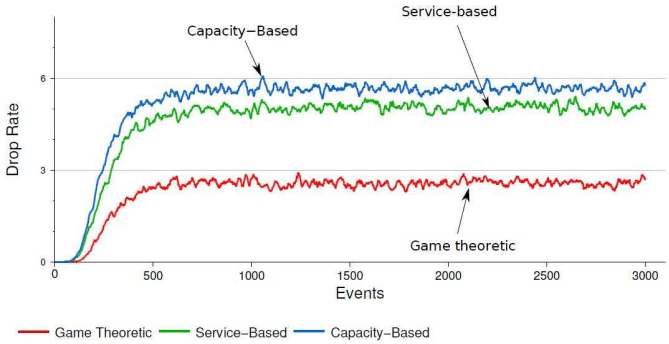

(d) Area a_4

Figure 6.14.: Call Blocking Probability vs. Simulation Steps.

7. Control Problem

Control Problem is involved in calculating policies that the RAN agents will base their cooperate or not cooperate decisions. The NOC Agents calculate these policies and send them to their RAN Agents.

7.1. Problem Description

We are concerned with the decision under uncertainty problem of a software agent that runs in an operator RAN. The agent makes delay measurements in its own RAN. It also queries the user QoE database to update its beliefs about the congestion states of the RANs in its neighborhood. If the delay in its own RAN is not satisfactory for the users, it chooses another RAN in the area, for which the agents belief that this RAN is not congested is the maximum among all the RANs in the vicinity. The software agent negotiates with its peer agent in the chosen peer RAN the proportion of traffic that it will transfer by following the results of Chapters 6 and 5. After call admission, the agreed proportion of users are forwarded to the peer RAN. During the cooperative phase the agents query the QoE database to update their beliefs about the congestion states of the peer RANs. The borrower RAN stops transferring traffic if its belief that the donor RAN is congested is above a threshold. Similarly, the donor operator stops accepting traffic when its belief that the borrower is normal again is larger than a threshold. The optimum decision problem is the definition of these thresholds and de development of a controller that automates this closed loop control problem.

Each agent abstracts the dynamics of its own RAN and peer RAN by using a Processor Sharing(PS) model as described in the Chapter 4. PS service discipline was originally studied by Kleinrock as an idealization of round-robin discipline. It can also be interpreted as a variable service rate discipline, in which the total service rate is shared equally by all the jobs in the system. It is latter interpretation that motivates using PS as a model for wireless networks, which goes back to the early work by Telatar [26]. It has recently been used to model 802.11g based wireless LANs [84] and GPRS [85] and HSDPA [48]. It has been shown both analytically [86] and experimentally [87] that TCP traffic over WLANs can be abstracted by a PS discipline.

Partially Observable Markov Decision Process (POMDP) is a generalization of the classical Markov Decision Process (MDP) to problem domains in which agents can only make stochastic observations about the states [88]. To their disposal are *a priori* observation probability functions $O(a, S_i, o)$, which gives the probability of making the discrete observation o after taking the action a and arriving at state S_i. Agent keeps a set of beliefs over each state, $\mathbf{b} = \{b(S_i)\}$, which it updates after making observations in

a Bayesian manner. The beliefs are in fact conditional probabilities based on the observation function. The main difficulty of POMDP is the representation of policies, which should assign optimal actions over the continues belief space. Owing to the piecewise linear nature of rewards over the belief state, a finite representation of an optimum policy is possible. An optimum policy π in the case of POMDP consists of a set of vectors $\{\alpha_{\mathbf{i}}\}$. Each vector is associated with a certain action. The optimal policy is to take the action associated with the vector that maximizes the dot product $< \alpha_{\mathbf{i}} \cdot \mathbf{b} >$.

The chapter is organized as follows. First we give a conceptual description of the mathematical formalisms that can be used to formulate the controlling problem in Section 7.2. These are centralized and decentralized sequential decision problems. We then analyze the various options according to the design criteria we introduce in Section 7.3. We choose to employ independent POMDP controllers in both RANs, which interact according to the strategy-proof negotiation mechanisms we developed in Chapter 6. We present the derivation of the POMDP controllers in Section 7.4. We finally present the solutions of the POMDP models for WLAN-WLAN load balancing in Section 7.5 and WLAN-HSDPA load balancing in Section 7.7.

POMDP has been used in the context of 802.11 coordinated MAC designs [89] and opportunistic spectrum access [90]. To the best of our knowledge they have not been employed in 802.11 [91] or WLAN-HSDPA load balancing scenarios.

7.2. Overview of Sequential Decision Problems

7.2.1. Centralized Sequential Decision Problems

Traditionally decision theory is concerned with the design of agents, which can be humans or machines, that take one-time decisions. An decision-theoretic agent observes its environment, compares it with its goals and decides on the action [92]. The approach is to combine utility theory with probability theory, in order to maximize the utility of an agent on an average sense.

Formally, an agent resides in an environment which can be described by a possibly infinite, yet countable state space S. The agent makes an set of observations that can be described by the vector $\mathbf{O}$. The goal is to choose an action a based on the current state and the observations in order to maximize a suitable reward function or minimize a cost function. The cost and reward are functions of s and a, and are chosen to describe the environment that the agent operates as accurately as possible. They describe the desirability of states from agent's perspective. Cost and reward functions can be used alternatively, by a suitable transformation. For example minimizing a cost function $C(s, a)$ is equivalent to maximizing the reward R(s,a) which is equal to $-C(s, a)$. For the sake of clarity, we assume reward maximizing agents.

In sequential decision problems, the agent is required to take multiple decisions in consecutively. The next state of the system is determined by the current state of the action of the agent. The agent's goal is to maximize the total reward over certain number of stages. The number of stages may be known in advance, but it can also be unknown. Also, the sequential decision problems can last after finite stages, or may

continue forever. The agent must take into account that its current actions will affect the future state of the system, which will ultimately define future reward. There is a tradeoff between immediate rewards and total reward. A certain action may have large instantaneous reward, but it may lead to a state trajectory that lowers the total reward. Therefore the traditional decision theoretic tools such as decision networks or influence diagrams are not sufficient for sequential decision problems.

Sequential decision problems can be modeled in a variety of ways, depending on the the nature of the states, the timely relationship between observations, decisions and actions. We are specifically interested in finite state space and discrete time models. We can formally define these models with discrete time dynamic systems. Specifically we are concerned with stationary discrete time dynamic systems, whose system properties do not vary over time. Such systems can be described by the system equation:

$$s_{k+1} = f(s_k, a_k, w_k) \tag{7.1}$$

$s_k \epsilon S$ is the state, $a_k \epsilon U(x_k) \subseteq A$ is a control action and $w_k \epsilon D$ is a discrete random variable and k and $k+1$ represent consecutive stages or time steps. a_k is chosen from the possible actions at stage k, $U(s_k)$, which itself is a subset of all possible actions A. w_k represents the random nature of the problem, in the sense that it is chosen from a probability distribution $P(w_k|s_k, a_k)$, that depend on s_k and a_k. Thus the next state can only be described by a probability distribution, that is a function of current state and the control action that is the result of the decision at that stage. It is important to note that the states before the stage k do not influence the next state in the next interval $k+1$. Such systems are said to have Markovian [38] property. This property allows us to develop tractable solution methods for sequential decision problems. Markov Decision Processes (MDP) are well established frameworks with which sequential decision problems can be solved.

Markov Decision Problems

A MDP is defined as a mathematical object $< S, A, R(s,a), T(s,a,s') >$, where:

- $S = \{s^i\} \quad i = 0, 1, 2...$ is a countable state space.
- $A = \{a^i\} \quad i = 0, 1, ..., N^a$ is a finite and countable set of actions.
- $R : S \times A \to \mathbb{R} - \{\infty, -\infty\}$ is the finite real reward function.
- $T : S \times A \to \Delta(S)$ is the transition probability function, that gives the probability of arriving at state s' after executing action a in state s. It is calculated from the system equation (7.1)

One solves a of a MDP is a in order to obtain an optimal *policy*. A policy $\pi_k(s_k)$ is simply a rule that the agent can employ to decide the action a_k given the system state at stage k, $s_k \epsilon S$. The policies which are independent from k are called *stationary policies*. In this case, the policy π is simply a mapping from states to actions. The goal in MDP

is to find a policy that achieve optimal long term reward. The definition of the long term reward depends on the duration of the MDP. Let us define the reward obtained at stage k as $R_k(s_k, a_k)$. Then for a *finite-horizon* MDP that lasts K stages the long term reward is given by:

$$R = E\left[\sum_{k=0}^{K-1} R_k(s_k, a_k)\right] \tag{7.2}$$

If the horizon length is unknown or infinite, one can use the *infinite-horizon discounted* long term reward given by:

$$R = \lim_{K\to\infty} E\left[\sum_{k=0}^{K-1} \gamma^k R_k(s_k, a_k)\right] \tag{7.3}$$

The discount factor γ which is between zero and one has two interpretations. In one, it models a sequential decision process, in which the decision process is terminated with probability $(1-\gamma)$ after each decision stage. In the other interpretation, γ models the relative importance of immediate and future rewards. Specifically, human agents or machine agents that are designed for humans, tend to value immediate rewards more than rewards in the future. Put in another words, the agents are more willing to take more risks on events further in the future. When γ is close to zero, the rewards in the future are insignificant. When γ is one all the rewards are equally important and the optimality is equivalent to *infinite-horizon additive* model. If the number of stages of a MDP is not known in advance, the discounted model with an appropriate discount factor is used.

Optimal policies differ for infinite and finite horizon MDPs form their stationarity properties. Generally, policies for finite horizon problems are not stationary, since the optimum actions at the last stages differ from the actions at the beginning stages. Infinite horizon MDPs on the other hand admit stationary optimal policies which are unique as shown by Howard in 1970 [93]. This optimal stationary policy, which is composed of state action pairs can be calculated using the classical Dynamic Programming (DP) algorithm due to Bellman [94].

Dynamic Programming Solution to MDPs

In order to compute optimal policies, we have to define the value of a policy, which is the long term reward obtained by applying the policy. For a given stationary policy π, its value depends on the initial state s_0 which we denote with $J_\pi(s_0)$. Given the initial state s_0 the agent chooses the action dictated by the policy $\pi(s_0)$. The system leaves s_0 and enters next state $s_1 \epsilon s^i$ with probabilities given by $T(s_0, \pi(s_0), s^i)$.

For infinite horizon problems the rewards that the agent collect after jumping to state s_1 and following policy π are the same as starting at initial state s_1 and following the policy π, owing to the Markov and stationary property of the policy. Thus we can drop the stage dependency in $J_\pi(s_0)$ and obtain:

$$J_\pi(s) = R(s, \pi(s)) + \gamma \sum_{s' \epsilon S} T(s, a, s') J_\pi(s') \quad \forall s \epsilon S \tag{7.4}$$

For a finite state MDP with a state space of size $|S|$, equations (7.4) constitute $|S|$ linear equations for $|S|$ unknowns, which can be solved trivially. This allows one to calculate the long term expected reward of any arbitrary policy. The next question to ask is how to find the optimal policy among all the possible policies.

The Dynamic Programming solution to MDPs finds the optimal valued policy π^* by making use of the *Principle of Optimality* due to Bellman [94]:

> *PRINCIPLE OF OPTIMALITY*: An optimal policy has the property that whatever the initial state and initial decisions are, the remaining decisions must constitute an optimal policy with regard to the state resulting from the first decisions.

This means that the agent can attain the optimal long term reward by choosing the action that maximizes the sum of one step reward plus the expected optimal long term reward associated with next states. This gives us a set of non-linear equations, derived from Equation (7.4), which is are called the *Bellman Equations*:

$$J_{\pi^*}(s) = \max_a \left[R(s, a) + \gamma \sum_{s' \epsilon S} T(s, a, s') J_{\pi^*}(s) \right] \qquad \forall s \epsilon S \tag{7.5}$$

Unlike calculating the value of a given policy, these set of equations are non-linear and thus cannot be solved trivially. An iterative approach involving the repetitious application of the one step DP update, i.e. the right-hand side of the Equation (7.5) can be used to solve the equations. This approach is called *Value Iteration* in the literature.

Let us donate the vector of all state values with $\mathbf{J}$. With this definition the Bellman Equations (7.5) can be interpreted as a non-linear transformation on the value function vector J, which we denote with T. We can rewrite the Bellman equations:

$$\mathbf{J}_{\pi^*} = (T)\mathbf{J}_{\pi^*} \tag{7.6}$$

Thus the optimal value function $\mathbf{J}_{\pi^*}$, i.e. the value attained by the optimal policy π^*, is the fixed point of the non-linear transformation T. In fact, the transformation T belongs to a class of transformations called *contractions* [92]. The important property of contractions is that applied to a vector, the contraction will always transform the input vector to another vector which is closer to the fixed point. Since the optimal value function is the fixed point in MDP formulation, repetitive application of the one step DP update to any arbitrary initial vector will approach to the optimal value function. If we define

$$\begin{aligned} (T^2)\mathbf{J} &= (T)((T)\mathbf{J}) \\ (T^N)\mathbf{J} &= (T)((T^{N-1})\mathbf{J}) \end{aligned} \tag{7.7}$$

We have for any arbitrary initial $\mathbf{J}$:

$$\mathbf{J}_{\pi^*} = \lim_{N\to\infty}(T^N)\mathbf{J} \tag{7.8}$$

By making use of (7.8) we can find the value attained by the optimal policy. However the aim of MDP is not to find just what optimum long term reward is, but to find a policy that achieves this value. The necessary and sufficient condition for a policy to be the optimal policy is to obtain the minimum in the Bellman Equations (7.5) for each state [95]. Thus, once the optimal value vector is found via value iteration using Equation (7.8), the optimal policy is simply given by:

$$\pi^*(s) = \underset{a\epsilon A}{\operatorname{argmax}}\left[R(s,a) + \gamma\sum_{s'\epsilon S} T(s,a,s')J_{\pi^*}(s)\right] \qquad \forall s\epsilon S \tag{7.9}$$

Obviously, the value iteration will not be continued to infinity in practical world. The following error bounds are useful in choosing the number of iterations and the discount factor:

$$\begin{aligned} \frac{2\gamma^N R_{\max}}{1-\gamma} &\leq \epsilon \\ \max_{s\epsilon S}|J_{\pi^*}(s) - J^N_{\pi^*}(s)| &\leq 2\frac{\epsilon\gamma}{1-\gamma} \end{aligned} \tag{7.10}$$

The first error bound relates the error in the approximation of the optimal value function to the discount factor γ, maximum reward $R_{\max}$ and the number of iterations. It is can be inferred that increasing γ to one will also increase the number of iterations required to keep the error under the desired value. Second error bound is related to the *policy error*. It represents the loss in the total reward when the agent employs a policy making use of approximation of N iterations length. In other words, how much does the long term reward deviates from the optimum when the agent uses the $N-th$ iteration $\mathbf{J}^{\mathbf{N}}_{\pi^*}$ instead of $\mathbf{J}_{\pi^*}$ in Equation (7.9).

For the sake of completeness, it is worth noting that an alternative method called *policy iteration* can be used to solve MDPs, and in some cases is more efficient than the value iteration. In short, the policy iteration starts with randomly associating each state with an action. The policy iteration consists of two sub-steps. In the policy evaluation sub-steps the value of the current policy is evaluated by making use of the linear set of equations given in (7.4). In the policy improvement sub-step the state-actions pairs are updated by using the value of the policy calculated at the previous sub-step. To illustrate this, let us assume that at iteration i the policy is $\pi^i(s)$ with a value $\mathbf{J}^{\mathbf{i}}_{\pi}$. The policy at the next iteration is updated as follows:

$$\pi^{i+1}(s) = \underset{a\epsilon A}{\operatorname{argmax}}\left[R(s,a) + \gamma\sum_{s'\epsilon S} T(s,a,s')J^i_{\pi}(s)\right] \qquad \forall s\epsilon S \tag{7.11}$$

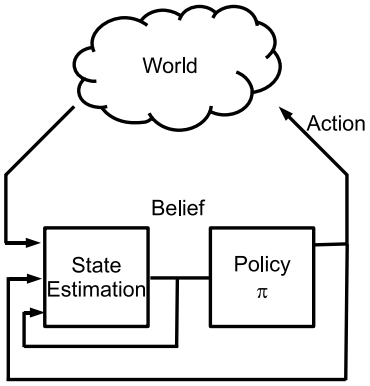

Figure 7.1.: The conceptual model for POMDPs.

Centralized Sequential Decision Problems with Partial Information

Centralized sequential problems which can be solved by MDPs are applicable for environments, where the decision making agent is able to determine the state of the world without any ambiguity. The class of problems, in which the agent makes observations that reflect the world state with a certain level of uncertainty are called *partially observable* problems.

MDP policies are not applicable to partially observable problems, since they directly associate actions with states. In partially observable domains, an agent doesn't have access to the actual state, it can at the maximum a set of *beliefs* over the world states. Beliefs are simply state estimations, and represent how likely it is, that the world is at a given state based on the observations of the agent.The agent should consider the relative likelihoods of current and future states in taking decisions. Figure 7.1, taken from [96], depicts the model that we are referring to. A policy in partially observable environments is a mapping from beliefs about the world states to the set of actions. The belief is computed progressively using the current and previous observations and the previous actions. The beliefs are in fact estimations of the states.

What are optimal policies in the model described above? The most straight forward approach would be associate actions to observations. This naive approach is not optimal, since different states may result in the same observations. Randomizing the actions associated with observations leads to general *memoryless policies* [97], which perform better than the naive approach, but yet are inferior to policies that make use of the entire history of observations.

The next question is how to account for the previous observations. For finite-length problems, one can depict policies depending on the entire history of observations via policy trees, similar to the one given in Figure 7.2. Each circle in the tree defines the action to be taken at a given stage, as a response to the previous path and the current observation. At stage 1 the agent can only chose 1 action among $|A|$ different possible actions. Depending on the observations, the policy determines the next action. In the figure there are two possible observations. The tree grows until the k-th stage. Different

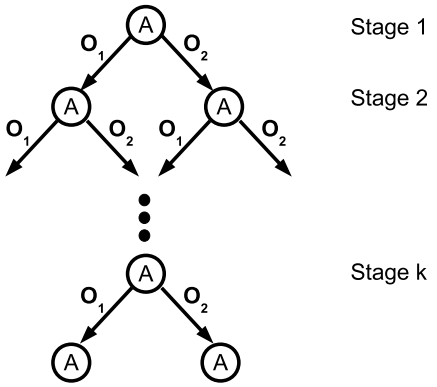

Figure 7.2.: An example policy tree with two observations.

actions associated each circular leaf determines different policies. In this sense each policy is a distinct policy tree.

The question of finding optimal policies that take into account the entire history of observations is complicated by the exponential manner the policies grow. A brute force approach would compute the expected value of every possible policy and choose the highest expected value. However, this problem is shown to be *PSPACE-complete*, which is a complexity class that is thought to contain P and NP and therefore intractable [98]. Sondik tackled this problem of intractability by converting the original problem into an equivalent MDP problem involving a continuous state space [99], [100]. This body of research is termed *Partially Observable Markov Decision Process* (POMDP) . We will discuss the complexity properties of POMDP and its decentralized versions in Section 7.3.1. First we introduce POMDP formalization in the next section.

Partially Observable Decision Processes

Formal definition of a POMDP extends the mathematical object that is used to define MDPs described in Section 7.2.1. A POMDP is given by $< S, A, T, R, \Omega, O >$. As in MDPs S represents the countable state set, A represent the finite and countable set of actions. $T(s, a, s')$ is the probability of reaching s' and $R(s, a)$ is the reward after executing a in state s. On top of the MDP, POMDP formulation adds the following:

- $\Omega = \{o^i\}, \quad i = 1, 2, ..., N^o$ is a set of finite observations.
- $O : S \times A \to \Delta(\Omega)$ is the observation function. In other words, $O(s', a, o)$ gives the probability of taking action a, landing in s' and making the observation o.

POMDPs, which cannot be solved via a brute force method, can be solved using a neat transformation step that allows the construction of an equivalent MDP. MDPs can be solved using the DP algorithm, and optimal policies can be developed based on the value functions obtained by the DP algorithm. This approach involves the notion of a *belief state*. The reason behind the intractability of the brute force solution is the size

of the policy trees that grow exponentially with time, owing to the number of different observations possible at each stage as discussed earlier. A proper calculation of the belief state, is a compact representation of the possibly infinite observation history.

Formally, belief state is a probability distribution over the world states. It represents the relative likelihood of the world being in a particular state, given the observations up to the current time step. It can be represented by the vector $\mathbf{b} =< b(s_1), b(s_2), ...) >$, where $b(s_i)$ is the probability that the world is in state s_i. Total probability requires the sum of individual beliefs to be equal to one.

The challenge is to be able to update the belief state recursively with the observations, so as to make use of all the observations. In other words, we are looking for a function f, such that:

$$\mathbf{b}_{k+1} = f(o_k, \mathbf{b}_k) \tag{7.12}$$

Aström proved in [101], that a recursive Bayesian filtering is one such function. Furthermore, it has the property of being a *sufficient statistic*. What this means is no further information about past observations can be used to improve the probability distribution. The Bayesian update computes $b'(s') = P(s'|o, a, b)$ from the observation o and the previous belief states $b(s)$. The Bayesian update equation is given by [96]:

$$b'(s') = \frac{1}{P(o|a, \mathbf{b})} \cdot O(s', a, o) \sum_{s \epsilon S} T(s, a, s') b(s) \tag{7.13}$$

The update works as follows. Once the observation o is made after taking action a and landing in state s', one step prediction of arriving at state s' given the old belief states $b(s)$ is computed with the term $\sum_{s \epsilon S} T(s, a, s') b(s)$. This prediction is then updated with the likelihood of the new observation, given by the $O(s', a, o)$ term. The term $\frac{1}{P(o|a,\mathbf{b})}$ is a constat that satisfies the total probability condition.

It is crucial to note that the next belief state depends only on the current belief state and the action. The transitions are random, and described by the stationary probability distributions given by O and T. In fact the evolution of the belief state can be represented in the canonical dynamical system representation given by Equation (7.1). And since the next belief state depends only on the current belief state, one can cast the POMDP as an equivalent *belief MDP*. The equivalent belief MDP is given by $< S, A, \tau(\mathbf{b}, a, \mathbf{b}'), \rho(\mathbf{b}, a) >$. The transition probability $\tau(\mathbf{b}, a, \mathbf{b}')$ is calculated from the transition and observation functions of the original POMDP.

The belief state reward function $\rho(\mathbf{b}, a)$ deserves an attention. It is calculated by the formula:

$$\rho(\mathbf{b}, a) = \sum_{s \epsilon S} b(s) R(s, a) \tag{7.14}$$

One might be tempted to think that assigning artificially large beliefs to the states with higher rewards may increase the reward. However the agent is fixed to the Bayesian update given by Equation (7.13) for the proper calculation of the beliefs and therefore

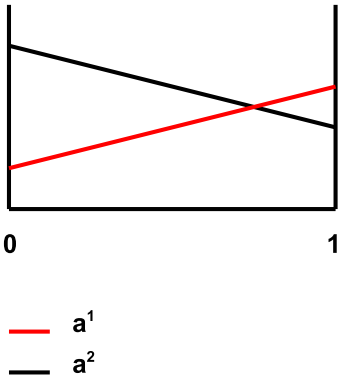

(a) One step value vectors

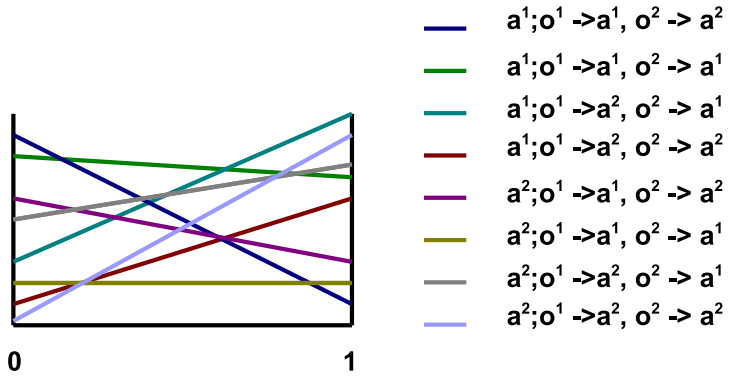

(b) Two step value vectors

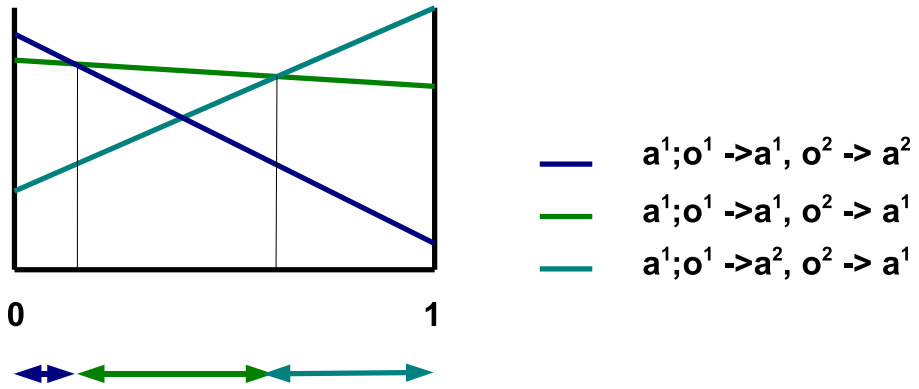

(c) Two step value function

Figure 7.3.: Value iteration steps.

cannot associate arbitrary beliefs to states.

The fact that there is an equivalent MDP process for every POMDP solves the intractability problem. However this is achieved with the cost of having a continuous state space which is multi-dimensional. Even though the DP algorithm can be extended to

account for continuous state spaces, the effective representation of the state space has to be tackled, in order to come up with solutions that are computationally feasible. Fortunately, this is possible owing to the *piecewise linear and continuous*(PWLC) nature of the value functions of the policy trees, which we discuss shortly.

At the heart of every application of DP lies the one step DP update, which calculates the value of a k-step policy from a $k-1$-step policy. We demonstrate the update for a POMDP with two actions and two observations. One step value of a policy π is given simply by:

$$V_\pi^1(s) = R(s, \pi(s)) \tag{7.15}$$

However, the agent is not certain about the state s. Therefore the value of one step policy is given as an expectation over the world states, calculated using the belief state:

$$\begin{aligned} V_\pi^1(\mathbf{b}) &= \sum_{s \epsilon S} b(s) V_\pi^1(s) \\ &= \mathbf{b} \cdot \boldsymbol{\alpha}_\pi^1 \end{aligned} \tag{7.16}$$

The second version of Equation (7.16) can be interpreted geometrically. The belief state $\mathbf{b} = (b_1, b_2, ..., b_N)$ represent a vector in a $N-1$ dimensional space. The reduction in dimensionality is due to the total probability condition that allows one belief state to be expressed in terms of all other belief states. The value of a policy is then the dot product of the belief state vector with a coefficient vector $\boldsymbol{\alpha} = (\alpha_1, \alpha_2, ..., \alpha_N)$. To compare policies for all possible belief values, an alternative geometric interpretation is possible. The belief states are represented by the $N-1$ axes of a coordinate system. Then the value functions are linear planes defined for the hyper cube $[0,1]^{N-1}$. Figure 7.3a demonstrates this for a two state POMDP. In such a POMDP the x-axis represent the belief state of state s_1, since $b(s_2)$ is given by $1 - b(s_1)$. The linear vectors are the value functions of both actions as calculated by Equation (7.16).

The value functions of two step policies can be calculated using the vectors associated with one step policies.

$$V_\pi^2(s) = R(s, \pi(s)) + \gamma \sum_{s' \epsilon S} T(s, \pi(s), s') \sum_{o \epsilon \omega} O(s', \pi(s), o) V_\pi^{o,1}(s') \tag{7.17}$$

In this calculation, $V_\pi^{o,1}(s')$ represents the value of the action in the one step policy that is associated with the observation o in the two step policy tree. The calculation is an expectation over all the possible transitions and observations. Again, the state dependent two step value functions are multiplied with the belief values to obtain the value functions in the belief state space. This calculation transforms the value functions of one step policies in Figure 7.3a into value functions of all the two step policy trees given in Figure 7.3b. Five of the eight policy trees have value functions that are smaller than the remaining three for all belief values. These policy trees are said to be *dominated* and are eliminated. The remaining three policy trees dominate each other on different

partitions of the belief space. Since we are dealing with reward maximizing problems, the optimal policy is to calculate the belief state, and choose the policy tree that is maximum at that particular belief value. This is depicted in Figure 7.3c, where belief partitions in which a particular policy tree is dominant is given with an arrow of the same color.

The one step value iteration for belief MDP is composed of two sub-steps. During the *generation* step, $k+1$-step policies are generated from the non-dominated k-step policies. These are then *pruned* to remove the dominated policies. Effective pruning can reduce the computational complexity of POMDP significantly. In the end of POMDP DP algorithm, one is left with a set of vectors $A_{\pi^*} = \{\alpha_k\}$, similar to the set in Figure 7.3c. The value of the optimal policy can be given in a compact form by using the expression:

$$V_{\pi^*}(\mathbf{b}) = \max_{\alpha \epsilon A_{\pi^*}} \mathbf{b} \cdot \boldsymbol{\alpha} \tag{7.18}$$

Equation 7.18 suggests that the optimal value function at any given belief state can be calculated by performing the inner product operation with the belief state with the vectors in A_{π^*} and taking the maximum value. The output vectors of a POMDP DP algorithm can than be used to calculate the optimum policy. Each vector is associated with a certain policy tree, in a manner similar to Figure 7.3b.

For finite-step problems, the agents computes the belief state that it is in, performs the inner product operation, and than follows the policy tree that is associated with the vector with the maximum inner product result. This means that the agent can base its subsequent decisions on the observations and not on the belief values.

The value functions of discounted infinite problems can also be represented by vectors, and hence do have a PWLC form. However, theoretically the number of vectors that define the infinite value function can be infinite. Optimal infinite stage policies are approximated by sufficiently long finite policies. After a certain step of DP algorithm, the vectors differ only within an acceptable error range, similar to the completely observable case, i.e. Equation (7.10). The vectors are still associated with individual policy tress, however these trees are very long. Thus the strategy of computing belief state initially, and following the policy tree based on observations is not an efficient way. Sondik proposed a more effective method in [99]. In this method, optimal policy π^* is composed of N_p of vector-action pairs:

$$\pi^* = \{< \boldsymbol{\alpha}^1, a^1 >, ..., < \boldsymbol{\alpha}^{N_p}, a^{N_p} >\} \tag{7.19}$$

The agent computes belief state at each step according to the Bayesian belief update given by Equation (7.13). Given the current belief vector $\mathbf{b}_k$, the inner products $\mathbf{b} \cdot \boldsymbol{\alpha}^1$ to $\mathbf{b} \cdot \boldsymbol{\alpha}^{N_p}$ are calculated. The controller chooses the the action that is associated with the vector with the largest inner product at the current belief state.

Yet a more efficient representation of infinite step policies is possible, if the policy has the *finite transience* property, as described first by Sondik and extended later by Cassandra [102]. In such problems the all the belief states in a certain partition dictated

by the vectors are mapped to the same partition after the belief update. This means there is a structured optimal sequence of action-observation-actions for the POMDP, which can be implemented as an Finite State Controller (FSC) . FSC is a simple controller that takes the action in the current state, and jumps to another state according to the next observation. Such an implementation makes the keeping the belief state update unnecessary. Unfortunately not all the POMDPs have this property.

Both pruning and generation steps in the POMDP DP algorithm are linear programming operations, for which efficient algorithms exist. Given a particular linear programming algorithm, different POMDP algorithms have been proposed in the literature such as the original enumerated elimination algorithm by Sondik, Incremental Pruning by Cassandra [103] and Witness Algorithm by Littman [104]. These differ in their computational complexities. Witness algorithm is able to compute optimal policies in polynomial time, as long as the algorithm converges. There is however no guarantee that this will be the case for all classes of problems. Approximations that are time-bound, such as [105], use a grid approach. In these approaches the belief state is divided into finite subsets, for which value functions are computed. It is also worth noting that Hansen developed a policy-iteration solution in [106] [107].

7.2.2. Decentralized Sequential Decision Problems with Partial Information

Decentralized sequential decision problems are the generalization of the centralized problems, in which more than one agent inhibit the world. The agents have their own observation functions. Problems with more than one agent in which the observation functions are shared can be casted as centralized problems with extended action sets. The agents may or may not share the reward function, meaning that the problem may or may not be cooperative or competitive.

The conceptual model is used for the cooperative problems is the following.The agents act according to their local policies that are based on the local observations. The state transition occurs as a result of their joint actions, which change the world state. The agents make individual observations on the new state, and gather jointly the generated global reward.

There are two main models in the literature developed for handling cooperative decentralized problems [108]. They differ from one another in the way they handle the belief states. In addition to the beliefs about the state of the world in centralized problems, the decentralized problems must also include beliefs about the other agents. These beliefs are handled either explicitly or implicitly. In implicit models the state space is augmented with the policies of the other agents. In explicit formulations, agents posses explicit models of the other agents, and have beliefs about the models of the other agents.

Implicit Belief Models

Decentralized POMDP (DEC-POMDP) [109] and Multi-agent Team Decision Problem (MTDP) [110] formalisms are the two leading approaches to decentralized cooperative POMDPs. In both of these approaches, actions and observations are in vector forms.

MTDP conceptually allows a state estimator function, that should be capable of producing a compact belief state, similar to the Bayesian update in centralized POMDPs. Unfortunately, no such compact belief state for decentralized problem has been proposed in the literature, and therefore MTDP state estimator uses the history of all the observations up to the current step. This means, without a compact belief representation, MTDP and DEC-POMDP are equivalent. Both of these formalisms can be extended to account for explicit message exchange between agents. This can be done easily by introducing communicating states to the state space, augmenting the action sets with communication actions and treating the messages themselves as observations. Seuken showed in [108] that MTDP, DEC-POMDP and their communicative variants are computationally equivalent. For the sake of brevity, we will use DEC-POMDP in the following discussions.

Without an compact belief representation like POMDP that allows the formulation as a continuous MDP, the agents in DEC-POMDP have to keep the entire history of observations. Thus the policy trees should cover all the possible observations. The size of the policy tree grows extremely rapidly with the number of decision stages. Given that there are t decision horizons, n agents $|A|$ possible actions, $|O|$ possible observations the size of the policy tree is given by:

$$\left\{ |A|^{\frac{|O|^t-1}{|O|-1}} \right\}^n \epsilon \quad O\left(|A|^{|O|^t}\right) \tag{7.20}$$

The factor n is included, since the agent should choose its policy tree, by taking into account the possible policies that can be used by other agents. This means that in the worst-case, the optimal solution will use double exponential time. There are more efficient algorithms than the brute search such as DP [111] or heuristic search [112] in the literature, but their worst case time behavior is still doubly exponential. Furthermore, the optimal DP solution that Hansen provided runs out of memory after four steps. Therefore the optimal solutions are of theoretical importance and approximate methods are used.

Among various approximation algorithms proposed in the literature Improved Memory Bounded Dynamic Programming (IMBDP) developed by Seuken ([113], [114]) and Approximate Dynamic Programming (ADP) presented by Cogill et. al. in [115]. IMBDP is a hybrid heuristic approach. First most possible belief states are calculated, identifying the policy trees which are associated with these belief states. In the second step DP algorithm is applied among these policy trees. IMBDP outperforms other approximation algorithms in selected benchmark problems. ADP is relevant, since it can be applied to discounted infinite step problems. The main idea in ADP is to separate the state space into partitions, which are associated to individual agents. Each agent employs the DP algorithm in their own partitions, ignoring the other agents. The value function of these local policies approximate the optimal global value function. The error in the approximation can be arbitrarily large depending on the structure of the state space characteristics. There has to be a high correlation between the world states, so that acting based on local observations can approximate acting on global observations.

Explicit Belief Models

All the methods mentioned to now were developed for cooperative scenarios, in which the agents try to maximize a global reward. Furthermore, the solution methods are off-line in nature, where the policies are solved externally and communicated to the agents. There are many problems in which the agents are self-interested, meaning that each agent has its own reward function. Gmytrasiewicz and Doshi present their formalism Interactive POMDP (I-POMDP) [116]. I-POMDP formalism can be used to model both competitive and cooperative problems. It sacrifices optimality with expressiveness as we describe shortly.

I-POMDPs differ from DEC-POMDP variants from the manner the behavior of other agents are handled. DEC-POMDP these beliefs are implicit in the transition functions. I-POMDP on the each agent has explicit beliefs about the behavior of the agents. This is accomplished by defining models of other agents, $m_j \epsilon M_j$ and extending the state space into the interactive state space $IS = S \times M_j$. The models of agents comes in different forms, sub-intentional and intentional models. Sub-intentional models are mappings from observations to a probability distribution over the actions. Intentional models augment the sub-intentional models with belief states. In other words, agents ascribe beliefs to to other agents. This extension comes with the problem of nested beliefs. In an environment with two agents i, j, agent i's model of agent j includes agent j's belief about agent i model, which includes again a belief about agent j model. The nesting can be extrapolated to infinity. Since such an infinitely nested model would not be computable, I-POMDP consults to limiting nesting to finite levels. Even for non-intentional models, where infinite nesting is not an issue, there is the problem of handling the infinite possibilities, in which observations can be mapped to actions for the other agent. Thus an optimal solution to I-POMDP does not exist, and finite model, finite nesting approximations are used. If there are $|M|$ models in consideration and l nesting levels, I-POMDP is equivalent to solving $|M|^l$ individual POMDPs. Again bounds for approximation errors are not known.

I-POMDPs can be regarded from a Game Theoretic perspective as *best response* controllers. This means that the agents build beliefs about the actions of other agents based on the observations and choose the best actions accordingly. On the other hand Game Theory is traditionally interested in finding equilibrium points, from which the agents would not deviate. Partially Observable Stochastic Games (POSG) [111] is an approach coming from this strand of Game Theory, which can be used to model both cooperative and competitive problems like I-POMDP. As a matter of fact, the DP algorithm used to solve POSG is the same algorithm to solve optimal DEC-POMDP problems. The DP algorithm used for solving POSGs employ in conjunction the pruning methods used for POMDP and iterative elimination of dominated strategies used in solving normal-form games. In normal form games, beliefs are about the strategies of the agents. Hansen introduces the generalized belief state, which is similar to the interactive belief state in I-POMDPs. Generalized belief state is defined as the belief over the cross product of world states and the strategy of the other agents. In solving DP for POSG, agents eliminate strategies one by one, by assuming the other agent is following that particular

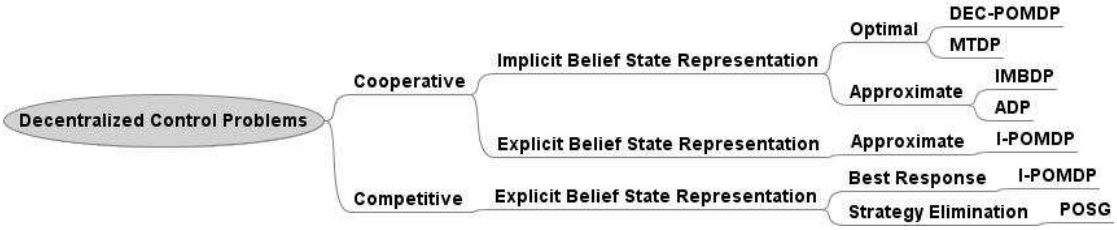

Figure 7.4.: A hierarchy of the algorithms discussed in this section.

strategy. This elimination is continued in an alternating fashion until none of the agents can eliminate any more strategies. This process leaves in the end a number of strategies which are value-equivalent. The question of which strategies are Nash equilibria, i.e. the equilibrium selection problem is still an open question. In [117] Kumar et. al. use the concepts developed for IMBDP to improve the scalability of the original Hansen algorithm, which runs out of memory after four steps. Their algorithm can solve problems up to forty stages.

In Figure 7.4, we present a hierarchy of the algorithms discussed in this section for summary purpose.

7.3. Design Decisions

We essentially have a decentralized problem in controlling the resource sharing among two operators. The software agents running on the RANs are interacting sequentially in a resource-sharing problem. Since they represent different operators, they are unwilling to share information about their internal states. The agents use the distributed user QoE to make imperfect observations about the internal congestion state of the other operators RAN. Based on their beliefs about the conditions on the peer RAN each take a cooperation decision. Decision to cooperate or not to cooperate change the internal states of both operators.

The questions we would like to answer in this section are:

- Which of the formulations we described in Section 7.2 is appropriate for our problem formulation and domain?
- What modifications are necessary to the proposed formalizations are required for a practical control algorithm for inter-operator resource sharing?

Two important criteria we take into account in answering these questions are the complexity of the solution and how realistically the formalization can represent the actual sequence of interactions. In this section we first cover the complexity properties of centralized and decentralized sequential decision making approaches. We begin this subsection with a short primer on Computational Complexity. We will show that applying the newly developed approaches for decentralized sequential making formalizations have serious complexity requirements. We will present an hybrid approach that tries

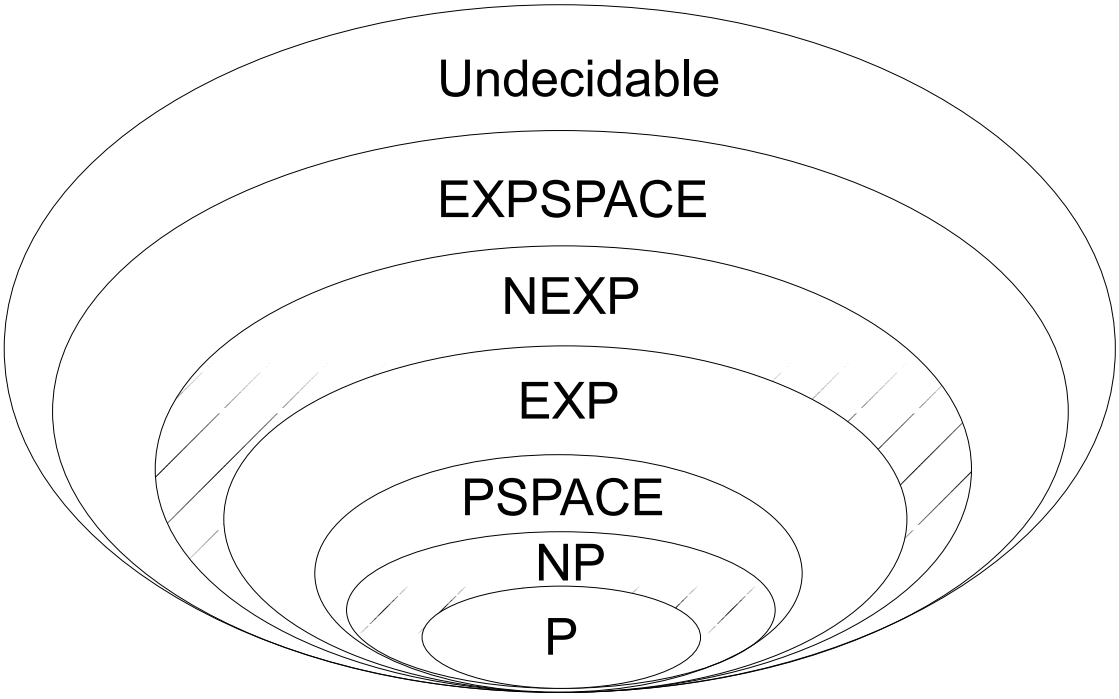

Figure 7.5.: A hierarchy of the complexity classes.

to minimize the time-complexity by formulating the problem as a single agent decision making problem and making sure that this simplification is realistic by using the negotiation mechanisms we present in Chapter 6. We then discuss the selection of the horizon length and the approximation types used in the design.

7.3.1. Complexity

A Primer on Computational Complexity Theory

Computational Complexity [118] is a branch of theoretical computer science that explores the theoretical performance limits of *classes* of computational problems. A class of problems is the set of all computational problems that can be solved with similar performance using hypothetical *models of computation*, such as *Turing Machines* or *Random Access Machines*. These hypothetical machines are able to simulate the logic of any algorithm. The performance measures that is of interest are worst case running times and memory needs as a function of input sizes.

Complexity theory problems are *decision problems*, which are formal "yes/no" questions. The sequential decision making problems, both centralized and decentralized versions, are on the other hand *optimization problems*. In an optimization problem the goal is to find a policy that maximizes the expected reward. In order to apply the rich results of complexity theory, the optimization problems should be converted into decision problems. This is done by formulating the optimization problem as a *threshold problem*

and asking the question "is there a joint policy whose reward exceeds the threshold." The actual determination of the optimal policy cannot be easier than this problem, so in this sense one obtains a limit on the complexity of the optimization problem. *Reduction* is an important concept in complexity theory. A problem A is reducible to problem B, if the answer to problem A is yes if and only if the answer to problem B is yes. Complexity theorists show complexity of particular algorithms by reducing them to known algorithms that belong well-known and well-defined *complexity classes*.

Figure 7.5 depicts the major complexity classes. Complexity class Polynomial Time (P) describes all the problems that whose worst case computation takes an amount of time that is polynomial in the number of inputs. According to *Cobham-Edmonds Thesis* [119] these are the problems that are computable with realistic models of computations, that can be implemented by real life components. Next complexity class in the hierarchy is the class Non-Deterministic Polynomial Time (NP) , which is the set of decision problems that can be computed in a polynomial time by a *non-deterministic Turing machine*. A non-deterministic Turing machine (NTM) is an theoretical extension of the *deterministic Turing machine* (DTM) , which can take multiple computation paths simultaneously. Obviously, this is not possible in reality. NTMs can be simulated in real-life by DTMs in exponential time. It is proven, that the complexity class P is a subset of NP, however the question, if it is a proper subset, i.e. $P \subset NP$, is one of the biggest open problems in theoretical computer science. Many theorists believe this is the case. This is represented by the dashes in the NP class in the figure.

Polynomial Space ($PSPACE$) complexity class covers the problems that require memory space, which is polynomial with the size of the input. $PSPACE$ covers both NP and P, since problems that can be solved in polynomial time with the inputs will require polynomial storage space. If a problem takes exponential time in the worst case when it is computed on a deterministic Turing machine, it belongs to the complexity class Exponential Time (EXP) . Since $PSPACE$ is a superset of NP, which can be computed in exponential time, $PSPACE$ problems form a subset of EXP. Thus the instances of $PSPACE$ require exponential time in the worst case.

In a fashion similar to the relation between P and NP, the class of problems which take exponential time when computed by a NTM is a superset of EXP and belong to the class Non-Deterministic Exponential ($NEXP$) . Owing to the fact that NTMs can be simulated in exponential times with DTMs, problems in this class require doubly exponential running times. Again, it is conjured, yet not proven that EXP is a proper subset of $NEXP$. The largest set for which an answer can be given to the decision problem is the class Exponential Space ($EXPSPACE$) . The problems in this class require exponential amount of memory to run.

A given problem A is said to be C-$HARD$ in a complexity class C, if any problem in class C can be reduced to problem A. These are the hardest problems in the class C in the sense that providing an efficient solution to problem A would mean providing a solution to all the problems in class C. A further description in Computational Complexity is the concept of C-$COMPLETENESS$. A problem A is C-$COMPLETE$ if it is C-$HARD$ and contained in the class C.

Complexity of Centralized Decision Problems

The first complexity results for sequential decision problems is due to Papadimitrou and Tsitsiklis. They established that all forms of MDPs, that is finite or infinite horizon and irrespective of the cost function definitions, are *P-COMPLETE* in [120]. Furthermore, they showed that the MDP problems belong to a complexity class *NC*, which is a subset of the class *P*. Such problems can be computed even more efficiently using parallel processors. Their results for POMDP were less encouraging. Specifically, they showed that even for short horizons, i.e. the time horizons shorter than the number of states, POMDP problems are *PSPACE-COMPLETE*. This means the POMDP algorithms will take exponential times in the worst-case. Even if one accepts exponential time and settles for an off-line algorithm that computes an optimal policy finite-horizon policy, there are problems with the applicability of the computed policy as an online controller. The authors show that it is not possible to represent such a finite horizon policy in a string that is exponential with the input size. The results of Papadimitrou and Tsitsiklis were extended more recently by Madani et. al. [121] and Mundhenk et. al. [122]. Madani et. al. show that the infinite horizon POMDP problems are undecidable. This disheartening result for infinite horizon problems are relieved by Mundhenk et. al.. They show that long term horizon POMDPs belong to the class *PSPACE*. The problems in *PSPACE* are computable, as opposed to undecidable problems. They have exponential worst case running times, and reasonable heuristics are possible.

In the face of their complexity properties we summarized, there are three questions to be asked regarding the practical applicability of POMDP solution algorithms described in Section 7.2.1. These are:

- How likely is the occurrence of worst-case exponential running times?
- How do approximations perform?
- How do heuristics perform?

The answer to the first question depends on the actual POMDP model under use. Unfortunately, a general theoretic answer to this question has not been given in the literature. The question can be answered experimentally, by using different POMDP models. This is the approach that Cassandra took in his thesis [102]. Unfortunately, the number of POMDP models that are accepted as benchmarks is not large in the literature. This is why Cassandra worked with randomized POMDP models. The results for Witness algorithm is depicted in Figure 7.6. It can be said that for small state spaces and observations less than five algorithms are suitable for at least off-line solutions.

Finding approximation algorithms that achieve to the optimal policy with a given error bound is an approach taken for certain complexity classes. However this is not the case for POMDP algorithms. Condon et. al. [123] show that finding a policy that gives an expected reward within a vanishing error bound for *PSPACE* is also *PSPACE*.

Thus heuristics is the only viable option. Cassandra's thesis [102] analyzes a wide variety of heuristics. Since the optimal POMDP policy is unknown, he compares the

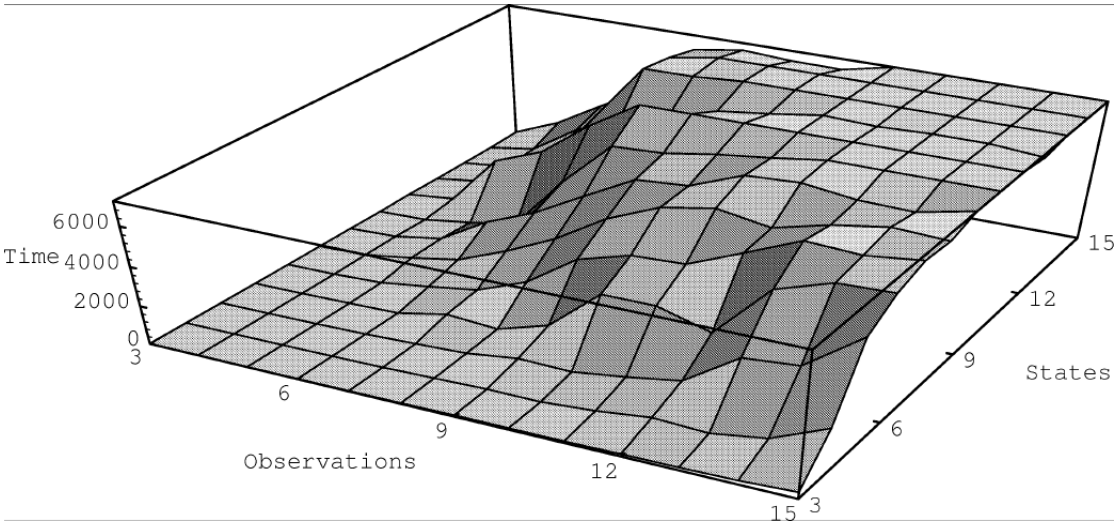

Figure 7.6.: Average running time of Witness algorithm for POMDPs, taken from [102].

expected rewards of the heuristics with that of an *omniscient* policy. Omniscient policy is a fictitious non-realizable policy that is able to see the system states at all times. The heuristics considered in the thesis include the *most likely state* (MLS), *action voting* (AV), *Q-MDP* and *weighted entropy control* and finally *Approximate Value Iteration*. In MLS, the idea is to update the belief state with observations, solve the problem as if it were completely observable MDP, and take the action associated with the state that has the highest probability. MLS completely ignores states except the most likely state, which is improved by Action Voting. AC chooses the action that maximizes the expected reward over the belief state over a single step. Both MLS and AV are myopic control policies, which do not consider the results of the actions in terms of the resulting path of future states. Q-MDP takes into account the future states, by choosing the action that maximizes the expected value functions over the belief states. The value functions of individual states are calculated as if the system is completely observable using Equation (7.4). Weighted entropy control is a method from the control theory, in which actions are chosen to minimize the entropy associated with belief states and maximize reward simultaneously.

Approximate Value Iteration control policy involves solving the Value Iteration Algorithms with efficient approximate algorithms such as Witness or Incremental Pruning we mentioned in Section 7.2.1 until they converge, and use it as the true optimal value function. Across a wide range of POMDP problems, Cassandra shows that the heuristic control policy *Approximate Value Iteration* performs consistently not worse, and in some cases considerably better than all the other heuristics.

Complexity of Decentralized Decision Problems

The complexity characteristics of the decentralized problem is even more troublesome than its centralized counterpart. It was again Papadimitrou and Tsitsiklis who provided the first results on the complexity of decentralized sequential decision problems. In 1986 [98] they showed that the decentralized control of MDPs is at least *NP-Hard*, but did not provide any upper bounds on the complexity. The next important result was provided by Bernstein et. al. in 2000 ([124], [109]), when they showed that the decentralized control of a two agent MDP is *NEXP-complete*. As discussed in Section 7.3.1 it is proven that $P \subset NEXP$, which means that optimal control of decentralized MDPs and POMDPs are infeasible according to *Cobham-Edmonds Thesis*. Furthermore since it is widely believed, but not yet proven, that $EXP \neq NEXP$, decentralized control of MDPs and POMDPs will require doubly exponential time in the worst case. This is inline with the complexity analysis results given in Equation (7.20). As discussed in Section 7.2.2, the jump in complexity going from single agent to two agents stems from the impossibility to represent the multi-agent beliefs in a compact manner. This leads to the necessity to store and process observations, that grow doubly exponentially over time.

Similar to the central decision problem, reduction in complexity is not possible using approximations that guarantee a maximum error compared to the optimal policy. Rabinovich et. al. proves in [125] that obtaining so called ϵ-*approximate* solutions that guarantee the approximation error to be smaller than the value ϵ for DEC-POMDPs is also *NEXP-hard*. The only reduction in complexity the authors could report was in the case of free communication, in which case the agents can exchange information about their observation histories without incurring a cost. In this case the complexity class was *PSPACE*, same as a centralized POMDP. This is not surprising, since with free communications the problem can be transformed into a centralized problem. Pyandah provided similar results for MTDP in [126], which is consistent with Seuken and Zilberstein's results, showing the equivalence between MTDP and DEC-POMDP formalizations.

I-POMDP attacks the complexity problem by extending the state space with models of the interacting agents. As discussed in Section 7.2.2, this leads to the problem of the need for infinitely nested belief states. Such a formulation is undecidable. The authors of I-POMDP [116] can only provide complexity results for models with finite models and finite strategy levels. For fixed strategy level l, which is also the level of belief nesting, and M models for the other agents I-POMDP is equivalent to solving M^l individual POMDPs. This means that I-POMDP has the same complexity properties as POMDP, i.e. *PSPACE-complete*. However as soon as the strategy level is made a variable value, the complexity increases substantially, even though there is no formal reduction proof is provided yet.

Our Approach

Let us review the presented formalizations in the light of the design criteria we presented in Section 7.3.

DEC-POMDP DEC-POMDP formalization is the one that has received most interest. It is conceptually equivalent to MTDP. However the main shortcoming of DEC-POMDP, which makes it not suitable for our problem, is its common reward structure. This reward structure only allows cooperative problems to be formulated. One of the main features of our problem formulation is the fact that two competing operators will be sharing resources only if it benefits both of them at the same time. This means that there might be instances when one of the operator is willing to cooperate, while the other one does not. Such a situation cannot be modeled with DEC-POMDP.

Furthermore, the workflow by which the problem is solved and the policies are executed in DEC-POMDP is not compatible with the dynamic resource sharing workflow. DEC-POMDP assumes that there is a central entity which can solve for the policies. The policies would then be executed in an decentralized manner. This contradicts the two interacting operators scenario that we propose.

POSG The first formalization that accommodates non-common reward structure and therefore can model cooperative encounters is the POSG formalization. There are two drawbacks that are associated with POSG, that makes it unsuitable for our purposes.

First of all solution of POSG gives us not single policy, but a set of Bayes-Nash optimal policies. A proper solution to the decentralized sequential decision making on the other hand would involve a single strategy set for the involved agents. There are coordination protocols in the literature that allow a single policy to be chosen, however they add to the complexity of the solution. Secondly, the POSG workflow is similar to the DEC-POMDP workflow, in the sense that the solution that gives the set of policies is given by a centralized entity.

I-POMDP Similar to POSG I-POMDP is able to model cooperative encounters. Furthermore, unlike POSG and DEC-POMDP the decision workflow is comparable to the dynamic resource sharing since the solution for policies are taken by the agents independently. These properties make I-POMDP a good candidate formalism for dynamic resource sharing.

Unlike POSG or an DEC-POMDP, an optimal solution for I-POMDP is not available. This is due to the problem of infinite nesting of beliefs and the infinite cardinality of the model space that describe the peer agents. Only computationally viable solution I-POMDPs are possible when a finite strategy level is chosen and the number of models is taken to be finite. The question here is than, how one can choose an appropriate value for the model order and the strategy level. Before answering this question, it is important to note that any agent designed with an arbitrary but finite strategy level or model order will be outperformed by an competing agent, whose strategy level or model order is larger. This property makes the answering of the aforementioned question futile. No matter how optimally we were to set the strategy level and the model order, another designer who is willing to add one more level or order would benefit from this.

In the face of this apparent deadlock, we answer the question by not answering it. To be more precise, we are proposing enforcing a strategy level of 0, i.e. 0-level I-

POMDP. This approach is equivalent to folding the behavior of the other agent as noise in the system. Such a solution is of course sub-optimal to an agent even with a single level of strategy, i.e. a model which models the beliefs of the peer agent about the agent itself. We are proposing using *strategy-proof mechanisms* to be used in the inter-agent interactions to make this undertaking irrational. Specifically, strategy-proof mechanisms are negotiation mechanisms in which lying is irrational for the participating agents. When such a mechanism is in place, agents behave according to the rules of the negotiation mechanism, and there is no need for second guessing what the peer agents beliefs. We present two such mechanisms in Chapter 6. For the rest of this chapter, we assume that there is a strategy-proof negotiation protocol implemented between the agents of the operators.

7.3.2. Horizon Length

After we finalize the formalization, we are left with two important design decisions. First one is to decide on the length of the horizon. Based on the this one should also opt for the type of approximation will be used to solve for the policies.

Let us recapitulate dynamic resource sharing scenario, in order to find a suitable horizon length. In a certain location a RAN belonging to one operator becomes overloaded. The operator begins a negotiation with a peer operator who owns a RAN in the vicinity, in order to transfer some of its traffic. If the peer operator has enough capacity to support the additional traffic, the operators agree on a transfer probability, which can also be denoted by an equivalent transfer throughput. Once this step is completed, both operators submit periodical queries to the QoE database to make observations about the load situation in the peer operator's RAN. The transfer of resources continue until *(i)* the donor operator RAN becomes overloaded or *(ii)* the congestion in borrower operator subsides. Neither of the RAN agents are able to foresee how many observation steps will it take, before one of the aforementioned conditions will take place in which one of the operators will take a do not cooperate decision. It this were possible, both of the operators would be able to agree on a static time period in which the resource exchange would take place, and the whole discussion in this chapter would be unnecessary.

In the literature, uncertainty in the time steps after which the interaction finishes is handled with infinite horizon models with exponential discounts. This approach allows interactions of varying lengths to be represented. As we discussed in Section 7.2.1 an infinite horizon model with a discount factor γ is equivalent to a sequential decision process, in which the decision process is terminated with probability $(1 - \gamma)$ after each decision stage. Such a formulation has two other advantages compared to a finite horizon length formulation.

First of all, this formulation is in line with the practice used in economics to model the investors behavior, which correspond in our case to the operator. In this interpretation the modeler is able to represent the risk-avoidance preferences of the investor. This is possible because γ is a measure of relative importance of future rewards compared to the current reward. A smaller γ represents a risk-averse investor, for whom the current reward is the most important reward. On the other hand, a larger and a closer to one γ

represents a risk-taking operator, who is willing to exchange future rewards with current rewards.

Secondly, as we again discussed in Section 7.2.1, the optimal policies differ for finite and infinite horizon formulations. In finite horizon problems the optimal policy is not stationary, since knowing that the end of the interaction is approaching changes the optimum action during the final stages. Having finite state non stationary policies is problematic, since the size of the non-stationary policy can be arbitrarily large for it to be represented efficiently. This is not the case for infinite horizon models, which can be represented with a finite set of vectors or as a FSC . For the aforementioned reasons we have decided to use an infinite horizon model with a properly set discount factor.

7.3.3. Approximation Type

Once we have decided for the infinite horizon formulation, the exact solution of both centralized and decentralized sequential decision making problems is not possible anymore, since these solutions are shown to be undecidable [120]. We therefore should use approximate methods.

Approximation has different semantics in the fields of Theoretic Computer Science and Artificial Intelligence [108]. The Theoretic Computer Science community uses the term approximation in the same manner as the ϵ-*approximation* we discussed, i.e. an approximation algorithm is able to provide a solution which is within an ϵ error bound of the optimal solution. There is only a single such solution in the literature for infinite horizon cases presented by Poupart and Boutilier for centralized problems [127] and Bernstein et. al. for decentralized problems [128]. Both of these approaches are based on policy iteration and are distinguished by their reliance on what is called a *correlation device*. A correlation device is an stochastic finite state machine with at least two states. It is assumed that both agents are able to simultaneously observe the state of the correlation device perfectly. The agents policy uses this observation in addition to the proper observations about the world in deciding the actions. It must be noted that correlation device is used strictly to synchronize the randomness in both agents, and is not used for communication. Even though the correlation device can be implemented implicitly with an pre-shared sequence of pseudo-noise sequence, without any direct communication, we do not use this approach. The reason for this is the increase in complexity. It must be noted that this line of research is an efficient approach that may be used in the future work.

We use the term approximate algorithms less strictly, as they understood in the Artificial Intelligence (AI) community. When theoretic optimal solutions are available, but computationally not feasible, AI approximations use computationally feasible heuristics based on the optimal solutions. These approximations do not provide guarantees on the quality of the solution, and their performance are compared to *(i)* each other or *(ii)* to an optimal solution to a superset problem which is computationally feasible. In our case this superset problem is the completely observable counterpart of dynamic resource sharing, and the optimal solution to the superset problem is the omniscient policy we discuss in 7.3.1.

There are two motivating factors for our decision to use approximate solutions to POMDPs. First of all, being heuristics, the quality of algorithms can only be gauged relative to each others. This is done in the literature, by using benchmark problems that is accepted by the community. Establishment of the benchmark problems is a time consuming process, and in the end there are limited number of such problems. As a result of their relative age, the number of benchmark problems for centralized sequential decision making is larger than decentralized case. This means that the results in centralized decision making is more established.

Secondly, relative complexity of POMDP compared to CO-POMDP is less. To be more precise, the worst case time complexity of POMDP is exponential, where are CO-POMDP is doubly exponential in the input size. It is true that exponential worst case time complexity is not a particularly nice feature, but it has been shown for a large set of benchmark problems that POMDPs rarely exhibit the worst case time. Secondly, since CO-POMDP belong to the complexity class *NEXP*, which is a proper superset of PSPACE, the solution policies are problematic to represent in an efficient manner.

7.4. Solution

7.4.1. Overview of Derivation

After choosing the formalization and choosing the horizon length and the solution method, we are in a position to present the derivation of the control algorithm which will be used by the RAN agents. Before we present the details, it is beneficial to present an overview of the derivation.

In the following sections we will first describe the equality between Discrete Time Markov Chains (DTMC) and Continuous Time Markov Chains (CTMC) and the method of *uniformization* that allows us to transform CTMCs into DTMCs, and vice versa. We will first generate a CTMC description of the the queueing network description of the dynamic resource sharing. Then we will use uniformization is needed for us to formulate a MDP out of the model, which is a CTMC. We will see that level of granularity of the obtained DTMC will be too detailed for the application of POMDP control to the problem. For this purpose we will present a method of state lumping, that allows us to build larger macro states, which lend themselves to POMDP control algorithms. We present the whole process on a load balancing scenario between two WLAN RANs. We finally present the solutions, i.e. the controllers, for load balancing between tho WLAN RANs and a between WLAN and HSDPA.

7.4.2. Uniformization & Construction of a DTMC

Uniformization

Let us start with reviewing CTMCs, DTMCs and the link between them. Our discussion follows [55] and [129]. DTMCs are used to model systems, in which the transition between states occur on periodic intervals. The periodicity maybe due to the natural characteristics of the system, such as in clocked digital systems, or due to a sampling

process that is used to capture a continuous process. In both cases, a homogenous DTMC is described by a *transition probability matrix* $\mathbf{P} = [p_{ij}]$. The element p_{ij} gives the probability of the system making a transition from state s_i to state s_j. Due to the total probability condition the rows should add to one, i.e. $\sum_j p_{ij} = 1 \quad \forall i$. If the sampling period or clock period is given by τ, the probability that the system spends $n\tau$ seconds in a particular state s_i, or equivalently state holding time $V(i)$ being equal to $n\tau$ is distributed geometrically with parameter p_{ii}:

$$Pr(V(i) = n\tau) = (1 - p_{ii})p_{ii}^{n-1} \tag{7.21}$$

If we let $\boldsymbol{\pi} = [Pr(s_1)Pr(s_2)...Pr(s_n)]$ denote the vector of steady state probabilities of the states, the solution of a stationary and homogenous DTMC can be obtained by simultaneously solving the following set of linear equations:

$$\begin{aligned} \boldsymbol{\pi} &= \boldsymbol{\pi}\mathbf{P} \\ \boldsymbol{\pi}\mathbf{1}^T &= 1 \end{aligned} \tag{7.22}$$

The first equation is derived from the fact that transition probabilities cannot change the state probabilities once the steady state is reached. Second linear equation is just the total probability condition.

CTMCs in contrast are used to model systems in which the state transitions can occur at any given time instant. Instead of actual probabilities of transitions, we are interested in *transition rates*:

$$q_{ij} = \lim_{\Delta t \to 0} \frac{p_{ij}(t, t + \Delta t)}{\Delta t} \tag{7.23}$$

q_{ij} represent the instantaneous rate with which transitions occur between states s_i and s_j. For Markovian processes with Poisson arrivals, this is equivalent to the Poisson rate λ_{ij} of the process that causes the transition. Differentiating the total probability condition results in the condition $-q_{ii} = \sum_{j \epsilon S} q_{ij}$, which means that the term q_{ii} represent the total rate with which the process leaves the state s_i.

Similar to DTMCs, CTMCs can be solved for the steady state probabilities $\boldsymbol{\pi} = [Pr(s_1)...Pr(s_n)]$ by using the following set of linear equations:

$$\begin{aligned} \mathbf{0} &= \boldsymbol{\pi}\mathbf{Q} \\ \boldsymbol{\pi}\mathbf{1}^T &= 1 \end{aligned} \tag{7.24}$$

In these equations, $\mathbf{Q}$ is a the transition matrix, whose elements are q_{ij} and $\mathbf{0}$ is a row vector of all zeros. The intuition behind the first equation is that at steady state the the transition between states should be balanced, and the thus transition rates between states should add up to zero. This is the the *global balance condition*. One can calculate the state holding times using the term q_{ii}. Unsurprisingly the state holding time

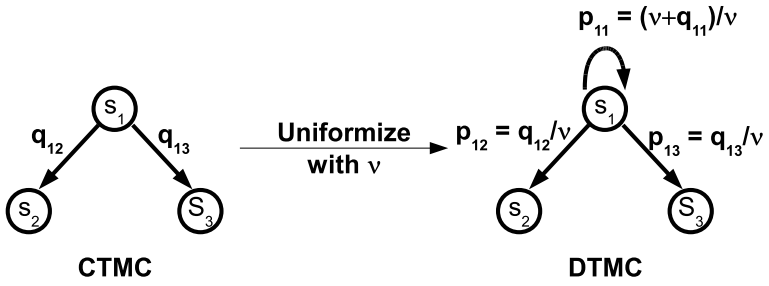

Figure 7.7.: Uniformization example.

$V(i)$ is distributed exponentially, which is the continuous time counterpart of Geometric distribution in Equation (7.21):

$$Pr(V(i) = \tau) = 1 - e^{\lambda_{ii}} \tag{7.25}$$

This relation between the channel holding times is key to the process of uniformization, which allows us to build an equivalent DTMC model out of a given CTMC model. Let us assume that we have a CTMC described by its transition rate matrix $\mathbf{Q} = [q_{ij}]$. As we described earlier, the terms $-q_{ii} \quad \forall i$ represent the total transition rates out of the states. Let us denote this transition rate out of state s_i with $\Lambda(i) = -q_{ii}$. One chooses an uniform rate ν such that $\nu \geq \Lambda(i) \quad \forall i$. One can than use this uniform rate as the "sampling" rate that is associated with an equivalent DTMC. This is equivalent to assuming system changes with a rate ν, where the changes include "real" transitions between states, and fictitious transitions from states unto themselves. In fact, these fictitious self-transitions have a rate of $\nu - \Lambda(i)$. With this uniform rate, the probability of transitioning from state s_i to s_j is then simply the ratio of transition rate q_{ij} to the total transitions associated with the state s_i which is given by ν. This process is demonstrated by Figure 7.7, and by the following equations:

$$p_{ij} = \begin{cases} \frac{q_{ij}}{\nu} & j \neq j \\ \frac{\nu + q_{ii}}{\nu} & i = j \end{cases} \tag{7.26}$$

The need to use uniformization stems from the fact that we have chosen to apply 0-level I-POMDP approach on a system described by a queueing network. I-POMDP formulation is based on a DTMC , and the BCMP solution to the queueing network is based on a CTMC model. It is standard practice in the area of controlled Markov Chains to reduce CTMC descriptions of real world systems to DTMCs via uniformization, and this is the path we follow. When reducing a CTMC description of a system to a DTMC with an uniformization rate ν, the discount factor and reward per stage have to be adjusted.

Formally, let us define the expected reward with a discount factor β associated with a CTMC under the control of a policy π with:

$$E_\pi \left[\int_{t=0}^{\infty} e^{\beta t} R(s(t), a(t)) \right] \tag{7.27}$$

Our goal is to obtain the equivalent reward of the uniformized DTMC under the same policy. The derivation in Section 7.3.2 in [129] makes use of the relation between channel holding times of the CTMC and DTMC. Cassandras uses the following facts: *(i)* the reward stays the same between transitions, *(ii)* the transitions -including the fictitious transitions- occur with a combined uniformized rate rate of ν and therefore the state holding times are exponential with ν, to derive the following equality:

$$E_\pi \left[\int_{t=0}^{\infty} e^{-\beta t} R(s(t), a(t)) \right] = \frac{1}{\beta + \nu} E_\pi \left[\sum_{k=0}^{\infty} \left(\frac{\nu}{\beta + \nu} \right)^k R(s_k, a_k) \right] \tag{7.28}$$

With this relation, the uniformization process is complete. When we are given a CTMC model with its transition rate matrix Q, reward structure $R(s, a)$ and discount rate β, we can construct an equivalent DTMC by:

- Constructing transition probability matrix P by making use of the Equation (7.26),
- Using modified rewards: $R_{DTMC}(s, a) = R_{CTMC}(s, a)/(\beta + \nu)$,
- Using a modified discount factor $\alpha = \nu/(\beta + \nu)$.

Construction of an DTMC

Unfortunately, we do not have access to the CTMC directly. This is because the BCMP solution bypasses the generation of the CTMC in providing the separable solution. However, since BCMP makes use of a special structure in the CTMC, it is not hard to obtain a a CTMC. It is worth noting that this is not trivial either, since this it is essentially a reverse problem: we are interested in the CTMC formulation, given the solution to it.

We give a short summary of the BCMP model from Chapter 5, which is depicted in Figure7.8. Each operator is modeled by a tandem of an infinite server (IS) and a processor sharing (PS) queue. For each operator the IS node models the call admission process (CAC), whereas the PS node represents the actual contention among the users for resources within an RAN. We concentrate on PS delay as the system delay, since it is larger. User requests arrive according to a Poison process described by λ. The users choose one of the operators for their session requests with probabilities P_A and P_B. Each RAN employs a CAC mechanism that rejects session requests with a probability $P_{(R,i)}$, for operator i. Given the capacities of the RANs and the current tendencies of the users to choose an operator, RAN A is a borrower of resources and transfers some of its users to donor RAN B with probability P_T. It may seem like the RAN A has an incentive to give as much traffic as possible; however, this is not the case since the transferred traffic increases the delay in RAN B, which would also affect the users who chose RAN A initially but were transferred. Therefore RAN A tries to minimize the expected delay

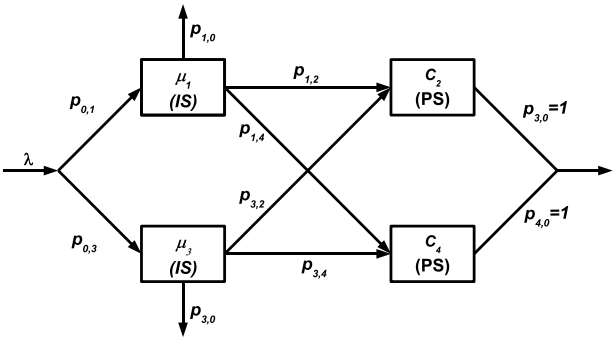

Figure 7.8.: Queueing network model for dynamic resource sharing between two operators A and B.

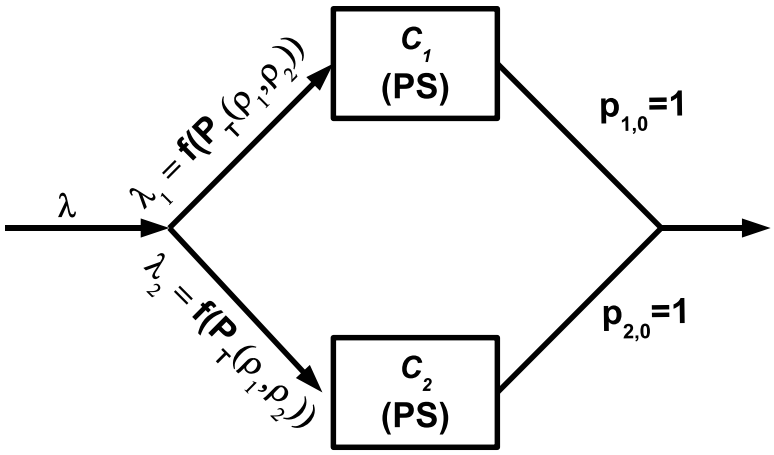

Figure 7.9.: Simplified queueing model

among all the users who chose RAN A. This formulation makes the average delay of RAN A concave and us to derive an optimal P_T value. After the traffic equations are written, BCMP formulation gives us a product form solution which we exploit in order to come up with the POMDP state transition probabilities.

For the purpose od POMDP derivations we concentrate on the processor sharing queues of the RANs, that model the actual air interface. For this purpose we use the simplified queueing model given in Figure 7.9. In this model the external traffic is shared as a function of the transfer probability P_T, which itself is a function of the

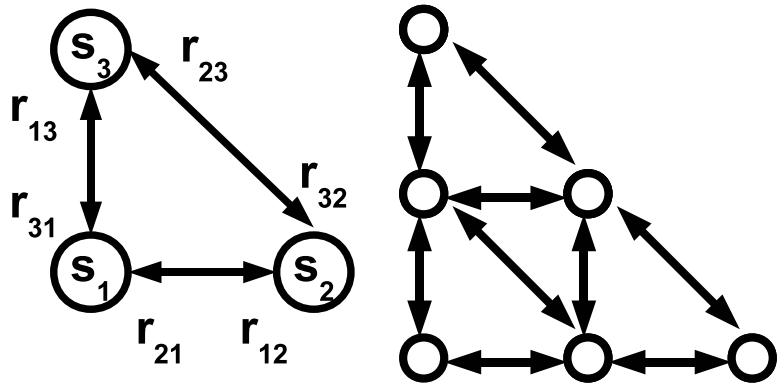

(a) Atomic transition diagram. (b) Two job extension.

Figure 7.10.: Construction of CTMC from atomic transition diagram.

utilizations of the individual RANs. We represent the joint probability of N_1 jobs in the first operator and N_2 jobs in the second operator with $\pi_{N_1N_2}$. Since we are using PS node models for which M→M property holds, the joint probability can be described as a product form solution of the marginal probabilities, i.e. $\pi_{N_1N_2} = \frac{1}{C}\pi_1(N_1) * \pi_2(N_2)$. Lazar presented a geometrical construction method for the construction of CTMC from the physical description of the queueing system in [130]. This method uses a atomic queueing network with two queues with post processing job sharing to build arbitrary queueing networks. The atomic CTMC is depicted in Figure 7.10a. This atomic CTMC is replicated by connecting at the edges to increase the number of users in the system. Different rates can be assigned for different replicas, which makes the description of state-dependent routing possible.

For our scenario, we do not have post processing job sharing, this is why we have $r_{23} = r_{32} = 0$. Since we have an open network, the size of the CTMC is infinite in both sides. We obtain the CTMC depicted in Figure 7.11 following the procedure proposed by Lazar. To show the validity of the CTMC, one has to compute the consistency graph. The consistency graph is a directed graph equivalent to the CTMC, whose nodes represent the probabilities of the corresponding states. The multiplication of the node value and the value on the directed edge to a neighbor node gives the value on the neighbor state. A consistently constructed CTMC should have all the closed paths in the consistency graph equivalent to 1. In order to show the consistency of the CTMC, we should show that the local balance equations have solutions.

For this purpose we first write down the global balance equation for node $(0, 0)$:

$$\underbrace{\pi_{00}\lambda_1}_{\text{departures due to 1}} + \underbrace{\pi_{00}\lambda_2}_{\text{departures due to 2}} = \underbrace{\pi_{10}\mu_1}_{\text{arrivals due to 1}} + \underbrace{\pi_{01}\mu_2}_{\text{arrivals due to 2}} \tag{7.29}$$

Equating the transitions associated with both nodes, and writing the state probabilities in terms of the marginal probabilities we obtain:

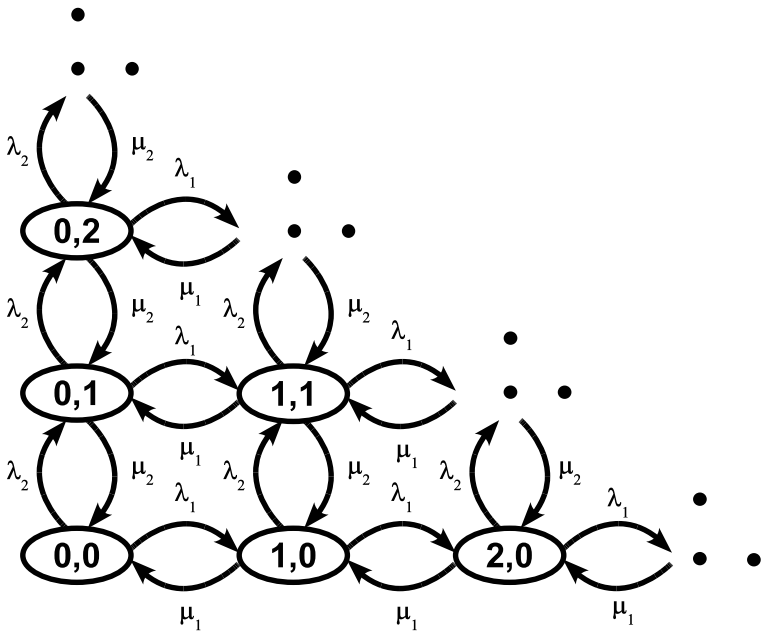

Figure 7.11.: Proposed CTMC model.

$$\begin{aligned}\pi_1(1) &= \rho_1\pi_1(0)\\ \pi_2(1) &= \rho_3\pi_2(0)\end{aligned} \tag{7.30}$$

We similarly we write the global balance equation for node $(1,0)$:

$$\underbrace{\pi_{10}\lambda_1 + \pi_{10}\mu_1}_{\text{departures due to 1}} + \underbrace{\pi_{10}\lambda_2}_{\text{departures due to 2}} = \underbrace{\pi_{00}\lambda_1 + \pi_{20}\mu_1}_{\text{arrivals due to 1}} + \underbrace{\pi_{11}\mu_2}_{\text{arrivals due to 2}} \tag{7.31}$$

We again equate local flows, substitute (7.30) in the local balance equations and write the node probabilities in terms of the marginal probabilities to obtain the following results:

$$\begin{aligned}\pi_1(2) &= \rho_1\pi_1(1) = \rho_1^2\pi_1(0)\\ \pi_2(1) &= \rho_2\pi_2(0)\end{aligned} \tag{7.32}$$

Similar steps gives us the following local balance equations for the state (01):

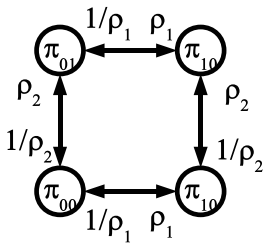

Figure 7.12.: Consistency graph.

$$\begin{aligned}\pi_2(2) &= \rho_2\pi_2(1) = \rho_2^2\pi_2(0)\\ \pi_1(1) &= \rho_1\pi_1(0)\end{aligned} \tag{7.33}$$

Thus moving in the horizontal axis gives the relation $\pi_1(k+1) = \rho\pi_1(k)$ and moving in the horizontal axis gives us $\pi_2(k+1) = \rho_2\pi(k)$. With these information we are able to construct the consistency graph, given in Figure 7.12. Any closed loop that is constructed from this atomic diagram will have product of 1, so the proposed CTMC is a proper CTMC. The corresponding solution is just the part of the original BCMP solution that include PS nodes:

$$\pi_{N_1N_2} = \frac{1}{(1-\rho_1)(1-\rho_2)}\rho_1^{N_1}\rho_2^{N_2} \tag{7.34}$$

Finally, we are in a position to construct the DTMC. We have to choose an uniformization rate that is guaranteed to be larger than all the transition rates in the CTMC. We choose the uniformization rate $\nu = \lambda_1 + \lambda_2 + \mu_1 + \mu_2$, which is guaranteed to be larger than all the rates in the CTMC.With this choice, the DTMC is constructed, which is given in Figure 7.13.

7.4.3. State Aggregation and Capacity Boundaries

State Aggregation

Due to the complexity results we discussed it is of prime importance to keep the number of states in the POMDP as small as possible. However the DTMC description we obtained has infinite number of states. Obviously, there is a need for reduction in the number of states. In classical problems in which interacting servers are modeled as CO-MDPs , infinite number of states is handled by finding boundaries between groups of states. These groups include those states, for which a common action satisfies the DP inequality for all of the states. The policy can then be implemented by finding which group of states the current state belongs to, and executing the action for that group. We will employ an approach that is influenced by this method.

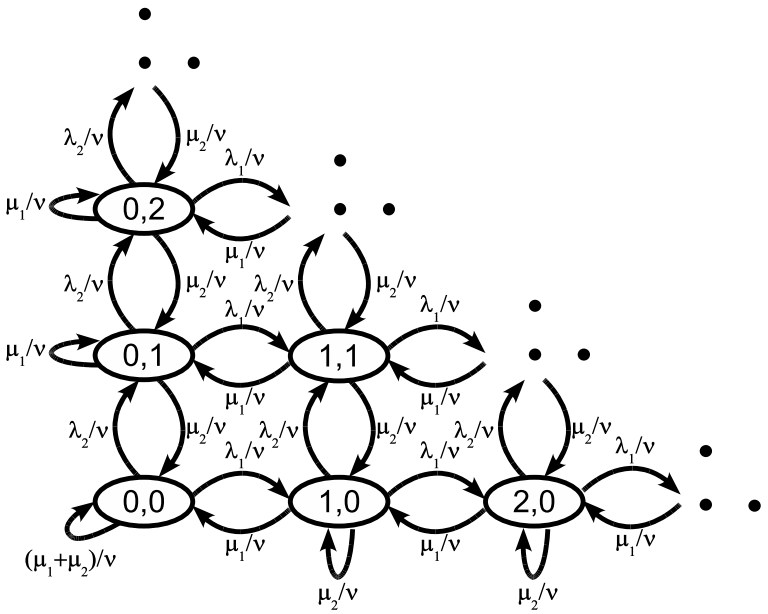

Figure 7.13.: Final DTMC.

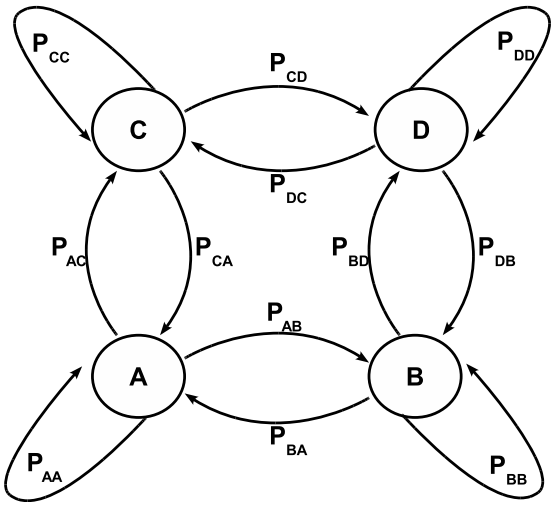

Figure 7.14.: Macro state transition diagram.

We will distinguish between *micro* and *macro* states. The individual DTMC states represents the highly dynamical micro behavior of the system. The micro states represent the number of active sessions in each system, and they change proportional to the combined external arrival rate. It is not the responsibility of the RAN agent running the POMDP to take decisions on a user session request by request basis, this is the responsibility of CAC . The RAN agents should take decisions in the case of severe changes

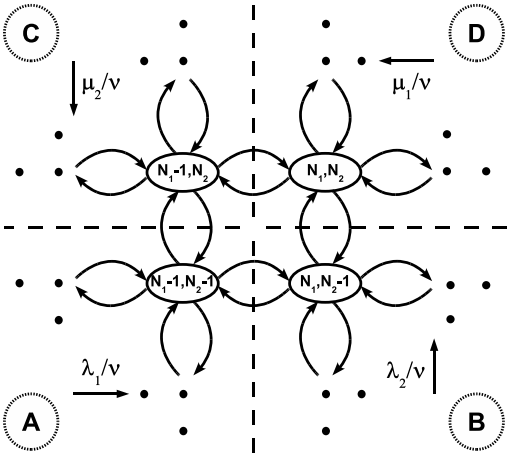

Figure 7.15.: DTMC state transition diagram and calculation of capacities.

in the overall load of the RANs. Thus, the macro states capture the conditions in the individual RANs as to whether or not they are able to deliver the QoS guarantees. A RAN is said to be in a normal state, when it is able to meet a QoE guarantee given in terms of a delay or throughput requirement. Since we have two RANs under consideration we have four macro states in which are depicted in 7.14. In state A both RANs are operating normally, as opposed to state D, in which both RANs are in congestion. In state B the RAN for which POMDP solution is applied is in congestion, while the peer operator is in normal operation mode. State C is the opposite. What we have done is to simply to lump micro-states into macro-states according to their congestion status'. Our aim is to formulate the macro transition probabilities, Figure 7.14, from the micro transition probabilities, Figure 7.13.

What we are looking for is a correspondence between the performance metrics associated with macro states and the micro states. The macro states A through D divides the state space S of the micro states into four partitions, such that $S = S_A \cup S_B \cup S_C \cup S_D$ and $S_i \cap S_j = \emptyset$ where $i \neq j$ and $i, j \epsilon \{A, B, C, D\}$. These partitions are rectangular, as depicted in Figure7.15. The intuition behind such an rectangular state aggregation of micro states is the PS abstraction. Service rate is inversely proportional to the the user number in a RAN. This means that there will be a limit on the number of users in each operator, N_1 and N_2, above which QoS requirements cannot be met. For example in all all micro states for which $n_1 \geq N_1$ and $n_2 \geq N_2$ holds, the QoS guarantees will not be met. Therefore all such micro states belong to the the macro state D. We propose different methods for drawing these capacity boundaries in the next section, Section 7.4.3. Until then, we assume that the capacity boundaries $(N1, N2)$ has been found according to one of the methods we propose in the next section. We are primarily involved with calculating macro transition probabilities from micro transition probabilities.

Once the N_1 and N_2 values that define the region boundaries are found, the transition

Transition	$(\mathbf{K_1}, \mathbf{L_1})$	$(\mathbf{K_2}, \mathbf{L_2})$	$\gamma_{\mathbf{ij}}$
$\mathbf{p_{AB}}$	$(N_1 - 1, N_1 - 1)$	$(0, N_2 - 1)$	λ_1
$\mathbf{p_{BA}}$	(N_1, N_1)	$(0, N_2 - 1)$	μ_1
$\mathbf{p_{AC}}$	$(0, N_1 - 1)$	$(N_2 - 1, N_2 - 1)$	λ_2
$\mathbf{p_{CA}}$	$(0, N_1 - 1)$	(N_2, N_2)	μ_2
$\mathbf{p_{CD}}$	$(N_1 - 1, N_1 - 1)$	$(N_2 - 1, \infty)$	λ_1
$\mathbf{p_{DC}}$	(N_1, N_1)	$(N_2 - 1, \infty)$	μ_1
$\mathbf{p_{BD}}$	(N_1, ∞)	$(N_2 - 1, N_2 - 1)$	λ_2
$\mathbf{p_{DB}}$	(N_1, ∞)	(N_2, N_2)	μ_2

Table 7.1.: The summation limits used for calculating macro transition probabilities.

probabilities can be obtained utilizing the micro DTMC state and transition probabilities. The transition probability between aggregate state i and j, $i, j \epsilon \{A, B, C, D\}$, can be computed by using the following relation given in [95]:

$$p_{ij} = \sum_{s \epsilon S_i} \pi(s) \sum_{t \epsilon S_j} p_{st}$$

This formula can be interpreted as follows. The for each micro state s in the originating partition S_i related with macro state i, we sum the probabilities of ending up in a micro state t which is in the destination partition S_j associated with macro state j and multiply the total probability with the probability of being in the micro state s. We finally sum these values for all micro states in the originating partition to come up with the transition probability between macro states. Owing to the birth-death nature of our system and the rectangular boundaries we set, transition between aggregate states occur only between boundary micro states and there is a single path between these micro states. Inserting the BCMP solution for the micro state probabilities, we obtain the following general formula for macro state transitions:

$$p_{ij} = \sum_{n_1 = K_1}^{L_1} \sum_{n_2 = K_2}^{L_2} \gamma_{ij} (1 - \rho_1)(1 - \rho_2) \rho_1^{n_1} \rho_2^{n_2}$$

The limits of the sums are functions of N_1 and N_2, and the depend on the boundaries that separate the states S_i and S_j. Similarly the parameter γ_{ij} takes values from the set $\{\mu_1/\nu, \lambda_1/\nu, \mu_2/\nu, \lambda_2/\nu\}$ depending on the direction of the transition as depicted in Figure7.15. For example for the computation of the transition probability p_{AB} these parameters takes the values $K_1 = L_1 = N_1 - 1$; $K_2 = 0$,$L_2 = N_2 - 1$ and $\gamma_{AB} = \lambda_1/\nu$. For the probability p_{DB} they are given by $K_1 = N_1$,$L_1 = \infty$; $K_2 = L_2 = N_2$ and $\gamma_{DB} = \mu_2/\nu$. The summations are over geometric sequences involving utilizations and therefore converge. We give the summation limits in the Table 7.1 and results of the summations in Equation (7.35).

$$
\begin{aligned}
p_{AB} &= \frac{\lambda_1}{\nu}(1-\rho_1)\rho_1^{N_1-1}(1-\rho_2^{N_2}) \\
p_{BA} &= \frac{\mu_1}{\nu}(1-\rho_1)\rho_1^{N_1}(1-\rho_2^{N_2}) \\
p_{AC} &= \frac{\lambda_2}{\nu}(1-\rho_2)\rho_2^{N_2-1}(1-\rho_1^{N_1}) \\
p_{CA} &= \frac{\mu_2}{\nu}(1-\rho_2)\rho_2^{N_2}(1-\rho_1^{N_1}) \\
p_{CD} &= \frac{\lambda_1}{\nu}(1-\rho_1)\rho_1^{N_1-1}(\rho_2^{N_2}) \\
p_{DC} &= \frac{\mu_1}{\nu}(1-\rho_1)\rho_1^{N_1}(\rho_2^{N_2}) \\
p_{BD} &= \frac{\lambda_2}{\nu}(1-\rho_2)\rho_2^{N_2-1}\rho_1^{N_1} \\
p_{DB} &= \frac{\mu_2}{\nu}(1-\rho_2)\rho_2^{N_2}\rho_1^{N_1}
\end{aligned} \tag{7.35}
$$

The probabilities of transitions from macro states onto themselves can be calculated by exploiting the total probability condition, $p_{ii} = 1 - \sum_{j \neq i} p_{ij}$:

$$
\begin{aligned}
p_{AA} &= 1 - p_{AB} - p_{AC} \\
p_{BB} &= 1 - p_{BA} - p_{BD} \\
p_{CC} &= 1 - p_{CA} - p_{CD} \\
p_{DD} &= 1 - p_{DB} - p_{DC}
\end{aligned} \tag{7.36}
$$

The open question is of course if this state aggregation is valid. The condition for legitimate aggregate sets of underlying Markovian states is the protection of the Markovian property. That means, the macro states should have the Markovian property. This is the case for our macro states. This is because the transition probabilities of the macro states are computed directly from the micro state probabilities. If macro states were not Markovian, this would mean that the micro states were not Markovian. But the micro states are states of a DTMC and Markovian. So the macro states being non-Markovian leads to a contradiction, which proves that this state aggregation is legitimate by contradiction.

It can be seen from Equations (7.35), that transition probabilities are functions of λ_1, λ_2 and ρ_1, ρ_2. All four of these variables are in turn functions of the transfer probability P_T. To borrow resources, to donate resources or not to get involved in the cooperation are actions that change these probabilities, and thus effect the state space trajectory. The POMDP formulation will be constructed in order to choose the best actions according to the Approximate Value Iteration heuristic. Before we formulate the POMDP, we discuss how we define the state aggregation boundaries.

Capacity Limits

In the previous section we assumed linear capacity boundaries divided the state space into four rectangular regions. In this section elaborate how we derive the capacity limits.

Capacity limits for different RANs depend on two factors. First one is the raw data transfer capacity of the individual RAN, which is reflected by the service rate μ. Second one is the QoS requirements of different application types. Modeling the QoS requirements of applications is a multi stage process. Firstly a source model should be developed, to model the physical process behind the application. An example for a source model is the *ON-OFF* model used for voice sources. The source model is than used to build up the traffic model, that model the actual data traffic seen by the network. Associating different Poisson rates for the ON and OFF states would be an example of the traffic model. The number of traffic models are very large for the network operators to handle them individually. This is why most of the data networks have defined *service classes* that gather together similar traffic models. We will be deriving capacity limits assuming the operators are trying to fulfil the requirements defined for different service classes.

We are considering three types of service classes:

- Delay bounded,
- Throughput bounded,
- Interference bounded.

For all of classes our strategy is to formulate the QoS guarantee associated with the service class as an decreasing function of the number of active sessions, and find the maximum value of number of sessions for which the QoS guarantee is met.

Delay Bounded Applications For delay bounded applications, the QoS guarantee that the operator is aiming at is the minimization of processing delay d exceeding a threshold $D_{\max}$:

$$Pr(d > D_{\max}) << 1 \tag{7.37}$$

The calculation of this probability would require the probability distribution of the delay as a function of number of active sessions n in a PS system. The the probability distribution is given by Yashkov for the unconditional case in [32], specifically Equation 2.45, as complex integral involving exponential functions of trigonometric functions of the utilization, which could only be solved numerically. A conditional distribution for the delay in a PS system given an arbitrary job size distribution is not known in the literature.

However we can make use of Cantenelli's Inequality, single sided version of the Tchebychev inequality. Cantenelli's Inequality gives an upper bound to the probability in Equation (7.37), for any type of probability distribution, as long as the mean and variance are given for the random variable under investigation. This is indeed the case for the

conditional mean and variance for PS servers serving exponentially distributed packet size, and in Appendix C we derive results for deterministic packet sizes. Cantenelli's inequality is given by:

$$Pr(d \geq E_n[d] + k \cdot \sqrt{Var_n(d)}) \leq \frac{1}{1+k^2} \tag{7.38}$$

We set the value of k to 10, which guarantees a probability less than 10^{-2}. Note that Tchebychev is a very loose bound, and actual probabilities will be less than this bound. Setting the value of k establishes an upper bound on the delay value for which a guarantee can be made, which is given by the expression $E_n[d]+k\cdot\sqrt{Var_n(d)}$. Equating this expression to the QoS goals of the operators, i.e. the delay bound$D_{\max}$, we obtain a boundary on the number of active sessions in a RAN.This is possible by making use of the expressions for mean and variance conditioned on the number of sessions in a M/M/1-PS system given by Coffman [30]:

$$E_n(d) = \frac{\tau}{1-\rho} + \{n(1-\rho)-\rho\}\frac{1-e^{-(1-\rho)\mu\tau}}{\mu(1-\rho)^2} \tag{7.39}$$

$$\begin{aligned}\sigma_n^2(d) = {} & \frac{2\rho\tau}{\mu(1-\rho)^3}\left\{1+(1+\rho)e^{-a\tau}\right\} - \frac{\rho^2}{\mu^2(1-\rho)^4}\left\{1-e^{-2a\tau}\right\} \\ & - \frac{4\rho}{\mu^2(1-\rho)^4}\left\{1-e^{-at}\right\} + \frac{n(1+\rho)}{\mu^2(1-\rho)^3}\left\{(1-e^{-2a\tau}) - 2(1-\rho)\mu\tau e^{-a\tau}\right\} \\ a = {} & \mu(1-\rho)\end{aligned} \tag{7.40}$$

Due to the non-linear nature of these equations, we resort to numeric a simple numerical solution of increasing n sequentially, until $D_{\max}$ is exceeded. Non-critical WWW traffic or interactive traffic can be modeled using this approach. It is also possible to model mission critical real-time applications.

Throughput Bounded Applications There are applications such as FTP-like downloads and video streaming applications that have throughput requirements, i.e. there exists a minimum $T_{\min}$. We are able to model these applications by resorting to the PS abstraction. Explicitly, the PS abstraction suggests that the maximum capacity of the RAN is shared equally between the number of sessions in the system. Therefore $N(T_{min})$ for a given minimum throughput T_{min} is the largest integer N satisfying the condition $\frac{C}{N} > T_{min}$.

Interference bounded Finally, there are applications such as VoIP or teleconferencing for which detailed capacity planning investigations have been made. In these cases these capacity bounds can be used naturally as the boundaries in the POMDP model.

	Normal	*Congested*
GOOD	0.7	0.1
OK	0.2	0.2
BAD	0.1	0.7

Table 7.2.: Observation probability distributions.

7.4.4. POMDP Model

We are in a position to define the POMDP model that will be used by the donating and borrowing RAN agents. A POMDP is defined by the n-tuple $< S, T, A, R, \Omega, O >$. In our POMDP formulation, the states S are the macro states depicted in Figure 7.14. We have shown how the transition probabilities can be calculated in the previous section. We will define the remaining elements in this section.

Actions

We define our set actions to be borrow(BOR) , donate(DON) or no interaction(NOP) . As we discussed earlier, the transition probabilities between the macro states depend on the micro state transition probabilities and the action. For example, the probability of going from a normal state to an congested state will increase for the donor operator, if it accepts additional traffic as compared to not cooperating. Similarly, the probability of making a transition form a congested state to a normal state will increase for the borrower operator, as opposed to not cooperating.

Observations

The next component in the POMDP definition is the description of the observations. The observations model the inaccurate nature of queries that the RAN agent makes to the user QoE database to gauge the condition in the peer RAN. The user delay reports can be grouped into three groups: good ($GOOD$), satisfactory (OK), bad (BAD). The RAN agent has the *a priori* distribution of these observations, i.e. it knows how possible an observation is, given the condition of the peer operator. We present a methodology for obtaining these probabilities in Chapter 8. These values can be entered manually, and than can be updated via a learning mechanism which is outside the scope of our work. We use the values given in Table 7.2. These probabilities are same for all the actions. The basic intuition is that it is more likely to get a BAD observation when the peer operator is congested.

Rewards

Finally, we define the rewards associated with each state-action pair. In order to account for the trade-off between increase in utilization that is for the benefit of the operators and increase in delay which is not beneficial, we propose two types of rewards. The

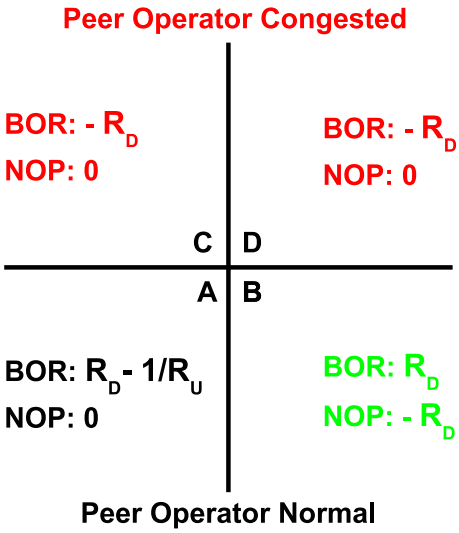

Figure 7.16.: Borrower Reward Assignments.

delay reward $R_d(a)$ and utilization reward $R_u(a)$. We combine these two reward definitions differently and allocate them to different aggregate states for donor and borrower formulations.

The delay reward is the ratio of the average initial delay to the average delay after a particular action,i.e. $R_D(a) = \bar{D}_{init}/\bar{D}(a)$. With this reward we represent the relative benefit of an action in decreasing the delay. The larger an action is able to reduce the delay, larger the associated delay reward will be. Its a positive real number larger than 1 for borrowing, and smaller than one for donating resources. By using the formula for the average delay for a PS queue we obtain the following expression for $R_D(a)$:

$$R_D(a) = \frac{1-\rho(a)}{1-\rho_{init}} \tag{7.41}$$

The utilization reward is defined to be the ratio of the utilization after a particular action to the original utilization. Its a positive real number larger than 1 for donating, and smaller than one for borrowing resources. The utilization reward is given by the following expression:

$$R_D(a) = \frac{\rho(a)}{rho_{init}} \tag{7.42}$$

Borrower Rewards Borrower wants to avoid borrowing resources from an congested peer operator. This is reflected in the Figure 7.16, in which the states for which the peer operator is congested is denoted with red. For states C and D the donating operator is congested, and they have to be avoided. So we punish borrowing with value $-R_d(BOR)$, and assign 0 for NOP. State B is the state where borrowing is compulsory. Therefore we reward borrowing by $R_d(BOR)$, and punish no operation is $-R_d(BOR)$. State A is

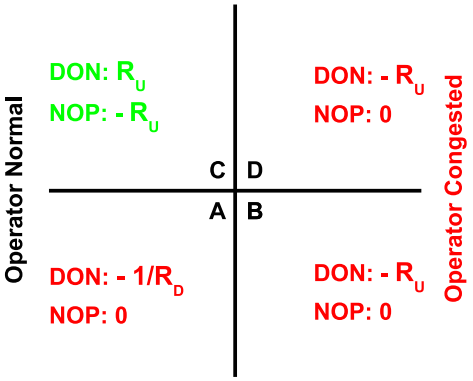

Figure 7.17.: Donor Reward Assignments.

ambiguous: from the perspective of the borrowing operator, it can decrease the delay, albeit with the drawback of decreasing it's utilization. In order to balance these factors, we associate the reward $R_d(BOR) - 1/R_u BOR$. $R_u(\cdot)$ is nominally smaller than 1 for borrowing resources. In order to make it comparable with the decrease in delay, which is larger than one, we use the inverse of $R_u(BOR)$. Not cooperating in this state brings a reward of 0.

Donor Rewards The donor on the other hand, has two goals to satisfy. Firstly, it wishes to avoid congestion in its own network. This means that states B and D should be avoided. For these states we punish donating with $-R_u(DON)$ and not cooperating with 0. Secondly, it only wishes to help a borrower, if it is sure that the borrower is in a congested state. The donor operator can increase its utilization by donating to a borrower in normal state, but in the expense of increasing its own average delay. But we assume that the operators do not want to help a competitor, when there is no congestion in the competitor network. This means the strategic agreement between the operators is of a tit-for-tat type. From this perspective the state C is the most suitable state for the donor operator to donate, since it is normal and the borrower is congested. For this state donating brings a reward $R_u(DON)$, and not donating is punished by a reward of $-R_u(DON)$. Finally, we punish donating to normal peer operator by the value $-1/R_d(DON)$.

7.5. Application of Inter-Operator Real-time Resource Sharing

We demonstrate our dynamic resource sharing approach via a load balancing problem in a 801.11g based Wireless LAN setting. In this scenario, two access points (AP) belonging to two different administrative domains are situated in a close proximity. These APs are optimized for plain World Wide Web browsing. It is well known that users tend to accumulate in certain APs which become hot spots and that the utilization of individual APs vary in the time scale of hours [131]. We assume that there exists a user QoE database available to the users of the two APs. Furthermore there are RAN agents are

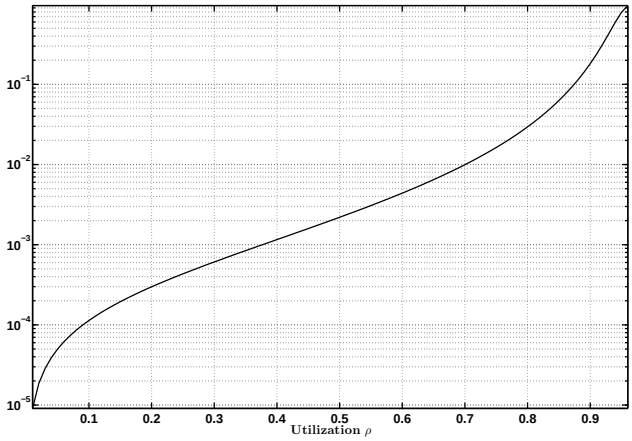

Figure 7.18.: Tchebychev bounds used for negotiation.

running on the APs or any gateway server in the RAN and these agents can communicate with each other. We focus on the decision taking but not on the execution. The actual sharing of resources, which consist of forwarding users from borrower operator to donor operator, can be implemented via any network-initiated layer 2 or layer 3 handover mechanism [132].

We represent the traffic generated by users with an exponential distribution, of mean *130 KBytes*, since this value is the most accurate estimate of the average web-page size we could obtain in the public domain [133]. The shortcomings of exponential distribution in representing self-similar data traffic is well known. We postulate that a leaky bucket type traffic shaper is available to the users. An alternative is to use Pareto model, and fit hyper-exponential distribution, from which mean and variance of delay can be calculated using symbolic mathematics packages as proposed by Xu in [134].

7.5.1. Definition of Donor and Borrower Roles

Two important aspects of a load balancing algorithm is the definition of the concepts of load an overload conditions. In our model chose delay as the performance criterium which the operators of the APs optimize their systems and define these concepts using delay. PS abstraction allows us to calculate utilization, or equivalently the load of an each AP, based on the average delay the completed jobs experience. An AP can measure the average delay $\overline{d}(u)$ for a given request size u in among the users its serving. It can also query the user QoE database for the average delay in the other AP. Using this value, the utilization or equivalently the load can be found using the following relation:

$$\rho_i = 1 - u/\left(C_i \cdot \overline{d}(u)\right) \tag{7.43}$$

In (7.43) C_i represents the MAC layer capacity of AP i. We use the value $31.9Mbps$ for both 802.11g APs. Each operator provides delay limits to the users. We choose this

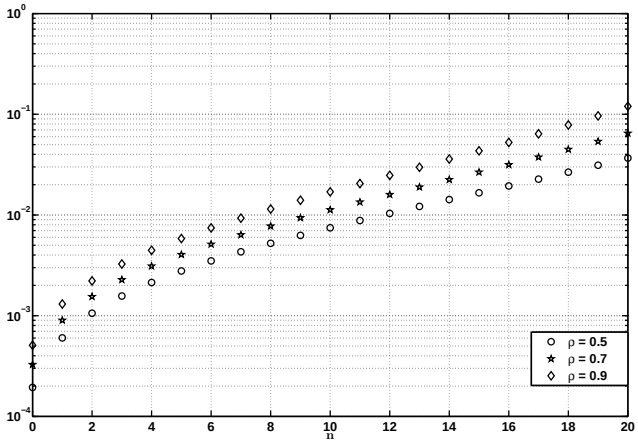

Figure 7.19.: Tchebychev bounds used for POMDP boundaries.

delay limit as 1 second for a request of size $130KByte$. Industry benchmarks [135] show that only the top 20 web-sites have a delay smaller than 1 second. An AP is said to be overloaded when it is not able to meet this delay guarantee with a high probability. The probability, that the delay experienced by a $130KByte$ request is larger than 1 second can be bounded by Tchebychev's inequality, using the formulas linking utilization to the mean and the variance of the delay conditioned on the request size [32]. For the scenario we described, the one sided Tchebychev bound on $P(d(130kb) > 1)$ is given in Figure 7.18 as a function of the utilization ρ. We believe a probability limit of 10^{-2} will be satisfactory, considering the how loose the Tchebychev bound is. This choice means that an AP is overloaded if its utilization is larger than 0.7. Each AP tracks its utilization and initiates a negotiation with the peer AP if the utilization is above 0.7. The result of the negotiation is a transfer probability value P_T.

7.5.2. Macro States and POMDP Models

As we discussed in Section 7.4.3, the solution of the decision problem via POMDP requires the transition probabilities between macro states. These probabilities depend on the limits on the number of simultaneous sessions. These limits are found similarly using bounds on $P(d(130kb) > 1)$, this computed using delay mean and variance conditioned on the number of simultaneous sessions, using the relations given in [30]. They are given for varying utilizations in Figure 7.19. Under the given conditions an AP can support $7, 9, 12$ simultaneous sessions with respective utilizations of $0.9, 0.7, 0.5$

In the scenario the initial borrower and donor utilizations are 0.9 and 0.5 respectively. They agree on a transfer probability of $P_T = 0.3$, which reduces the borrower utilization to 0.630 and increases the donor utilization to 0.597, both below the congestion limit. We plot the Tchebychev bounds versus the number of active sessions for before and after resource sharing. Borrower is able to accommodate seven simultaneous users before

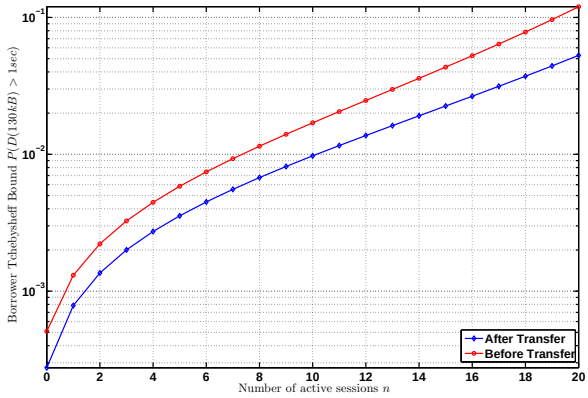

(a) Borrower

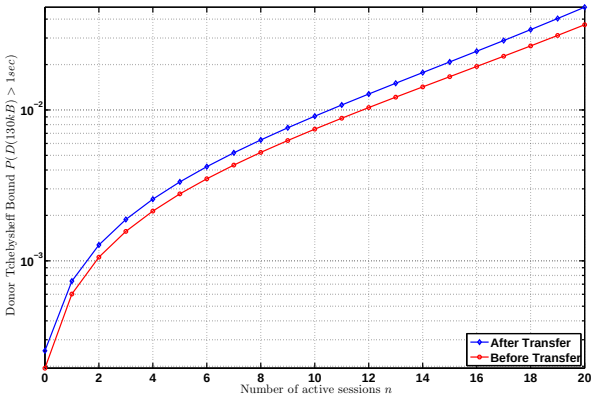

(b) Donor

Figure 7.20.: Tchebychev bounds used for POMDP boundaries.

resource sharing, which increases to ten as depicted in Figure 7.20a. On the other hand donor is able to accommodate twelve users before accepting additional traffic from the borrower. After sharing, it is able to serve eleven users simultaneously as depicted in Figure 7.20b. In total, the operators are able to serve 21 sessions simultaneously compared to 19 users. This is the trunking gain associated with the dynamic resource sharing.

Borrower POMDP Model

The transition probabilities obtained from Equations (7.35) for the described borrower model is given in Table 7.3.

Both donor and borrower POMDP models use the observation probabilities described in the Table 7.4.

Action	Start State	End State	Probability
no-op	A	B	0.01481710646952658
no-op	A	C	0.00003947675210489538
no-op	A	A	0.9851434167783685
no-op	B	A	0.01481710646952658
no-op	B	D	0.00003619224833787636
no-op	B	B	0.9851467012821356
no-op	C	D	0.000007238449667575271
no-op	C	A	0.00003947675210489538
no-op	C	C	0.9999532847982275
no-op	D	B	0.00003619224833787636
no-op	D	C	0.000007238449667575271
no-op	D	D	0.9999565693019946
borrow	A	B	0.001123063383474185
borrow	A	C	0.0007054789386521665
borrow	A	A	0.9981714576778736
borrow	B	A	0.001123063383474185
borrow	B	D	0.00000717594180476163
borrow	B	B	0.9988699190223453
borrow	C	D	0.000006433829708825937
borrow	C	A	0.0007054789386521665
borrow	C	C	0.9992880872316391
borrow	D	B	0.00000717594180476163
borrow	D	C	0.000006433829708825937
borrow	D	D	0.9999865485761108

Table 7.3.: Borrower Transition Probabilities.

State	Observation	Probability
A	MOS1	0.1
A	MOS2	0.2
A	MOS3	0.7
B	MOS1	0.1
B	MOS2	0.2
B	MOS3	0.7
C	MOS1	0.7
C	MOS2	0.2
C	MOS3	0.1
D	MOS1	0.7
D	MOS2	0.2
D	MOS3	0.1

Table 7.4.: Donor and Borrower Model Observations.

Action	State	Reward
no-op	A	0.0
borrow	A	-1.4286
no-op	B	-3.700
borrow	B	3.700
no-op	C	0.0
borrow	C	-3.700
no-op	D	0.0
borrow	D	-3.700

Table 7.5.: Borrower Model Rewards.

For the borrower model, the reward assignments are described in Table 7.5.

Donor POMDP Model

Similarly, the donor transition probabilities for each action is given in Table 7.6.

Donor operator rewards are listed in Table 7.7.

7.6. WLAN Load Balancing Models

We present the solution of the individual POMDP models for the borrower and donor in this section. For solving the POMDP models we presented in Section 7.5.2 we used the POMDP-Solve software developed by Cassandra [136]. We first briefly discuss how we will present the results.

Action	Start State	End State	Probability
no-op	A	B	0.00003947675210489538
no-op	A	C	0.014817106469527
no-op	A	A	0.985143416778368
no-op	B	A	0.00003947675210489538
no-op	B	D	0.000072738449667575271
no-op	B	B	0.999953284798228
no-op	C	D	0.00003619224833787635
no-op	C	A	0.014817106469527
no-op	C	C	0.985146701282135
no-op	D	B	0.000072738449667575271
no-op	D	C	0.00003619224833787636
no-op	D	D	0.999956569301995
donate	A	B	0.0007054789386521665
donate	A	C	0.001123063383474
donate	A	A	0.998171457677874
donate	B	A	0.0007054789386521665
donate	B	D	0.000026433829708825937
donate	B	B	0.999288087231639
donate	C	D	0.000027017594180476163
donate	C	A	0.001123063383474
donate	C	C	0.998869919022346
donate	D	B	0.000026433829708825937
donate	D	C	0.000027017594180476162
donate	D	D	0.999986548576111

Table 7.6.: Donor Transition Probabilities.

Action	State	Reward
no-op	A	0.0
donate	A	-1.24
no-op	B	0.0
donate	B	-1.193
no-op	C	-1.193
donate	C	1.193
no-op	D	0.0
donate	D	-1.193

Table 7.7.: Donor Model Rewards.

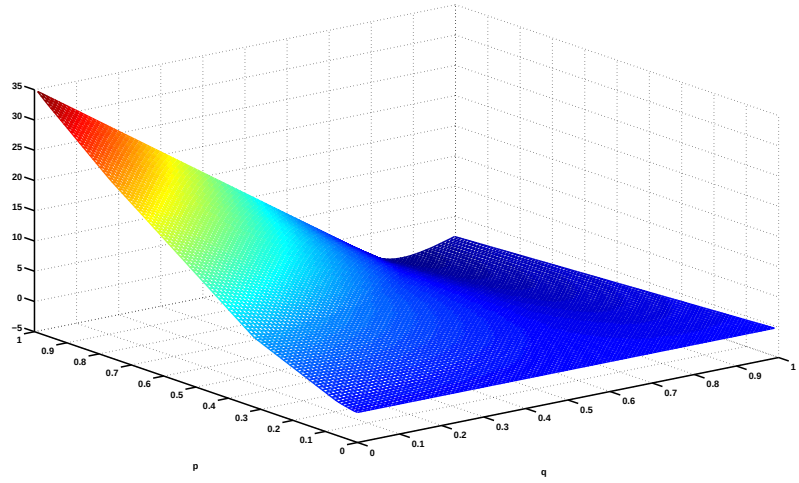

Figure 7.21.: Value functions.

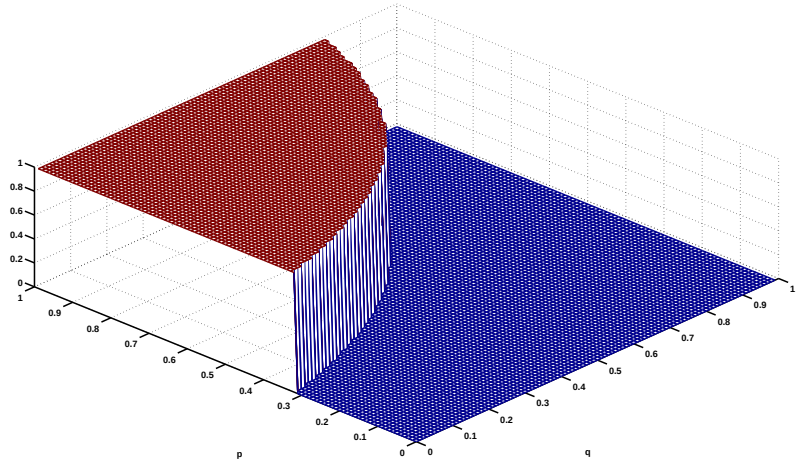

Figure 7.22.: Sample Action Mappings.

POMDP-Solve program gives two outputs. The first output is a list of vectors and their associated actions. This output correspond to the vectors defined in the Equation (7.19), which are used to calculate the optimal value function given in Equation (7.18). In our problem, there are four states, and thus the vectors are four dimensional. However the states are not independent in our scenario, but are cross products of two random variables. We denote the belief that the RAN for which the POMDP is solved, is in a normal condition with q. This means that the belief that this RAN is in a congested state is $1-q$. Similarly we note the belief that the peer operator is in a normal condition

with p, and its complementary belief with $1 - p$. With these definitions, the beliefs in states A, B, C, D are given by $b(A) = q \cdot p$, $b(B) = (1 - q) \cdot p$, $b(C) = q \cdot (1 - p)$ and $b(D) = (1-q) \cdot (1-p)$. This we are able to represent the optimal value function with two variables. For each value of (p, q) we take the value of the maximum vector in order to plot the optimal value function. At the same time, we note the action that is associated with the maximizing vector for each (p, q) value. One sample optimal value function is given in Figure 7.21. We also plot the optimal action as a function of beliefs, in what we term the action mappings, such as the one given in Figure 7.22. In these figures the z-axis value of 0 represents the *NOP* action, and 1 *DON* or *BOR* actions. For better visualization we present the contour of the action mappings on a two dimensional (q, p) graph.

In the coming sections we investigate the different parameters of the approximate value iteration algorithms we use for solving the donor and borrower models. We then present the finite state controller implementations of the policies.

7.6.1. Precision

The quality of the solutions obtained by the POMDP-Solve depend on the quality of the linear programming solver used for each iteration. Cassandra uses a publicly available linear program solver for Linux. However it is mentioned that the quality of the solutions are increased if a proprietary commercial solver is used. The main problem with the linear programming solution quality is mainly numerical. The optimal value function tends to include many vectors that differ in their slopes with a very small difference. This leads to very narrow regions of the belief space to be partitioned by vectors which are associated with the same action. Another result of this is the fact that these vectors cannot be eliminated during the iterations, even though they are dominated by other vectors in almost all the belief space.

A remedy for this problem is decreasing the precision used in the linear programming solution. Decreasing the precision also brings with it the danger that the solution of the POMDP is not precise. In order to gauge the effects of using different precision in the solution, we present the borrower action mapping contours with two different precision degrees in Figure 7.23. The contour map divides the (q, p) space into two regions. On the top-left region the action *BOR* is optimal, on the rest action *NOP* is optimal. It can be seen that the difference between the contours are negligible. Therefore we use the highest precision that allows the shortest solution time possible in our solutions.

7.6.2. Methods

Cassandra implements an comprehensive list of POMDP solution algorithms. This list includes the original Enumeration and Two Pass algorithms by Sondik [137], the Linear Support algorithm by Cheng [138], the Incremental Pruning algorithm by Zhang and Lui [103], the Witness algorithm by Littman and Cassandra [104] and finally an implementation of the Grid Based Value Iteration. We have found out that the Witness, the Incremental Pruning and the Grid algorithms are the algorithms that give the most

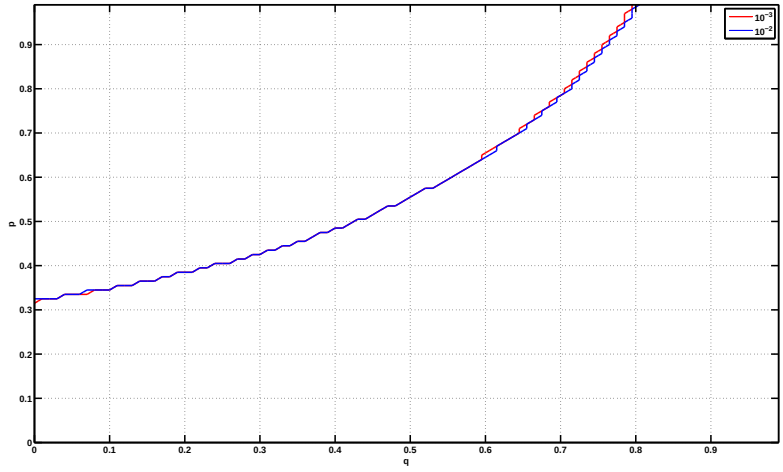

Figure 7.23.: Action mapping contours for two different precisions.

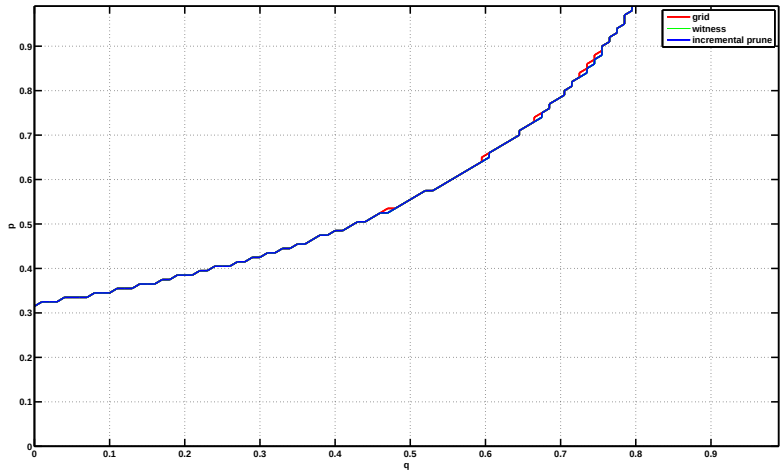

Figure 7.24.: Action Mapping Contours for different methods.

stable results. It was observed in the older algorithms that the vector set grew in size, instead of converging into a stable number of vectors.

We compare the three algorithms that converge into a finite set of vectors in Figure 7.24. As it can be seen the Action Mapping contours are very similar. For the same model, the performance of different methods is summarized in Table 7.8. As it can be seen the grid algorithm is superior to the others in terms of the number of vectors and the running time. It is important to remember that the smaller the number of vectors, the smaller will the finite state controller will be. Thus we will use grid to solve the

Algorithm	Number of Vectors	Solution Time
Incremental Prune	32	38 sec.
Witness	31	45 sec.
Grid	5	1 sec.

Table 7.8.: Performances of different methods.

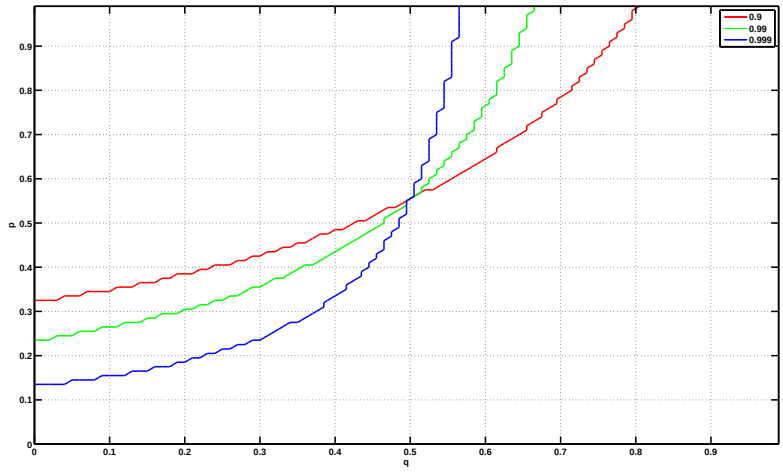

Figure 7.25.: Action Mapping Contours for different discount rates.

POMDP problems.

7.6.3. Discount Factor

Discount rate is a measure of the risk-taking behavior of the operators. A smaller discount factor α means that the future rewards have less value compared to the current reward. Therefore a smaller discount factor represent a more risk averse operator. This can be observed in Figure 7.25. The model is solved for a borrower. In the case of congestion, the belief of the operator that the RAN is normal will be close to zero. For a risk averse operator, let us assume that the α is set to 0.9. If the operator is certain, that its RAN in a congested state, i.e. $q = 0$, the minimum belief in the normal donor state for which borrowing is optimal is 0.32. The same value for an operator with an $\alpha = 0.999$ is 0.12.

The α value has also a physical interpretation in terms of the time spent between decisions. The discount factor α weighs the rewards in a sequential decision problem. The important question is the calculation of the equivalent weighing in continuous time. For this one has to refer back to Equation (7.28), which defines $\alpha = \nu/(\beta + \nu)$, where β is the rate with which rewards are exponentially weighted in continuous time, i.e. $R(a,t) = R(a) \cdot e^{-\beta t}$, and ν is the uniformization rate. The uniformization rate is set by

the arrival rates and the capacities of the individual rates. Then, we can solve for β in terms of α and ν:

$$\beta = \nu(\frac{1}{\alpha} - 1) \tag{7.44}$$

$1/\beta$ is the time-constant of the reward scaling exponential function. This is the time when the reward is scaled with a value of $1/e$. For the alpha values 0.9, 0.99, and 0.999 the corresponding time-constants are 0.06, 0.7 and 7 seconds. We present results for 0.99 and 0.999, since these give us more realistic time-constants.

7.6.4. Borrower Model

We have already presented the optimal value function, Figure 7.21 and the action mappings, Figure 7.22 and the action mapping contours for the borrower in Figure 7.25.

Let us explore the action mapping contours a little more in detail. The value q represents the belief of the borrower that its own RAN is congested. The value p is the belief of the borrower that the donor is in normal condition. For a congested borrower the q value will be close to 0. If the borrower is certain that it is in a congested state, it requires a minimal belief of 0.22 that the donor is in normal condition. As the borrowers uncertainty about its own congestion state decreases, i.e. as q increases, the borrower requires more evidence that the donor is not congested. If the borrowers belief, that its own RAN is not congested is above the value 0.68, borrowing becomes non-optimal.

Luckily, our model is finitely transient, which means that the optimal policy can be implemented as a finite state controller. We present the finite state controllers for α values 0.99 and 0.999 in Figures 7.26 and Figure 7.27 respectively. A congested borrower starts with the leftmost borrow state. For the operator which is more risk averse, and set the α to 0.99, it takes four consecutive poor MOS readings, i.e. MOS1, to stop borrowing. For a less risk-averse operator, whose α is set to 0.999 this value is five.

7.6.5. Donor Model

We finally present the donor model. The optimal value function for the donor model is given in Figure 7.28, which is distinguished from the borrower value function by the large plateau. Notice that we plot the value function on a $(q, (1-p))$ plane. This is because the donor is willing to donate when the borrower is in a congested state. This means that it is interested not in the probability that the borrower is in a normal state, i.e. p, but in the probability that the borrower is in a congested state, i.e. $(1-p)$. The corresponding action mapping is given in Figure 7.29.

The characteristics of the decision problem can be explored more easily in the contours of the action maps, which are given in Figure 7.30. The donor operator will be willing to donate, when the belief that its own RAN is normal is close to one. If the RAN is certain that is normal, i.e. $q = 1$, it requires a minimum belief value of 0.4 that the borrower is congested. As the certainty of the donor in its normal status decreases, it requires more evidence for the congestion state of the borrower. When the donor belief

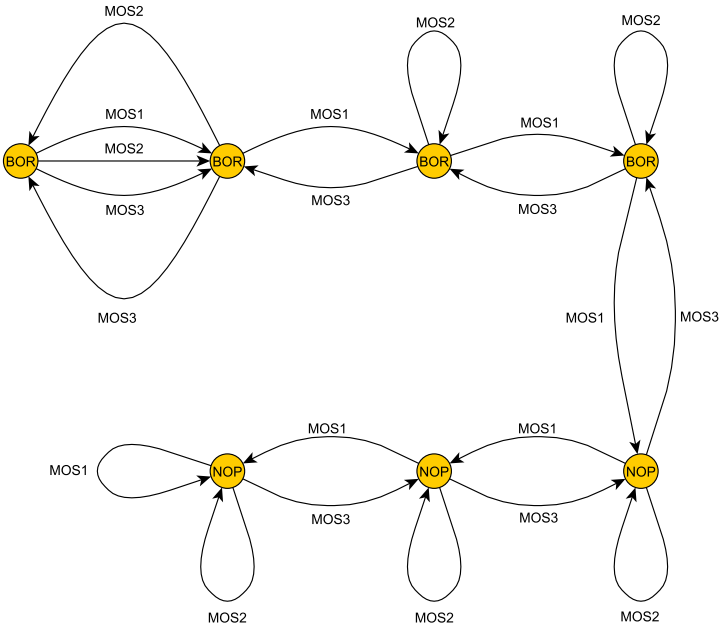

Figure 7.26.: The borrower finite state controller for discount rate $\alpha = 0.99$

q drops below 0.28, donating is not optimal anymore.

Similar to borrower we are able to formulate a finite state controller for the optimal policy. This is given in Figure 7.31. A normal donor starts with the action *DON* on the top left corner of the finite state controller. It takes three good MOS observations, i.e. *MOS3*, for the donor to decide that the borrower is not congested anymore, and to stop donating.

7.7. HSDPA-WLAN Load Balancing Models

We also applied the POMDP formulation to a load sharing scenario between a HSDPA RAN and a 802.11g RAN. We use the PS model for HSDPA networks that we introduced in Section 4.4.3. According to this model, a cellular data RAN employing HSDPA on five channeling codes and using 7 Watts, can be modeled as a PS server with capacity 1.4 Mbps. As depicted in Figure 7.32 the delay guarantee of 10^{-2} is to optimistic for the limited capacity of HSDPA. We therefore choose a grade of service of 10^{-1}, which allows the HSDPA to be occupied up to $\rho = 0.5$. In the scenario a congested HSDPA RAN borrows resources from the normal WLAN RAN.

Borrower value function and action mappings do not differ from the WLAN Balancing versions. They are depicted in Figures 7.33 and 7.34.

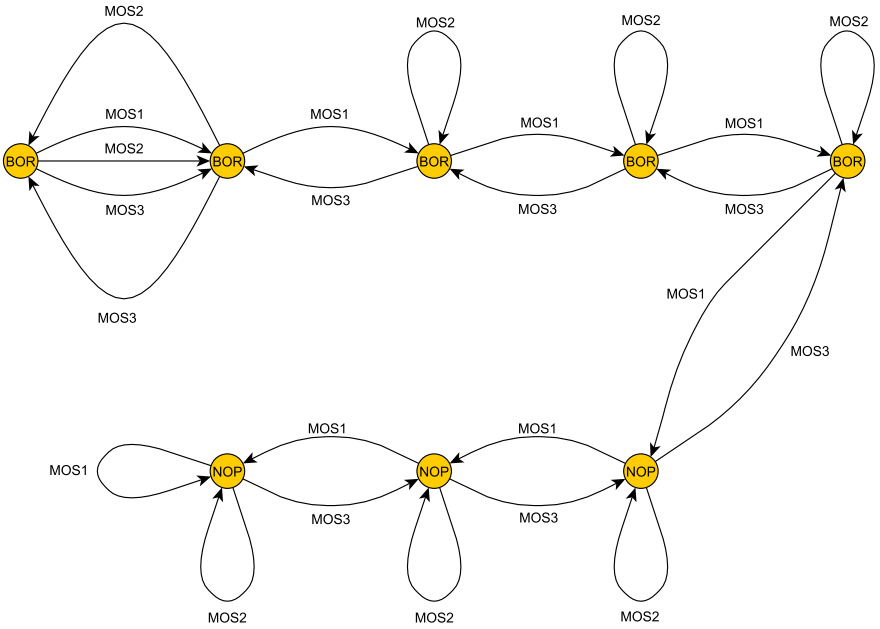

Figure 7.27.: The borrower finite state controller for discount rate $\alpha = 0.999$

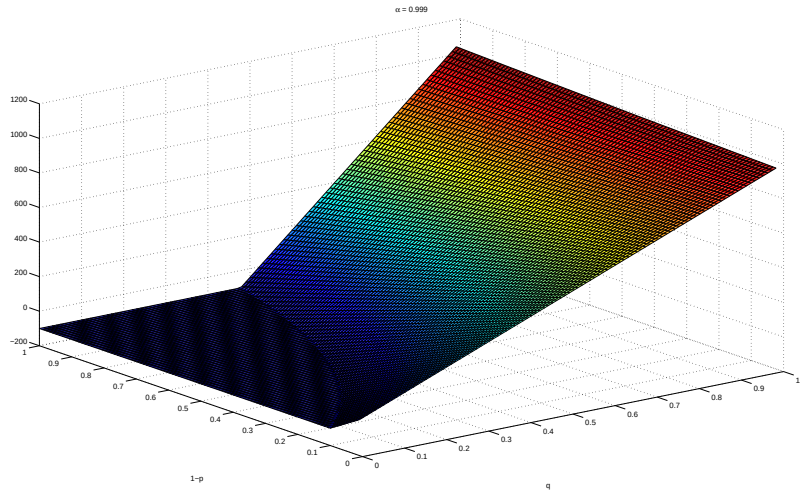

Figure 7.28.: Donor Value Function.

Since the action mappings are the same, the borrower finite state controller is similar to the WLAN balancing case. This finite state controller for HSDPA borrower is given

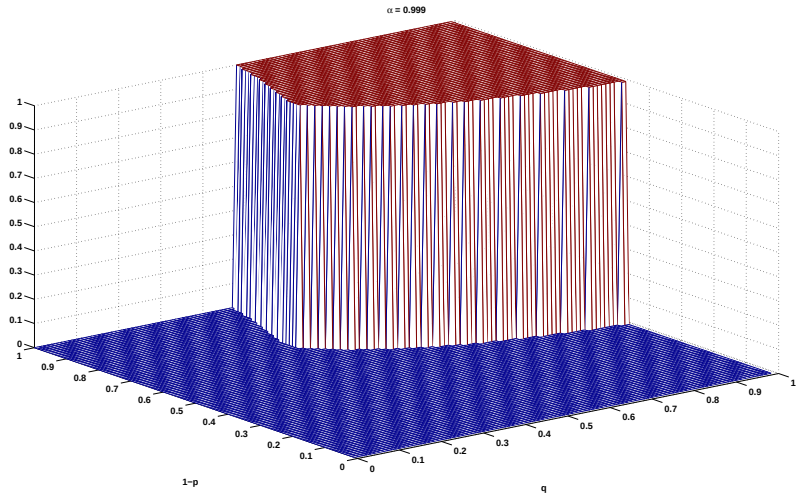

Figure 7.29.: Donor Action Map.

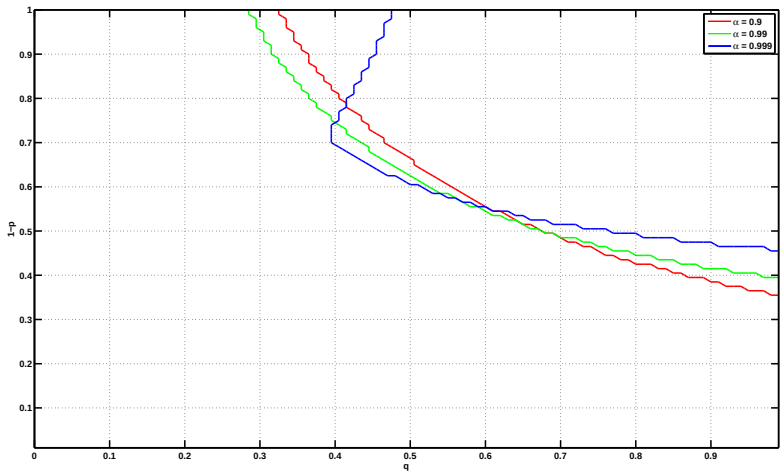

Figure 7.30.: Donor Action Mapping Contours.

in Figure 7.35.

Donor value function and action mapping differ from their WLAN only counterparts. They are given in Figures 7.36 and 7.37.

The difference of the action mapping and the value function reflects itself in the structure of the finite state controller for the donor. The FSC depicted in Figure 7.38 is more complex than the ones we presented so far. However, the overall structure remains, in which negative observations move the agent from donating states closer to non cooperative states, and positive observations moving the agent closer to donating

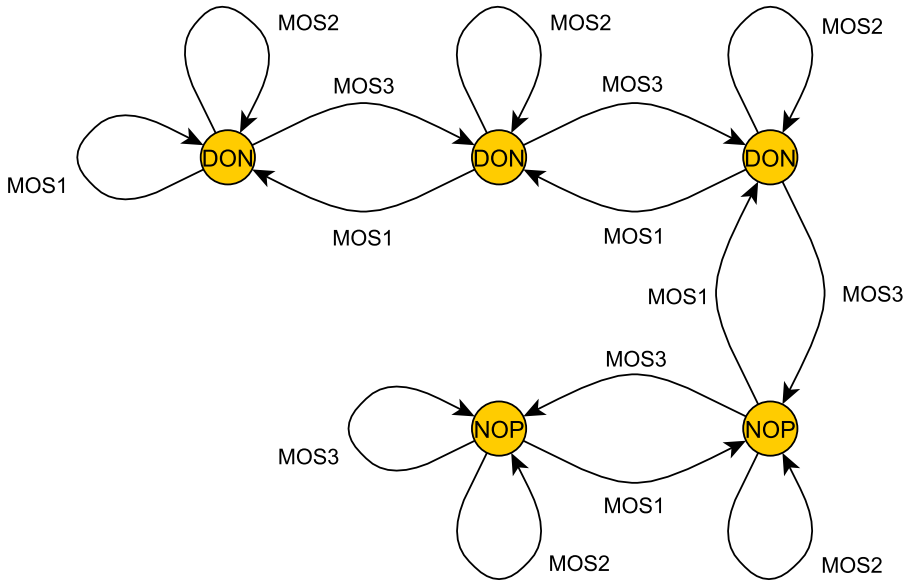

Figure 7.31.: Donor Finite State Controller.

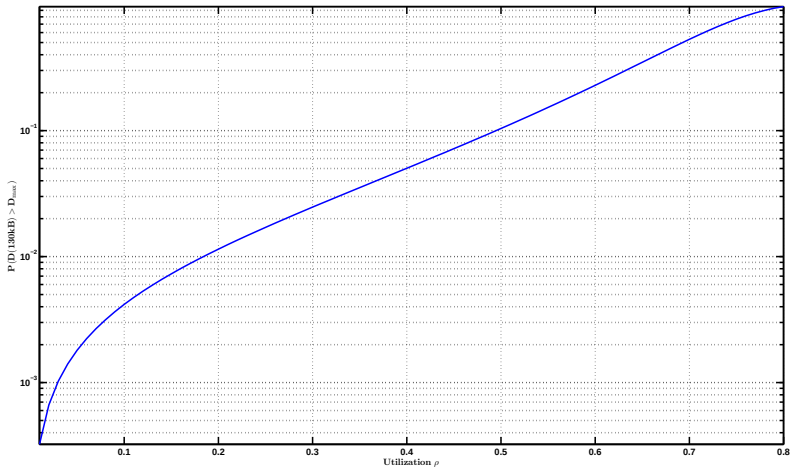

Figure 7.32.: HSDPA Tchebychev bound.

states. For example starting at the stable donating state, the second donating stage on the left, it takes three MOS3 observations for the agent to decide that the borrower is not congested anymore, and go to a non cooperative state. Similarly, after the agent stabilizes at the stable non cooperative state, i.e. the left most non-cooperative state, it takes three MOS1 observations to switch to a donating state.

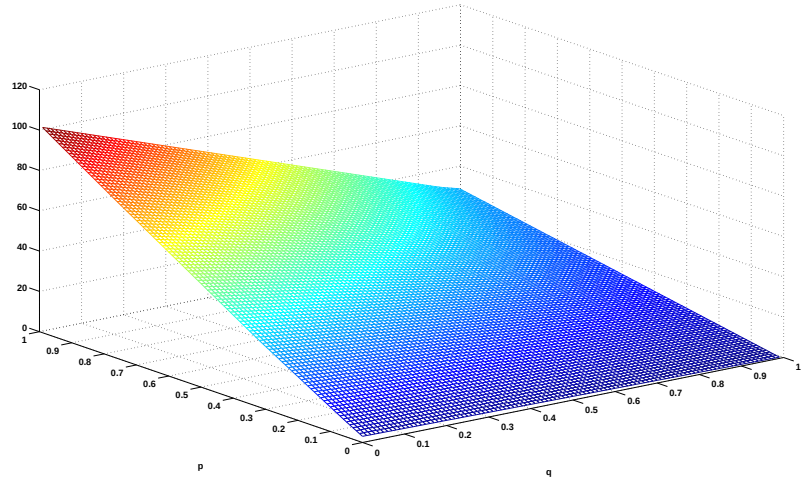

Figure 7.33.: HSDPA Borrower Value Function.

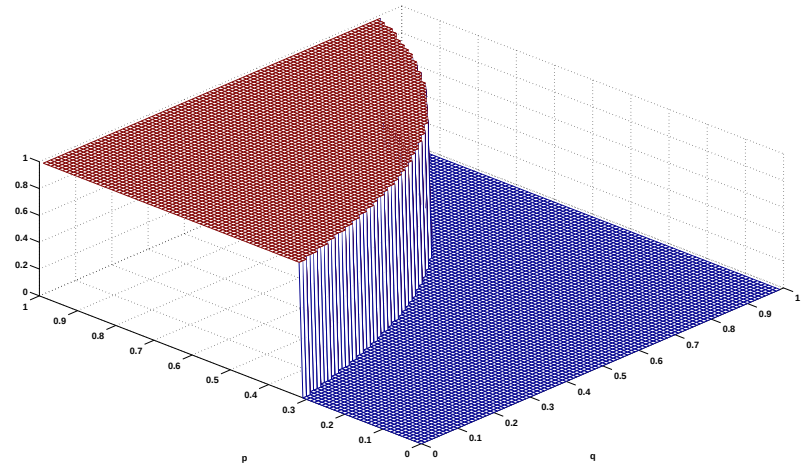

Figure 7.34.: HSDPA Borrower Action Mapping.

7.8. Conclusion

In this Chapter we motivated how single agent decision making solution POMDPs can be used for the multi-agent problem we have. This necessitates the condition that the POMDP controllers be used in conjunction with the negotiation mechanisms given in Chapter 6. In the next Chapter we present the results of the tests of the controllers under realistic traffic conditions.

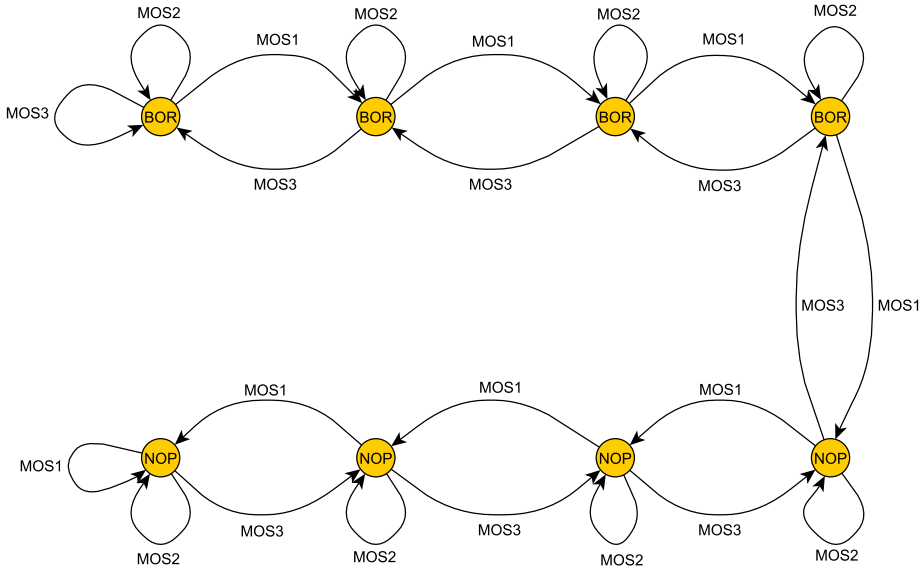

Figure 7.35.: HSDPA Borrower Policy Graph.

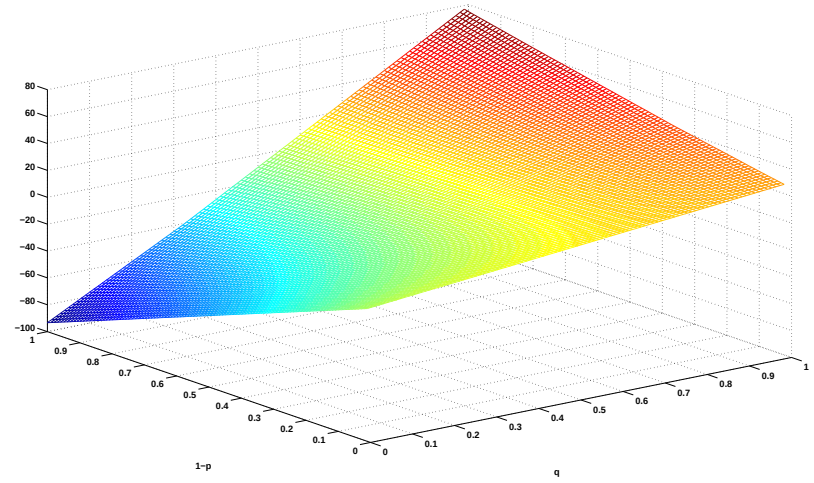

Figure 7.36.: HSDPA Donor Value Function.

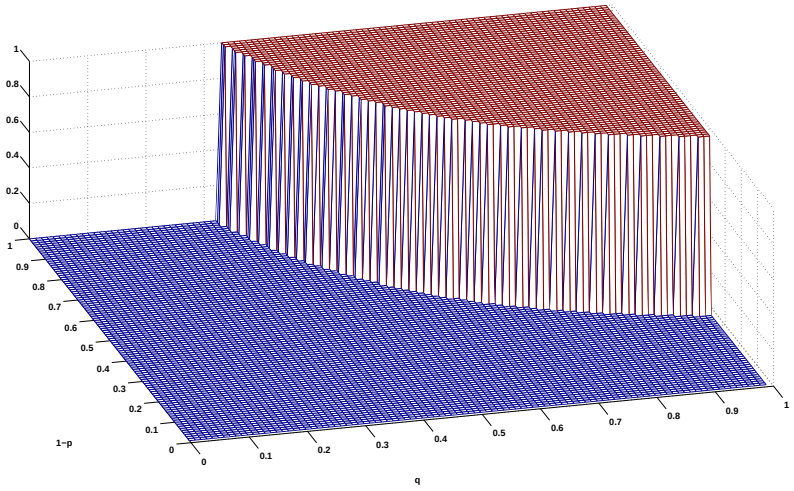

Figure 7.37.: HSDPA Donor Action Mapping.

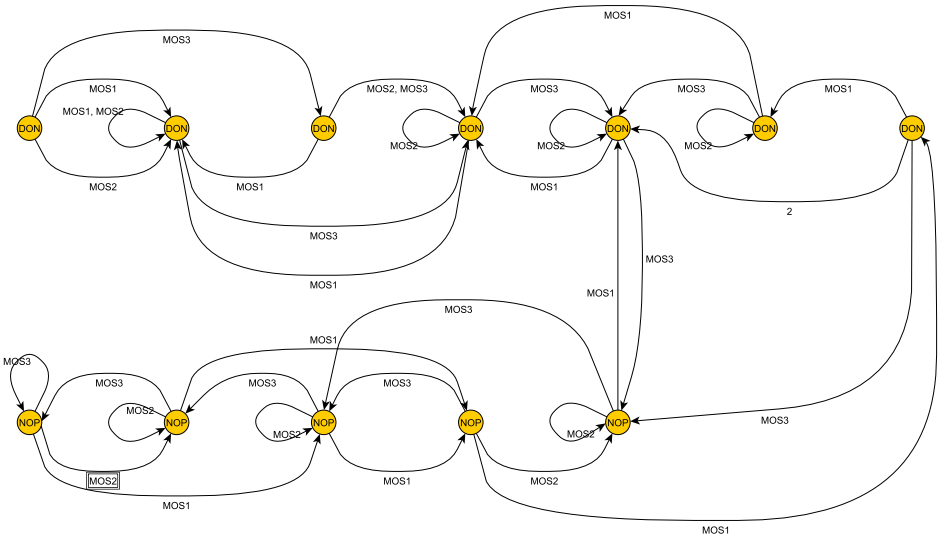

Figure 7.38.: HSDPA Donor Finite State Controller.

8. Results

In this chapter we put the developed controller models to a test against realistic traffic conditions. To achieve this we developed a small-scale WLAN testbed and traffic generation set-up to simulate arrival of a large number of user traffic. We then conducted a survey of the traffic measurements in the cellular and WLAN networks, and developed a stochastic model to generate realistic synthetic arrival processes. We than used sample traffic arrival rates generated by this model as input to the traffic generators in the testbed. POMDP controllers were tested against these arrival processes.

8.1. Test Scenarios

We will use the following scenarios to test the implementation of user-centric WLAN load sharing based on POMDP controllers.

- **No Sharing:** This is the baseline scenario, in which two APs belonging to two different operators do not share traffic in the case of congestion.
- **Agnostic Sharing:** In this scenario APs transfer traffic to their peers without consulting to the QoE database to query the congestion status at the peer AP.
- **Omniscient Controller:** In this scenario a centralized controller with a priori knowledge of the traffic fluctuations in both APs balance traffic between the APs.
- **POMDP Controller:** Both APs run the POMDP controller, and consult the QoE database to query the congestion status at the peer AP.

We use the *No Sharing* scenario as the reference scenario against which the benefits of sharing will be demonstrated. The *Agnostic Sharing* scenario demonstrates the danger of load balancing in the absence of congestion information of the peer RAN. *Omniscient Controller* is a hypothetical reference scenario used in performance comparison of POMDP heuristics, which has access to changes in the system load instantaneously. Since the optimal solution is not computationally feasible, the omniscient controller is used as a best case benchmark.

8.2. Test Setup

In order to evaluate the processor sharing modeling and the performance of the POMDP controllers, a testbed was set up. The network diagram of the testbed is illustrated in the Figure 8.1. The testbed consists of six Linux laptops that emulate the actual users,

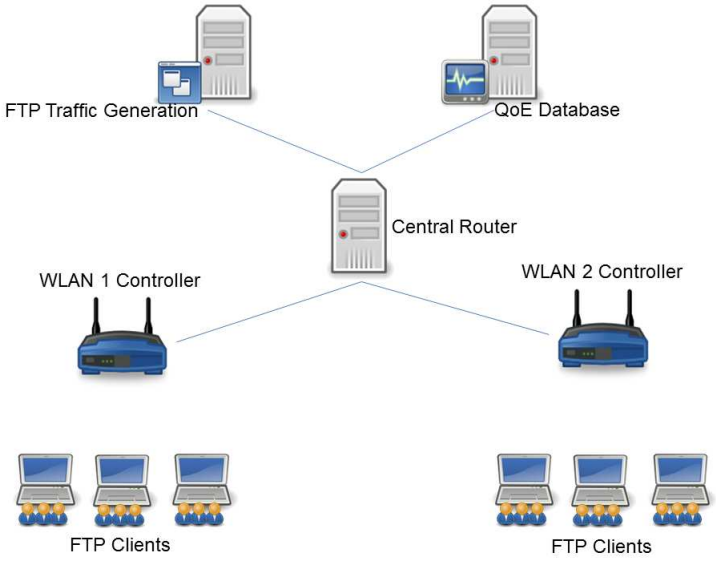

Figure 8.1.: Testbed diagram.

two WLAN APs running embedded Linux serving these users, a central router linking these APs to two servers. One of the servers is the source of the FTP traffic, and the other one is used as the central QoE database. Server-grade Linux operating systems are running on the servers and the router.

Since it is not possible to emulate congestion in the current high capacity WLAN access points with the actual user populations that we have to our disposal, we opted to use a traffic generator based approach. We chose the Distributed Internet Traffic Generator (DITG) software developed by the Universita degli Studi di Napoli [139], due to its flexibility and modularity. DITG is based on the well-known TCP performance measurement tool Iperf [140]. On top of the TCP/UDP traffic generation capabilities of Iperf, DITG gives the possibility to generate generalized IP traffic with tunable packet interarrival times, packet sizes and protocols. It can run on different machines, as it comes with a internal distributed protocol that synchronizes DITG instants running on different network nodes. A DITG Sender can send packets to a DITG Receiver, running on different "flows" allocated to different ports. After the packet generation and packet reception, timing information is sent to a DITG Log entity, which then computes the detailed delay, jitter, and bandwidth measurements for all the flows. Finally, a DITG Manager entity is able to trigger and control another DITG Sender remotely, using the internal protocol.

In our set-up, a DITG Sender runs on the FTP traffic generator. It is controlled by the two independent DITG Manager instances running on the individual APs. The FTP traffic is sent on flows that are received by the DITG Receiver instances running on the laptops. On each flow, we generate TCP packets corresponding to a request size that is exponentially distributed with a mean 150 Kbytes, with interarrival times

also exponential with average 1 second. Each flow can be thought of as 10 users with exponential page request rate of 0.1 packets per seconds. We increase the number of flows to increase the offered load to the system. We run tests for 5 minute intervals, and at the end of these intervals timing information is sent to the DITG Logging component running on the QoE Database. DITG Logging software calculates the delay and jitter of each individual packet. We then use the GNU matrix calculation package Octave [141] to calculate the probability that the delay values exceed 1 seconds for each AP. These values are written to a file, that can be accessed by the WLAN APs, and therefore constitute the observations in the POMDP model. We assign the probabilities to MOS values as follows: If the expected delay is smaller than 10^{-2}, this corresponds to excellent QoE, and given a MOS of 3. If the expected delay is in the range of 10^{-2}, this is acceptable, but not excellent. Therefore we assign a MOS of 2. Otherwise, we assign a MOS of 1, corresponding to an unacceptable QoE.

The APs run the POMDP controller developed in the Chapter 7. At the beginning of each hour each AP makes an observation on their own RANs to determine their roles, i.e. if they need to be borrowers, or they can be donors. After their roles are set, they query the QoE Database for the MOS values in the peer networks at five minute intervals. The POMDP controllers are implemented as FSCs . Depending on the action taken, they determine the aggregate traffic that will be accommodated during the next five minutes. With this value, they use DITG Manager to configure the DITG Sender on the FTP server to send traffic with the calculated traffic intensity. The value of the traffic intensity depends on the actions, as well as the inherent traffic intensity within the RANs that vary over time.We define the used hourly traffic profiles that determine the incoming traffic intensity in individual RANs in the next section

Finally, we use off-line Octave scripts to gather delay and bandwidth measurements for each five minute interval.

8.3. Traffic Profiles

8.3.1. Cellular Systems

There are two possible approaches that can be followed to characterize the spatio-temporal behavior of the traffic in cellular networks. The first option is to track the RF channel occupancy in different locations via spectrum analyzers. The other option is to analyze the AAA records in order to extract the aggregate user behavior associated with a certain base station.

RF Spectrum Measurement Based Surveys

Wideband RF spectrum measurements were undertaken first by regulators to analyze the spectrum utilization. It was the result of these measurements that led DARPA to lead the efforts on dynamic spectrum access, summarized well in [21]. One of the most recent spectrum occupancy surveys was undertaken in two separate locations in Germany and Netherlands by Wellens et. al. [142], which also contains an exhaustive

list of previous measurement studies. In their setup, they scan the frequencies from 20 MHz to 3 GHz with an advanced spectrum analyzer for 47 days. They concentrate purely on the received RF signal power, and perform no demodulation to analyze the actual contents of the transmissions at different frequency ranges. Since their aim is to characterize the spectrum holes and their evolution in time and frequency, an actual demodulation is not necessary. In the following paper [143], the authors use the results to develop empirical stochastic models that can be used to generate synthetic spectrum usage data. The main result from this paper that is relevant for our purposes is the model of the *burst intervals*. A *burst* is a series of spectrum measurements, during which the spectral energy in a given frequency bin is consistently larger than a given threshold. A burst is the exact opposite of a spectrum hole, and therefore represent the intervals for during which opportunistic secondary users are nor allowed to transmit. They show by statistical methods, that the burst periods can be modeled by lognormal or exponential distributions depending on the load.

A similar energy-detection-only measurement campaign was undertaken by Holland et. al. during the 2006 Football World Cup in Germany [144]. Their spectrum scans include a wide range of frequencies: GSM900 (915 MHz - 995MHZ) , DCS1800 (1805 MHz - 1885 MHz), UMTS (2110 MHz -2170 MHz) and Wi-Fi (2.4 GHz). The authors make spectrum scans in the mentioned frequency ranges before, during, and after World Cup matches in two different cities. In their paper they present the results only for the 1800 MHz band. The RF activity stays relatively stable before and decrease during the matches. Half times cause 15 minute long peaks, with similar peaks occurring right after the games. The authors also demonstrate that the rate of change in the activity is smaller for high load periods. Another interesting result is the spatial variation between two venues, which the authors attribute to the social context. One of the games was a high emotion game involving the host nation Germany, where as the other one was a relatively less exciting match. What this shows is that the level of activity is related to social factors that are completely out of control of the operators, such as the end result of a football game.

Energy-detection-only studies account for the total emission in a given spectrum, that includes the signal, the interference and the noise. In order to extract the signal out of the total emission a demodulation process is necessary. The drawback of this approach is the increased sampling time, due to the demodulation. The widest study we could find in the literature is by Kamakaris et. al. [145]. The authors scan the spectrum and decode the signals for six different operators, three of them using CDMA and three of them GSM for 27 hours in two different locations in New Jersey, one being a rural city, the other urban neighborhood with a sampling interval of seven minutes. The main goal of the authors was to quantify the amount of spectrum being under-utilized due to the overprovisioning prevalent in the cellular network planning practice. They show that on the average a CDMA operator overbooks 3 codes out of the maximum 32 codes, and a GSM operator overbooks 10 channels out of 25 channels to 74 channels at its disposal. Furthermore the authors characterize the cross-correlation between the load of different operators during different time frames. The results indicate that 2 hour correlations vary from 0.4 to 1 and half day correlations between 0.8 and 1. Apart from the different

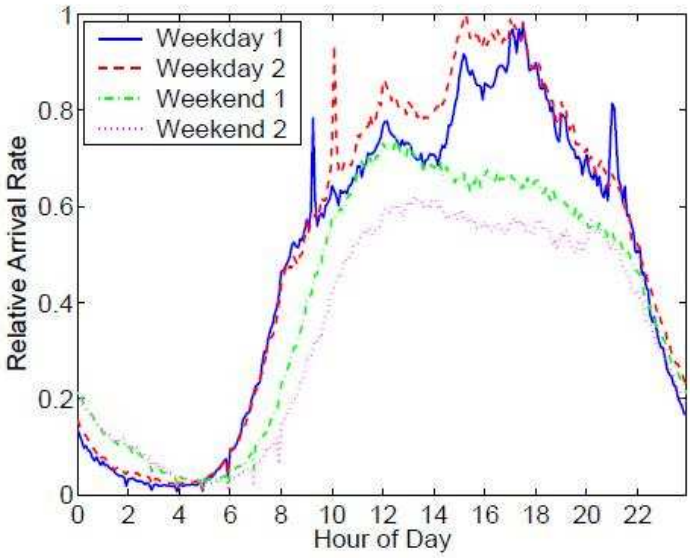

Figure 8.2.: Relative arrival rate versus hour of day from [146]

in the peak loads, the other results are similar for urban and low-density test locations.

AAA Records Based Surveys

The second method of profiling the load variations in the cellular networks is to analyze the call records that the operators hold for AAA purposes. These records are very large in size, and the operators are not willing to share these confidential records. However, these records contain direct information about the call durations, call arrivals and partial information about user mobility. This is in contrast to spectrum measurements, which allows researchers to deduce the overall utilization indirectly.

One of the most recent and most extensive studies of this sort is by Willkomm et. al. [146]. This work was also initiated to determine the behavior of cellular users. Whereas the focus of Kamakaris et. al. is to share the overbooked spectrum among bidding operators, Willkomm et. al. are interested in allowing secondary users to transmit during the periods of low utilization. The authors analyze three weeks worth of call records from a major US operator, Sprint, coming from hundreds of base stations stationed in urban North California. The call records indicate the call start times, end times as well as the start end base stations. The granularity of the records are in the order of milliseconds. Authors first analyze the aggregated call records, which contain records from all the base stations, and thus are statistically more informative.

The calls are modeled by the interarrival random process T and call duration random process D. This is a classical stationary queuing theory type of model. The stationarity interval for the models is shown to be an hour, which means the distributions of these two random processes are stable in hourly intervals. The arrival process is shown to

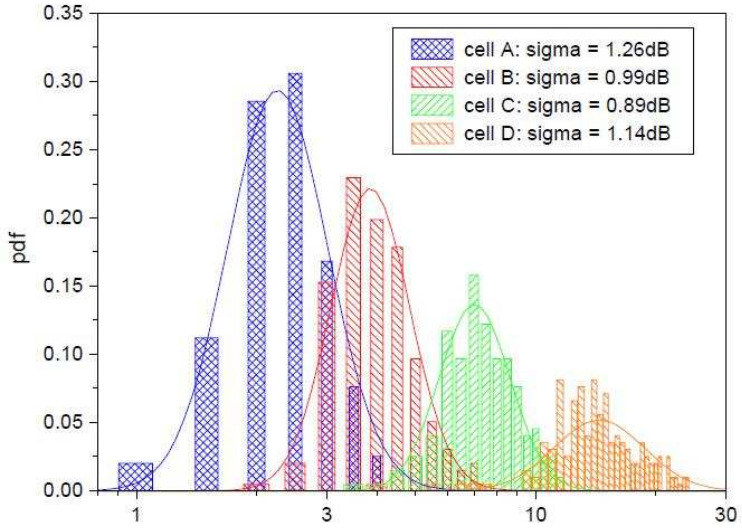

Figure 8.3.: Distribution of call arrival rates from [147].

be Poisson with a rate that changes with the hour of the day. The arrival rate shows a bimodal or diurnal characteristic, with low relative low activity during the day and high activity during the night, depicted in Figure 8.2. A similar diurnal pattern of channel activity is also noted in the work of Kamakaris described earlier [145]. The call duration times are not exponential like the interarrival times, mainly due to the abundance of short calls to the mail boxes of the clients who did not answer the calls. The call duration process is described with two separate lognormal processes for the night and day, similar to the burst interval in the work of Wellens et. al [143]. It is also noted that there are short peaks in both arrival rates and call durations that pertain to the social context, such as a popular TV quiz show. The authors than verify that the models developed using the aggregate data are able to describe the individual cells, by the virtue of goodness-of-fit tests. The system model with variable rate Poisson arrivals and two lognormal call length passes the %95 confidence level tests. The final temporal characteristic that the authors investigate is the level of variation of load within the one hour of stationarity. They show that the standard variation of minute long arrival rate is relatively stable around 0.2 relative to the hourly arrival rate. The ratio of maximum and minimum minute long arrival rate varies between 0.2 and 0.8 relative to the hourly arrival rate. Finally the authors show that there is a considerable spatial variation in usage by calculating the *variogram* of the one minute arrival rate in non adjacent cells. The variogram varies between 0.1 and 0.7. The variogram value γ is defined as the expected mean square difference between the arrival rate in a neighbor location $A(\acute{x}, \acute{y})$ and at a reference location $A(x, y)$

$$\gamma = \frac{1}{2} E\left[A(\acute{x}, \acute{y}) - A(x, y)^2\right] \tag{8.1}$$

Another long call record analysis is due to Hampel et. al. from Bell-Lucent laboratories [147]. Their motivation for visiting call-records is to estimate the capacity of cellular base stations for growth planing by taking into consideration the fluctuations in the traffic seen by the base stations. In this effort they model the load on an base station as the sum of two components, one representing the mean traffic and one representing the stochastic variations around this mean. They investigate 49 day long call records to match the call arrival rates to lognormal distribution depicted in Figure 8.3. Their main result is that the arrival process is Poisson, whose mean is time variant. Hourly arrival rate is distributed lognormally around a mean dependent on the time of the day. The variance of the lognormal distribution is proportional to the time-dependent mean.

In [148] Williamson et. al. used yet more fine grained data than the individual call records, namely the base station traces of low-level events such as registration of mobile nodes. They provide a sample 24 hour data-set from a larger data-set spanning several weeks. They concentrate on the data services, as compared to voice services that Hampel [147] and Willkomm [146]. They are able to reproduce time-varying Poisson arrival process similar to the aforementioned works. However they spot a difference in the peaks that occur in the arrival rate process compared to wired data networks and cellular voice networks. The authors attribute this difference to the pricing schemes used for data services.

Other call record based studies of importance are the 2007 study of call duration distributions from a large GSM network in China by Gui et. al. [149], results from the analysis of a pioneering data service from 2003 by Tang and Baker [150] and finally the work of Hollick [151], [152]. Gui shows that the call duration can be modeled by a lognormal process. Tang and Baker use the wireless modem association data to model the spatial and temporal characteristics of a pioneering wireless network based on Ricochet packet radio infrastructure that was deployed in the United States during the early 2000 and late 90s. Bimodal pattern in changing arrival rate was also a feature of this early radio network. In his work Hollick divided the German city Darmstadt of population 145.000 into zones such as residential, academic, shopping, leisure. He than defines user types such as students, workers, consumers. By analyzing statistical data obtained from off-line databases he than defines the notion of attraction of a zone for different user types, which varies with the time of the day. He finally associates different session rates and session lengths for different user types. This hybrid model allows simulation of the spatio-temporal variation of the traffic across the city.

8.3.2. Wireless LAN

One of the first of these measurement studies was carried out by Afanasyev et. al. on the Google WLAN network deployed in Mountain View, California [131] [153]. The Google network is composed of 500 wireless lan APs that are part of a mesh network. The access to the network is unrestricted and free, but Google imposes a 1 Mbps speed limit to the connections. The authentication uses the Radius protocol. The authors collect Radius association and de-association messages for 28 days. Furthermore, in order to correlate the WLAN network usage with Internet usage they collect 5 days of header information

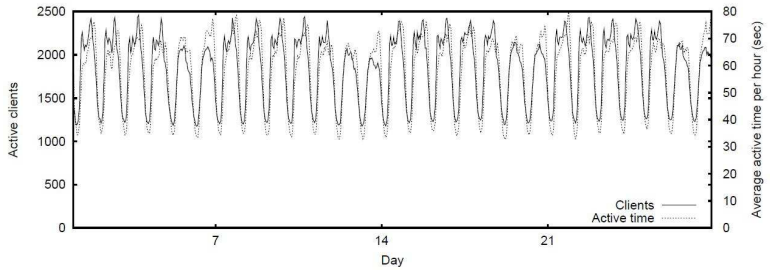

Figure 8.4.: Distribution of call arrival rates from [153].

from the gateway server that connects the Google WLAN node to the global Internet. In collecting the Radius reports, the authors chose the value of 15 minutes as the polling interval. The authors claim that this interval is the period during which the arrival rates are stationary.

The authors discern three different types of end devices, by observing the MAC address hardware manufacturer components. There are users that access Google network by a fixed modem, which acts as a DSL replacement. There are users that prefer their smartphones, and finally users that treat the mesh network like a traditional hotspot, and connecting with their laptops. The maximum number of instantaneous devices is around 2500. For modem-like users the traffic profile is constant, where as diurnal variations are present in the hotspot and smartphone users, as well as in the aggregate traffic depicted in the Figure 8.4. There is a pronounced asymmetry in the download and upload traffic, 3.15 times more download traffic than upload in the aggregate. This ratio is as much as 7 in smartphones. The dominating protocol in use is TCP. The authors also quantify the spatial characteristics of the usage. The most busy AP supports 15 clients on the average, and 95% of the APs serve at least one user on the average. This spatial variation should be put in context by comparing it to the next recent and important measurement study we describe.

In [154] Brik et. al. present the results of an intensive measurement study of a commercial WLAN mesh network operational in Madison Wisconsin. In contrast to Google, which provisions the network access without any contractual bounds, the MadMesh network under study is available on a subscription basis. The network is composed of 250 MAPs (Mash Access Points) which connect to each other on 5 GHz using 802.11 protocols, and act as APs in the 2.4 GHz. The authors undertake three forms of measurement over a period of months. First of all they collect SNMP logs from all the MAPs with three minute intervals. Secondly they use sniffing software to track the network usage passively. Finally they also use active measurements to gauge the end user throughput. The results indicate a diurnal pattern similar to cellular networks and the Google network. However the peaks occur very late in the night, reflecting the young user base of the network who tend to use the network after coming home. The spatial distribution is not uniform, as opposed to Google Mesh: 40% of users connect to the 20 % of the installed mesh networks. Another key result of this study is the observation of traffic sharing among users of TCP protocol, i.e. the more users sharing a link, the less TCP

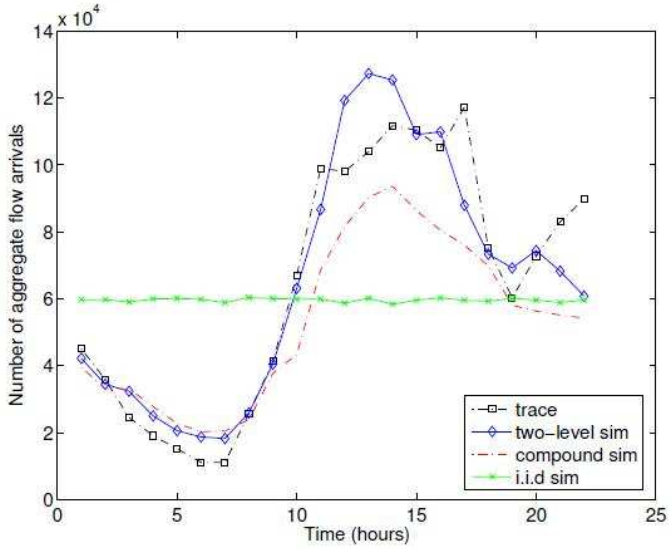

Figure 8.5.: Distribution of call arrival rates from [160].

throughput they obtain. Finally the authors find many coverage holes, even though the network has been engineered to provide full coverage in downtown Madison. They relate the cause of this to the low power setting used by the end user devices: the MAPs can send packets to the end users, but the end users cannot reply back since their power is not enough for reaching the MAP.

Before these wide-area measurement studies came out, the WLAN traffic characteristics were investigated extensively in different settings. Blinn et. al. investigate the traffic conditions in a network of hot-spots operated by a major US operator in New York [155]. Kotz, one of the co-authors of the aforementioned study, and Essien present the analysis of a campus-wide WLAN network in Darmouth college, where the ownership of a laptop is mandatory, in [156]. Sevtsuk et. al. demonstrate a real-time system that tracks and demonstrates the network load in MIT WLAN network in [157]. Castro and Balazinska measure the traffic in three buildings of the IBM campus in [158]. In all these works the diurnal characteristic of the traffic demand is visible. In [159] Jardosh et. al. attempt to analyze the development of congestion in 802.11b WLANs, by tracking the WLAN usage via passive sniffing during a two day long IETF event. The set-up for the meeting included 38 WLAN APs. Three sniffers are placed in strategic locations to track the overall activity in three WLAN channels. This approach is similar to the energy-detection only measurements done for the cellular networks. The results indicate that the different channels occupied by different APs experience utilizations between 20% and 99%. Furthermore, the authors define utilization thresholds based on the overall throughput: an AP is under-utilized if the utilization is less than 30%, and it is congested if the utilization is above 84%.

Finally, Hernandez-Campos et. al. develop an empirical model for the spatio-temporal

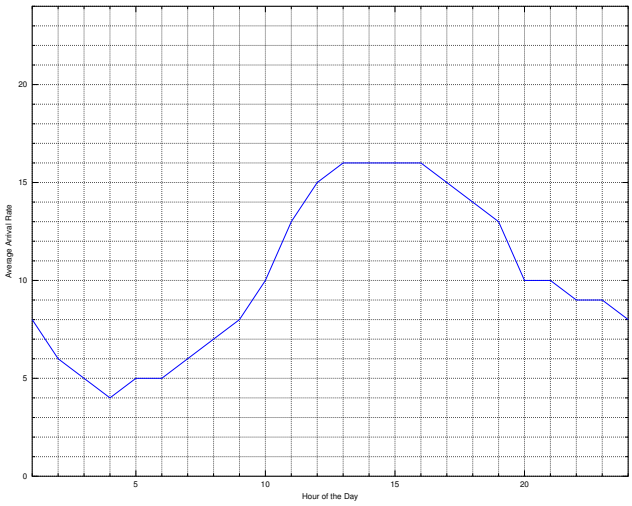

Figure 8.6.: Baseline arrival rate.

characteristics of campus WLANs in [160]. Their model is the result of their previous measurements undertaken in the University of North Caroline Campus [161]. After comparing the empirical results of spatio-temporal measurements to the Darmouth College study and showing that diurnal temporal nature of the traffic as well as the log-normal spatial distribution are valid irrespective of the location, the authors develop a stochastic model to describe wireless traffic in campus WLANs. Their model is two leveled. In the bottom level they describe the session arrival, which correspond to the arrival of new users, with a time varying Poisson process similar to what has been proposed for cellular traffic temporal variations. The users than generate a number of flows, whose inter arrival times are described by a Lognormal process. The size of the individual flows are described by a BiPareto distribution. The synthetic arrival process produced by this model is able to replicate the diurnal characteristic of WLAN traffic as depicted in Figure 8.5.

8.3.3. Hybrid Traffic Model

For generating synthetic arrival processes that are used as inputs to the simulations, we use various aspects of the WLAN and cellular traffic models.

It is well established that the hourly arrival process follows a time-varying Poisson process, whose parameter follows a diurnal pattern. In the simulations we use two variants of the baseline average hourly arrival rate. The profile depicted in Figure 8.6 is used by two co-located independent access networks, which serve a similar user population.

Another set of baseline average hourly arrival rates is depicted in Figure 8.7. These arrival rates belong to co-located access networks, which serve different user populations. It has been observed in campus-wide studies summarized in Section 8.3.2, that the

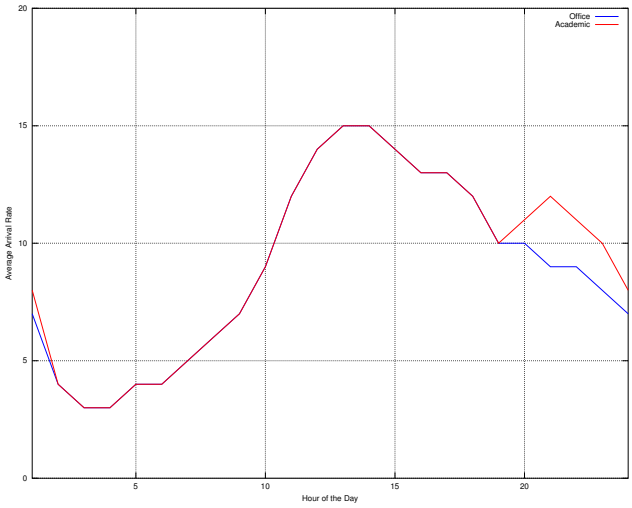

Figure 8.7.: Differential arrival rates.

residential and academic WLAN networks experience a second peak into the late hours of the night, compared to the relative lack of activity in commercial WLAN networks. This trend is replicated in the differential arrival rate averages in the aforementioned figure.

If these patterns were deterministic, there would be very few periods, during which dynamic resource sharing would make sense. However, this is not the case. The hourly arrival rates fluctuate around the mean given in the diurnal baseline. Hernandez-Campos et. al. provide the minimum, maximum, average and median hourly arrival rates in [161], but do not propose a distribution with which the hourly arrival rates vary. Hampel provides such a distribution for cellular networks in [147]. According to this model, the hourly arrival rates follow a log-normal distribution around the baseline hourly averages with a standard deviation of 20% of the hourly average. We extend Hernandez-Campus model with Hampel's model, and write the hourly arrival rate λ_{ik} of operator i at hour k as:

$$\lambda_{ik} = d_{ik} + v_{ik} \tag{8.2}$$

The deterministic component d_{ik} is taken from the baseline hourly average arrival profiles. To this the stochastic component v_{ik} is added, which is a zero mean lognormal random variable with a standard deviation one fifth of the hourly average d_{ik}.

Another important property that needs to be taken into account is the amount of correlation between different access networks. To the best of our knowledge, Salami et. al. are the only authors who have provided correlation values for traffic on cellular networks. In [162] they use correlation coefficient values between 0.5 and 1.

We use the following procedure to generate synthetic yet realistic traffic profile. First

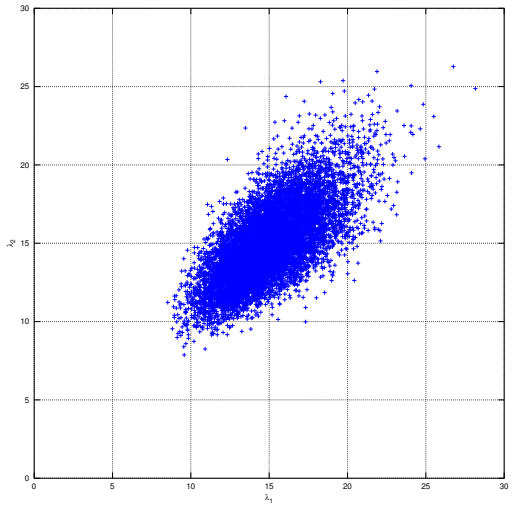

Figure 8.8.: Scatter diagram of arrival rates of correlated operators.

we use the baseline hourly average rates. We use the standard deviations which are scaled versions of the hourly average rates and the correlation coefficient generate a covariance matrix. By using this covariance matrix, we generate two correlated normal variables. We then use the exponential function to obtain the correlated lognormal random variables. We employ the necessary numerical transformations to assure that the resulting processes have the desired standard deviations and means. Figure 8.8 presents a scatter plot of two arrival processes with mean 15 and correlation coefficient 0.6 and ten thousand samples. It is worthwhile to not that the arrival rates can grow as large as 29 and shrink as low as 8.

We present two sample daily traffic profiles in Figure 8.9 and Figure 8.10. Figure 8.9 uses the differential baseline hourly arrival rate averages given in Figure 8.7. Figure 8.10 uses the arrival profile given in 8.7. What one can infer from these sets of figures are the following. First of all, dynamic resource sharing opportunities occur not during low utilization hours, but during peak hours. Secondly, as expected, these opportunities are ample when there is a differential between the baseline hourly arrival rate averages, such as the case for residential/academic vs. commercial networks. Finally, even if two operators share the same baseline hourly arrival rate averages, their hourly average rates may differ substantially to make room for dynamic resource sharing. Furthermore, the networks change their donor/borrower roles. This is evident for example the hours 12 and 15 in Figure 8.10.

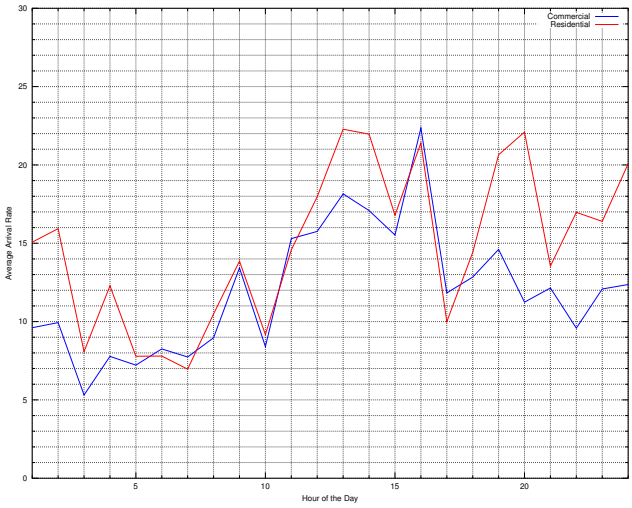

Figure 8.9.: Synthetic arrival rates for uneven demands.

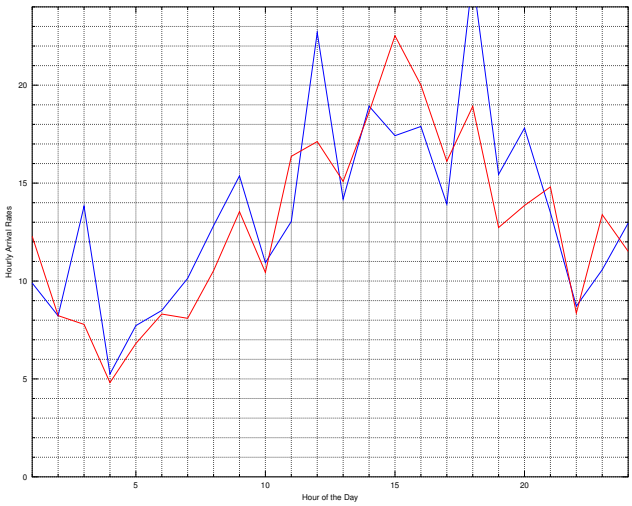

Figure 8.10.: Synthetic arrival rates for even demands.

8.4. Test Results

8.4.1. Processor Sharing Modeling

We first verified the validity of PS model for 802.11g RAN. In order to do this, we gather the delay values experienced by sessions for a period of ten minutes. We then calculate

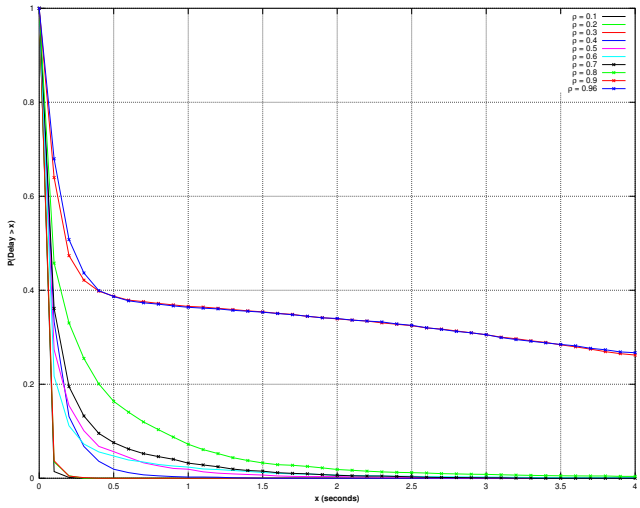

Figure 8.11.: Complementary Cumulative Distribution Function

the Complementary Cumulative Distribution Function (cCDF) of the delay values. For a given x, $CCDF(x)$ gives the probability that the delay values are larger than this value x. We plot this function in Figure 8.11.

In our model our performance goal was set to strictly less than 0.01. However we observe that the delay values are in the order of 0.01, and not below. There are two reasons for not meeting the tighter bound. First of all there is a slight over estimation of the total capacity of the 802.11 RAN in our model. We used a theoretically computed capacity of 31 Mbps, as proposed in the literature. The practical RAN capacity is smaller than this value. However, there is also the important factor about the packet sizes. In our derivations in Section 7.5.1, we set bounds on delay for demands with a constant size of 130 kbps. In other words, the tighter limit is for conditional delay. The measurements on the other hand are for the delay average for all the demand sizes, where the demand size is distributed exponentially. We assume that the larger delays associated with larger packets is a contributing factor to increased delay limit. Nevertheless, we are able to meet a looser delay bound with the original model. The well-known saturation phenomena is also visible in the plots. After a utilization of 0.7, the delay distributions remain the same for increasing utilizations.

We can deduce that the PS model we developed for WLAN RANs and TCP traffic in Section 7.5 can be used for practical purposes. If one concentrates on the value of the cCDF at $x = 1$, the values grow to unacceptable levels i.e. $P(\text{delay} > 1) > 0.1$ after utilization exceeds 0.7. A tighter bound $P(\text{delay} > 1) > 0.1$ is possible for utilizations smaller than 0.4.

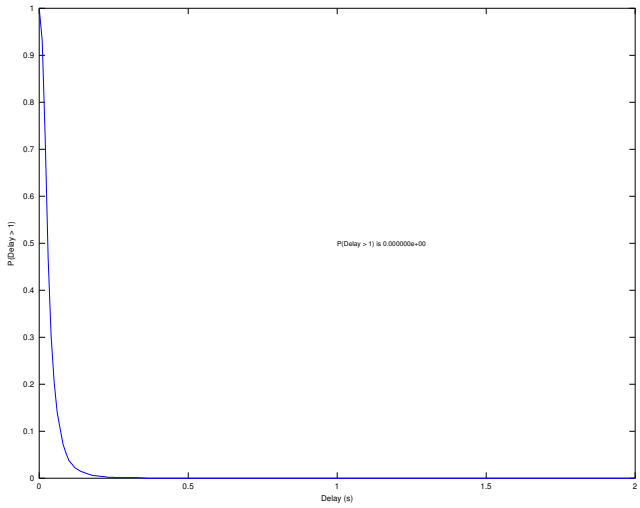

(a) $\lambda = 8$

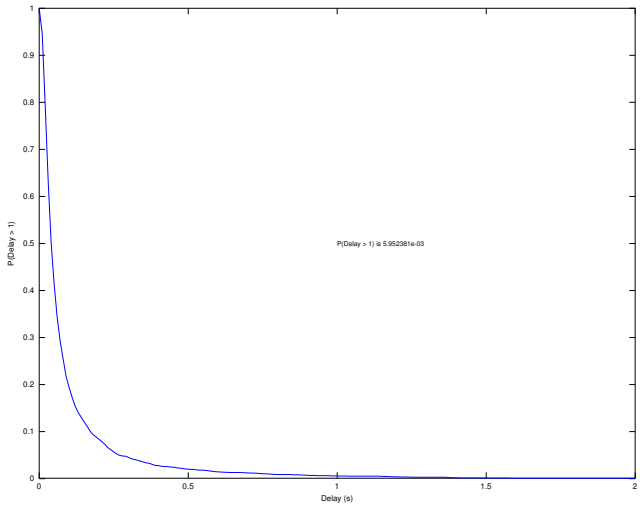

(b) $\lambda = 17$

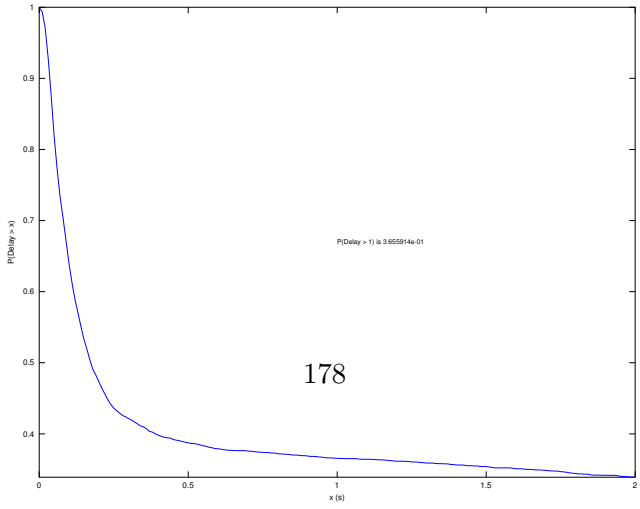

(c) $\lambda = 24$

Figure 8.12.: cCDF of delay for different arrival rates.

8.4.2. Calculating A Priori Probabilities

In Section 7.4.4, we used intuitive values for the a priori probabilities of the observations. In this subsection we discuss how these values could be determined from our test results.

To calculate the a priori observation probabilities, one needs to calculate the distribution of delay values for a given arrival rate. Complementary CDFs calculated for three different values of arrival rates, $\lambda = 8, 17, 24$, is given in Figure 8.12. It can be seen that there is a one to one correspondence between the traffic arrival rates and the probability that the delay exceeds 1 seconds. The empirical delay exceedance probability is respectively 0, 6×10^{-3}, 3.6×10^{-1} for increasing arrival rates. These exceedance probabilities are also used as observations in our model. If this probability is between 0 and 10^{-2}, the observation is MOS3. If the exceedance probability is in the order of 10^{-2}, then observation is MOS2. MOS1 corresponds to larger exceedance probabilities.

To calculate the a priori probability of an observation, one has to find the correspondence between arrival rate and the empirical exceedance probabilities. This correspondence can be obtained by gradually increasing the arrival rate, collecting delay values, and calculating the empirical exceedance probabilities. Once such a correspondence is established, the a priori probabilities of the observations can be expressed as probability that the arrival rate is between certain threshold values. In our experiments, we found that arrival rates less than 13 Erlangs result in exceedance probability less than 10^{-2}. Arrival rates between 13 and 20 result in exceedance probabilities in the order of 10^{-2}. Larger arrival rates result in higher exceedance probabilities. Therefore, the a priori probability of MOS3 is equivalent to the probability that the arrival rate is less than 13 Erlangs. The a priori probability of MOS2 is equivalent to probability that the arrival rate is between 13 and 20. Thus, an operator with access to long term arrival rates can easily calculate the observation probabilities. Without access to these measurements, we opted to use intuitive values.

8.4.3. Performance of POMDP Controllers

We tested our implementation over a 70 minute period by using the traffic profiles depicted in Figure 8.13. In this scenario the donor has a stable arrival rate of 16 Erlangs. Borrower on the other hand is facing 22 Erlangs, and cannot meet the QoE requirements. In the next hour, borrowers traffic demand decreases to 14 Erlangs. The POMDP controller in the donor is able to deduce this change after three observations, amounting to 15 minutes. The required time to sense the change in the peer network is a function of the structure of the POMDP controller given in Figure 7.31 and the length of the observation periods which is 5 minutes in our implementation.

We present the QoE and the throughput measurements at the donor operator in Figure 8.14. What we observe is that the donor operator is able to increase its average throughput 9%, while at the same time keeping the unsatisfied request less than %8.

On the borrower side, it can be observed that borrower is able to reduce the number of unsatisfied requests from 40% to less than 12%.

Since we varied the arrival rates on hourly basis, there were no sudden spikes in the

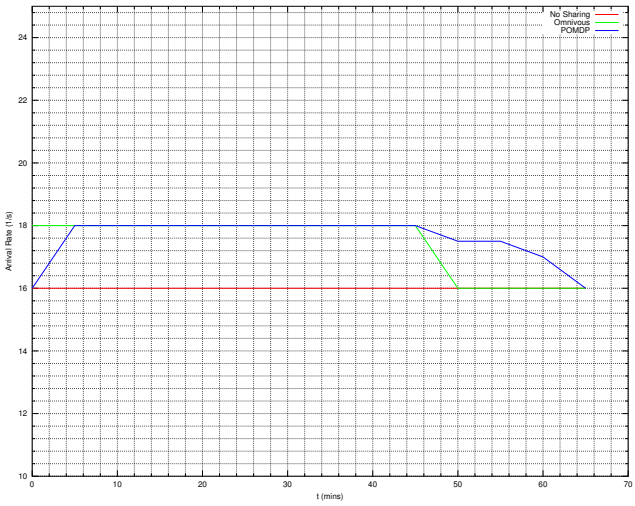

(a) Donor Arrival Rate.

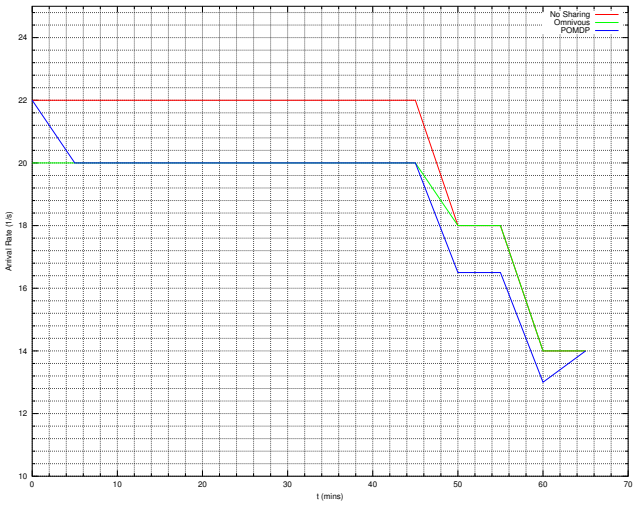

(b) Borrower Arrival Rate.

Figure 8.13.: Donor and Borrower Arrival Rates.

traffic profiles. This meant that comparing the performance of the POMDP with the agnostic controller was not possible. However it is well demonstrated that the traffic arrival rates can vary, and cause a sudden increase in the arrival rate. If the changes in the arrival rates in two different operators are not simultaneous, which is the case in our set-up but more are more realistic, an agnostic controller will not be able to deduce

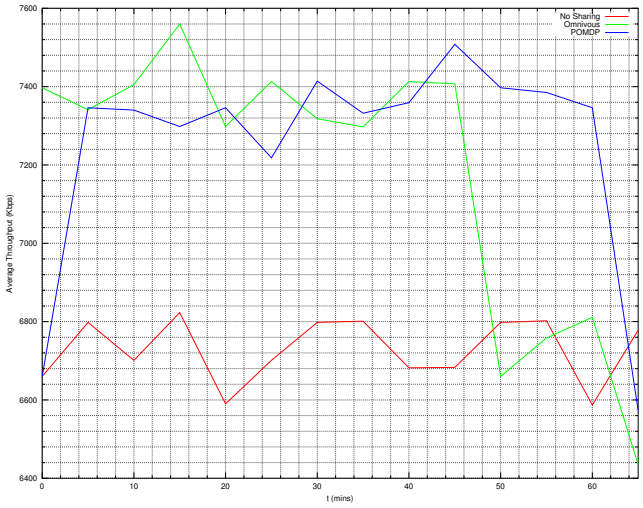

(a) Donor Average Throughput.

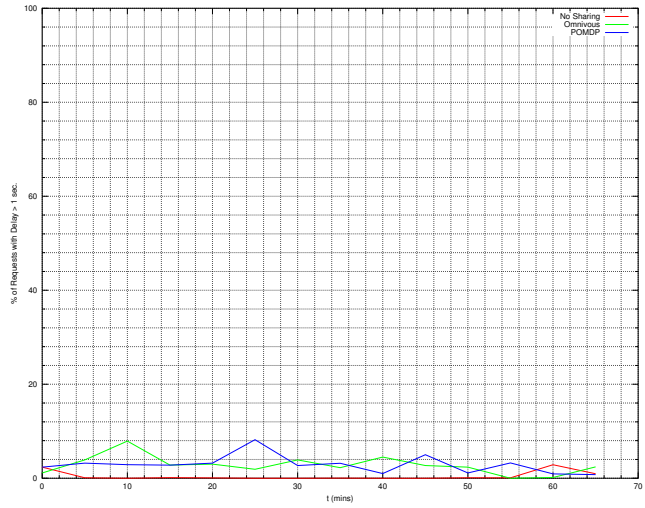

(b) Donor QoE.

Figure 8.14.: Donor Performance Metrics.

this, whereas POMDP controller would be able to.

We can conclude that our POMDP modeling has the limitation that results in a less tight delay limit to be guaranteed. If one accepts this larger limit, POMDP controllers are able to increase the throughput of the donor operator, and decrease the probability that delay guarantees are not met in the borrower operator. An alternative approach

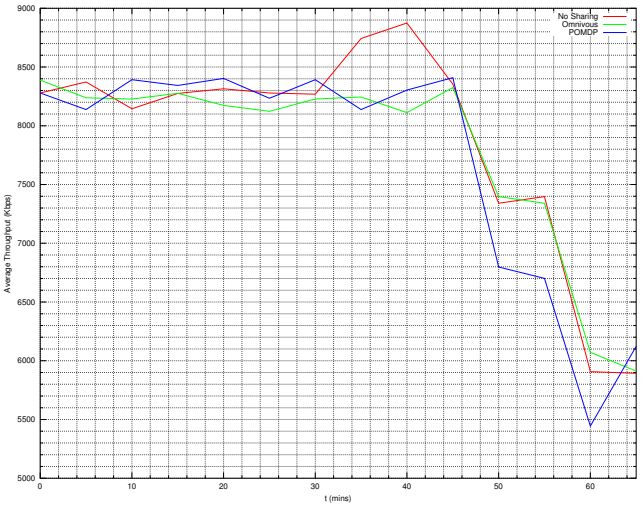

(a) Borrower Average Throughput.

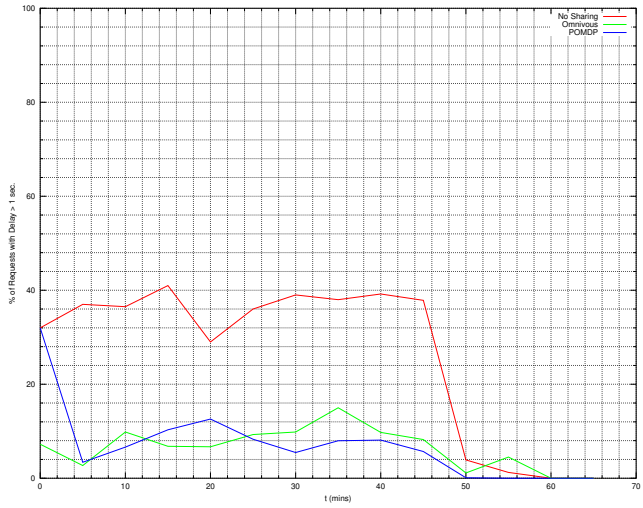

(b) Borrower QoE.

Figure 8.15.: Borrower Performance Metrics.

to the non-matching limit problem would be to include a safety vector in the model development process in Chapter 7. Instead of choosing the utilization corresponding to 0.01 in Figure 7.18, one can choose a lower utilization corresponding to 0.1. However, this would mean that it would be harder for operators to be considered as donors.

9. Conclusions

At the beginning of this work we set out to demonstrate that real-time resource sharing between operators can be realized by introducing an open database to which users anonymously report their experiences with different radio access networks owned by these operators. We believe such a dynamic exchange of resources is necessary, especially in the face of increasing demand for wireless data access and the long time frames with which new technologies such as cognitive radio or LTE are accepted on mass scales. We tried to motivate this by examples in Chapter 2.

It is a point shared by many in the telecommunications industry, that the future of the wireless landscape is a heterogenous one. Therefore the operators for which we develop the real-time dynamic resource sharing will be owning radio access networks of different technologies. At this point, it is crucial to have an modeling approach that can be used to abstract these different technologies. In Chapter 4, we argued that Processor Sharing Queue Model is one option for this. One of the shortcomings of the models we developed in this Chapter is their fixed capacity property. In reality the overall capacity of a radio access network changes with the number of users associated with it. We have assumed that this capacity is constant. We have chosen a capacity value, that corresponds to the saturation capacity, meaning that our model is more conservative to the reality, which is not necessarily a bad design decision. Nevertheless, one of our future work points is to introduce load dependence in our models for WLAN and HSDPA.

When two operators must take decisions on how much resources they will exchange, they must have a framework with which they can combine the processor sharing models of their radio access networks. We have used Queueing Networks as this framework in Chapter 5. There are room for improvements in the queueing networks we developed in this Chapter. Specifically, we have used fixed probabilities for user preferences of network operators. In real life, and especially in a user-centric environment, the preference of the users for network operators is dependant on the relative loads of the radio access networks. This can be incorporated as load dependent routing probabilities in the queueing network. Such queueing networks with load dependant routing probabilities can be used to investigate the feedback effects user congestion. Furthermore, single operator common radio resource management techniques can also be modeled by this extensions.

When it comes to negotiating the parameter of resource sharing, our aim was to provide a peer to peer mechanism. The other option is to have a trusted third party acting as an intermediary. This option requires establishing trust between multiple large corporations, and can be expected to take years. Peer to peer agreements are easier to establish, and becoming more common in the industry. We were able to provide such a negotiation mechanism for single class resource sharing in Section 6.1. For multi-class

sharing we provided an auctioning mechanism, that can be used by a trusted third party solution, in Section 6.2. We will work on providing a peer to peer mechanism for multi-class sharing in the future.

We handled the real-time control problem of resource sharing, after the negotiation phase in Chapter 7. We provided finite state controllers for borrower and donor radio access networks, for the single class scenario. We used POMDP framework to develop these finite state controllers. The individual decision makers considered the actions of their peers as an environment variable. This means, they did not model the intelligence of their peers in their decision making. This was not necessary, when the incentive compatible negotiation mechanism developed in Chapter 6 is used, since cheating is futile with this mechanism. However for multi-class control, for which no incentive compatible mechanism was developed, agents should take into account the possibility that the peer agents might be cheating. To this end we will use i-POMDP abstraction from multi-agent modeling in our future work.

Finally, we plan to develop an OPNET simulation to validate the performance of the single class controllers we developed for resource sharing between HSDPA and WLAN RANs.

Bibliography

[1] AT&T Wireless CEO Calls For Action To Avert Capacity Crunch. [Online] Available: http://blogs.wsj.com/digits/2010/03/23/att-wireless-ceo-calls-for-action-to-avert-capacity-crunch/.

[2] R. Marvedis. (2009, July) Mobile Operators Threatened More by Capacity Shortfalls than Growth of WiMAX. [Online]. Available: http://maravedis-bwa.com/Issues/5.6/Syputa_readmore.html

[3] E. Halepovic, C. Williamson, and M. Ghaderi, "Wireless Data Traffic: A Decade of Change," *IEEE Network*, vol. 23, no. 2, pp. 20–26, 2009.

[4] [9]. (2009) AT&T Investment in 2009 Will Add More Than 40 New Cell Sites throughout Illinois. [Online]. Available: http://www.att.com/gen/press-room?pid=4800&cdvn=news&newsarticleid=26690.

[5] (2010) KINETO SMART Wi-Fi OFFLOAD SOLUTION ADDRESSES NETWORK CHALLENGES CREATED BY SMARTPHONES. [Online]. Available: http://www.kineto.com/pdf/press_releases/kineto_Smart_WiFi_Solution.pdf

[6] T. Miki, "Community networks as next generation local network planning concept," in *Communication Technology Proceedings, 1998. ICCT'98. 1998 International Conference on.* IEEE, 2002, pp. 8–12.

[7] *The Milan Civic Network experience and its roots in the town*, August 2002. [Online]. Available: http://dx.doi.org/10.1109/CN.1995.509584

[8] FON Corporate Homepage. [Online] Available: http://www.fon.com/.

[9] *Building Wireless Community Networks with 802.16 Standard*, December 2008. [Online]. Available: http://dx.doi.org/10.1109/BROADCOM.2008.55

[10] M. H. Manshaei, P. Marbach, and J. P. Hubaux, "Evolution and market share of wireless community networks," June 2009, pp. 508–514. [Online]. Available: http://dx.doi.org/10.1109/GAMENETS.2009.5137439

[11] A. C. Toker, F. Cleary, M. Fiedler, L. Ridel, and B. Yavuz, "PERIMETER: Privacy-Preserving Contract-less, User Centric, Seamless Roaming for Always Best Connected Future Internet," in *Proceedings of 22th World Wireless Research Forum*, 2009.

[12] M. Dohler, D. E. Meddour, S. M. Senouci, and A. Saadani, "Cooperation in 4G - Hype or Ripe?" *Technology and Society Magazine, IEEE*, vol. 27, no. 1, pp. 13–17, March 2008. [Online]. Available: http://dx.doi.org/10.1109/MTS.2008.918035

[13] L. Giupponi, R. Agusti, J. Pérez-Romero, and O. Salient, "Improved Revenue and Radio Resource Usage through Inter-Operator Joint Radio Resource Management," in *Communications, 2007. ICC'07. IEEE International Conference on*. IEEE, 2007, pp. 5793–5800.

[14] L. Giupponi, R. Agusti, J. Perez-Romero, and O. Sallent, "Inter-operator agreements based on QoS metrics for improved revenue and spectrum efficiency," *Electronics Letters*, vol. 44, no. 4, pp. 303–304, February 2008. [Online]. Available: http://dx.doi.org/10.1049/el:20083431

[15] T. Frisanco, P. Tafertshofer, P. Lurin, and R. Ang, "Infrastructure Sharing and Shared Operations for Mobile Network Operators: From a Deployment and Operations View," in *Communications, 2008. ICC '08. IEEE International Conference on*, May 2008, pp. 2193–2200. [Online]. Available: http://dx.doi.org/10.1109/ICC.2008.419

[16] A. Tolli, P. Hakalin, and H. Holma, "Performance evaluation of common radio resource management (CRRM)," in *Communications, 2002. ICC 2002. IEEE International Conference on*, vol. 5, 2002. [Online]. Available: http://dx.doi.org/10.1109/ICC.2002.997467

[17] A. Furuskar and J. Zander, "Multiservice allocation for multiaccess wireless systems," *Wireless Communications, IEEE Transactions on*, vol. 4, no. 1, pp. 174–184, 2005. [Online]. Available: http://dx.doi.org/10.1109/TWC.2004.840243

[18] *Common radio resource management: functional models and implementation requirements*, vol. 3, 2005. [Online]. Available: http://dx.doi.org/10.1109/PIMRC.2005.1651803

[19] *Congestion Control Strategies in Multi-Access Networks*, 2006. [Online]. Available: http://dx.doi.org/10.1109/ISWCS.2006.4362365

[20] *Understanding Dynamic Spectrum Access: Models,Taxonomy and Challenges*, June 2007. [Online]. Available: http://dx.doi.org/10.1109/DYSPAN.2007.88

[21] I. F. Akyildiz, W. Y. Lee, M. C. Vuran, and S. Mohanty, "NeXt generation/dynamic spectrum access/cognitive radio wireless networks: a survey," *Comput. Netw.*, vol. 50, no. 13, pp. 2127–2159, September 2006. [Online]. Available: http://dx.doi.org/10.1016/j.comnet.2006.05.001

[22] G. Salami, A. U. Quddus, D. Thilakawardana, and R. Tafazolli, "Nonpool based spectrum sharing for two UMTS operators in the UMTS extension band," September 2008, pp. 1–5. [Online]. Available: http://dx.doi.org/10.1109/PIMRC.2008.4699855

[23] G. Salami, S. Thilakawardana, and R. Tafazolli, "Dynamic spectrum sharing algorithm between two UMTS operators in the UMTS extension Band," in *Communications Workshops, 2009. ICC Workshops 2009. IEEE International Conference on.* IEEE, 2009, pp. 1–6.

[24] S. K. Jayaweera and T. Li, "Dynamic spectrum leasing in cognitive radio networks via primary-secondary user power control games," *Wireless Communications, IEEE Transactions on*, vol. 8, no. 6, pp. 3300–3310, 2009.

[25] L. Kleinrock, "Time-shared Systems: a theoretical treatment," *J. ACM*, vol. 14, no. 2, pp. 242–261, 1967. [Online]. Available: http://dx.doi.org/10.1145/321386.321388

[26] I. E. Telatar and R. G. Gallager, "Combining queueing theory with information theory for multiaccess," *Selected Areas in Communications, IEEE Journal on*, vol. 13, no. 6, pp. 963–969, 1995. [Online]. Available: http://dx.doi.org/10.1109/49.400652

[27] A. K. Parekh and R. G. Gallager, "A generalized processor sharing approach to flow control in integrated services networks: the single-node case," *IEEE/ACM Trans. Netw.*, vol. 1, no. 3, pp. 344–357, August 1993. [Online]. Available: http://dx.doi.org/10.1109/90.234856

[28] F. Baskett, K. M. Chandy, R. R. Muntz, and F. G. Palacios, "Open, Closed, and Mixed Networks of Queues with Different Classes of Customers," *J. ACM*, vol. 22, no. 2, pp. 248–260, 1975. [Online]. Available: http://dx.doi.org/10.1145/321879.321887

[29] Kitayev, "Analysis of a Single-Channel Queueing Systems with the Discipline of Uniform Sharing of a Device," *Engineering Cybernetics*, vol. 17, no. 6, pp. 42–49, 1979.

[30] E. G. Coffman, R. R. Muntz, and H. Trotter, "Waiting Time Distributions for Processor-Sharing Systems," *J. ACM*, vol. 17, no. 1, pp. 123–130, 1970. [Online]. Available: http://dx.doi.org/10.1145/321556.321568

[31] T. J. Ott, "The Sojourn-Time Distribution in the M/G/1 Queue with Processor Sharing," *Journal of Applied Probability*, vol. 21, no. 2, pp. 360–378, 1984. [Online]. Available: http://dx.doi.org/10.2307/3213646

[32] S. Yashkov and A. Yashkova, "Processor sharing: A survey of the mathematical theory," *Automation and Remote Control*, vol. 68, no. 9, pp. 1662–1731, September 2007. [Online]. Available: http://dx.doi.org/10.1134/S0005117907090202

[33] Ietf, "RFC 3475: An Architecture for Differentiated Services," [Onlone] Available: http://tools.ietf.org/html/rfc2475, Tech. Rep., 1998.

[34] ——, "RFC 1633: Integrated Services in the Internet Architecture an Overview," [Online] Available: http://tools.ietf.org/html/rfc1633, Tech. Rep.

[35] S. Mangold, S. Choi, G. R. Hiertz, O. Klein, and B. Walke, "Analysis of IEEE 802.11 e for QoS support in wireless LANs," *Wireless Communications, IEEE*, vol. 10, no. 6, pp. 40–50, 2004.

[36] G. Bianchi and Others, "Performance analysis of the IEEE 802. 11 distributed coordination function," *IEEE Journal on selected areas in communications*, vol. 18, no. 3, pp. 535–547, 2000.

[37] A. Kumar, E. Altman, D. Miorandi, and M. Goyal, "New insights from a fixed-point analysis of single cell IEEE 802.11 WLANs," *IEEE/ACM Transactions on Networking*, vol. 15, no. 3, pp. 588–601, 2007.

[38] A. Papoulis, *Probability, random variables, and stochastic processes*. McGraw-Hill Science, Engineering & Mathematics, 1991.

[39] D. Miorandi, A. A. Kherani, and E. Altman, "A queueing model for HTTP traffic over IEEE 802.11 WLANs," *Computer networks*, vol. 50, no. 1, pp. 63–79, 2006.

[40] R. Litjens, "Capacity allocation in wireless communication networks: Models and analyses," Ph.D. dissertation, Universiteit Twente, Twente, 2003.

[41] K. Medepalli and F. A. Tobagi, "System centric and user centric queueing models for IEEE 802.11 based wireless LANs," in *Broadband Networks, 2005. BroadNets 2005. 2nd International Conference on*, 2005. [Online]. Available: http://dx.doi.org/10.1109/ICBN.2005.1589666

[42] R. Bruno, M. Conti, and E. Gregori, "Analytical modeling of TCP clients in Wi-Fi hot spot networks," *NETWORKING 2004, Networking Technologies, Services, and Protocols; Performance of Computer and Communication Networks; Mobile and Wireless Communications*, pp. 626–637, 2004.

[43] G. Kuriakose, S. Harsha, A. Kumar, and V. Sharma, "Analytical models for capacity estimation of IEEE 802.11 WLANs using DCF for internet applications," *Wireless Networks*, vol. 15, no. 2, pp. 259–277, 2009.

[44] A. Ferragut and F. Paganini, "A connection level model for IEEE 802.11 cells," in *Proceedings of the 5th International Latin American Networking Conference*. ACM, 2009, pp. 32–40.

[45] A. Mäder, D. Staehle, and H. Barth, "A Novel Performance Model for the HSDPA with Adaptive Resource Allocation," in *Managing Traffic Performance in Converged Networks*, ser. Lecture Notes in Computer Science, L. Mason, T. Drwiega, and J. Yan, Eds. Berlin, Heidelberg: Springer Berlin / Heidelberg, 2007, vol. 4516, ch. 82, pp. 950–961–961. [Online]. Available: http://dx.doi.org/10.1007/978-3-540-72990-7_82

[46] M. e. a. Andreas, "Spatial and temporal fairness in heterogeneous HSDPA-enabled UMTS networks," *EURASIP Journal on Wireless Communications and Networking*, vol. 2009, 2009.

[47] K. I. Pedersen, T. F. Lootsma, M. Stottrup, F. Frederiksen, T. E. Kolding, and P. E. Mogensen, "Network performance of mixed traffic on high speed downlink packet access and dedicated channels in WCDMA," in *IEEE VTC*. Citeseer, 2004, pp. 4496–4500.

[48] S. Borst, "User-level performance of channel-aware scheduling algorithms in wireless data networks," *IEEE/ACM Trans. Netw.*, vol. 13, no. 3, pp. 636–647, June 2005. [Online]. Available: http://dx.doi.org/10.1109/TNET.2005.850215

[49] Y. Wu, C. Williamson, and J. Luo, "On processor sharing and its applications to cellular data network provisioning," *Performance Evaluation*, vol. 64, no. 9-12, pp. 892–908, 2007.

[50] S. C. Borst, R. Núñez-Queija, and M. J. G. Van Uitert, "User-level performance of elastic traffic in a differentiated-services environment," *Performance Evaluation*, vol. 49, no. 1-4, pp. 507–519, 2002.

[51] M. Ivanovich and P. Fitzpatrick, "Throughput metrics in beyond 3G wireless systems with complex rate variability and QoS," in *2008 IEEE 19th International Symposium on Personal, Indoor and Mobile Radio Communications*. IEEE, September 2008, pp. 1–5. [Online]. Available: http://dx.doi.org/10.1109/PIMRC.2008.4699615

[52] E. S. G. Qualcomm, "Air Interface Cell Capacity of WCDMA Systems," [Online] Available: http://www.qualcomm.com/common/documents/, Qualcomm, Tech. Rep., 2007.

[53] *Performance Modelling of a Wireless 4G Cell under GPS Scheme*, January 2005. [Online]. Available: http://dx.doi.org/10.1109/SAINTW.2005.1620031

[54] *Performance modeling of a wireless 4G cell under a GPS scheme with hand off*, April 2005. [Online]. Available: http://dx.doi.org/10.1109/NGI.2005.1431695

[55] G. Bolch, S. Greiner, H. de Meer, and S. Trivedi, *Queueing Networks and Markov Chains: Modeling and Performance Evaluation*, 2nd ed. Wiley, 2006.

[56] *Queueing network modeling of signaling system No.7*, December 1990. [Online]. Available: http://dx.doi.org/10.1109/GLOCOM.1990.116572

[57] D. Kouvatsos, "Performance modelling and cost-effective analysis of multiservice integrated networks," vol. 9, no. 3, pp. 127–135, August 2002. [Online]. Available: http://ieeexplore.ieee.org/xpls/abs_all.jsp?arnumber=599232

[58] D. D. Kouvatsos, I. Awan, and K. Al-Begain, "Performance modelling of GPRS with bursty multiclass traffic," vol. 150, no. 2, pp. 75–85, May 2003. [Online]. Available: http://dx.doi.org/10.1049/ip-cdt:20030278

[59] E. T. Jaynes, "Prior Probabilities," *Systems Science and Cybernetics, IEEE Transactions on*, vol. 4, no. 3, pp. 227–241, February 2007. [Online]. Available: http://dx.doi.org/10.1109/TSSC.1968.300117

[60] *Impact of mobility on traffic distribution in seamless interworking environments*, vol. 6, 2004. [Online]. Available: http://dx.doi.org/10.1109/VETECF.2004.1404910

[61] *Modelling Cellular/Wireless LAN Integrated Systems with Multi-Rate Traffic Using Queueing Network*, October 2008. [Online]. Available: http://dx.doi.org/10.1109/WiCom.2008.29

[62] A. K. Salkintzis, "Interworking techniques and architectures for WLAN/3G integration toward 4G mobile data networks," *Wireless Communications, IEEE*, vol. 11, no. 3, pp. 50–61, June 2004. [Online]. Available: http://dx.doi.org/10.1109/MWC.2004.1308950

[63] M. Reiser, "A Queueing Network Analysis of Computer Communication Networks with Window Flow Control," vol. 27, no. 8, pp. 1199–1209, January 2003. [Online]. Available: http://ieeexplore.ieee.org/xpls/abs_all.jsp?arnumber=1094531

[64] B. Urgaonkar, G. Pacifici, P. Shenoy, M. Spreitzer, and A. Tantawi, "Analytic modeling of multitier Internet applications," *ACM Trans. Web*, vol. 1, no. 1, pp. 2+, May 2007. [Online]. Available: http://dx.doi.org/10.1145/1232722.1232724

[65] Y. Chen, A. Das, W. Qin, A. Sivasubramaniam, Q. Wang, and N. Gautam, "Managing server energy and operational costs in hosting centers," in *SIGMETRICS '05: Proceedings of the 2005 ACM SIGMETRICS international conference on Measurement and modeling of computer systems*. New York, NY, USA: ACM, 2005, pp. 303–314. [Online]. Available: http://dx.doi.org/10.1145/1064212.1064253

[66] H.-J. Bartsch, *Tachenbuch Mathematischer Formeln*, C. Fritzsch, Ed. Leipzig: Carl Hanser Verlag, 2007, vol. 21.

[67] J. Wong, "Queueing Network Models f o r Computer Systems," Ph.D. dissertation, Berkley University, School of Engineering arid Applied Science, October 1975.

[68] E. Altman, K. Avrachenkov, and U. Ayesta, "A survey on discriminatory processor sharing," *Queueing Systems*, vol. 53, no. 1, pp. 53–63, June 2006. [Online]. Available: http://dx.doi.org/10.1007/s11134-006-7586-8

[69] A. K. Parekh and R. G. Gallager, "A generalized processor sharing approach to flow control in integrated services networks: the multiple node case," pp. 137–150, 1993.

[70] J. Sodenschein and G. Zlotkin, *Rules of Encounter: Designing Cenventions for Automated Negotiation among Computers*, J. Sodenschein and G. Zlotkin, Eds. Cambridge, Massachusetts: MIT Press, 1998.

[71] H. Lin, M. Chatterjee, S. K. Das, and K. Basu, "ARC: an integrated admission and rate control framework for CDMA data networks based on non-cooperative games," in *Proceedings of the 9th annual international conference on Mobile computing and networking*. ACM, 2003, pp. 326–338.

[72] D. Niyato and E. Hossain, "A Cooperative Game Framework for Bandwidth Allocation in 4G Heterogeneous Wireless Networks," in *Proc. IEEE International Conf on Communications ICC '06*, vol. 9, 2006, pp. 4357–4362. [Online]. Available: http://dx.doi.org/10.1109/ICC.2006.255766

[73] I. M. Suliman, C. Pomalaza-Rez, J. Lehtomki, and I. Oppermann, "Radio resource allocation in heterogeneous wireless networks using cooperative games," in *Proc. Nordic Radio Symposium 2004 / Finnish Wireless Communications Workshop*, 2004.

[74] S. K. Das, H. Lin, and M. Chatterjee, "An econometric model for resource management in competitive wireless data networks," *IEEE Network*, vol. 18, no. 6, pp. 20–26, 2004. [Online]. Available: http://dx.doi.org/10.1109/MNET.2004.1355031

[75] D. Niyato and E. Hossain, "Bandwidth Allocation in 4G Heterogeneous Wireless Access Networks: A Noncooperative Game Theoretical Approach," in *Proc. IEEE Global Telecom. Conf. GLOBECOM '06*, 2006, pp. 1–5. [Online]. Available: http://dx.doi.org/10.1109/GLOCOM.2006.637

[76] N. Halder and J. B. Song, "Game Theoretical Analysis of Radio Resource Management in Wireless Networks: A Non-Cooperative Game Approach of Power Control," *IJCSNS International Journal of Computer Science and Network Security*, vol. 7 (6), pp. 184–192, 2007.

[77] L. Badia, C. Taddia, G. Mazzini, and M. Zorzi, "Multiradio resource allocation strategies for heterogeneous wireless networks," in *Proc. Wireless Personal Multimedia Communications Conference (WPMC '05)*, 2005.

[78] M. Ahmed Khan, F. Sivrikaya, and S. Albayrak, "Network Level Cooperation for Resource Allocation in Future Wireless Networks," in *Proceedings of the IFIP Wireless Days Conference '08*, 2008.

[79] M. J. Osborne and A. Rubinstein, "Bargaining and Markets," UCLA Department of Economics, Levine's Bibliography, Feb 2005.

[80] E. Kalai, "Solutions to the Bargaining Problem," Northwestern University, Center for Mathematical Studies in Economics and Management Science, Discussion Papers 556, Mar 1983.

[81] E. Rasmusen, *Games and Information: An Introduction to Game Theory*, 4th ed. Wiley-Blackwell, December 2006.

[82] H. Vartiainen and Y. J. Foundation, "Bargaining without Disagreement," in *Discussion Papers*. University of Helsinki, Faculty of Social Sciences, Department of Economics, 2003.

[83] N. Dagan and O. Volij, "The Bankruptcy Problem: a Cooperative Bargaining Approach," Nir Dagan, Economic theory and game theory 001, 1993. [Online]. Available: http://ideas.repec.org/p/nid/ndagan/001.html

[84] A. Ferragut and F. Paganini, "A connection level model for IEEE 802.11 cells," in *LANC '09: Proceedings of the 5th International Latin American Networking Conference*. New York, NY, USA: ACM, 2009, pp. 32–40. [Online]. Available: http://dx.doi.org/10.1145/1636682.1636687

[85] N. K. Shankaranarayanan, Z. Jiang, and P. Mishra, "Performance of a shared packet wireless network with interactive data users," *Mobile networks and applications*, vol. 8, no. 3, pp. 279–293, 2003.

[86] G. Kuriakose, S. Harsha, A. Kumar, and V. Sharma, "Analytical models for capacity estimation of IEEE 802.11 WLANs using DCF for internet applications," *Wireless Networks*, vol. 15, no. 2, pp. 259–277, February 2009. [Online]. Available: http://dx.doi.org/10.1007/s11276-007-0051-8

[87] D. Miorandi, A. A. Kherani, and E. Altman, "A queueing model for HTTP traffic over IEEE 802.11 WLANs," *Computer networks*, vol. 50, no. 1, pp. 63–79, 2006.

[88] K. P. Murphy, "A survey of POMDP solution techniques," University of Toronto, Tech. Rep., 2003.

[89] Z. Hu and C. K. Tham, "CCMAC: coordinated cooperative MAC for wireless LANs," in *MSWiM '08: Proceedings of the 11th international symposium on Modeling, analysis and simulation of wireless and mobile systems*. New York, NY, USA: ACM, 2008, pp. 60–69. [Online]. Available: http://dx.doi.org/10.1145/1454503.1454518

[90] K. Liu and Q. Zhao, "Channel Probing for Opportunistic Access with Multichannel Sensing," in *Proceedings of IEEE Asilomar Conference on Signals, Systems, and Computers*, 2008.

[91] L. H. Yen, T. T. Yeh, and K. H. Chi, "Load Balancing in IEEE 802.11 Networks," *IEEE Internet Computing*, vol. 13, no. 1, pp. 56–64, 2009.

[92] S. J. Russell, P. Norvig, J. F. Canny, J. Malik, and D. D. Edwards, *Artificial intelligence: a modern approach*. Prentice hall Englewood Cliffs, NJ, 2003.

[93] R. A. Howard, *Dynamic programming and Markov processes*. The MIT Press, 1960.

[94] R. Bellman, "The theory of dynamic programming," *Proceedings of the National Academy of Sciences of the United States of America*, vol. 38, no. 8, pp. 716–719, 1952.

[95] D. Bertsekas, *Dynamic Programming and Optimal Control*, D. Bertsekas, Ed. Belmont, Massachusetts: Athena Scientific, 1995, vol. I.

[96] L. Kaelbling, M. Littman, and A. Cassandra, "Planning and acting in partially observable stochastic domains," *Artificial Intelligence*, vol. 101, no. 1-2, pp. 99–134, May 1998. [Online]. Available: http://dx.doi.org/10.1016/S0004-3702(98)00023-X

[97] M. L. Littman, "Memoryless policies: Theoretical limitations and practical results," in *From Animals to Animats 3: Proceedings of the Third International Conference on Simulation of Adaptive Behavior*, 1994, pp. 238–247.

[98] C. H. Papadimitriou and J. N. Tsitsiklis, "Intractable problems in control theory," in *Decision and Control, 1985 24th IEEE Conference on*, vol. 24, 1985.

[99] R. D. Smallwood and E. J. Sondik, "The optimal control of partially observable Markov processes over a finite horizon," *Operations Research*, pp. 1071–1088, 1973.

[100] E. J. Sondik, "The optimal control of partially observable Markov processes over the infinite horizon: Discounted costs," *Operations Research*, vol. 26, no. 2, pp. 282–304, 1978.

[101] K. J. Astrom, "Optimal control of Markov decision processes with incomplete state estimation," *Journal of Mathematical Analysis and Applications*, vol. 10, no. 1, pp. 174–205, 1965.

[102] A. R. Cassandra, "Exact and approximate algorithms for Partially Observable Markov Decision Processes," Ph.D. dissertation, Brown University, May 1998.

[103] A. Cassandra, M. L. Littman, N. L. Zhang, and Others, "Incremental pruning: A simple, fast, exact method for partially observable Markov decision processes," in *Proceedings of the 13th Conference on Uncertainty in Artificial Intelligence*. Citeseer, 1997, pp. 54–61.

[104] M. L. Littman, "The witness algorithm: Solving partially observable Markov decision processes," *Brown university department of computer science technical report cs-94-40*, 1994.

[105] H. Kurniawati, D. Hsu, and W. S. Lee, "SARSOP: Efficient point-based POMDP planning by approximating optimally reachable belief spaces," in *Proc. Robotics: Science and Systems*, 2008.

[106] E. A. Hansen, "Solving POMDPs by searching in policy space," in *In Proceedings of UAI*, 1998.

[107] ——, "An improved policy iteration algorithm for partially observable MDPs," *Advances in Neural Information Processing Systems*, pp. 1015–1021, 1998.

[108] S. Seuken and S. Zilberstein, "Formal models and algorithms for decentralized decision making under uncertainty," *Autonomous Agents and Multi-Agent Systems*, vol. 17, no. 2, pp. 190–250, 2008.

[109] D. S. Bernstein, R. Givan, N. Immerman, and S. Zilberstein, "The complexity of decentralized control of Markov decision processes," *Mathematics of operations research*, vol. 27, no. 4, pp. 819–840, 2002.

[110] D. V. Pynadath and M. Tambe, "Multiagent teamwork: Analyzing the optimality and complexity of key theories and models," in *Proceedings of the first international joint conference on Autonomous agents and multiagent systems: part 2*. ACM, 2002, pp. 873–880.

[111] E. A. Hansen, D. S. Bernstein, and S. Zilberstein, "Dynamic programming for partially observable stochastic games," in *Proceedings of the National Conference on Artificial Intelligence*. Menlo Park, CA; Cambridge, MA; London; AAAI Press; MIT Press; 1999, 2004, pp. 709–715.

[112] D. Szer, F. Charpillet, and S. Zilberstein, "MAA*: A heuristic search algorithm for solving decentralized POMDPs," in *Proceedings of the twenty-first conference on uncertainty in artificial intelligence*. Citeseer, 2005, pp. 576–590.

[113] S. Seuken and S. Zilberstein, "Improved memory-bounded dynamic programming for decentralized POMDPs," in *Proceedings of the twenty-third conference on uncertainty in artificial intelligence*, 2007.

[114] ——, "Memory-bounded dynamic programming for DEC-POMDPs," in *International Joint Conference on Artificial Intelligence*, 2007, pp. 2009–2016.

[115] R. Cogill, M. Rotkowitz, B. Van Roy, and S. Lall, "An approximate dynamic programming approach to decentralized control of stochastic systems," *Control of Uncertain Systems: Modelling, Approximation, and Design*, pp. 243–256, 2006.

[116] P. J. Gmytrasiewicz and P. Doshi, "A framework for sequential planning in multiagent settings," *Journal of Artificial Intelligence Research*, vol. 24, no. 1, pp. 49–79, 2005.

[117] A. Kumar and S. Zilberstein, "Dynamic Programming Approximations for Partially Observable Stochastic Games," 2009.

[118] C. Papadimitriou, *Computational Complexity*, C. Papadimitriou, Ed. Reading, Mass.: Addison Wesley, 1993.

[119] A. Cobham, "he intrinsic computational difficulty of functions," *Proc. Logic, Methodology, and Philosophy of Science II*, 1965.

[120] C. H. Papadimitriou and J. N. Tsitsiklis, "The complexity of Markov decision processes," *Mathematics of operations research*, vol. 12, no. 3, pp. 441–450, 1987.

[121] O. Madani, S. Hanks, and A. Condon, "On the undecidability of probabilistic planning and infinite-horizon partially observable Markov decision problems," in *Proceedings of the National Conference on Artificial Intelligence*. JOHN WILEY & SONS LTD, 1999, pp. 541–548.

[122] M. Mundhenk, J. Goldsmith, C. Lusena, and E. Allender, "Complexity of finite-horizon Markov decision process problems," *Journal of the ACM (JACM)*, vol. 47, no. 4, pp. 681–720, 2000.

[123] A. Condon, J. Feigenbaum, C. Lund, and P. Shor, "Probabilistically checkable debate systems and nonapproximability of PSPACE-hard functions," *Chicago Journal of Theoretical Computer Science*, vol. 19, 1995.

[124] D. S. Bernstein, R. Givan, N. Immerman, and S. Zilberstein, "The complexity of decentralized control of markov decision processes," pp. 32–37, June 2000.

[125] Z. Rabinovich, C. V. Goldman, and J. S. Rosenschein, "The complexity of multiagent systems: The price of silence," in *Proceedings of the second international joint conference on Autonomous agents and multiagent systems*. ACM, 2003, pp. 1102–1103.

[126] D. V. Pynadath and M. Tambe, "Multiagent teamwork: Analyzing the optimality and complexity of key theories and models," in *Proceedings of the first international joint conference on Autonomous agents and multiagent systems: part 2*. ACM, 2002, pp. 873–880.

[127] P. Poupart and C. Boutilier, "Bounded finite state controllers," *Advances in neural information processing systems*, vol. 16, 2004.

[128] D. S. Bernstein, E. A. Hansen, and S. Zilberstein, "Bounded policy iteration for decentralized POMDPs," in *INTERNATIONAL JOINT CONFERENCE ON ARTIFICIAL INTELLIGENCE*, vol. 19. Citeseer, 2005, p. 1287.

[129] C. G. Cassandras, *Discrete Event Systems: Modeling and Performance Analysis*, R. D. Irwin, Ed. Aksen Associates Incorporated Publishers, 1993.

[130] A. A. Lazar and T. G. Robertazzi, "The geometry of lattices for Markovian queueing networks," *Performance Evaluation*, vol. 6, no. 1, pp. 85–86, 1986.

[131] M. Afanasyev, T. Chen, G. M. Voelker, and A. C. Snoeren, "Analysis of a mixed-use urban wifi network: when metropolitan becomes neapolitan," in *IMC '08: Proceedings of the 8th ACM SIGCOMM conference on Internet measurement*. New York, NY, USA: ACM, 2008, pp. 85–98. [Online]. Available: http://dx.doi.org/10.1145/1452520.1452531

[132] T. Melia, A. de la Oliva, A. Vidal, I. Soto, D. Corujo, and R. Aguiar, "Toward IP converged heterogeneous mobility: A network controlled approach," *Computer Networks*, vol. 51, no. 17, 2007. [Online]. Available: http://www.sciencedirect.com/science/article/B6VRG-4PD4XJY-1/2/9d7aba6a2eb68e366c2f9f3dfffa5b3e

[133] A. King. (2010) The Average Web Page. [Online]. Available: http://www.optimizationweek.com/reviews/average-web-page/

[134] S. Xu, B. Xu, and D. Peng, "The Waiting Time Distribution of a Pareto Service Self-Similar Queuing Model for Wireless Network Nodes," sept 2006. [Online]. Available: http://dx.doi.org/10.1109/WiCOM.2006.379

[135] Webmetrics. WM100 - The Web Performance Standard.

[136] A. R. Cassandra. (2010) POMDP solver software. [Online]. Available: http://www.pomdp.org/pomdp/code/index.shtml

[137] E. J. Sondik, "The Optimal Control of Partially Observable Markov Processes Over the Infinite Horizon: Discounted Costs," *Operations Research*, vol. 26, no. 2, pp. 282–304, 1978. [Online]. Available: http://dx.doi.org/10.2307/169635

[138] Cheng, "Algorithms for Partially Observable Markov Decision Processes," Ph.D. dissertation, University of British Columbia, 1988.

[139] S. Avallone, D. Emma, A. Pescap, and G. Ventre, "A distributed multiplatform architecture for traffic generation," in *International Symposium on Performance Evaluation of Computer and Telecommunication Systems, San Jose, CA, USA*. Citeseer, 2004.

[140] Iperf project website. [Online] Available: http://sourceforge.net/projects/iperf/.

[141] GNU Octave Reference Manual. [Online] Available: http://www.gnu.org/software/octave/doc/interpreter/.

[142] M. Wellens and P. M"ah"onen, "Lessons learned from an extensive spectrum occupancy measurement campaign and a stochastic duty cycle model," *Mobile Networks and Applications*, vol. 15, no. 3, pp. 461–474, 2010.

[143] M. Wellens, J. Riihij"arvi, and P. M"ah"onen, "Empirical time and frequency domain models of spectrum use," *Physical Communication*, vol. 2, no. 1-2, pp. 10–32, 2009.

[144] O. Holland, P. Cordier, M. Muck, L. Mazet, C. Klock, and T. Renk, "Spectrum Power Measurements in 2G and 3G Cellular Phone Bands During the 2006 Football World Cup in Germany," in *2007 2nd IEEE International Symposium on New Frontiers in Dynamic Spectrum Access Networks*. IEEE, April 2007, pp. 575–578. [Online]. Available: http://dx.doi.org/10.1109/DYSPAN.2007.81

[145] T. Kamakaris, M. M. Buddhikot, and R. Iyer, "A case for coordinated dynamic spectrum access in cellular networks," in *New Frontiers in Dynamic Spectrum Access Networks, 2005. DySPAN 2005. 2005 First IEEE International Symposium on*, 2005, pp. 289–298.

[146] D. Willkomm, S. Machiraju, J. Bolot, and A. Wolisz, "Primary user behavior in cellular networks and implications for dynamic spectrum access," *IEEE Communications Magazine*, vol. 47, no. 3, pp. 88–95, 2009.

[147] G. Hampel, M. J. Flanagan, L. M. Drabeck, J. Srinivasan, P. A. Polakos, and G. Rittenhouse, "Capacity Estimation for Growth Planning of Cellular Networks in the Presence of Temporal and Spatial Traffic Fluctuations," in *2005 IEEE 61st Vehicular Technology Conference*. IEEE, 2005, pp. 2116–2122. [Online]. Available: http://dx.doi.org/10.1109/VETECS.2005.1543708

[148] C. Williamson, E. Halepovic, H. Sun, and Y. Wu, "Characterization of CDMA2000 Cellular Data Network Traffic," in *The IEEE Conference on Local Computer Networks 30th Anniversary (LCN'05)l*. IEEE, 2005, pp. 712–719. [Online]. Available: http://dx.doi.org/10.1109/LCN.2005.37

[149] J. Guo, F. Liu, and Z. Zhu, "Estimate the call duration distribution parameters in GSM system based on kl divergence method," in *International Conference on Wireless Communications, Networking and Mobile Computing, 2007. WiCom 2007*, 2007, pp. 2988–2991.

[150] D. Tang and M. Baker, "Analysis of a metropolitan-area wireless network," *Wirel. Netw.*, vol. 8, no. 2/3, pp. 107–120, 2002. [Online]. Available: http://dx.doi.org/10.1023/A:1013739407600

[151] M. Hollick, T. Krop, J. Schmitt, H. Huth, and R. Steinmetz, "A hybrid workload model for wireless metropolitan area networks," in *2003 IEEE 58th Vehicular Technology Conference. VTC 2003-Fall (IEEE Cat. No.03CH37484)*. IEEE, 2003, pp. 1989–1993. [Online]. Available: http://dx.doi.org/10.1109/VETECF.2003.1285373

[152] M. Hollick, T. Krop, and J. Schmitt, "Modeling mobility for cellular networks based on statistical data collection," 2003.

[153] M. Afanasyev, T. Chen, G. M. Voelker, and A. C. Snoeren, "Usage Patterns in an Urban WiFi Network," *IEEE/ACM Transactions on Networking*, 2010. [Online]. Available: http://dx.doi.org/10.1109/TNET.2010.2040087

[154] V. Brik, S. Rayanchu, S. Saha, S. Sen, V. Shrivastava, and S. Banerjee, "A measurement study of a commercial-grade urban wifi mesh," in *IMC '08: Proceedings of the 8th ACM SIGCOMM conference on Internet measurement*. New York, NY, USA: ACM, 2008, pp. 111–124. [Online]. Available: http://dx.doi.org/10.1145/1452520.1452534

[155] D. P. Blinn, T. Henderson, and D. Kotz, "Analysis of a Wi-Fi hotspot network," in *WiTMeMo '05: Papers presented at the 2005 workshop on Wireless traffic measurements and modeling*. Berkeley, CA, USA: USENIX Association, 2005, pp. 1–6. [Online]. Available: http://portal.acm.org/citation.cfm?id=1072430.1072431

[156] D. Kotz and K. Essien, "Analysis of a campus-wide wireless network," *Wirel. Netw.*, vol. 11, no. 1-2, pp. 115–133, January 2005. [Online]. Available: http://dx.doi.org/10.1007/s11276-004-4750-0

[157] A. Sevtsuk, S. Huang, F. Calabrese, and C. Ratti, *Mapping the MIT campus in real time using WiFi*. Hershey, PA: IGI Global, 2009.

[158] M. Balazinska and P. Castro, "Characterizing mobility and network usage in a corporate wireless local-area network," in *MobiSys '03: Proceedings of the 1st international conference on Mobile systems, applications and services*. New York, NY, USA: ACM, 2003, pp. 303–316. [Online]. Available: http://dx.doi.org/10.1145/1066116.1066127

[159] A. P. Jardosh, K. N. Ramachandran, K. C. Almeroth, and E. M. Belding Royer, "Understanding congestion in IEEE 802.11b wireless networks," in *IMC '05: Proceedings of the 5th ACM SIGCOMM conference on Internet Measurement*. Berkeley, CA, USA: USENIX Association, 2005, p. 25. [Online]. Available: http://portal.acm.org/citation.cfm?id=1251086.1251111

[160] F. H. Campos, M. Karaliopoulos, M. Papadopouli, and H. Shen, "Spatio-temporal modeling of traffic workload in a campus WLAN," in *WICON '06: Proceedings of the 2nd annual international workshop on Wireless internet*. New York, NY, USA: ACM, 2006, pp. 1+. [Online]. Available: http://dx.doi.org/10.1145/1234161.1234162

[161] F. Hernandez-Campos and M. Papadopouli, "A comparative measurement study of the workload of wireless access points in campus networks," in *16th Annual IEEE International Symposium on Personal Indoor and Mobile Radio Communications*. Citeseer, 2005.

[162] G. Salami and R. Tafazolli, "On the performance evaluation of spectrum sharing algorithms between two UMTS operators," in *2009 International Conference on Telecommunications*. IEEE, May 2009, pp. 260–265. [Online]. Available: http://dx.doi.org/10.1109/ICTEL.2009.5158655

[163] "OPNET Modeller 15.0," http://www.opnet.com/solutions/, 2010.

[164] N. E. Sayed, "A mathematical framework for the analysis and design of dynamic inter-operator resource sharing mechanisms," Master's thesis, Technische Universität Berlin, 2010.

[165] P. Gill, M. Arlitt, Z. Li, and A. Mahanti, "Characterizing User Sessions on YouTube," *In IEEE Multimedia Computing and Networking (MMCN)*, 2008.

[166] S. F. Yashkov, "THE M/D/1 PROCESSOER SHARING QUEUE REVISITED," *INFORMATION PROCESSES*, vol. 9, no. 3, pp. 216–223, 2009.

[167] M. Shalmon, "Explicit formulas for the variance of conditioned sojourn times in M/D/1-PS," *Operations Research Letters*, vol. 35, no. 4, pp. 463–466, 2007.

List of Figures

List of Tables

Appendices

A. Derivation of Optimal Sharing Parameter

Operator A is the donor operator, and Operator B is the borrowing one. Furthermore we assume that $P_{T,A} = 0$, i.e. the donor does not transfer traffic, Operator B (the borrowing one) knows the advertised initial delay of the donor operator A termed $D_{A,init}$, and The average service demand x is fixed.

We now define the problem, that is to find a suitable $P_{T,B}$, which satisfies the following inequalities:

$$D_A(P_{T,B}) \leq D_{A,max}$$

$$D_B(P_{T,B}) \leq D_{B,max}$$

where D_A and D_B represent the average delays experienced by the users that choose operator A or operator B respectively.

The borrowing operator B he would have to take into account that $P_{T,B}$ of his users will experience the delay at the donor operator A $D_{PS,A}$ and $1 - P_{T,B}$ of his users is going to experience the delay of his own $D_{PS,B}$. Thus we can write

$$D_B = P_{T,B} \cdot D_{PS,A} + (1 - P_{T,B}) \cdot D_{PS,B} \leq D_{max,B}$$

Theoretically, for operator B to be able calculate $D_{PS,A}$, it needs to know $P_{r,A}$, which is not directly available. However, since operator B can query $D_{A,init}$, it can also calculate $D_{PS,A}$ without $P_{r,A}$ by:

$$D_{PS,A}(P_{T,B}) = \frac{\frac{x}{C_A}}{1 - \rho_{PS,A}}$$

$$D_{PS,A}(P_{T,B}) = \frac{\frac{x}{C_A}}{1 - \rho_{A,init} - \frac{\lambda}{\mu C_A} \cdot P_B \cdot P_{T,B}}$$

$$D_{PS,A}(P_{T,B}) = \frac{\frac{x}{C_A}}{\frac{x}{C_A \cdot D_{A,init}} - \frac{\lambda}{\mu C_A} \cdot P_B \cdot P_{T,B}}$$

and since we assumed that $P_{T,A} = 0$ we obtain:

$$\rho_{PS,B} = (P_B \cdot (1 - P_{T,B} - P_{r,B})) \cdot \frac{\lambda}{\mu C_B}$$

Hence we can write:

$$D_{PS,B}(P_{T,B}) = \frac{\frac{x}{C_B}}{1 - \rho_{PS,B}}$$

$$D_{PS,B}(P_{T,B}) = \frac{\frac{x}{C_B}}{1 - (P_B \cdot (1 - P_{T,B} - P_{r,B})) \cdot \frac{\lambda}{\mu C_B}}$$

These can be further simplified to:

$$D_{PS,A}(P_{T,B}) = \frac{x}{\frac{x}{D_{A,init}} - \frac{\lambda P_B}{\mu} \cdot P_{T,B}}$$

$$D_{PS,A}(P_{T,B}) = \frac{1}{\frac{1}{D_{A,init}} - \frac{\lambda P_B}{\mu x} \cdot P_{T,B}}$$

Finally by substituting $\frac{1}{D_{A,init}}$ we obtain:

$$D_{PS,B}(P_{T,B}) = \frac{1}{\frac{C_B}{x} - \frac{\lambda P_B}{\mu x} + P_{r,B}\frac{\lambda P_B}{\mu x} + \frac{\lambda P_B}{\mu x} \cdot P_{T,B}}$$

Let's set $k = \frac{\lambda P_B}{\mu x}$:

$$D_{PS,A}(P_{T,B}) = \frac{1}{\frac{1}{D_{A,init}} - k \cdot P_{T,B}}$$

$$D_{PS,B}(P_{T,B}) = \frac{1}{\frac{C_B}{x} - k + kP_{r,B} + k \cdot P_{T,B}}$$

Furthermore we set $m = \frac{1}{D_{A,init}}$ and $n = \frac{C_B}{x} - k + kP_{r,B}$ and obtain:

$$D_{PS,A}(P_{T,B}) = \frac{1}{m - k \cdot P_{T,B}}$$

$$D_{PS,B}(P_{T,B}) = \frac{1}{n + k \cdot P_{T,B}}$$

We can now write as:

$$D_B(P_{T,B}) = \frac{P_{T,B}}{m - k \cdot P_{T,B}} + \frac{1 - P_{T,B}}{n + k \cdot P_{T,B}}$$

We substitute $P_{T,B}$ with y and get:

$$\boxed{D_B(y) = \frac{y}{m - k \cdot y} + \frac{1 - y}{n + k \cdot y}}$$

$$D_B(y) = \frac{ny + ky^2 + (m - ky)(1 - y)}{(m - ky)(n + ky)}$$

$$D_B(y) = \frac{ny + 2ky^2 + m - ky - my}{(m - ky)(n + ky)}$$

$$D_B(y) = \frac{2ky^2 + (n-k-m)y + m}{(m-ky)(n+ky)}$$

$$\Rightarrow \boxed{D_B(y) = \frac{2ky^2 + (n-k-m)y + m}{-k^2y^2 + k(m-n)y + mn}}$$

Meaning of the Parameters

Let's try to make a sense of the parameters n, m, k:

For k we have:

$$k = \frac{\lambda P_B}{\mu x}$$

$$k = \frac{C_B}{x(1-P_{r,B})} \cdot \frac{\lambda P_B(1-P_{r,B})}{\mu C_B}$$

$$\boxed{k = \frac{C_B}{x(1-P_{r,B})} \cdot \rho_{r,init}}$$

For m we have:

$$\boxed{m = \frac{1}{D_{A,init}}}$$

which is the inverse of the initial delay of the donor operator. And finally for n:

$$n = \frac{C_B}{x} - k + kP_{r,B}$$

$$n = \frac{C_B}{x} - \frac{\lambda P_B}{\mu x} + \frac{\lambda P_B P_{r,B}}{\mu x}$$

$$n = \frac{C_B}{x}(1 - \frac{\lambda P_B}{\mu C_B}(1-P_{r,B}))$$

$$n = \frac{C_B}{x}(1-\rho_{B,init})$$

$$\boxed{n = \frac{1}{D_{B,init}}}$$

To summarize we have $n = \frac{1}{D_{B,init}}, m = \frac{1}{D_{A,init}}, k = \frac{C_B \rho_{B,init}}{x(1-P_{r,B})}$.

Now let's consider the term $\frac{k}{n}$:

$$\frac{k}{n} = \frac{\frac{C_B \cdot \rho_{B,init}}{x(1-P_{r,B})}}{\frac{1}{D_{r,init}}}$$

$$\frac{k}{n} = \frac{D_{B,init} \cdot C_B}{x} \cdot \frac{\rho_{B,init}}{1-P_{r,B}}$$

$$\frac{k}{n} = \frac{1}{1-\rho_{B,init}} \cdot \frac{\rho_{B,init}}{1-P_{r,B}}$$

Let $b = \frac{k}{n} = \frac{1}{1-\rho_{B,init}} \cdot \frac{\rho_{B,init}}{1-P_{r,B}}$ Thus we have $k = b \cdot n$.

Domain and Constraints

From the precious section we recall that:

$$D_B(y) = \frac{y}{m - k \cdot y} + \frac{1-y}{n + k \cdot y}$$

and:

$$m = \frac{1}{D_{A,init}}, n = \frac{1}{D_{B,init}}, k = n \cdot b$$

$$b = \frac{k}{n} = \frac{1}{1-\rho_{B,init}} \cdot \frac{\rho_{B,init}}{1-P_{b,B}}$$

Range

First the two following conditions must hold. We derive these in the next subsection.

$$\rho_{A,PS} < 1 \Rightarrow y < \frac{m}{k}$$

$$\rho_{B,PS} < 1 \Rightarrow y > \frac{-n}{k}$$

Thus:

$$y \in]\frac{-n}{k}, \frac{m}{k}[$$

Since y represents a probability we have $y \in [0, 1]$. This leads to the domain of y:

$$y \in [0, 1] \cap]\frac{-n}{k}, \frac{m}{k}[$$

Using the fact that $n = \frac{1}{D_{B,init}} > 0$ we get:

$$y \in [0, 1], \frac{m}{k} > 1$$
$$y \in [0, \frac{m}{k}[, \frac{m}{k} \leq 1$$

Derivations of Range Conditions

For the first condition:

$$\rho_{A,PS} < 1$$

$$0 < 1 - \rho_{A,PS}$$

$$\rho_{A,PS} = (P_A(1 - P_{b,A}) + P_B \cdot P_{T,R}) \frac{\lambda}{\mu \cdot C_A}$$

$$\rho_{A,PS} = \rho_{A,init} + \frac{P_B P_{T,R} \lambda}{\mu C_A}$$

$$0 < 1 - \rho_{A,init} - \frac{P_B P_{T,R} \lambda}{\mu C_A}$$

$$0 < \frac{x/C_A}{D_{A,init}} - \frac{P_B P_{T,R} \lambda}{\mu C_A}$$

$$0 < \frac{1}{D_{A,init}} - \frac{P_B P_{T,R} \lambda}{\mu x}$$

$$0 < m - k P_{T,R}$$

Since $P_{T,R} = y$ we get

$$\boxed{y < \frac{m}{k}}$$

For the second condition:

$$\rho_{B,PS} < 1$$

$$0 < 1 - \rho_{B,PS}$$

$$0 < 1 - (P_B(1 - P_{b,B} - P_{T,R})) \frac{\lambda}{\mu C_B}$$

$$0 < (1 - \rho_{B,init}) + P_B P_{T,R} \frac{\lambda}{\mu C_B}$$

$$0 < \frac{C_B \, (1 - \rho_{B,init})}{x} + P_B P_{T,R} \frac{\lambda}{\mu x}$$

$$0 < \frac{1}{D_{B,init}} + y \frac{\lambda P_B}{\mu x}$$

$$0 < n + ky$$

Thus we get:

$$\boxed{y > \frac{-n}{k}}$$

Derivatives

From:

$$\boxed{D_B(y) = \frac{y}{m - k \cdot y} + \frac{1 - y}{n + k \cdot y}}$$

we get:

$$\boxed{D_B^{'}(y) = \frac{m}{(m-ky)^2} - \frac{n+k}{(n+ky)^2}}$$

and

$$\boxed{D_B^{''}(y) = \frac{2m}{(ky-m)^3} + \frac{2(n+k)}{(n+ky)^3}}$$

Extrema

Now we set $D_B^{'}(y)$ to 0 and we get:

$$\boxed{y_1 = \frac{m}{k} \cdot \frac{\sqrt{\frac{n+k}{m}} - \frac{n}{m}}{\sqrt{\frac{n+k}{m}} + 1}}$$

$$\boxed{y_2 = \frac{m}{k} \cdot \frac{\sqrt{\frac{n+k}{m}} + \frac{n}{m}}{\sqrt{\frac{n+k}{m}} - 1}}$$

Simplifications

For the recipient operator to be able to calculate the transfer probability $P_{T,R}$, it acquires the value $D_{A,init}$ from the QoE database.

Knowing its initial delay $D_{B,init}$ it will calculate the ratio $\frac{D_{A,init}}{D_{B,init}}$. which intuitively should be less than 1. We note that this ratio equals $\frac{n}{m}$, which again appears frequently in our derivations. For this reason we will use the following simplification :

$$\boxed{r^2 = \frac{n}{m}}$$

Finally with r^2 and $k = n \cdot b$ we have:

$$y_1 = \frac{m}{k} \cdot \frac{\sqrt{\frac{n+k}{m}} - \frac{n}{m}}{\sqrt{\frac{n+k}{m}} + 1} = \frac{m}{k} \cdot \frac{r\sqrt{1+b} - r^2}{r\sqrt{1+b} + 1}$$

$$y_2 = \frac{m}{k} \cdot \frac{\sqrt{\frac{n+k}{m}} + \frac{n}{m}}{\sqrt{\frac{n+k}{m}} - 1} = \frac{m}{k} \cdot \frac{r\sqrt{1+b} + r^2}{r\sqrt{1+b} - 1}$$

$$D_B^{''}(y) = \frac{2m}{(ky-m)^3} + \frac{2(n+k)}{(n+ky)^3} = \frac{2}{m^2}\left[\frac{1}{\left(\frac{k}{m}y - 1\right)^3} + \frac{r^2(1+b)}{\left(r^2 + \frac{k}{m}y\right)^3}\right]$$

Discussion

In this section we show that y_1 is the only candidate for the minimum. We achieve this by showing that y_2 lies outside the domain of the function. Recall that we defined the domain:

$$y \in [0,1], \tfrac{m}{k} > 1$$
$$y \in [0, \tfrac{m}{k}[, \tfrac{m}{k} \leq 1$$

and we have:

$$y_1 = \frac{m}{k} \cdot \frac{r\sqrt{1+b} - r^2}{r\sqrt{1+b}+1}$$
$$y_2 = \frac{m}{k} \cdot \frac{r\sqrt{1+b} + r^2}{r\sqrt{1+b}-1}$$

It is obvious that y_2 lies outside the domain of the function for all values of r^2 as

$$r^2 < \frac{1}{1+b} \Rightarrow y_2 < 0$$
$$r^2 \geq \frac{1}{1+b} \Rightarrow y_2 > \frac{m}{k}$$

As for y_1 and since we assume that $r^2 < 1$, we have:

$$r > r^2 \wedge \sqrt{1+b} > 1 \Rightarrow r\sqrt{1+b} > r^2 \Rightarrow y_1 > 0$$
$$\frac{r\sqrt{1+b}}{r\sqrt{1+b}+1} < 1 \wedge \frac{-r^2}{r\sqrt{1+b}+1} < 0 \Rightarrow \frac{r\sqrt{1+b}-r^2}{r\sqrt{1+b}+1} < 1 \Rightarrow y_1 < \frac{m}{k}$$

Now we know that $y_1 < \frac{m}{k}$, but since it is possible that $\frac{m}{k} \geq 1$ we need to know for what values of r^2 we have that $y_1 > 1$. In order to find out we note that $\frac{m}{k} = \frac{1}{r^2 b}$ Thus we need to solve this inequality:

$$y_1 < 1 \Rightarrow \frac{1}{br^2} \cdot \frac{r\sqrt{1+b} - r^2}{r\sqrt{1+b}+1} < 1$$
$$\Rightarrow \sqrt{1+b} - r < br^2\sqrt{1+b} + br$$
$$\Rightarrow 0 < b\sqrt{1+b}r^2 + (1+b)r - \sqrt{1+b}$$
$$\Rightarrow 0 < br^2 + \sqrt{1+b}r - 1$$
$$\Rightarrow r > \frac{-\sqrt{1+b} + \sqrt{1+b+4b}}{2b} \Rightarrow r > \frac{-\sqrt{1+b} + \sqrt{1+5b}}{2b}$$
$$\Rightarrow r^2 > \frac{(1+b) + (1+5b) - 2\sqrt{1+b}\sqrt{1+5b}}{4b^2}$$
$$\Rightarrow \boxed{r^2 > \frac{1+3b-\sqrt{5b^2+6b+1}}{2b^2}}$$

Minimum

Recall:

$$y_1 = \frac{m}{k} \cdot \frac{r\sqrt{1+b} - r^2}{r\sqrt{1+b}+1}$$

In order to prove that y_1 is the actually a minimum we need to make sure that $D_B^{''}(y_1) > 0$

$$D_B^{''}(y_1) = \frac{2}{m^2}\left[\frac{1}{\left(\frac{k}{m}y_1 - 1\right)^3} + \frac{r^2(1+b)}{\left(r^2 + \frac{k}{m}y_1\right)^3}\right] > 0$$

$$\Rightarrow \left[\frac{1}{\left(\frac{r\sqrt{1+b}-r^2}{r\sqrt{1+b}+1} - 1\right)^3} + \frac{r^2(1+b)}{\left(r^2 + \frac{r\sqrt{1+b}-r^2}{r\sqrt{1+b}+1}\right)^3}\right] > 0$$

$$\Rightarrow \left[\frac{1}{\left(\frac{-(r^2+1)}{r\sqrt{1+b}+1}\right)^3} + \frac{r^2(1+b)}{\left(\frac{r\sqrt{1+b}(r^2+1)}{r\sqrt{1+b}+1}\right)^3}\right] > 0$$

$$\Rightarrow \left(\frac{r\sqrt{1+b}+1}{r^2+1}\right)^3 \cdot \left(\frac{1}{r\sqrt{1+b}} - 1\right) > 0$$

$$\Rightarrow \boxed{r^2 < \frac{1}{1+b}}$$

Summary

Thus we have shown that the minimum occurs at minimum at y_1:

$$y_1 = \frac{m}{k} \cdot \frac{\sqrt{\frac{n+k}{m}} - \frac{n}{m}}{\sqrt{\frac{n+k}{m}} + 1}$$

under the assumption that:

$$\frac{1 + 3b - \sqrt{5b^2 + 6b + 1}}{2b^2} < r^2 < \frac{1}{1+b}$$

B. OPNET Simulation

B.1. Simulation Scenario

In Section 5.6 we provided a mathematical model for multi-class sharing between multiple operators with possibly different technologies. In this section, we verify this model and its associated derivations, by a Discrete Event Simulation, using OPNET [163]. For this we consider two co-located wireless networks, with different technologies. OP-A is an 802.11g based WLAN-AP with capacity is $C_A = 31.9$ Mbps. Called Op-B, is another WLAN-AP using 802.11b, which we also model as a Processor Sharing Queuing Station, with a capacity $C_B = 5.5$ Mbps. In the simulation scenario, Op-A is under utilized and Op-B is congested. We consider a single role resource sharing, in which OP-A is the donor and the OP-B is the borrower. Two classes of services are considered. Class-1 stands for HTTP-session requests, and Class-2 stands for YouTube Session requests. These requests, handled, in a user centric environment, where user can decide which operator to choose for what type of traffic. The details of the OPNET model can be found in [164].

The Tchebychev boundaries are calculated using the following parameters:

- $D_{max,1} = 4$ seconds for HTTP sessions
- $D_{max,2} = 1120$ seconds, for YouTube sessions
- $g = 1\% = 10^{-2}$ as Grade of Service

The rationale behind choosing the Youtube delay limit is the following. According to most recent measurement studies [165] and [165] the average Youtube session is 1120 seconds. We assume a relatively constant throughput is available to the user, and that the video will be interrupted if the download time is above the session duration. Same authors measured the average session size to be 27 MBps, which means that our delay guarantee is equivalent to an minimum average throughput guarantee of $27 \times 8 \times 10^6/1120 = 192.8$Kbps.

The initial states of the operators are depicted in Figure B.1 and Table B.1. Using those values, we can calculate the debt of Op-B and the surplus of Op-A in terms of utilization. The results are retained in Table B.2.

We run the simulation with these parameters for a ten hours period. We measure the actual response time for each session request. In this way we are able to determine if the grade of service is met or not for each traffic type.

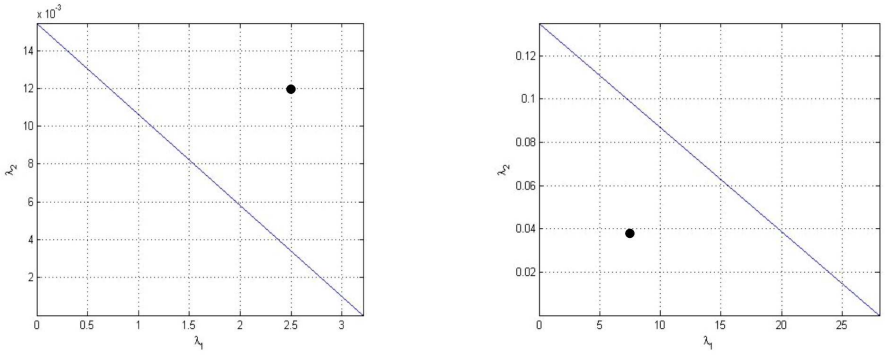

(a) Overloaded 802.11b based WLAN AP (b) Underloaded 802.11g based WLAN AP

Figure B.1.: State Spaces and boundary lines.

Operator	C	λ_1	λ_2	ρ_{max}
Op-B	5.5 Mbps	2.5	$12 \cdot 10^{-3}$	0.607
Op-A	31.9 Mbps	7.5	$38 \cdot 10^{-3}$	0.915

Table B.1.: Initial state of the operators.

Operator	$\rho_{init,i,1}$	$\rho_{init,i,2}$	surplus / debt
Op-B	$4727 \cdot 10^{-4}$	$4712 \cdot 10^{-4}$	$\alpha_B = 3369 \cdot 10^{-4}$
Op-A	$2445 \cdot 10^{-4}$	$2573 \cdot 10^{-4}$	$\alpha_A = 4132 \cdot 10^{-4}$

Table B.2.: Initial utilizations, debt/surplus

B.2. Simulation Results for the Initial State

The simulation results, for the initial case where we have the overloaded Op-B, and the under-loaded Op-A are depicted in the Figure B.2. It shows the response time probability distribution over the response times, for each class and each Operator.

The results show that Op-B is clearly overloaded with, Response times for Class-1 traffic up to 15 seconds. The dashed red line show our chosen Grade of Service boundary for each class. For class-1 (HTTP) 31.21% of the sessions response times is above the acceptable threshold of 4 seconds. As for Class-2 traffic (YouTube), we get response times up to 2311 seconds. 26.42% of the Class-2 sessions response times is above the acceptable threshold 1120 seconds. On the other side, Op-A is under-loaded with fast response times below 0.45 seconds for Class-1, and below 50 seconds for Class-2 sessions.

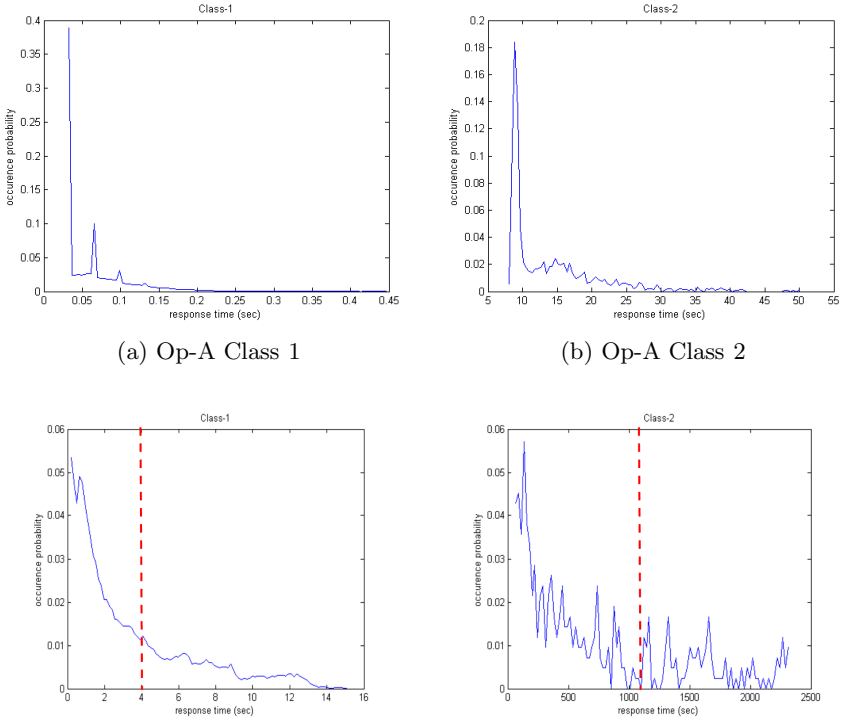

(a) Op-A Class 1

(b) Op-A Class 2

(c) Op-B Class 1

(d) Op-B Class 2

Figure B.2.: Initial Simulation results

B.3. Sharing

In order to overcome the excess of load, Op-B has, he chooses to use a sharing mechanism with Op-A, which would improve the his Quality of Service on one side, and elevate the Op-A's utilization on the other side. Since the condition $C_A\alpha_A \geq C_B\alpha_B$ holds, we know, that the two operators are able to enter a sharing agreement, so that they both profit.

Two operators have many options for selecting the suited sharing parameters, dependent on the sharing case they decide to follow. A summary of all possible sharing cases is depicted in Table 5.2. We choose to single role sharing case as discussed in section 5.6.4, where we derive the constraints on the sharing parameters. The main goal of these simulations is to verify the theoretical results, derived in the sections 5.6.4 and 5.6.5. For this reason we choose the following four cases of sharing parameters as depicted in the Figure B.3.

Figures B.3a and B.3b represent cases where the Op-B shares only Class-1 or Class-2 traffic respectively. We show that, In terms of performance, there is no big difference what type of traffic to share. The decision here is strategic, and depends on the Service Layer Agreements (SLA) between the two operators. We compare the number of transfered sessions which corresponds to borrowed resources for each case, and compare these

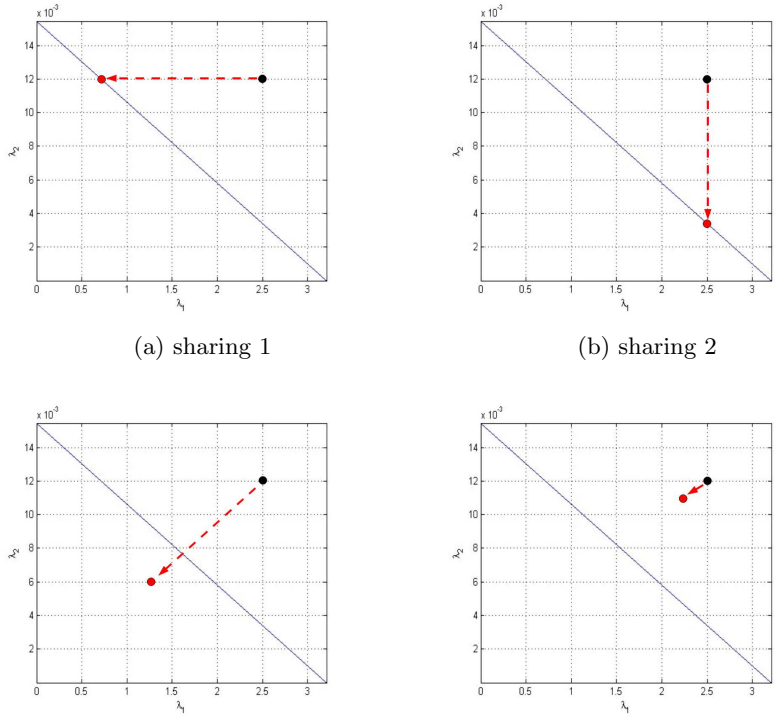

(a) sharing 1

(b) sharing 2

(c) sharing 3

(d) sharing 4

Figure B.3.: Different sharing simulations

Case	$P_{T,B,1}$	$P_{T,B,1}$
1	0.713	0
2	0	0.715
3	0.5	0.5
4	0.1	0.1

Table B.3.: Different sharing parameters

numbers with the derivations of section 5.6.5. These two cases are referred to as **One Dimensional Sharing** cases.

Next the figures B.3c and B.3d represent cases where the Op-B shares both Class-1 and Class-2 traffic. These cases are referred to as **Two Dimensional Sharing** We show that, it is necessary for the overloaded Operator to reach a sate below the boundary line, to guarantee the desired QoS. For this we compare the two final states, both applying Class-1 and Class-2 sharing. The first (Figure B.3c) has the final state of Op-B below his boundary line, and the second (Figure B.3d) has the final state Op-B still above his boundary line.

B.3.1. One Dimensional Sharing Simulation results

The first two sharing cases, represent two options, that Op-B can follow, to overcome the overload situation. Each one of these option brings Op-B back to exactly his boundary line, by sharing only one type of traffic. In the following discussion we show when it is profitable for Op-B to choose which option.

Class-1 Sharing

This is the case depicted in the Figure B.3a. As described in Table B.3, we use $P_{T,B,1} = 0.713$ and $P_{T,B,2} = 0$. The resulting response times probability distributions are depicted in Figure B.4.

Figure B.4 shows that with these parameters, an good result in terms of load balancing is achieved. All the session response times are below their respective thresholds. It also shows that for Op-A the response times start to get longer. For example, the YouTube session response is now up to 55 seconds, which is bigger that the 50 seconds we had in the initial state as shown in Figure B.2b. Nonetheless the response times are still below the maximum allowed 1120 seconds. On the other side Op-B response times for class-1 and class-2 traffic became much less, compared with the initial case shown in the Figures B.2c and B.2d.

We Note that, during the ten hours of simulation, Op-B has transfered 64878 HTTP-sessions to Op-A.

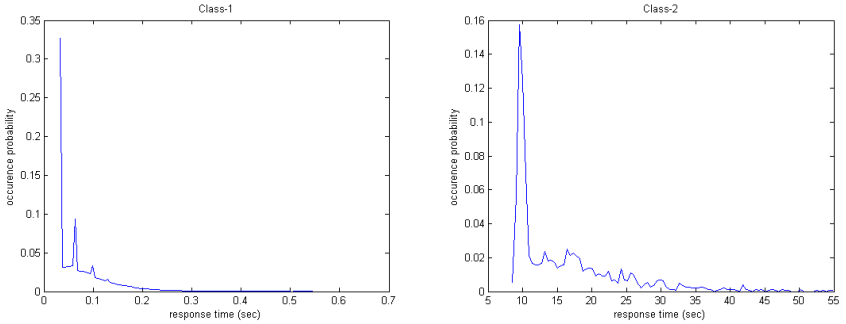

(a) Op-A Class 1

(b) Op-A Class 2

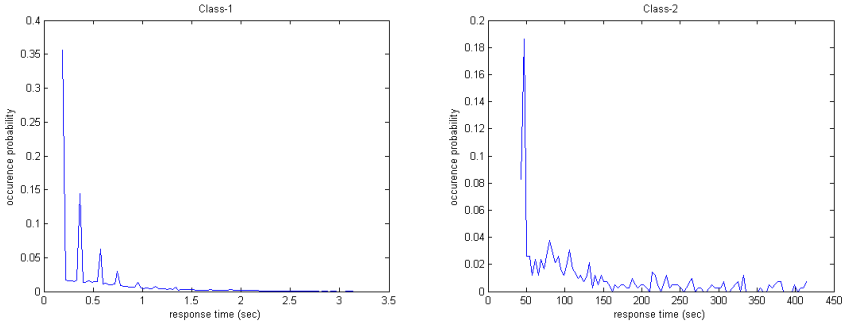

(c) Op-B Class 1

(d) Op-B Class 2

Figure B.4.: Sharing 1 Simulation results

Class-2 Sharing

This is the case depicted in the Figure B.3b. Only the Class-2 arrival is affected here. As described in Table B.3, we use $P_{T,B,1} = 0$ and $P_{T,B,2} = 0.715$. The resulting response times probability distributions are depicted in Figure B.5.

The results we get here are pretty comparable with the results we get from sharing only class-1 traffic. Figures B.5 and B.4 show same impact on the response time performance for the two one dimensional sharing cases. During the same simulation duration of ten hours, Op-B has transferred 302 YouTube (Class-2) sessions to Op-A. Furthermore we can see that Op-B is relaxed without hurting the performance of Op-A. All class-1 session responses are below the 4 seconds threshold., and all class-2 session responses are below the 1120 seconds threshold.

Discussion

The first what can be concluded, is that the model provide a valid framework for calculating the sharing parameters, that guarantee the profit of both sharing parties. This profit can be achieved by several. The equation 5.60 gives one possible solution, to help decide which way to design the sharing, by associating different costs to different session

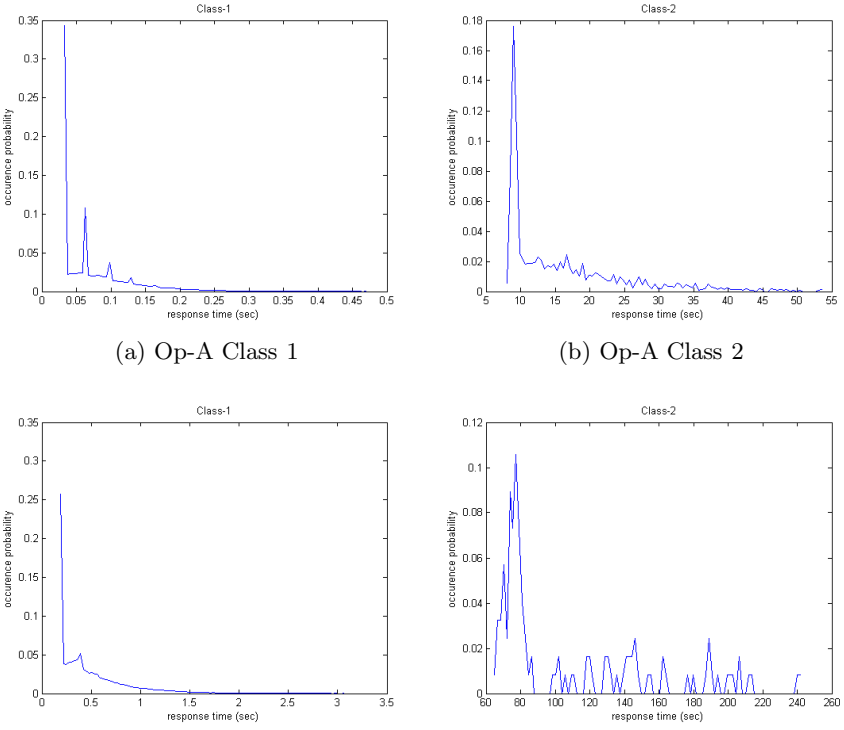

(a) Op-A Class 1

(b) Op-A Class 2

(c) Op-B Class 1

(d) Op-B Class 2

Figure B.5.: Sharing 2 Simulation results

request class transfers. This depends on the following term:

$$\frac{c_1}{\overline{x_1}} - \frac{c_2}{\overline{x_2}} \tag{B.1}$$

where c_1, and c_2 are the, per session class respective transfer cost, what the transferring operator pays for the Donor Operator, $\overline{x_1}$ and $\overline{x_2}$ are the respective average session lengths.

We have shown that in case

$$\frac{c_1}{c_2} = \frac{\overline{x_1}}{\overline{x_2}} \tag{B.2}$$

it will make no difference which sharing case to prefer by the borrower operator.The Simulation shows that Op-B has to either transfer 64878 HTTP sessions or 302 YouTube sessions.

These two options would yield the same cost in case:

$$64878 \cdot c_1 = 302 \cdot c_2 \tag{B.3}$$

This verifies the previous derivations since $\frac{302}{64878} \approx \frac{\overline{x_1}}{\overline{x_2}}$. This means in case:

- $\frac{c_1}{c_2} \leq \frac{\overline{x_1}}{\overline{x_2}}$ Op-B would prefer sharing 1.
- $\frac{c_1}{c_2} \geq \frac{\overline{x_1}}{\overline{x_2}}$ Op-B would prefer sharing 2.
- $\frac{c_1}{c_2} = \frac{\overline{x_1}}{\overline{x_2}}$ it would make no difference for Op-B

B.3.2. Two Dimensional Sharing

Now we examine the results of the Two Dimensional sharing, which corresponds to the Figures B.3c and B.3d. The difference between these two cases, is that, in the first one, Op-B has the final state below its boundary line, whereas for the second one, Op-B has its final state above its boundary line.

Two Dimensional Sharing with the Final State Below the Boundary Line

This is the case depicted in the Figure B.3c. For the simulation, we use $P_{T,B,1} = P_{T,B,2} = 0.5$ as described in Table B.3. In this case the final state of Op-B is below its boundary line. The results are depicted in the Figure B.6. This shows a more clear impact on Op-A than the cases in Figures B.4 and B.5, where the response times for class-2 traffic goes up to 60 seconds for Op-A compared with 55 seconds in Figures B.4 and B.5.

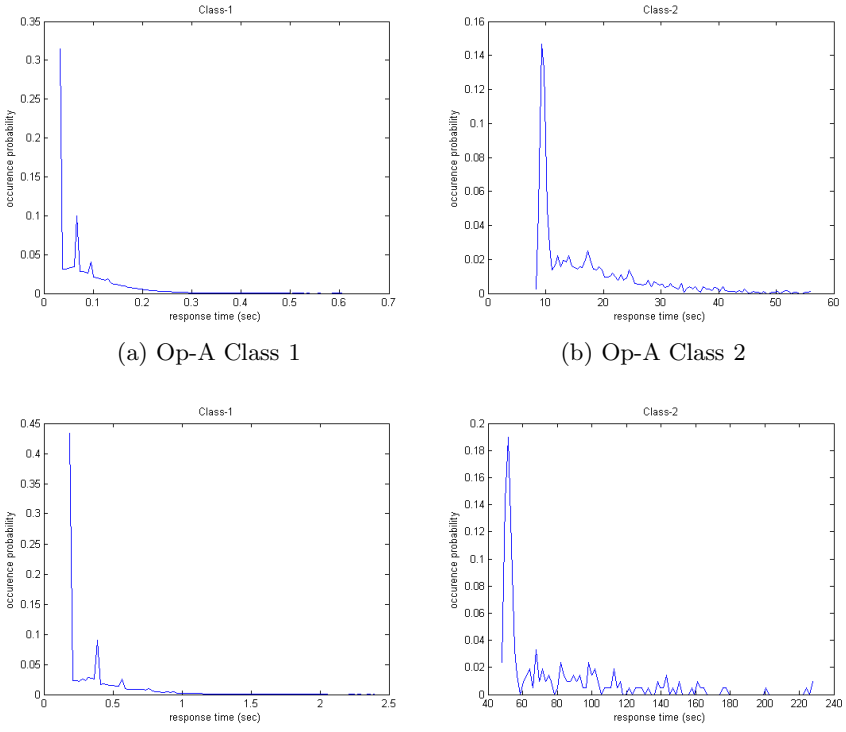

(a) Op-A Class 1

(b) Op-A Class 2

(c) Op-B Class 1

(d) Op-B Class 2

Figure B.6.: Sharing 3 Simulation results

During the ten hours simulation time, Op-B transfers 45651 HTTP sessions, and 214 YouTube sessions to Op-A. Even with balanced costs at the end Op-B will still have higher cost, compared with the costs it would have to pay in case it have chosen the transfer parameter that bring it back to his boundary line, and not below. However, comparing Figure B.4c and B.5c with the Figure B.6c, we can see that the response times for HTTP-sessions became much shorter, from up to 3 - 3.5 seconds, to up to almost 2 seconds. Thus transferring more traffic, would grant the Borrower even better QoS. On the other hand it should not have a final state above his boundary line, as it is shown in the next simulation case.

Two Dimensional Sharing with the final state above the boundary line

This is the case depicted in the Figure B.3d. For the simulation, we use $P_{T,B,1} = P_{T,B,2} = 0.1$ as described in Table B.3. In this case the final state of Op-B is still above its boundary line. The results are depicted in the Figure B.7.

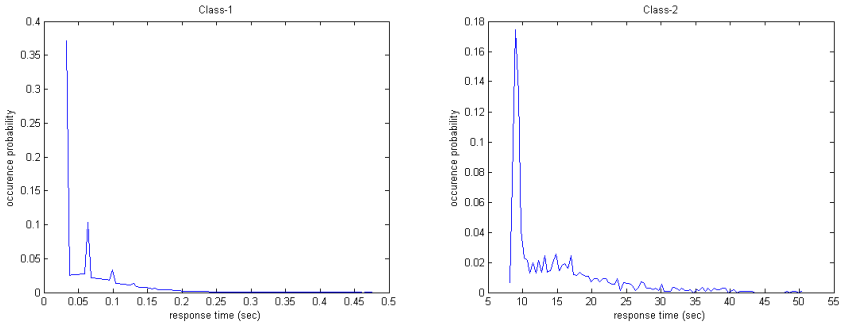

(a) Op-A Class 1 (b) Op-A Class 2

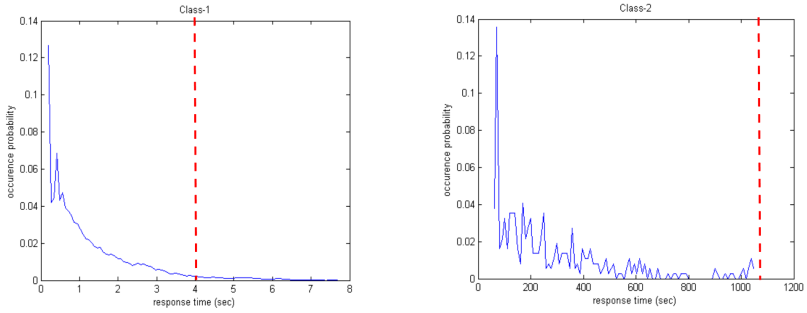

(c) Op-B Class 1 (d) Op-B Class 2

Figure B.7.: Sharing 4 Simulation results

As we can see, even all the YouTube session have a response time below the required threshold, more then 4% of the HTTP sessions take longer then the required 4 seconds threshold. This is shown in Figure B.7c, where we still have some occurrence on of

the right side of the dashed red line. For Youtube sessions of Op-B (Figure B.7d), it is shown that their response time is terse above the required threshold, since all the probabilities, in the probability distribution function, occurs on the left side of the dashed red line, which represents our required threshold of 1120 seconds. The difference in the performance between the two classes at Op-B can be explained by the different vulnerability of the different classes. As we set the maximum allowed utilization for the Op-B, as represented in Table B.1, we choose the maximum allowed utilization corresponding to HTTP traffic since it was the lower one. Thus YouTube traffic would tolerate a slightly higher utilization. This is why all of the YouTube sessions, have their response times below the correspondent threshold, even though HTTP traffic is suffering a service degradation.

C. Derivation of Conditional Delay Distribution

C.1. Introduction

Processor Sharing (PS) service discipline was introduced by Kleinrock as the limit of round-robin discipline with infinitesimal service time quanta. It can also be interpreted as a variable rate service discipline, in which the service capacity is shared equally between the number of customers in the system. This interpretation has gained interest among researchers in the telecommunications field, where PS models are used to model shared communication mediums. M/D/1-PS models, where the service sizes are known and deterministic are relevant for many types of communications applications. In scaling shared mediums among customers, it is of interest to calculate the expected delay as a function of number of customers in the system. This requires a closed form expression of the sojourn time in a M/D/1-PS system as a function of number of customers in the system. We derive such an expression in this paper.

Yashov [166] and Shalmon [167] provide closed form solutions for the variance of sojourn time in M/D/1-PS systems, which are not conditioned on the number of customers in the system. To the best of our knowledge the closest result in the literature is given by Coffman [30], who calculated the expected sojourn time conditioned on the number of customers in the system for M/M/1-PS queues.

C.2. Outline of the Derivation

We are considered with a M/D/1-PS system in which customers arrive according to a Poisson distribution of intensity λ and have a fixed service time of y seconds. Let us further denote the number of users that a tagged customer finds in the system with N. Let T_N be the sojourn time of a customer who finds N customers upon arrival. The probability density function sojourn time conditioned on number of customers in the system is $T_N(t)$, where $P(S < t|n = N) = \int_{u=0}^{t} T_N(u)du$. We are interested in finding a closed form expression for the expected sojourn time conditioned on the number of customers upon arrival, i.e. $E[T_N]$.

N is a discrete where as T_N is a continuous random variable. Their joint distribution can be described by the generating function of $w_N(t, s)$, which is the the Laplace transform of $T_N(t)$:

$$E\left[e^{-sT}\cdot z^N\right] = \sum_{N=0}^{\infty} z^N \int_{t=0}^{\infty} e^{-st} T_N(t)dt$$
$$= \sum_{n=0}^{\infty} z^N w_N(t,s) \tag{C.1}$$

Ott gives the expression for $E\left[e^{-sT}\cdot z^N\right]$ in [31]. It is well known that the derivative of $w_N(t,s)$ with respect to s evaluated at $s=0$ gives $-E\left[T_N\right]$:

$$\frac{\partial}{\partial s|_{s=0}} E\left[e^{-sT}\cdot z^N\right] = \sum_{n=0}^{\infty} z^N \int_{t=0}^{\infty} \frac{\partial}{\partial s|_{s=0}} w_N(t,s)$$
$$= \sum_{n=0}^{\infty} z^N \left(-E\left[T_N\right]\right) \tag{C.2}$$

(C.2) is the $\mathcal{Z}$-transform of the expected sojourn time conditioned on the number of customers in the system upon arrival times minus one. Our approach is to calculate the derivative with respect to s at $s=0$ and evaluate the inverse $\mathcal{Z}$-transform to obtain the expression for $E\left[T_N\right]$. This approach is similar to Coffman's for obtaining the expected sojourn time conditioned on N in M/M/1-PS queues [30].

C.3. Obtaining the $\mathcal{Z}$-transform

The expression for $E\left[e^{-sT}\cdot z^N\right]$ is given by:

$$E\left[e^{-sT}\cdot z^N\right] = \frac{(1-\rho)(\lambda+s)^2 e^{-y(\lambda+s)}}{s\left(s+\lambda(1-z)\right) + \left\{s(1+z(1-\rho)) + \lambda(1-\rho z)\right\}\lambda e^{-y(\lambda+s)}} \tag{C.3}$$

where $\rho = y\lambda$ is the utilization. Let us define intermediate variables A and B to make the derivative tractable:

$$\frac{\partial}{\partial s} E\left[e^{-sT}\cdot z^{-N}\right] = \frac{\partial}{\partial s}\frac{A}{B}$$
$$= \frac{B\cdot\frac{\partial}{\partial s}A - A\cdot\frac{\partial}{\partial s}B}{B^2} \tag{C.4}$$

We evaluate the terms one by one:

$$
\begin{aligned}
B^2 = &\left\{ s^4 + 2s^3\lambda(1-z) + s^2\lambda^2(1-z)^2 \right\} \\
&+ 2\Big\{ s^3\left[1+(1-\rho)z\right] + s^2\lambda(1-\rho z) + s^2\lambda(1-z)\left[1+(1-\rho)z\right]\ldots \\
&+ s\lambda^2(1-z)(1-\rho z)\Big\}\lambda e^{-y(\lambda+s)} \\
&+ \left\{ s^2\left[1+(1-\rho)z\right]^2 + 2s\left[1+(1-\rho)z\right]\lambda(1-\rho z^{-1}) + \lambda^2(1-\rho z)^2 \right\}\lambda^2 e^{2y(\lambda+s)}
\end{aligned}
\tag{C.5}
$$

The derivative terms of A and B are given by:

$$
\begin{aligned}
\frac{\partial}{\partial s}A &= (\lambda+s)(1-\rho)\left[2-y(\lambda+s)\right]e^{-y(\lambda+s)} \\
\frac{\partial}{\partial s}B &= 2s + \lambda(1-z) + \lambda(1-ys)\left[1+(1-p)z\right]e^{-y(\lambda+s)} \\
&\quad - \lambda\rho(1-\rho z)e^{-y(\lambda+s)}
\end{aligned}
\tag{C.6}
$$

Only the terms without a s term contribute when $s=0$, therefore we get the following shorter expressions:

$$
\begin{aligned}
B^2|_{s=0} &= \lambda^4 e^{-2\rho}(1-\rho z)^2 \\
A|_{s=0} &= \lambda^2 e^{-\rho}(1-\rho) \\
\frac{\partial}{\partial s}A|_{s=0} &= \lambda e^{-\rho}(1-\rho)(2-\rho) \\
B|_{s=0} &= \lambda^2 e^{-\rho}(1-\rho z) \\
\frac{\partial}{\partial s}B &= \lambda\left\{\left[1+e^{-\rho}(1-\rho)\right] + \left[e^{-\rho}(\rho^2-\rho+1)-1\right]z\right\}
\end{aligned}
\tag{C.7}
$$

We obtain the following rational function when we insert (C.7) in (C.4):

$$
\begin{aligned}
\mathcal{Z}\left\{-E\left[T_N\right]\right\} = &\frac{\lambda^2 e^{-\rho}(1-\rho z)\cdot\lambda e^{-\rho}(1-\rho)(2-\rho)}{\lambda^4 e^{-2\rho}(1-\rho z)^2} \\
&- \frac{\lambda^2 e^{-\rho}(1-\rho)\cdot\lambda\left\{\left[1+e^{-\rho}(1-\rho)\right] + \left[e^{-\rho}(\rho^2-\rho+1)-1\right]z\right\}}{\lambda^4 e^{-2\rho}(1-\rho z)^2}
\end{aligned}
\tag{C.8}
$$

Using the linearity of $\mathcal{Z}$-transform and grouping together the constant terms and the terms with z we obtain:

$$\mathcal{Z}\left\{E\left[T_N\right]\right\} = \frac{\lambda^{-1}(1-\rho)(e^{\rho}-1)}{(1-\rho z)^2} + \frac{\lambda^{-1}(1-\rho)(1+\rho-e^{\rho})z}{(1-\rho z)^2} \tag{C.9}$$

C.4. Inverting the $\mathcal{Z}$-Transform

When we define $K = \lambda^{-1}(1-\rho)(e^{\rho}-1)$ and $L = \lambda^{-1}(1-\rho)(1+\rho-e^{\rho})$, we have:

$$\mathcal{Z}\left\{T_N\right\} = \frac{K}{(1-\rho z)^2} + \frac{Lz}{(1-\rho z)^2} \tag{C.10}$$

Which correspond to the Z-transform of two sequences of the form $n\rho^n$. Lets re-write the terms to obtain familiar Z-transforms:

$$\mathcal{Z}\left\{T_N\right\} = \frac{\sqrt{K}}{(1-\rho z)} \cdot \frac{\sqrt{K}}{(1-\rho z)} + \frac{L}{\rho}\frac{\rho z}{(1-\rho z)^2} \tag{C.11}$$

Note that the Ott uses the definition of $\mathcal{Z}$-transform with the positive powers of z. It is usually given by the negative powers of z. Nevertheless, the forms are equivalent with only a change of the region of convergence. The sequence $\rho^N u(N)$, where $u(N)$ is the unit step function has the following $\mathcal{Z}$-transform:

$$\mathcal{Z}\left\{\rho^N u(N)\right\} = \frac{1}{1-\rho z} \quad |z| < 1/\rho \tag{C.12}$$

The region of convergence, $|z| < 1/\rho$ includes the unit circle for a stable queue, i.e. $\rho < 1$.

Multiplication of two $\mathcal{Z}$-transforms correspond to the convolution of the corresponding sequences in N. Thus, the first term correspond to the convolution of the sequence $x(N) = \rho^N u(n)$ with itself:

$$\begin{aligned} x(N) \otimes x(N) &= \sum_{k=-\infty}^{\infty} \sqrt{K}\rho^k u(k) \cdot \sqrt{K}\rho^{N-k} u(N-k) \\ &= K \cdot \rho^N \sum_{k=0}^{N} 1 \\ &= K \cdot (N+1)\rho^N \end{aligned} \tag{C.13}$$

The second term can be obtained using the differentiation property of $\mathcal{Z}$-transform:

$$\mathcal{Z}\{N \cdot x(N)\} = z \cdot \frac{d}{dz} X(z)$$
$$\mathcal{Z}\left\{N \cdot \rho^N u(N)\right\} = \frac{\rho z}{(1-\rho z)^2} \tag{C.14}$$

We obtain the final expression for $E[T_N(t)]$ after we insert (C.14) and (C.13) into (C.10) and expand K and L:

$$E[T_N] = \lambda^{-1}(1-\rho)\rho^N \left\{N\left[(1-e^{\rho}) + \rho^{-1}(e^{\rho}-\rho-1)\right] + (1-e^{\rho})\right\} \tag{C.15}$$

C.5. Discussion

The expression can be interpreted as an application of Little's theorem, $E[T_N] \cdot \lambda = E[\text{Number of users who leave behind N users}]$. Therefore the expression:

$$(1-\rho)\rho^N \left\{N\left[(1-e^{\rho}) + \rho^{-1}(e^{\rho}-\rho-1)\right] + (1-e^{\rho})\right\} \tag{C.16}$$

gives the average number of customers which leave N users behind.

Another interesting fact is the limiting behavior of the conditional expected sojourn time, $\lim_{N\to\infty} E[T_N] = 0$. On the one hand one expects the expected service time to be infinity as the number of jobs increase. On the other hand the actual probability that there are arbitrarily large numbers of users in the system is practically zero.